Biologie synthétique de la fixation du carbone chez Chlamydomonas reinhardtii

Nicolas Boisset

▶ **To cite this version:**

Nicolas Boisset. Biologie synthétique de la fixation du carbone chez Chlamydomonas reinhardtii. Biotechnologies. Université Paris-Saclay, 2023. Français. NNT : 2023UPASB033 . tel-04207798

HAL Id: tel-04207798

https://theses.hal.science/tel-04207798

Submitted on 14 Sep 2023

HAL is a multi-disciplinary open access archive for the deposit and dissemination of scientific research documents, whether they are published or not. The documents may come from teaching and research institutions in France or abroad, or from public or private research centers.

L'archive ouverte pluridisciplinaire **HAL**, est destinée au dépôt et à la diffusion de documents scientifiques de niveau recherche, publiés ou non, émanant des établissements d'enseignement et de recherche français ou étrangers, des laboratoires publics ou privés.

université PARIS-SACLAY

Biologie synthétique de la fixation du carbone chez *Chlamydomonas reinhardtii*

Synthetic biology of carbon fixation in *Chlamydomonas reinhardtii*

Thèse de doctorat de l'université Paris-Saclay

École doctorale n°567 : Sciences du végétal : du gène à l'écosystème (SEVE)
Spécialité de doctorat : Biologie
Graduate School : BioSphERA Référent : Faculté des sciences d'Orsay

Thèse préparée dans les unités de recherche **Laboratoire de Biologie Moléculaire et Cellulaire des Eucaryotes (Institut de Biologie Physico-Chimique, CNRS et Sorbonne Université) et Laboratoire de Biologie Computationnelle et Quantitative (Institut de Biologie Paris-Seine, Sorbonne Université et CNRS)**, sous la direction de **Stéphane LEMAIRE**, Directeur de recherches CNRS et le co-encadrement de **Pierre Crozet**, Maître de conférences,

Thèse soutenue à Paris, le 3 Juillet 2023, par

Nicolas Boisset

Composition du Jury

Membres du jury avec voix délibérative

Marianne Delarue Professeure, Université Paris-Saclay	Présidente
Nicolas Rouhier Professeur, Université de Lorraine	Rapporteur & Examinateur
Arnould Savouré Professeur, Sorbonne Université	Rapporteur & Examinateur
Emmanuelle Issakidis-Bourguet Chargée de recherche CNRS, Université Paris-Saclay	Examinatrice
Katia Wostrikoff Maitresse de conférences, Sorbonne Université	Examinatrice

THESE DE DOCTORAT

NNT : 2023UPASB033

Titre : Biologie synthétique de la fixation du carbone chez *Chlamydomonas reinhardtii*

Mots clés : biologie synthétique, blasticidine, *Chlamydomonas reinhardtii*, cycle de Calvin-Benson-Bassham, phosphoribulokinase, photosynthèse

Résumé : La photosynthèse permet l'assimilation du CO_2 atmosphérique en glucides tout en produisant de l'O_2. L'énergie lumineuse est convertie en énergie chimique qui est à son tour principalement utilisée pour fixer le carbone inorganique via le cycle de Calvin-Benson-Bassham (CBBC). Le CBBC se compose de 13 réactions qui sont catalysées par 11 enzymes, qui sont toutes fortement exprimées et étroitement régulées à plusieurs niveaux (abondance, modifications post-traductionnelles,...). Le principal facteur limitant la photosynthèse est le CBBC, qui présente des goulets d'étranglement cinétiques. Une meilleure compréhension de ces goulets d'étranglement *in vivo* est indispensable pour lever ces limitations afin de pouvoir améliorer la photosynthèse. Une approche consiste à modifier l'abondance de chaque enzyme individuellement afin de déterminer si elle est limitante. Pour contrôler l'abondance des enzymes du CBBC *in vivo*, des circuits génétiques synthétiques peuvent être utilisés. Les approches de biologie synthétique permettent de construire de tels circuits génétiques et de comprendre par construction plutôt que par déconstruction.

Dans cette thèse, nous avons étudié la phosphoribulokinase (PRK) chez l'algue unicellulaire *Chlamydomonas reinhardtii*, car son activité est unique et spécifique au CBBC, elle est codée par un seul gène nucléaire et un mutant d'insertion est disponible.

La caractérisation de la souche mutante a révélé que la PRK est essentielle à la photoautotrophie et que la complémentation fonctionnelle du mutant permet de restaurer la croissance en milieu minimum. Toutefois, pour obtenir plus de 40 % de PRK par rapport à la souche sauvage, nous avons dû construire un circuit génétique contenant le promoteur, le 5'UTR et la séquence incluant les introns du gène endogène de la PRK. Une collection de souches présentant des niveaux de PRK entre 16% et 250% des niveaux de PRK sauvage a été générée et caractérisée. Un contenu en PRK d'environ 86% est suffisant pour restaurer complètement la croissance photoautotrophe. Nos résultats suggèrent que la PRK est présente en excès modéré chez *C. reinhardtii*. De manière cohérente, la surexpression de la PRK n'a pas augmenté la croissance photosynthétique, indiquant que le niveau endogène de PRK chez *C. reinhardtii* n'est pas limitant pour le cycle de Calvin-Benson-Bassham dans des conditions optimales.

En parallèle, j'ai participé au développement d'outils de biologie synthétique. En particulier, nous avons développé et validé un nouveau marqueur de résistance à l'antibiotique blasticidine chez *C. reinhardtii* afin de faciliter la construction de nouvelles souches.

Title : Synthetic biology of carbon fixation in *Chlamydomonas reinhardtii*

Keywords : blasticidine, Calvin-Benson-Bassham cycle, *Chlamydomonas reinhardtii*, synthetic biology, phosphoribulokinase, photosynthesis

Abstract : Photosynthesis allows the assimilation of atmospheric CO_2 into carbohydrates while producing O_2. Light energy is converted into chemical energy which is in turn primarily used to fix inorganic carbon *via* the Calvin Benson Bassham cycle (CBBC). The CBBC consists of 13 reactions catalyzed by 11 enzymes, all of which are highly expressed and tightly regulated at multiple levels (abundance, post-translational modifications;…). The primary limiting factor for photosynthesis is the CBBC, which has kinetic bottlenecks. A better understanding of these bottlenecks *in vivo* is essential for overcoming these limitations to improve photosynthesis. One approach is to alter the abundance of each individual enzyme to determine if it is limiting. Synthetic genetic circuits can be used to control the abundance of CBBC enzymes *in vivo*. Synthetic biology approaches allow for the construction of such genetic circuits and understanding by construction rather than deconstruction.

In this thesis, we studied phosphoribulokinase (PRK) in the unicellular alga *Chlamydomonas reinhardtii*, as its activity is unique and specific to the CBBC, it is encoded by a single nuclear gene, and an insertion mutant is available. Characterization of the mutant strain revealed that PRK is essential for photoautotrophy, and functional complementation of the mutant restores growth in minimal media. However, to achieve more than 40% of PRK compared to the wild-type strain, we had to construct a genetic circuit containing the promoter, 5'UTR, and sequence including the introns of the endogenous PRK gene. A collection of strains with PRK levels between 16% and 250% of wild-type PRK levels was generated and characterized. A PRK content of approximately 86% is sufficient to fully restore photoautotrophic growth. Our results suggest that PRK is present in moderate excess in *C. reinhardtii*. Consistently, PRK overexpression did not increase photosynthetic growth, indicating that the endogenous level of PRK in *C. reinhardtii*. is not limiting for the Calvin-Benson-Bassham cycle under optimal conditions.

In parallel, I contributed to the development of synthetic biology tools. In particular, we developed and validated a new marker of resistance to the antibiotic blasticidine in *C. reinhardtii* to facilitate the construction of new strains.

Remerciements

Je tiens tout d'abord à remercier les membres de mon jury pour avoir accepté d'évaluer mon travail : la Pr. Marianne Delarue, la Dr. Emmanuelle Issakidis-Bourguet, le Pr. Nicolas Rouhier, le Pr. Arnould Savouré et la Dr. Katia Wostrikoff. Je remercie également les membres de mon comité de thèse, la Dr Alix Boulouis et la Dr. Corinne Cassier-Chauvat pour avoir suivi l'évolution de mon projet.

Je tiens également à remercier mon école doctorale, Science du végétal : Du gène à l'ecosystème (SEVE) pour m'avoir donné l'opportunité de vivre cette aventure. Marianne, encore une fois merci beaucoup, tu m'as énormément aidé, suivi et soutenu pour que je puisse finir ma thèse dans de bonnes conditions.

Un grand merci au Dr. Stéphane Lemaire, mon directeur de thèse qui m'a donné la chance de pouvoir vivre cette aventure au sein de son équipe. Un immense merci à Pierre Crozet qui a co-encadré mon travail de thèse et m'a suivi étroitement au cours de ma thèse. Votre compassion et votre bienveillance m'ont grandement aidé à traverser ma maladie. Je n'aurais pu trouver meilleur soutien humain que le vôtre durant et après cette épreuve et je ne serais pas là où j'en suis sans vous. Je ne pourrais même pas énumérer la quantité de choses que j'ai apprises auprès de vous ni exprimer la reconnaissance que j'ai à votre égard.

Merci au Dr. Antoine Danon, au Dr. Christophe Marchand et au Dr Julien Henri pour toutes les discussions et aides que vous m'avez apportées, pour le wine testing et les bons moments que nous avons passés autour d'un verre.

Merci à la Dr. Teresa Teixeira pour m'avoir accueilli au sein de son unité. Je remercie aussi vivement Félix de Carpentier et Théo Le Moigne avec qui nous avons partagé ce fameux petit bureau très étroit dans lequel nous avions de l'excellente musique et des discussions très scientifiques, d'une qualité à ne pas faire avancer grandement la science la plupart du temps.

Merci à l'IBPC, institut rempli d'histoire qui nous baigne dans une atmosphère inégalable, à ce mélange scientifique entre tous les membres de l'institut à l'occasion par exemple des "drinking Thursdays". En ce lieu j'ai trouvé une famille qui m'a beaucoup apporté. Un merci particulier à Isabelle, Margot, Denesh, Alejandro, Antonin C., Antonin N., Bechara, Cyrielle, Cynthia, Jeanne LP, Prisca et Tanguy. Vous avoir rencontrés est une chance et m'a permis de passer de très bons moments en votre compagnie ! Ferdinand ta rencontre à l'IBPC m'a valu une nouvelle et forte amitié, merci pour ton soutien tout au long de ma thèse et de ma maladie.

Au LCQB, je remercie Alessandra Carbone de m'avoir accueilli. C'est au sein de cette unité que j'ai pu rencontrer Achille, Mariette, Nicolas, Clémence, Jeanne G, Lou, Lucile, Martina, Maria mais aussi Giusi qui a grandement participé à ma thèse.

Merci à vous tous pour les moments que nous avons passés ensemble autour d'un verre, cafés, gâteaux et repas.

Enfin, j'aimerais remercier ma famille dont mes parents, Daniel et Brigitte, et ma sœur Emilie. Vous êtes les premières personnes à avoir cru en moi et vous m'avez soutenu tout du long. Je ne peux pas mentionner ma famille sans citer également Boubouille ainsi que Enola-Lou, Jean Descarpenterie et Dylan Tatara qui me suivent depuis le lycée et Fidji qui a partagé ma vie pendant une bonne partie de ma thèse.

Un dernier remerciement aux personnes qui ont cru en moi, m'ont accompagné et élevé : Stéphanie Florat Lohyer, Laurent Desfarges, Emmanuelle Bayer, Frédéric Delmas, Michel Hernould, Rima Menassa, Reza Saberianfar et également merci au Dr. Capera-Galeas et à Florence Ronco sans qui je n'aurais pas pu me relever de ma maladie, qui m'ont permis de me soigner et devenir plus fort.

Abréviations

1,3-PGA : 1,3-bisphosphoglycérate

3-PGA : 3-phosphoglycérate

ADN : acide désoxyribonucléique

ARN : acide ribonucléique

BCA : bicinchoninic acid

BSA : bovine serum albumin

CDS : coding sequence

CA : anhydrase carbonique

CAR : Chimeric antigen receptor

CBBC : cycle de Calvin-Benson-Bassham

CCM : mécanisme de concentration du carbone

CETCH : crotonyl-CoA/ethylmalonyl-CoA/hydroxybutyryl-CoA

Chlamydomonas : *Chlamydomonas reinhardtii*

C_i : carbone inorganique

CP12 : chloroplast protein of 12 kDa

DBTL : design, build, test, learn

DHAP : dihydroxyacétone phosphate

DTT : dithiothréitol

E4P : érythrose-4-phosphate

EC : enzyme commission number

EPYC1 : essential pyrenoid component 1

FBP : fructose-1,6-bisphosphate

F6P : fructose-6-phosphate

FBA : fructose-1,6-bisphosphate aldolase

FBPase : fructose-1,6-bisphosphatase

FPP : farnesyl pyrophosphate

G3P : glycéraldéhyde-3-phosphate

GAPDH : glycéraldéhyde-3-phosphate déshydrogénase

GED : Gnd-Entner-Doudoroff

GIEC : groupe d'experts intergouvernemental sur l'évolution du climat

CLiP : Chlamydomonas Library insertion Project

GRAS : generally recognized as safe

GS/GOGAT : glutamine synthétase/glutamine oxoglutarate aminotransférase

HSM : high salt medium

MoClo : modular cloning

NPQ : non-photochemical quenching

OMM : organisation météorologique mondiale

PCR : polymerase chain reaction

PETC : chaine photosynthétique de transfert des électrons

PGK : phosphoglycérate kinase

PNUE : programme des nations unies pour l'environnement

PRK : phosphoribulokinase

PTM : modification post-traductionnelle

QC : contrôle de qualité

R5P : ribose-5-phosphate

ROS : reactive oxygen species

RPE : ribulose-5-phosphate-3-épimérase

RPI : ribulose-5-phosphate isomérase

RT : room temperature

Rubisco : ribulose-1,5-bisphosphate carboxylase/oxygénase

RuBP : ribulose-1,5-bisphosphate

RuP : ribulose-5-phosphate

S7P : sédoheptulose-7-phosphate

SBP : sédoheptulose-1,7-bisphosphate

SBPase : sédoheptulose-1,7-bisphosphatase

SDS-PAGE : électrophorèse en gel de polyacrylamide contenant du dodécysulfate de sodium

TAP : Tris acétate phosphate

TBS : Tris buffered saline

TEM : microscopie électronique à transmission

TPI : triose phosphate isomérase

TRK : transketolase

TRX : thiorédoxine

TU : unité transcriptionnelle

UTR : untranslated region

WT : wild-type

X5P : xylulose-5-phosphate

Table des matières

1 INTRODUCTION

1.1 Problématique environnementale, écologique et sociétale.

Aujourd'hui et pour les décennies à venir, l'humanité est confrontée à un défi majeur auquel elle n'a jamais été confrontée auparavant. Cinq ans après la création de l'Organisation des Nations Unies en 1954, cette dernière avait estimé la population mondiale à près de 2,6 milliards de personnes. Le 15 novembre 2022, la population mondiale a atteint 8 milliards de personnes (Gaigbe-Togbe et al., 2022). Ce chiffre important n'est pas sans engendrer des conséquences sur notre planète et sur nos vies.

Tout comme les autres espèces, l'*Homo sapiens* utilise son environnement pour se développer et prospérer. Nous déforestons pour étendre les terres agricoles, nous utilisons l'agriculture pour produire des denrées alimentaires et nous utilisons des industries pour transformer ces ressources ainsi que pour produire des molécules d'intérêt industriel.

Les conséquences de l'activité humaine ont commencé à se manifester assez rapidement en raison de l'accroissement démographique. En 1988, le programme des nations unies pour l'environnement (PNUE) et l'organisation météorologique mondiale (OMM) ont créé le groupe d'experts intergouvernemental sur l'évolution du climat (GIEC), chargé de synthétiser l'état des connaissances sur le changement climatique et le rôle de l'activité humaine (https://www.ipcc.ch/). Assez rapidement, la corrélation entre les deux fut établie et il n'y a aujourd'hui plus de doute sur le fait que les bouleversements climatiques et environnementaux sont dues à l'activité humaine (Lee et al., 2021; IPCC, 2022).

Notre activité a un tel impact, qu'elle a déclenché une sixième extinction de masse sur Terre, qualifiée d'Holocène ou également d'Anthropocène (Barnosky et al., 2011; Cowie et al., 2022). La surpêche, la déforestation et l'appauvrissement des zones naturelles, le réchauffement climatique, la pollution des sols et des eaux à l'échelle

de la planète entraînent des conséquences très lourdes sur le biome de la planète. La concentration en CO_2 dans l'air est passée de 280 ppm à l'époque préindustrielle à 420 ppm aujourd'hui. Cela a déjà entrainé une augmentation de la température moyenne mondiale de 1,5°C (Figure 1) qui, même avec des mesures dites « zéro émission » pour tenter d'y remédier, bouleversera les écosystèmes pendant 100 générations, soit près de 10 000 ans (Hirt et al., 2023).

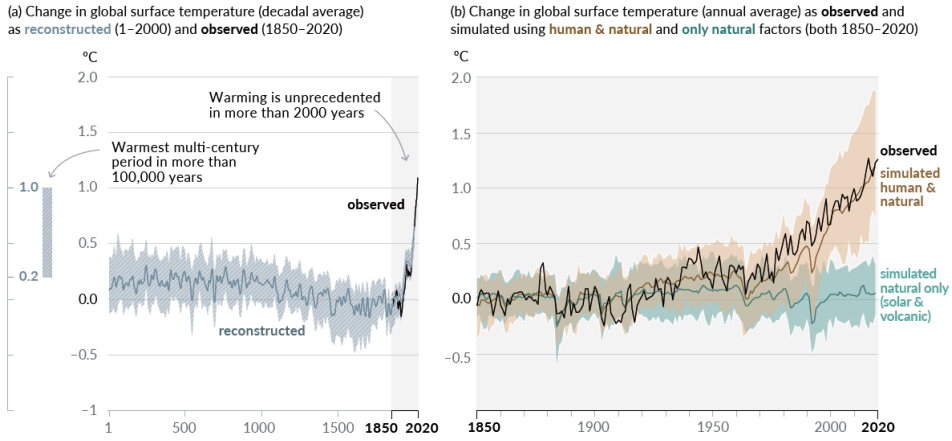

Figure 1. Graphique de l'augmentation de la température globale (a) sur 2000 ans (b) entre 1850 et 2020 (Lee et al., 2021)*)*

Le réchauffement climatique engendre déjà des sècheresses, des inondations et une diminution des capacités de production de l'agriculture. Les ressources de notre planète sont limitées. Avec notre système de production actuel, nous ne pouvons résoudre les problèmes que nous créons. L'un des plus grands défis de l'humanité est donc de réussir, dans ce contexte, à produire suffisamment de nourriture pour la population mondiale, de réduire les émissions de carbone et de capturer le CO_2 atmosphérique. En définitive, il s'agit de réduire l'impact de notre activité en changeant, entre autres choses, nos modes de production (Lee et al., 2021; IPCC, 2022).

Malgré notre progrès technologique, il nous reste encore beaucoup à développer et à apprendre pour transformer profondément nos modes de production, que ce soit dans l'agriculture ou dans l'industrie. Pour cela, il est intéressant de s'inspirer des stratégies présentes dans le vivant (Singh et al., 2012; Oguntona et Aigbavboa, 2023).

L'humanité est relativement jeune, apparue il y a seulement quelques centaines de milliers d'années, en comparaison avec la vie sur terre qui aurait débuté il y a environ 4 milliards d'années (Malaterre et al., 2022). La bio-inspiration est donc un vecteur d'avancées technologiques. Par exemple, nous pouvons envisager de remédier à la consommation énergétique très importante des *data-centers* en nous inspirant du vivant pour stocker l'information de manière plus efficace (*cf.* 1.2.2.5). L'information dans les cellules est portée par l'acide désoxyribonucléique (ADN), une molécule dont la compacité et la durabilité dans le temps demeurent jusqu'à présent inégalée par les inventions humaines (Dong et al., 2020). Une compréhension fondamentale du vivant, me semble un point clé pour l'évolution de la société humaine.

1.2 La biologie de synthèse en tant qu'approche de compréhension

1.2.1 La synthèse en biologie

« *Comme les autres sciences, la biologie doit être successivement descriptive, analytique puis synthétique* » S. Leduc, 1912.

Stéphane Leduc, un scientifique français du XIX^{éme} siècle, a pu observer le développement fantastique de la chimie organique de synthèse. Il a voulu témoigner de l'importance de ne pas se limiter uniquement à l'observation et à l'analyse des phénomènes biologiques pour les comprendre, et les utiliser à d'autres finalités (Tirard, 2015).

La synthèse vise à comprendre par la construction plutôt que par la déconstruction (analyse).

« *What I cannot create, I do not understand* » Richard Feynman.

Cette phrase de Richard Feynman illustre bien le concept sous-jacent de la synthèse : la construction est la preuve ultime de la compréhension. Imaginons que pour comprendre un vélo, l'approche analytique va retirer une roue ou le guidon et en observer les conséquences. La synthèse va construire une roue, un guidon, une selle, un dérailleur et ainsi observer que les connaissances que nous

avions jusque-là n'étaient pas suffisantes pour comprendre pleinement comment fonctionne un vélo. A chaque cycle, dit de *Design*, *Build*, *Test*, *Learn* (DBTL), une méthodologie empruntée à l'ingénierie (Endy, 2005), nous apprenons des concepts et les règles de conception (design) qui nous échappaient précédemment pour élaborer convenablement notre système (Figure 2). En conservant notre métaphore, une roue a besoin de rayons, et ses rayons ont besoin d'être légers, tout comme le châssis, le dérailleur doit être graissé...

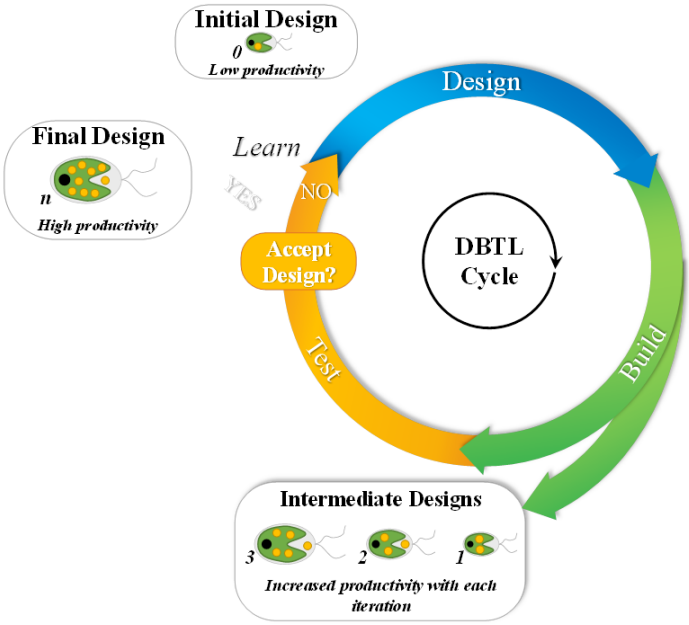

Figure 2. Le cycle Design/Build/Test/Learn appliqué pour une utilisation chez l'algue unicellulaire Chlamydomonas reinhardtii

En d'autres termes, la biologie synthétique vise à concevoir et construire des systèmes biologiques avec une (des) fonction(s) nouvelle(s). En répétant le cycle Design/Build/Test/Learn jusqu'à l'obtention du système le plus efficace pour la (les) fonction(s) donnée(s). L'organisme dans lequel le design est assemblé et testé est appelé le châssis.

Par exemple, pour produire des molécules d'intérêt dans un châssis à partir d'un design original peu productif, un nouveau design est construit et testé selon des critères prédéfinis. Si le nouveau design est

plus performant mais pas encore assez (générant un design intermédiaire), un nouveau design est réalisé en améliorant le précédent à la lumière des résultats du test (Learn). Cela marque le début d'une nouvelle itération. Comme chaque itération apporte de nouvelles connaissances (Learn), elle permet de guider la génération d'une nouvelle conception pour l'itération suivante. Après *n* itérations, le design *n* est hautement productif selon les critères attendus et devient le design final, mettant fin au cycle.

Quelle meilleure preuve de compréhension d'un système que de réussir à le (re)construire ? Pouvons-nous améliorer ce système ? Pouvons-nous lui donner de nouvelles fonctions ? Pour que cette logique de construction fonctionne, la biologie de synthèse s'appuie sur deux autres concepts d'ingénierie, l'abstraction et la standardisation (Endy, 2005).

Dans le but de construire des systèmes complexes, les designs s'avèrent également de plus en plus complexes. L'abstraction permet de créer une hiérarchie dans notre méthodologie, un système sera composé de dispositifs (*devices*), eux-mêmes composés de modules, ces derniers étant construits à partir de briques élémentaires. En montant ces niveaux de complexité, on peut faire *abstraction* des détails des niveaux précédents et ainsi concevoir (*design*) plus facilement (Figure 3).

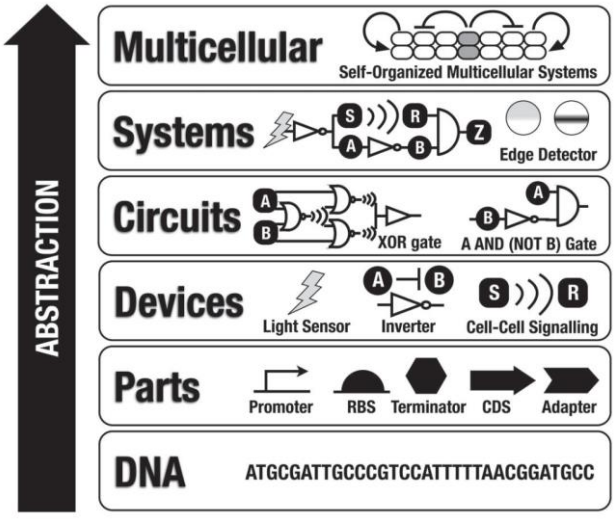

Figure 3. Représentation d'une hiérarchie d'abstraction, de l'ADN à l'ingénierie de systèmes multicellulaires (Federici et al., 2013)

En biologie, l'ADN *designé*[1] permet de faire construire aux cellules des systèmes élaborés par un être humain. Une hiérarchie d'abstraction en biologie aura donc comme niveau fondamental, celui des briques, des séquences d'ADN portant une fonction simple (comme un promoteur ou une séquence codante). Le niveau suivant de fonctionnalité sera le gène, ou unité de transcription, composé de ces briques. L'intégration fonctionnelle de ces gènes sera le niveau supérieur, et ainsi de suite.

Pour pouvoir construire ces systèmes efficacement, l'histoire de l'ingénierie a montré que la standardisation est cruciale. En effet, celle-ci permet un meilleur échange entre les designers, et évite donc de recréer continuellement les mêmes constructions. Cela garantit une meilleure efficacité et permet une meilleure diffusion des progrès (Meng et Ellis, 2020). Chaque niveau d'une hiérarchie d'abstraction possède donc ses propres standards. Le premier niveau, celui des briques géniques fonctionnelles, est donc celui ayant eu le plus de tentatives de standardisation (Casini et al., 2015). On a pu clairement voir au cours du temps, un engouement pour un standard particulier, associé à une méthodologie : le Modular Cloning (MoClo) (Weber et al., 2011; Patron et al., 2015) rendu possible grâce au Golden Gate Cloning (Engler et al., 2008). Nous détaillerons cette méthodologie ci-après (*cf.* 1.4).

L'avènement des biotechnologies nous a permis de ne plus exploiter certaines ressources naturelles pour la production de molécules spécifiques. La biologie de synthèse contribuera encore davantage à cette évolution. Cette discipline, bien que jeune, est prometteuse pour aborder un certain nombre de problématiques sociétales (Cameron et al., 2014; Meng et Ellis, 2020). Nous en illustrerons des exemples dans la partie suivante.

1.2.2 Quelques domaines de la biologie de synthèse

De nos jours, l'utilisation de la biologie de synthèse est devenue de plus en plus présente dans la recherche fondamentale comme dans

[1] Le terme correct en français serait « conçu rationnellement » mais il semble accepté aujourd'hui d'utiliser le terme anglais *design*, et ses variations (designé), dans notre contexte de biologie synthétique.

l'industrie. De nombreux projets ont vu le jour dans différents domaines. A travers quelques exemples, nous illustrerons cette diversité.

1.2.2.1 Programmation génétique

Les travaux de François Jacob, Jacques Monod et André Lwoff, qui leur ont valu le prix Nobel de physiologie ou médecine en 1965, ont démontré l'existence de circuits génétiques se comportant comme les opérateurs logiques fondamentaux à la base de l'électronique (Jacob et al., 2005). En effet, l'opéron lactose se comporte comme un opérateur A NIMPLY B de la logique de Boole. Il parait donc impératif d'être capable de programmer ces réseaux génétiques cellulaires afin d'en comprendre le fonctionnement (English et al., 2021). C'est donc sans surprise que les deux articles fondateurs de la biologie synthétique décrivaient des circuits génétiques synthétiques : le *toggle switch* (Figure 4), un interrupteur génétique contrôlé de façon exogène (Gardner et al., 2000), et le repressilator, un oscillateur génétique autonome (Michael B. Elowitz et Stanislas Leibler, 2000). Ainsi, des

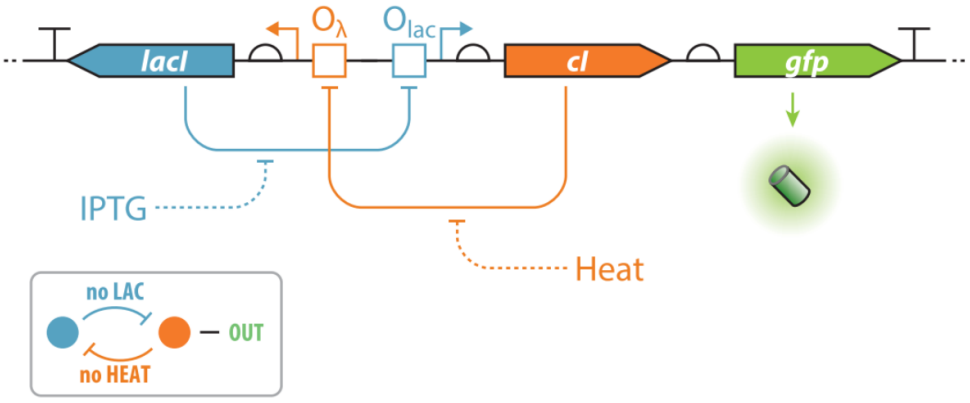

Figure 4. Représentation d'un interrupteur génétique, le toggle switch. *Deux répresseurs (LacI et cI) s'inhibent l'un l'autre par l'intermédiaire de leurs opérateurs apparentés, contrôllant l'output du circuit génétique, l'expression de la GFP* (English et al., 2021).

circuits génétiques de plus en plus complexes sont aujourd'hui littéralement programmés sur ordinateurs et leur efficacité est modélisée avant qu'ils ne soient testés *in vivo* (Nielsen et al., 2016).

1.2.2.2 Génomique synthétique

L'obtention d'un génome entièrement synthétique est un des succès de la biologie de synthèse. Cela permet de répondre à des questions fondamentales comme : est-ce qu'un génome défini une espèce ? quel est le nombre minimal de gènes pour obtenir une cellule viable ? En outre, cela permet également de disposer d'un châssis dont on peut contrôler intégralement le génome (Wang et al., 2018).

Le premier génome artificiel synthétisé fut celui d'un virus, le poliovrus (Cello et al., 2002). Cependant, la démonstration la plus significative, réalisée en deux étapes, a été la synthèse complète du génome de *Mycoplasma mycoides* (Gibson et al., 2010). Cette étude a permis de montrer qu'un génome est bien ce qui détermine l'espèce car le génome d'un mycoplasme (*capricolum*) a été remplacé par celui d'un autre (*mycoides*), transformant une cellule d'une espèce en une autre. La même équipe a ensuite utilisé ce génome artificiel pour le réduire jusqu'au minimum possible. Après de plusieurs cycles de D/B/T/L, ils ont réussi à obtenir le premier génome minimal d'une cellule capable de se diviser (Figure 5) (Hutchison et al., 2016). Cet exploit a permis de répondre à la question « quel est le nombre minimal de gènes strictement suffisant pour qu'une cellule soit capable de se diviser ». Pour ce mycoplasme, la réponse semble être 473 gènes. De façon surprenante, parmi ce faible nombre de gènes, plus d'un tiers (149) sont de fonction inconnue.

D'autres initiatives ont ensuite vu le jour, telles que le projet SC2.0, initié par Jef Boeke et Srinivasan Chandrasegaran, visant au redesign et à la construction d'un génome synthétique de la levure *Saccharomyces cerevisiae*. Ils ont en particulier choisi *a priori* d'enlever du génome de *S. cerevisiae* tous les introns et les télomères naturels (remplacés par des télomères artificiels) ou encore de déplacer les gènes des ARNs de transfert vers un nouveau chromosome (car connus pour provoquer de l'instabilité génomique). L'obtention de chromosomes synthétiques chez un eucaryote permet également d'adresser des questions concernant l'organisation des chromosomes linéaires (Richardson et al., 2017). Parmi les autres initiatives, nous pouvons citer des épisomes artificiels chez la diatomée *Phaeodactylum tricornutum* (Karas et al., 2015), des chromosomes artificiels chez *Homo*

sapiens (Kouprina et al., 2018), ou encore l'initiative *Human Genome Project Write* visant à synthétiser un génome humain complet (Boeke et al., 2016).

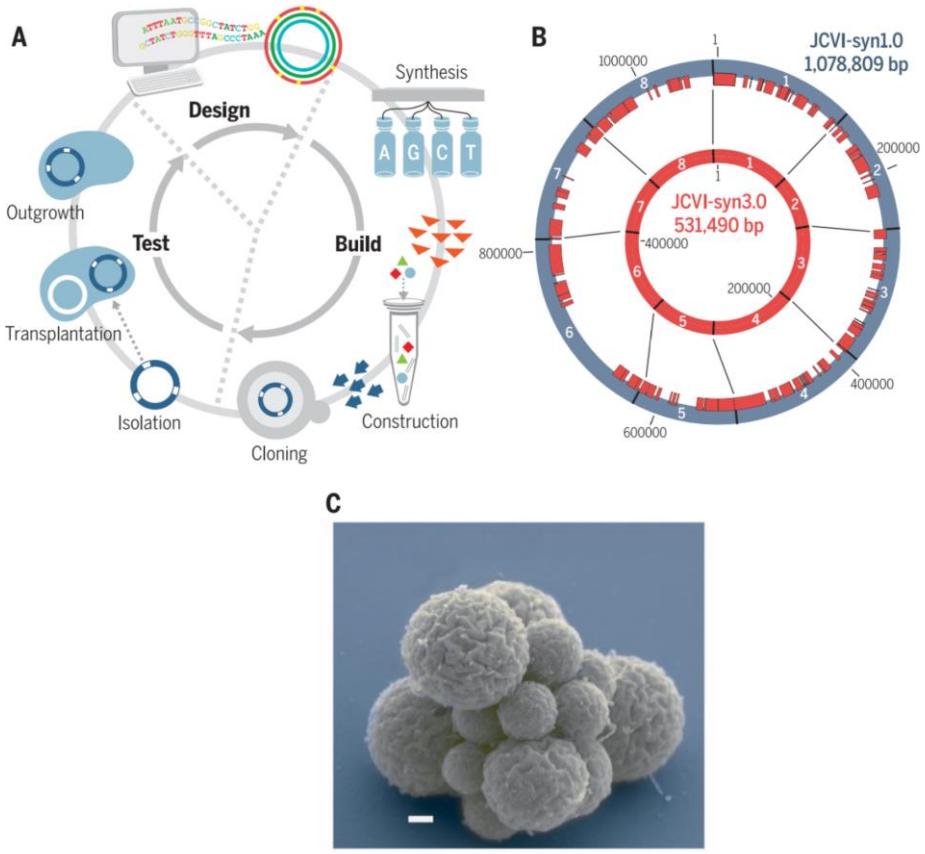

Figure 5. Quatre cycles de Design-Build-Test ont permis de produire JCVI-syn3.0. (A) Le cycle de conception du génome, de construction au moyen de la synthèse et du clonage dans la levure, et de test de la viabilité du génome. Après chaque cycle, l'essentialité des gènes est réévaluée par mutagénèse par transposon globale. (B) Comparaison de JCVI-syn1.0 (cercle bleu extérieur) avec JCVI-syn3.0 (cercle rouge intérieur), montrant la division de chacun en huit segments. Les barres rouges à l'intérieur du cercle extérieur indiquent les régions conservées dans JCVI-syn3.0. (C) Un groupe de cellules JCVI-syn3.0 montrant des structures sphériques de tailles variables (barre d'échelle : 200 nm). (Hutchison et al., 2016).

D'autres initiatives ont ensuite vu le jour, telles que le projet SC2.0, initié par Jef Boeke et Srinivasan Chandrasegaran, visant au redesign et à la construction d'un génome synthétique de la levure *Saccharomyces cerevisiae*. Ils ont en particulier choisi *a priori* d'enlever du génome de *S. cerevisiae* tous les introns et les télomères naturels (remplacés par des télomères artificiels) ou encore de déplacer les gènes des ARNs de transfert vers un nouveau chromosome (car connus pour provoquer de l'instabilité génomique). L'obtention de chromosomes synthétiques chez un eucaryote permet également d'adresser des questions concernant l'organisation des chromosomes linéaires (Richardson et al., 2017). Parmi les autres initiatives, nous pouvons citer des épisomes artificiels chez la diatomée *Phaeodactylum tricornutum* (Karas et al., 2015), des chromosomes artificiels chez *Homo sapiens* (Kouprina et al., 2018), ou encore l'initiative *Human Genome Project Write* visant à synthétiser un génome humain complet (Boeke et al., 2016).

1.2.2.3 Ingénierie métabolique

Même si l'ingénierie métabolique existe depuis l'avènement des biotechnologies grâce à la biologie moléculaire, l'application systématique des principes de l'ingénierie par la biologie synthétique (*cf.* 1.2.1) a bouleversé ce domaine (Endy, 2011). Cette discipline vise à faire produire à un châssis choisi une (des) molécule(s) d'intérêt que ce châssis ne produit pas naturellement à l'aide de circuits génétiques synthétiques.

L'exemple le plus cité est souvent la synthèse de l'artémisinine, un médicament antipaludique dont la découverte a valu le prix Nobel de Médecine à Tu Youyou en 2015. La plante *Artemisia annua* produit cette molécule mais sa culture ralentit la production d'artémisinine (Mark Peplow 2016). L'équipe de Jay Keasling a donc greffé une partie de sa voie de biosynthèse au métabolisme de la bactérie *Escherichia coli* (Martin et al., 2003) puis de la levure *S. cerevisiae* (Figure 6) (Ro et al. 2006).

L'utilisation de la biologie pour produire des molécules d'intérêt permet également de viser un objectif de réduction de la production de CO_2. Par exemple, il existe la possibilité de faire produire du ciment

par des microorganismes. Les émissions globales de CO_2 produites par cette industrie pourraient donc être réduite (Lezzi et al., 2019). D'autre part, il existe aussi des biomatériaux produits *via* la biologie de synthèse comme des textiles, issus de la production de soie d'araignée produite chez différents organismes (Poddar et al., 2020).

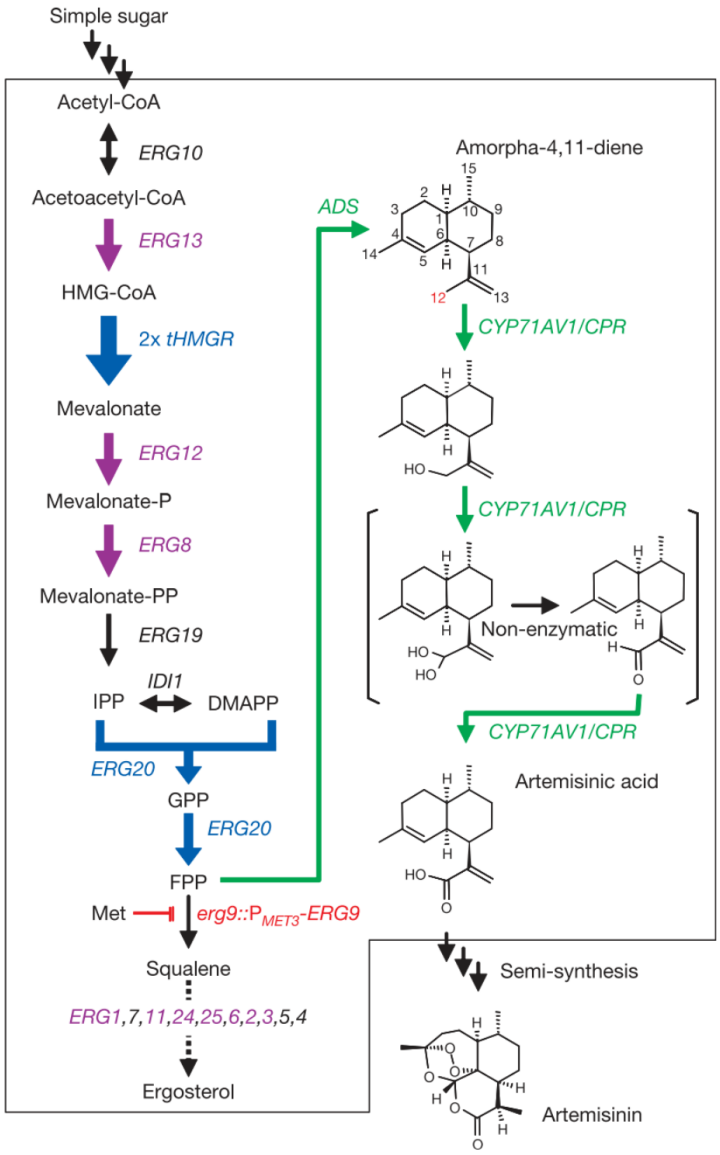

Figure 6. Représentation schématique de la voie de biosynthèse de l'acide artémisinique dans la souche EPY224 de S. cerevisiae exprimant CYP71AV1 et CPR. Les gènes de la voie du mévalonate chez S. cerevisiae *qui sont directement surexprimés sont indiqués en bleu ; ceux qui sont*

indirectement régulés par l'expression de upc2-1 sont en violet ; et la ligne rouge indique la répression de ERG9 dans la souche EPY224. Les intermédiaires de la voie IPP, DMAPP et GPP sont définis comme étant respectivement le pyrophosphate d'isopenténylе, le pyrophosphate d'allyle diméthylique et le pyrophosphate de géranyle. Les flèches vertes indiquent la voie biochimique menant du farnesyl pyrophosphate (FPP) à l'acide artémisinique, qui a été introduit dans S. cerevisiae *à partir d'*A. annua*. Les trois étapes d'oxydation convertissant l'amorphadiène en acide artémisinique par CYP71AV1 et CPR sont représentées* (Ro et al., 2006).

De nombreux exemples existent aussi dans l'agro-alimentaire où des colorants, conservateurs et enzymes sont produits *via* des bactéries ou des levures. Dans le domaine de la cosmétique, certaines huiles, arômes et parfums ne sont plus issus de plantes cultivées en champs, mais de microorganismes cultivés en bioréacteurs (Moses et Goossens, 2017; Moses et al., 2017).

1.2.2.4 Applications médicales

De nombreuses autres applications comme la synthèse d'anticorps, le développement de nouvelles thérapies, jusqu'au développement de tissus en laboratoire sont des domaines très actifs de recherche dans le secteur médical (Rosales-Mendoza et al., 2012; Rooke, 2013; Way et al., 2014). On peut en particulier citer les thérapies par CAR-T cell (Chimeric Antigen Receptor) qui sont une des pistes privilégiées dans la lutte contre le cancer. En effet, des récepteurs de lymphocytes T ont été modifiés afin qu'ils puissent reconnaitre spécifiquement des épitopes présents uniquement à la surface de cellules cancéreuses. Cela permet de diriger l'activation du système immunitaire directement contre ces cancers (Gross et Eshhar, 2016). Ces thérapies ont aussi été couplées à des circuits logiques permettant de mieux en contrôler l'activité (Meng et Ellis, 2020).

1.2.2.5 Stockage numérique sur ADN

Enfin, nous pouvons citer un cas particulier d'application de la biologie synthétique à l'informatique.

Le monde de l'informatique connait aujourd'hui une crise des données.

En effet, nos supports de stockage sont aujourd'hui insuffisants pour stocker les données que nous générons. De plus, ils sont fragiles, volumineux et énergivores (pour leur production, fonctionnement et maintenance) (Rapport de l'Académie des technologies, 2020).

Une solution possible apportée par la biologie de synthèse est de stocker ces données numériques sur de l'ADN. Ce stockage moléculaire est robuste, extrêmement compact et ne nécessite pas d'énergie pour sa conservation (dans des conditions appropriées). La première démonstration de cette technologie a été réalisée en 2012 par l'équipe de George Church (Church et al, 2012) et elle continue depuis d'être améliorée par un certain nombre d'acteurs, la plupart réunis au sein de la *DNA Data Storage Alliance* (https://dnastoragealliance.org/). En particulier, un de ces acteurs est la start-up Biomemory née au sein de notre laboratoire (www.biomemory.com). Contrairement aux autres acteurs du domaine, Biomemory stocke l'information numérique sur des grandes molécules d'ADN et non pas des oligonucléotides. Pour démontrer la faisabilité de leur méthodologie, ils ont encodé deux textes fondateurs de la révolution française sur ADN, la déclaration des droits de l'homme et du citoyen ainsi que la déclaration des droits de la femme et de la citoyenne d'Olympe de Gouges. Ces textes ont été officiellement déposés aux Archives Nationales en Novembre 2021 (Figure 7).

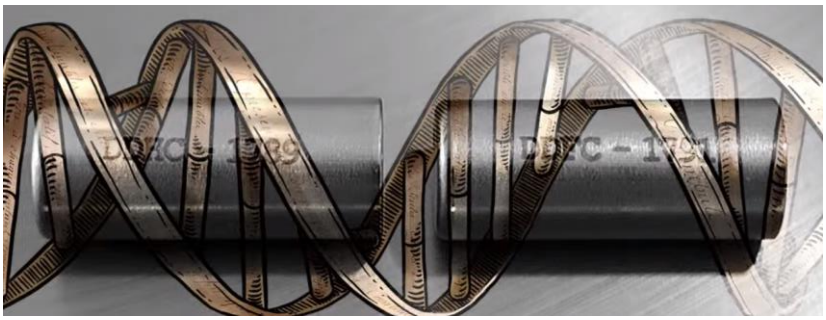

Figure 7. Dessin réalisé par Jeanne Le Peillet illustrant les capsules utilisées par la start-up Biomemory pour stocker l'ADN contenant l'information numérique.

A gauche la capsule DDHC 1789 contient la Déclaration des droits de l'homme et du citoyen, à droite la capsule DDFC 1791 contient la Déclaration des droits de la femme et de la citoyennne.

1.2.2.6 Vers de nouveaux châssis

De nos jours la majorité des projets en biologie synthétique utilisent des levures et des bactéries qui sont utilisées dans des bioraffineries. Ces installations permettent de produire des médicaments, des parfums et d'autres molécules. Pour la bioproduction, les châssis, c'est-à-dire les organismes dans lesquels on conçoit, construit et teste les systèmes biologiques, sont peu nombreux (Adams, 2016). Aussi, une partie de la communauté de la biologie synthétique plaide en faveur de l'utilisation de nouveaux châssis de production.

Ainsi, une partie de l'utilisation des sols pour l'agriculture sert à produire de la biomasse (glucose et autre sucres simples) afin de nourrir les châssis hétérotrophes de bioproduction. Face à la diminution prévue de nos capacités de production alimentaire dans un futur proche, en raison du réchauffement climatique et de la baisse des rendements, ces besoins en biomasse risquent d'entrer en compétition avec la production agricole pour les terres arables (Long et al., 2015).

Dans cette perspective, une alternative à ce problème consisterait à recourir à des microalgues comme châssis car elles ne nécessitent pas de matière organique ni de terres arables pour croitre et donc produire des biomolécules d'intérêt.

1.3 *Chlamydomonas reinhardtii* – Organisme modèle

Etant donné leur capacité à utiliser la photosynthèse pour augmenter leur biomasse ainsi que leur croissance rapide, comparativement aux plantes terrestres, les microalgues apparaissent comme de bons châssis pour la biologie de synthèse (Vavitsas et al., 2019).

Parmi la très grande diversité de microorganismes photosynthétiques, certaines espèces ont été choisies comme modèles. On peut citer par exemple *Synechococcus* et *Synechocystis* chez les cyanobactéries, *P. tricornutum* chez les diatomées, *Chlorella vulgaris* et *C. reinhardtii* chez les algues vertes (Vavitsas et al., 2021).

Depuis les années 1960, *Chlamydomonas reinhardtii* est utilisé pour de nombreuses études sur la photosynthèse, la biologie du chloroplaste, la structure et la fonction des cils, le contrôle du cycle cellulaire, ou

encore la signalisation par la lumière (Harris, 2001; Salomé et Merchant, 2019).

Chlamydomonas reinhardtii est un organisme phototrophe eucaryote unicellulaire (Figure 8). Son appareil photosynthétique est très similaire à celui des plantes terrestres. Des collections de mutants sont disponibles (http://chlamystation.free.fr/index.php), dont la plus complète, la banque CLiP (Chlamydomonas Library Insertion Project), a été obtenue récemment par mutagénèse insertionnelle (Li et al., 2015, 2019), comme cela a déjà été fait chez *Arabidopsis thaliana*. Ses génomes (mitochondrial, chloroplastique et nucléaire) ont été séquencés et annotés, et sont transformables (Gallaher et al., 2018; Craig et al., 2023). Elle possède une grande plasticité phénotypique et est reconnue comme GRAS (*Generally Reconized As Safe*) (Wollman et al., 1994). Sa génétique et sa physiologie sont bien connues et elle est capable de croitre en présence d'une source de carbone réduite (acétate) ce qui permet d'obtenir des mutants viables de gènes photosynthétiques, ce qui est un défi particulier chez les plantes terrestres (Merchant, 2019).

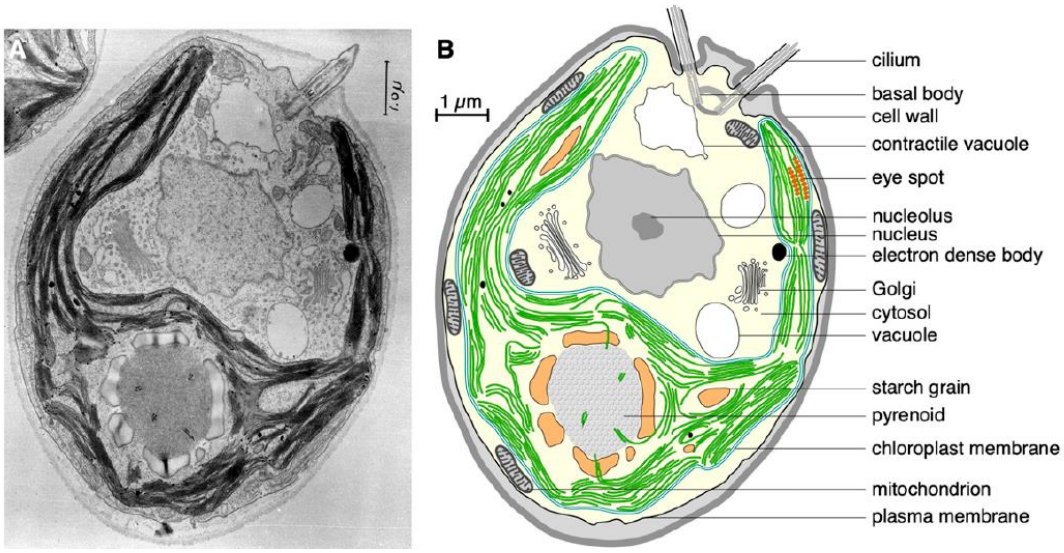

Figure 8. Anatomie de Chlamydomonas reinhardtii. *Tiré de* (Merchant, 2019). *(A) Micrographie électronique à transmission (TEM) d'une cellule. Publié à l'origine par Ohad et al.* (Ohad et al., 1967). *(B) Dessin d'une cellule de* C. reinhardtii *d'après l'image de TEM en (A).*

Chlamydomonas commence à être utilisé comme châssis de bioproduction pour des applications industrielles potentielles et a déjà été utilisé pour produire diverses molécules d'intérêts notamment des terpènes (Yahya et al., 2023), pigments (Amendola et al., 2023), lipides (Kong et al., 2019), et différentes protéines d'intérêt pharmaceutique (Yan et al., 2016).

Ces caractéristiques font de *C. reinhardtii* un choix judicieux pour la biologie de synthèse. De nombreux outils ont été développés offrant de nombreuses possibilités d'ingénierie (Scaife et al., 2015; Kong et al., 2019; Vavitsas et al., 2019; Schroda and Remacle, 2022). Nous pouvons citer par exemple l'édition du génome *via* CRISPR/Cas9 (Ferenczi et al., 2017; Greiner et al., 2017; Kim et al., 2020), ou bien le kit de Modular Cloning (*cf.* 1.4) généré par un consortium de scientifiques. Ce dernier a été initié et mené au sein de mon laboratoire avant mon arrivée. Depuis, le nombre de briques géniques n'a fait qu'augmenter pour passer de 119 briques à plus de 300 (Crozet et al. 2018).

1.4 Modular Cloning (MoClo)

Comme mentionné précédemment, la standardisation est un des points essentiels dans les approches de biologie de synthèse car elle permet de concevoir et de construire plus aisément et plus rapidement les systèmes voulus. Au cours des années, différents standards, et souvent leurs méthodologies associées de construction de circuits génétiques, ont été développés (Casini et al., 2015). Les biologistes ont sélectionné au cours du temps une méthodologie et son standard, le *Modular Cloning* (MoClo) (Weber et al., 2011). Le MoClo est basé sur la technologie du *Golden Gate cloning* qui consiste en l'utilisation d'enzyme de restriction de type IIS (Engler et al., 2008). Ces endonucléases ont la particularité de cliver l'ADN double brin cible en dehors de leur site de reconnaissance, laissant ainsi des extrémités saillantes dont la séquence est variable et donc pouvant être choisies (les sites de fusion). Cela permet donc un clonage directionnel et sans cicatrice. De plus, à l'aide d'un design approprié, la partie d'intérêt de la molécule clivée ne contient plus les sites de reconnaissance de l'enzyme de restriction, ce qui permet d'obtenir un produit final de ligation insensible à cette enzyme (Figure 9). Ces particularités font que le clonage *Golden Gate* permet de réaliser une digestion avec une

seule enzyme et qui peut être effectuée en même temps que la ligation (Engler et al., 2008).

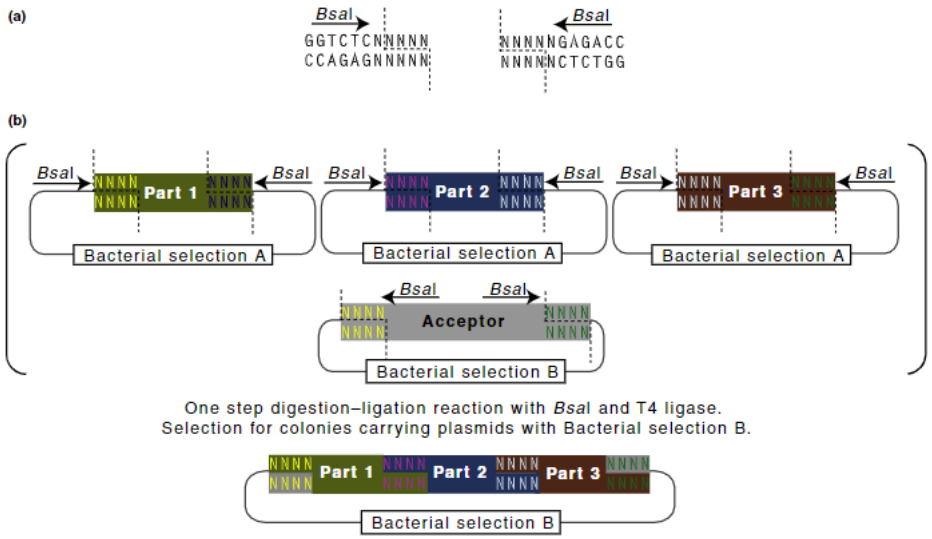

Figure 9. Représentation schématique du système de clonage modulaire basé sur l'utilisation d'une enzyme de restriction de type IIS (a) Les enzymes de restriction de type IIS telles que BsaI sont directionnelles, clivant en dehors de leurs séquences de reconnaissance non palindromiques. (b) Les squelettes plasmidiques flanqués d'une paire de sites de reconnaissance peuvent être assemblés en une seule réaction de digestion-ligature dans un plasmide accepteur (Patron et al., 2015).

En déterminant les enzymes à utiliser et les séquences des sites de fusion en fonction de leur position dans le construit final, et en répétant ce choix pour les différents niveaux de construction génétique (brique génique, unité de transcription, construit multigénique), on obtient un standard. Ce standard permet de construire en seulement 3 étapes, en utilisant au total deux enzymes (*Bsa*I et *Bbs*I) et une ligase, des construits de plusieurs gènes, chacun avec des briques potentiellement différentes (Figure 10). C'est cette standardisation extrême du *Golden Gate cloning* que l'équipe de Sylvestre Marillonet a appelé le MoClo (Weber et al., 2011)

Il est important de noter que le standard pour assembler des briques en modules (niveau 0 à 1) est différent de celui pour assembler des modules en dispositif (niveau 1 à M/2) (Weber et al., 2011; Werner et al., 2012).

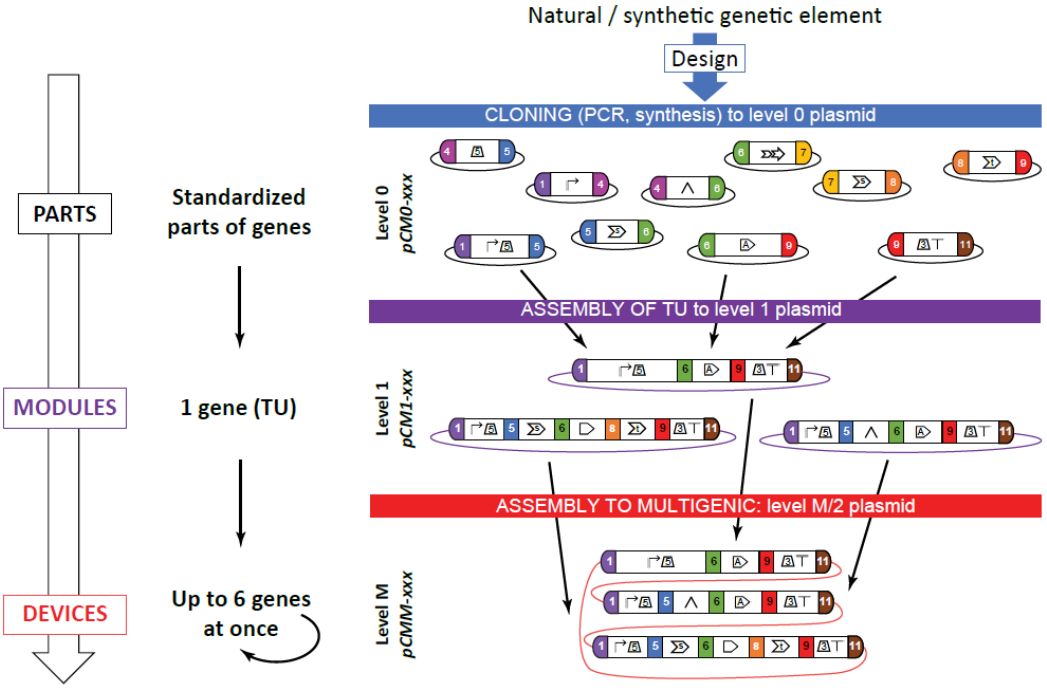

Figure 10. Processus d'assemblage MoClo reflétant la hiérarchie d'abstraction. Figure tirée de (Crozet et al. 2018). *La syntaxe utilisée est l'originale du MoClo* (Weber et al., 2011; Patron et al., 2015). *Après la conception d'une partie de gène contrôlée* in silico *pour une compatibilité totale jusqu'à l'assemblage de niveau M, la brique est clonée avec BpiI (équivalent à BbsI) dans le plasmide de niveau 0 approprié (résistance bactérienne à la spectinomycine). Après un contrôle de qualité (QC) par restriction et séquençage, le clone résultant est enregistré dans la base de données des briques en tant que niveau 0. Pour générer l'unité transcriptionnelle (TU) souhaitée, les briques compatibles sont assemblées avec BsaI dans le plasmide de niveau 1 approprié (résistance bactérienne à l'ampicilline). Après un contrôle de qualité par restriction, le clone est enregistré en tant que niveau 1 dans la base de données des modules. Enfin, pour assembler un dispositif, jusqu'à 6 modules à la fois sont assemblés, à l'aide de l'end-linker correspondant, par BpiI dans un plasmide de niveau M ou 2 (résistance bactérienne à la spectinomycine ou à la kanamycine, respectivement). Après un contrôle qualité par restriction, le clone est enregistré en tant que niveau M ou 2 dans la base de données des dispositifs. Un nouvel*

assemblage à partir de ce dispositif peut être effectué pour assembler d'autres modules au dispositif. Les briques géniques sont représentées dans le code visuel SBOL2.0. Les sites de fusion standardisés permettant le passage du niveau 0 à 1 sont représentés par des parties colorées et un numéro, correspondant au standard MoClo révisé (Patron, 2014). *Les sites de fusion standardisés permettant le passage du niveau 1 à M/2 ne sont pas représentés dans un souci de clarté.*

Le standard au niveau des briques (du niveau 0 à 1) peut dépendre du châssis utilisé, par exemple à cause du biais de codon (codons rares présents dans les sites de fusion, pourcentage de GC, etc.). Le standard original est celui présenté en Figure 11A. Il a ensuite été révisé et complété en 2014 pour aboutir au standard appelé Plant MoClo (Patron, 2014) présenté en Figure 11B.

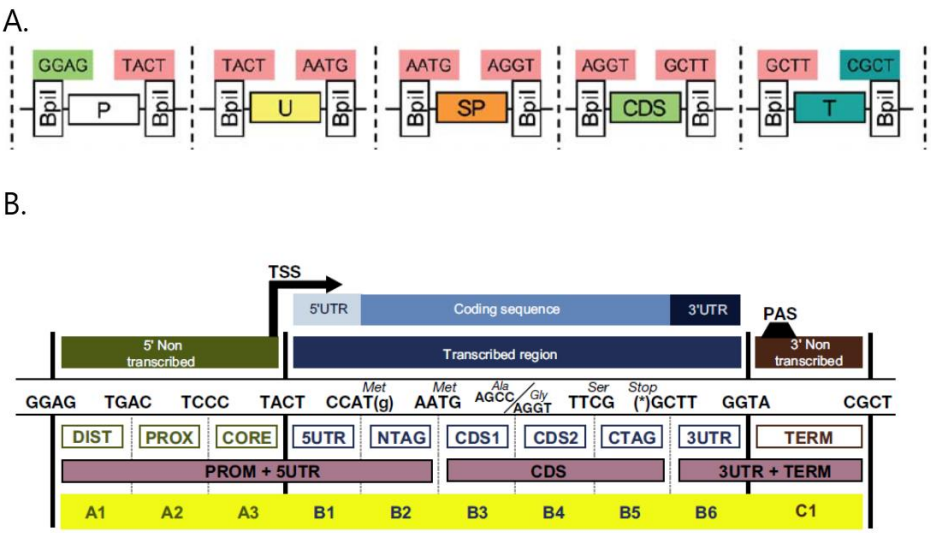

Figure 11. Standard original du MoClo et complété en 2015.

A. Standard original du Modular Cloning (Weber et al., 2011a). *Une unité de transcription est découpée en 5 positions standardisées : P : promoteur, U : 5'UTR, SP : Signal Peptide, CDS : Coding Sequence, T : 3'UTR et Terminateur.*

B. Standard du Plant MoClo (Patron et al., 2015a). *L'unité de transcription est maintenant partagée en 10 positions à partir du même standard qu'en A. : A1 à A3 : promoteur (Distal, Proximal, Core), B1 : 5'UTR, B2 : N-terminal Tag, B3 : CDS 1, B4 : CDS2, B5 : C-terminal Tag, B6 : 3'UTR, C1 : Terminateur. Les positions B sont toutes transcrites.*

Le MoClo est donc un outil formidable mais il demande un effort initial de la communauté car la banque initiale de briques compatibles - domestiquées- doit être générée. En effet, pour être assemblées correctement, les séquences ne doivent pas contenir de sites de reconnaissance des enzymes *Bbs*I et *Bsa*I et être clonées dans un plasmide donneur de niveau 0 avec les sites de fusion adéquats à la fonction de cette brique, et donc à la ou les positions utiles dans le standard (Figure 11).

Pour pouvoir mener des approches de biologie synthétique chez les microalgues, les outils standardisés manquaient. En effet, chaque brique devait être conçue et clonée à chaque fois en utilisant des enzymes de restriction classiques. Les briques n'étaient pas partagées par défaut par tous les laboratoires, et étaient donc refaites par chaque équipe, gaspillant du temps et des ressources.

Ce constat a été fait par la communauté de scientifiques européens travaillant sur *C. reinhardtii*. Un consortium composé de 8 équipes de 5 pays (Royaume-Uni, Espagne, Allemagne, Danemark et France) a généré un kit de clonage modulaire contenant les briques de bases nécessaires aux travaux de recherche chez *C. reinhardtii*. Le contenu de ce kit, fort de 119 briques à sa publication, permet de réaliser toutes les constructions communes (Figure 12). Parmi les différentes briques développées il y a les marqueurs de résistance aux antibiotiques, la zéomycin, la kanamycine, la spectinomycine, la paromycine, l'hygromycine ainsi que la blasticidine, dernière brique générée et à l'élaboration de laquelle j'ai participé au cours de ce travail de thèse.

Avec les outils rendant possible les approches de synthèse chez *C. reinhardtii*, il devient ainsi possible d'appliquer cette démarche à notre sujet d'étude, la photosynthèse.

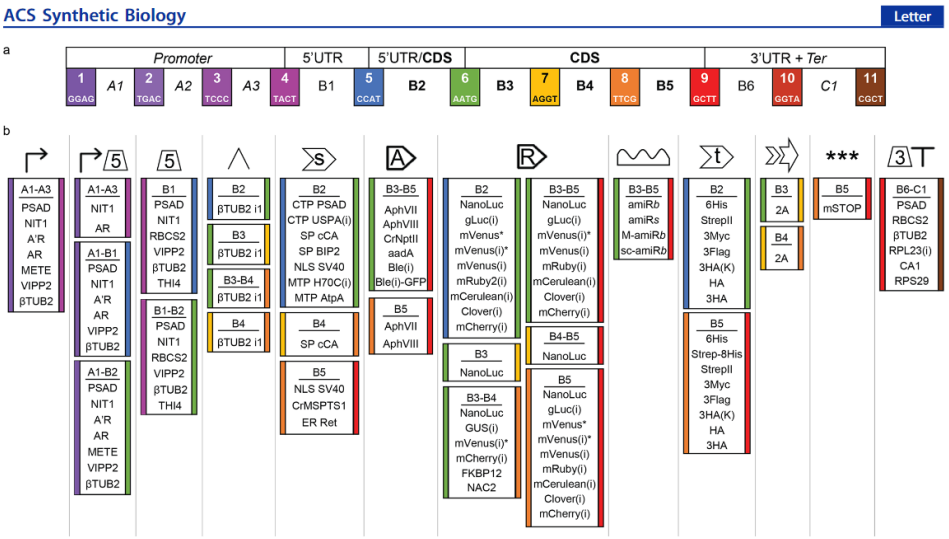

Figure 12. Représentation des différentes biobriques standardisées du Moclo chez Chlamydomonas (Crozet et al, 2018).

a- Standard utilisé pour le kit MoClo Chlamydomonas (identique à celui présenté en figure 11A). Le code couleur indique quel site de fusion est utilisé.

b. Liste des 119 briques composant le kit MoClo Chlamydomonas à sa publication en 2018. Les briques sont représentées en format SBOL 2.0 selon leur fonction.

1.5 Photosynthèse

Les acides nucléiques, les lipides, les glucides et les protéines sont les éléments fondamentaux qui composent le vivant. Ces éléments ont en commun qu'ils possèdent un squelette de carbone. La vie sur Terre s'est construite à partir du carbone. La photosynthèse est le mécanisme majoritaire capable de capturer le CO_2 atmosphérique, ou solubilisé dans l'eau, afin de construire de la matière organique (Matthew Johnson, 2016).

La photosynthèse est apparue chez un ancêtre des cyanobactéries. Ensuite, un phénomène d'endosymbiose s'est produit dans un organisme proto-eucaryote donnant naissance au chloroplaste du phylum *Viridiplantae*. Des événements d'endosymbiose secondaire ont eu lieu dans d'autres phyla des eucaryotes (Burki et al., 2007).

Dans ce processus nous pouvons différencier deux phases : 1) l'énergie lumineuse est convertie en énergie chimique qui va majoritairement être utilisée pour 2) assimiler du carbone inorganique (CO_2) en carbone organique (triose-P). Ce carbone organique est ensuite utilisé dans un ensemble de voies métaboliques pour soutenir la croissance et le développement de l'organisme. La phase dite « photochimique » se déroule dans les membranes des thylacoïdes alors que la phase « biosynthétique » a lieu dans le stroma chloroplastique chez les eucaryotes et dans le cytoplasme chez les cyanobactéries.

La phase photochimique est réalisée par la chaine photosynthétique de transfert des électrons (PETC) qui a pour rôle de capter l'énergie des photons *via* les chlorophylles qui changent alors d'état (stable à excité). La désexcitation de la chlorophylle va produire de l'énergie sous trois formes possibles : 1) par l'émission de chaleur (le Non-Photochemical Quenching, NPQ), 2) par l'émission d'un photon (fluorescence), ou 3) par photochimie (séparation de charge stable) associée à l'oxydation de l'eau qui produit du dioxygène, des électrons et des protons (Matthew Johnson, 2016). Les électrons vont pouvoir être transférés dans la membrane des thylacoïdes par des réactions successives d'oxydo-réduction entre les différents éléments de la chaine de transfert des électrons (Figure 13). Cette suite de réactions s'accompagne d'une translocation de protons à travers ces membranes, générant un gradient de protons (Matthew Johnson, 2016).

La *Ferredoxin NADP*$^+$ *reductase* permet à partir de ce transfert d'énergie jusqu'à l'accepteur final, la ferrédoxine, de régénérer du NADPH à partir de $NADP^+$ et de protons. L'ATP synthase quant à elle génère de l'ATP à partir d'ADP et de phosphate inorganique grâce à l'énergie du gradient de protons généré (Matthew Johnson, 2016).

Les thiorédoxines (TRX) sont des petites oxydoréductases régulant le métabolisme primaire, en particulier le cycle de Calvin-Benson Bassham. Elles seront abordées dans la partie 1.5.2. Elles sont réduites par la même source de pouvoir réducteur que celle utilisée pour réduire le NADPH, la ferrédoxine. Cette réaction est catalysée par la *Ferredoxin Thioredoxin Reductase*. Cela permet de lier directement le niveau de réduction du pool de thiorédoxines à l'activité de la PETC.

A.

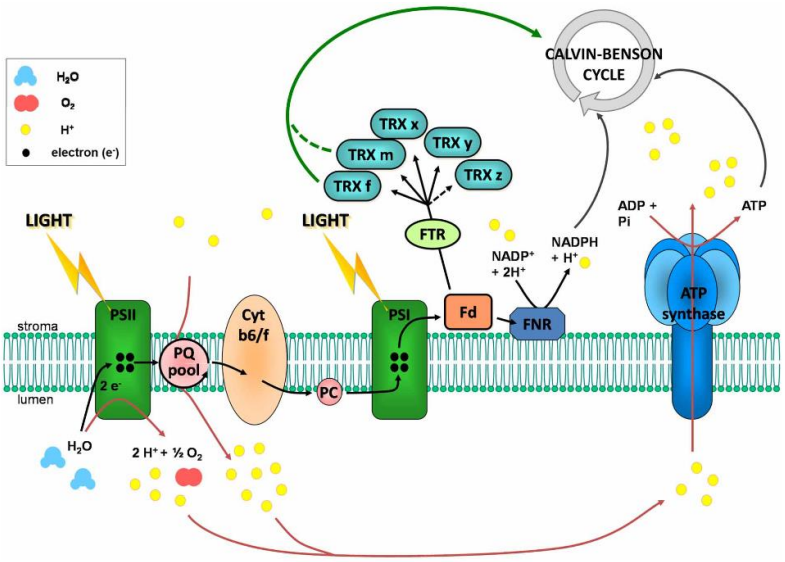

B.

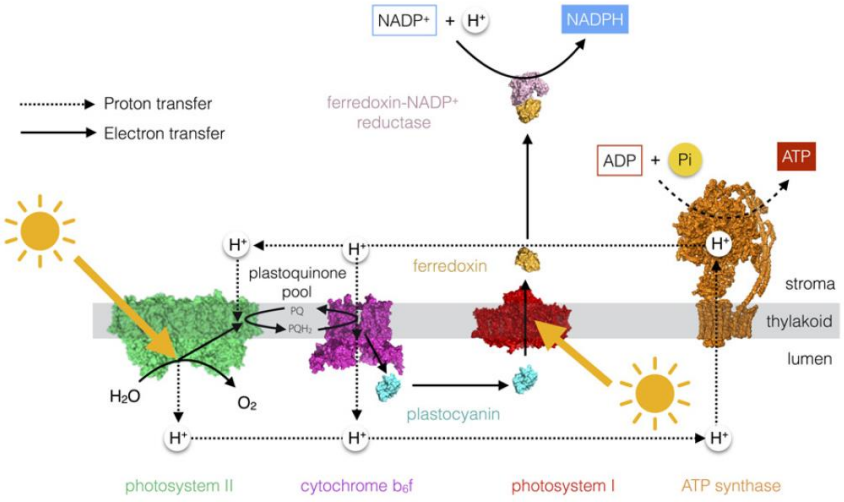

Figure 13. Représentation de la chaine de transfert linéaire des électrons chez un organisme photosynthétique eucaryote.

A. Schéma d'après (Michelet et al., 2013). *PS : Photosystème, PQ : plastoquinone, Cyt : Cytochrome, Fd : Ferrédoxine, FNR : Fd-NADP⁺ Réductase, TRX : Thiorédoxine.*

B. Représentation du transfert d'électron via la chaine de transfert linéaire des électrons avec les structures tridimensionnelles des complexes protéiques la composant (Matthew Johnson, 2016).

L'ATP et le NADPH générés vont être principalement utilisés au cours de la seconde phase de ce processus de photosynthèse, le cycle de Calvin Benson Bassham.

1.5.1 Le cycle de Calvin Benson Bassham

Le cycle de Calvin Benson Bassham (CBBC) a été découvert dans les années 1950 grâce notamment au travail du Pr Calvin, du Dr Benson et du Dr Bassham. Ils ont utilisé une culture de chlorelle injectée dans un tuyau *via* lequel du CO_2 radioactif était injecté et qui finissait sa course dans une solution de méthanol chauffée à 70°C. En analysant les fractions récoltées, cette équipe a pu suivre l'incorporation du carbone radioactif ^{14}C d'un état minéral à un état organique. En analysant les différents sucres marqués, ils ont ainsi pu découvrir le mécanisme de fixation du CO_2 dans la photosynthèse (Bassham et al., 1954).

Cette partie sera développée en détail dans L'article 1 correspondant au le chapitre 8 du Chlamydomonas Sourcebook (3ème édition, 2023) intitulé « *Photoproduction of reducing power and the Calvin-Benson cycle* » dont je suis co-premier auteur.

1.5.2 Article 1

1.5.2.1 Résumé du chapitre

Pendant mon travail de thèse, j'ai eu l'opportunité de participer à la rédaction du chapitre 8 du Chlamydomonas Sourcebook (3ème édition, 2023) intitulé « *Photoproduction of reducing power and the Calvin-Benson cycle* ». Le *Chlamydomonas Sourcebook*, publié en 1989, 2009 et 2023, rassemble toutes les connaissances actuelles sur Chlamydomonas et constitue donc une référence pour notre communauté.

Ce chapitre traite en détail de la photoproduction du pouvoir réducteur chez *C. reinhardtii*, et donc de l'accepteur final de la PETC, la ferrédoxine. Celle-ci sert de donneur de pouvoir réducteur pour réduire le NADPH mais aussi les TRX. Après une description de ce système, les TRXs sont présentées ainsi que leurs fonctions connues, en particulier celle de réguler le CBBC dans le chloroplaste. Le CBBC

est ensuite décrit, enzyme par enzyme, y compris au niveau structural, chez *C. reinhardtii*. En particulier, la régulation des enzymes du CBBC par les TRX, est détaillée. Le rôle central du NADPH, y compris dans la détoxication des *Reactive Oxygen Species* (ROS), est ensuite discuté. Enfin, les perspectives d'amélioration de la photosynthèse sont abordées, avec un focus particulier sur les approches de biologie de synthèse. Cette section présente les outils d'ingénierie développés pour Chlamydomonas, ainsi que son utilisation comme châssis afin de mieux comprendre et possiblement d'améliorer la fixation du carbone.

Mon travail de thèse s'inscrit plus spécifiquement dans les sections traitant du CBBC et de la biologie de synthèse.

1.5.2.2 Photoproduction of reducing power and the Calvin-Benson cycle

Chapter 8

Photoproduction of reducing power and the Calvin-Benson cycle

Théo Le Moigne[1,2,3,*], Nicolas D. Boisset[1,2,3,*], Félix de Carpentier[1,2,3], Pierre Crozet[1,2,4], Antoine Danon[1,2], Julien Henri[1,2], Christophe H. Marchand[1,2], Stéphane D. Lemaire[1,2] and Xenie Johnson[5]

[1]Sorbonne Université, CNRS, UMR7238, Institut de Biologie Paris-Seine, Laboratoire de Biologie Computationnelle et Quantitative, Paris, France, [2]Sorbonne Université, CNRS, UMR8226, Institut de Biologie Physico-Chimique, Laboratoire de Biologie Moléculaire et Cellulaire des Eucaryotes, Paris, France, [3]Faculty of Sciences, Doctoral School of Plant Sciences, Université Paris-Saclay, Saint-Aubin, France, [4]Sorbonne Université, Polytech-Sorbonne, Paris, France, [5]Aix Marseille Univ., CEA, CNRS, Biosciences and Biotechnology Institute Aix-Marseille, Saint Paul-Lez-Durance, France

8.1 Introduction to linear electron flow, water to NADPH

Photosynthesis proceeds from the capture of light energy to the conversion of this energy into high-energy chemical bonds, adenosine triphosphate (ATP) and reducing power, nicotinamide adenine dinucleotide phosphate (NADPH). *Chlamydomonas* grown in the absence of acetate relies on photosynthesis as the only source of ATP and NADPH, and the majority of this goes toward the Calvin-Benson cycle (CBC) and thus CO_2 fixation. Linear photosynthetic electron flow denotes the transfer of electrons from H_2O, the primary electron donor that is oxidized at the level of Photosystem II (PSII), to a terminal electron acceptor nicotinamide adenine dinucleotide phosphate ($NADP^+$) that is reduced at the acceptor side of Photosystem I (PSI). Plastoquinones, the cytochrome b_6f complex and plastocyanin act as intersystem electron carriers between PSII and PSI in the thylakoid membrane. The stromal electron carriers, including flavodiiron proteins, thioredoxins, and ferredoxins, exert control on intersystem electron transport, which helps optimize electron transfer in relation to inputs (light) and outputs (metabolites). This assures a tight integration of the electron transfer reactions with downstream metabolic processes, principally the CBC, in the chloroplast (Vol 2, Chapter 18 for details).

8.2 Ferredoxins orchestrate electron transfer downstream of Photosystem I

After the light reactions, carried out at the level of the thylakoid membranes, electrons from the stromal ridge of PSI (constituted by PsaC, PsaD, and PsaE, which harbor the Fe-S redox clusters F_X, F_A, and F_B; see Chapter 16) are transferred to Ferredoxin (FDX) in the chloroplast stroma. Marco and coworkers reported on a PsaC K35D mutant in which FDX binding to PSI was abolished (Marco et al., 2018; Marco, Elman, & Yacoby, 2019). Numerous biological processes are based on redox reactions that use electron carriers such as the FDXs, which are small (10–11 Da), soluble Fe-S cluster proteins that are widely distributed in microorganisms, plants, and animals. Indeed, they serve as low potential, single electron carriers with E_m values ranging from −310 to −455 mV. These electrochemical properties allow them to operate as electron donors in a multitude of metabolic and signaling pathways (Hanke & Mulo, 2013). FDXs play a central role in chloroplast metabolism. Once reduced, FDX can transfer electrons to proteins involved in diverse pathways including ferredoxin-$NADP^+$ reductase (FNR) for $NADP^+$ reduction, ferredoxin-thioredoxin reductase (FTR) for the reduction of thioredoxins (TRXs), which provide electrons for antioxidant and signaling functions, sulfite reductase (SiR) for sulfur assimilation, nitrite reductase (NiR) and ferredoxin-dependent glutamate synthetase (GOGAT) for nitrogen assimilation, hydrogenase for hydrogen production under anaerobic conditions (Winkler, Hemschemeier, Jacobs, Stripp, & Happe, 2010), fatty acid desaturases for the biosynthesis of lipids (Yang et al., 2015), and photosynthetic cyclic electron flow via ferredoxin-plastoquinone reductase (Hertle et al., 2013).

*These authors contributed equally.

The *Chlamydomonas* Sourcebook. DOI: https://doi.org/10.1016/B978-0-12-821430-5.00016-X
© 2023 Elsevier Inc. All rights reserved.

The *Chlamydomonas* genome encodes at least 13 FDX genes (Yang et al., 2015), mostly chloroplastic (Table 8.1), among which six FDXs (FDX1-FDX6) have been studied in more detail. The major FDX in *Chlamydomonas* (FDX1, previously named PETF) was initially purified by Paul Levine (Gorman & Levine, 1966). The function of FDXs can be inferred from their expression patterns and their substrate specificities. Under standard growth in the presence of acetate, FDX1 contributes 98% of the total ferredoxin-encoding transcript pool. FDX1 expression is regulated by light, and the circadian clock and the encoded protein is the most efficient electron donor to FNR and FTR. FDX1 is therefore likely the main electron donor for carbon fixation and redox homeostasis (Lemaire, Keryer et al., 1999; Terauchi et al., 2009). In contrast, FDX2 is not regulated by light but by nitrogen sources and is an efficient electron donor to NiR (Hirasawa et al., 2010; Strenkert et al., 2019; Terauchi et al., 2009). FDX2 can also transfer electrons to FNR; however, there is a significant preference for FDX1 (Mosebach et al., 2017), while mutating two residues from the kinetically slower FDX2 confers it with redox properties similar to FDX1 (Boehm et al., 2016). FDX3–6 are reduced in the light but are unable to supply FNR with electrons for the reduction of $NADP^+$ (Boehm et al., 2016). Therefore FDX1–6 exhibit distinct substrate specificities suggesting specialization for allocation of reducing power to specific metabolic pathways. FDX substrate specificities are likely mediated by key residues controlling electrostatic interactions with partner proteins (Boehm et al., 2016; Garcia-Sanchez et al., 1997; Jacquot, Stein, et al., 1997). FDX5 is specifically expressed under dark-hypoxic conditions and copper or sulfur deprivation, but it is not able to reduce hydrogenase, which is preferentially reduced by FDX1 (Jacobs, Pudollek, Hemschemeier, & Happe, 2009; Yacoby et al., 2011). FDX5 appears to be important for hydrogenase maturation, fatty acid desaturation, dark metabolism, maintenance of the thylakoid membrane, and responses to sulfur depletion (Subramanian et al., 2019; Yang et al., 2015). The FDX9

TABLE 8.1 Components of the chloroplast ferredoxin-thioredoxin system.

Name	Gene name	Locus ID (Phytozome 12)	Uniprot	MW (kDa) Pre/mat	Length (AA) Pre/mat
Ferredoxin 1	*FDX1*	Cre14.g626700	A8IV40	13.2 / 9.9	126 / 94
Ferredoxin 2	*FDX2*	Cre16.g658400	A0A2K3CTD8	13.2 / ND	121 / ND
Ferredoxin 3	*FDX3*	Cre06.g306350	Q2HZ24	19.7 / ND	187 / ND
Ferredoxin 4	*FDX4*	Cre07.g334800	Q2HZ23	14.0 / ND	131 / ND
Ferredoxin 5	*FDX5*	Cre17.g700950	Q2HZ22	14.4 / ND	130 / ND
Ferredoxin 6	*FDX6*	Cre03.g183850	Q2HZ21	34.1 / ND	314 / ND
Ferredoxin 7	*FDX7*	Cre01.g006100	A8JFX3	13.7 / ND	133 / ND
Ferredoxin 8	*FDX8*	Cre01.g005600	A0A2K3E509	20.6 / ND	197 / ND
Ferredoxin 9	*FDX9*	Cre12.g487900	A0A2K3D298	10.7 / ND	101 / ND
Ferredoxin 10	*FDX10*	Cre04.g225450	A0A2K3DUL5	14.5 / ND	130 / ND
Ferredoxin 11	*FDX11*	Cre06.g291650	A8J2J6	12.1 / ND	117 / ND
Ferredoxin thioredoxin reductase Catalytic subunit	*FTRC*	Cre03.g193950	A8IWK2	16.0 / 13.1	145 / 116
Ferredoxin thioredoxin reductase Variable subunit	*FTRV*	Cre16.g687294	A8JA70	12.3 / 10.4	113 / 93
Thioredoxin f1	*TRXf1*	Cre01.g066552	Q84XR8	18.2 / 12.6	173 / 115
Thioredoxin f2	*TRXf2*	Cre05.g243050	A0A2K3DSC9	19.9 / 13.2	180 / 116
Thioredoxin m (*aka* CH2)	*TRXm*	Cre06.g269752	P23400	15.1 / 11.6	140 / 106
Thioredoxin x	*TRXx*	Cre01.g052250	Q84XR9	15.8 / 12.8	145 / 116
Thioredoxin y	*TRXy*	Cre10.g446100	Q84XS2	16.7 / 12.9	152 / 115
Thioredoxin z (*aka* CITRX)	*TRXz*	Cre02.g142800	A8J0Q8	19.5 / 13.9	183 / 128
NADPH-dependent thioredoxin reductase C	*NTRC1/ NTR4*	Cre01.g054150	A0A2K3E888	58.9	536

pre, Premature protein MW; *mat*, mature protein MW.

gene is only expressed in the dark and was recently identified as coregulated with hydrogenase genes and may also play some role in hydrogen production (Strenkert et al., 2019). A ferredoxin interactome identified more than 200 putative partner proteins in *Chlamydomonas* (Peden et al., 2013), with 43 potential partners of FDX5 (Subramanian et al., 2019). For a more complete overview of *Chlamydomonas* FDXs, we refer the reader to dedicated reviews (Sawyer & Winkler, 2017; Terashima, Specht, & Hippler, 2011; Winkler et al., 2010). In the present chapter, we will further detail the functions of FDX1 linked to carbon fixation and redox homeostasis that is mediated by FNR and FTR.

8.3 Ferredoxin $NADP^+$ reductase and the NADPH/$NADP^+$ couple

In the light, FDX reduces the FAD containing FNR in two single-electron steps; FNR then transfers the two electrons to $NADP^+$ completing linear electron flow. Under aerobic conditions, the abundance of FNR is equal to that of plastocyanin in *Chlamydomonas*, providing an electron pathway for the reduction of $NADP^+$ (Nikolova, Heilmann, Hawat, Gabelein, & Hippler, 2018). The *Chlamydomonas* genome does not have orthologs of the conserved tethering proteins that allow close interaction of FNR with the thylakoid membranes as found in higher plants. However, a PSI-LHCI-FNR-LHCSR3 complex in cells in state I has been identified (Bergner et al., 2015), and this complex appears to be destabilized in the absence of PGR5/PGRL1 proteins (Mosebach et al., 2017). To facilitate this very close interaction between FNR and PSI, FNR (like FDX) localizes to the PSI stromal ridge, with possible interactions with PsaE, B, F, and at least one LHC1 (Marco et al., 2019).

$NADP^+$ is the major pyridine nucleotide found in the plastid and is considered the final acceptor of electrons issued from H_2O oxidation in oxygenic photosynthesis. Apart from CO_2 fixation, NADPH is required for other plastid-localized processes including tetrapyrrole synthesis, lipid biosynthesis, and detoxification of reactive oxygen species (ROS). As NADPH is the universal electron carrier for photosynthesis and chloroplast metabolism, both the flux and the directionality along these pathways are highly dependent upon the relative concentrations of NADPH and $NADP^+$. However, NADPH rarely accumulates in the light because it is rapidly utilized by these same metabolic reactions. The $NADP^+$/NADPH couple has a low oxidation-reduction potential (E'_0 at pH 7.0 = −320 mV), which makes NADPH a powerful reductant.

$$NADP^+ + H^+ + 2e^- \leftrightarrow NADPH$$

This can also be written as:

$$NADP^+ + 2H^+ + 2e^- \leftrightarrow NADPH + H^+$$

because it shows the 2 hydrogen ions generated as a consequence of water oxidation as well as the electrons that will serve as reductant.

8.4 The ferredoxin-thioredoxin system

8.4.1 Components and function of the ferredoxin-thioredoxin system

The ferredoxin-thioredoxin system, located in chloroplasts, is composed of ferredoxins (FDXs), FTR, and thioredoxins (TRXs) (Fig. 8.1, Table 8.1) (Michelet, Zaffagnini et al., 2013; Zaffagnini et al., 2019). This system converts a light-driven electron signal (photoreduced FDX1) into a thiol signal transmitted by FTR to different isoforms of TRXs. FTR is a thin, flat enzyme that allows docking of FDX on one side and TRX on the other side. It contains a [4Fe-4S] cluster

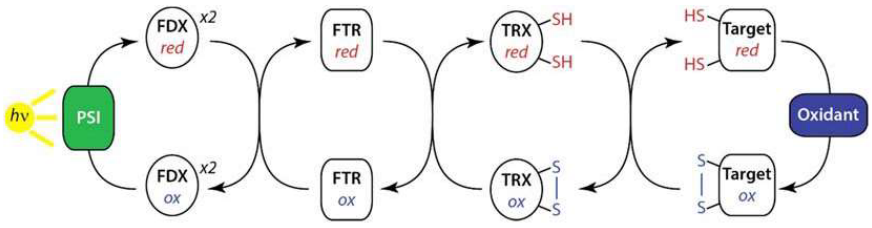

FIGURE 8.1 The ferredoxin/thioredoxin system. *FDX*, ferredoxin; *FTR*, ferredoxin thioredoxin reductase; *PSI*, Photosystem I; *ox*, oxidized; *red*, reduced.

functionally and physically connected with a redox active disulfide (Dai et al., 2007). FTR is heterodimeric, with a highly conserved catalytic subunit of 13 kDa (FTRC) and a variable subunit (FTRV) exhibiting different molecular masses among organisms (Dai, Johansson, Miginiac-Maslow, Schurmann, & Eklund, 2004; Schurmann, 2002). The coexpression of both subunits is required to produce a functional FTR, although the exact function of FTRV remains unknown (Keryer, Collin, Lavergne, Lemaire, & Issakidis-Bourguet, 2004). *Chlamydomonas* FTR, purified in 1990 (Huppe, de Lamotte-Guery, Jacquot, & Buchanan, 1990), is a typical FTRC/FTRV heterodimer with an FTRC of 13 kDa and an FTRV of 10 kDa. The nuclear genome of *Chlamydomonas* contains a single gene encoding each subunit (Table 8.1). The formation of the FDX–FTR complex requires the presence of the negatively charged Glu91 in FDX1 (Jacquot, Stein, et al., 1997).

TRXs are ubiquitous disulfide bond oxidoreductases found in all free-living organisms. They contain a canonical disulfide active site (W-C-G/P-P-C) responsible for disulfide oxidoreductase activity and a redox midpoint potential of between −270 and −300 mV at pH 7.0 (Aslund, Berndt, & Holmgren, 1997; Collin et al., 2003; Collin et al., 2004; Hirasawa et al., 1999). Since its discovery as a hydrogen donor for ribonucleotide reductase in *Escherichia coli* (Laurent, Moore, & Reichard, 1964; Sengupta & Holmgren, 2014), the TRX system has been extensively studied and recognized as having multiple roles in a myriad of cellular processes and human diseases (Buchanan, Holmgren, Jacquot, & Scheibe, 2012; Hanschmann, Godoy, Berndt, Hudemann, & Lillig, 2013; Lee, Kim, & Lee, 2013; Toledano, Delaunay-Moisan, Outten, & Igbaria, 2013).

In photosynthetic organisms, TRXs constitute multigenic families and phylogenetic analyses have revealed the existence of different types of TRX proteins localized in diverse subcellular compartments: 2 TRXf, TRXm, TRXx, TRXy, and TRXz are in chloroplasts while TRXo and TRXh are in mitochondria and the cytosol (Lemaire, Michelet, Zaffagnini, Massot, & Issakidis-Bourguet, 2007; Meyer, Belin, Delorme-Hinoux, Reichheld, & Riondet, 2012; Serrato, Fernandez-Trijueque, Barajas-Lopez, Chueca, & Sahrawy, 2013). Cytosolic and mitochondrial TRXs are reduced by NADPH-dependent thioredoxin reductases (NTRs) like TRXs in nonphotosynthetic organisms. By contrast, chloroplast TRXs are specifically reduced by FTR (Balsera, Uberegui, Schurmann, & Buchanan, 2014; Chibani, Wingsle, Jacquot, Gelhaye, & Rouhier, 2009; Jacquot, Eklund, Rouhier, & Schurmann, 2009; Michelet, Zaffagnini et al., 2013; Schurmann & Buchanan, 2008; Yoshida & Hisabori, 2017). Once reduced, TRXs can specifically reduce disulfide bonds on their target proteins.

The FDX-TRX system was initially identified as a light signaling mechanism controlling the activity of several CBC enzymes (Buchanan, 2016; Michelet, Zaffagnini et al., 2013). These enzymes have low activity in the dark and become activated in the light through reduction of one or several regulatory disulfide bonds. This reduction triggers a slow conformational change, shifting the target enzyme from a low to a high activity state. The FDX-TRX system ensures coupling of metabolism with the redox state of the PET chain and the availability of reducing equivalents. In addition to CBC enzymes, many other enzymes involved in diverse pathways are regulated by light through TRX-dependent reduction of disulfide bonds (Lemaire et al., 2007; Montrichard et al., 2009; Schurmann & Buchanan, 2008). This includes ATP synthase, which is responsible for the light-driven ATP production required for the functioning of the CBC (Buchert, Bailleul, & Hisabori, 2017; Sekiguchi et al., 2020), acetyl-CoA carboxylase, which catalyzes the first committed step of fatty acid biosynthesis (Sasaki, Kozaki, & Hatano, 1997), ADP-glucose pyrophosphorylase, glucan:water dikinase, and beta-amylase BAM1, which are involved in starch metabolism (Ballicora, Frueauf, Fu, Schurmann, & Preiss, 2000; Geigenberger, Kolbe, & Tiessen, 2005; Mikkelsen, Mutenda, Mant, Schurmann, & Blennow, 2005; Sparla, Costa, Lo Schiavo, Pupillo, & Trost, 2006), and the oxidative pentose phosphate pathway (OPPP) enzyme glucose-6-phosphate dehydrogenase, which is inactivated by TRX-dependent reduction in the light (Farr, Huppe, & Turpin, 1994; Nee, Zaffagnini, Trost, & Issakidis-Bourguet, 2009; Wenderoth, Scheibe, & von Schaewen, 1997). The mechanisms associated with TRX regulation are the best characterized redox signaling pathways in photosynthetic organisms (Foyer & Noctor, 2005); they have been investigated in detail at the molecular and structural levels in different model systems, including *Chlamydomonas*.

In addition to their role in the control of metabolic enzymes through reduction of regulatory disulfides where the electrons and protons provided by TRX are not used in the reaction catalyzed by the enzyme, TRXs can also reduce catalytic disulfides and thereby play a major role in detoxification of ROS and maintenance of redox homeostasis in the chloroplast. Indeed, TRXs serve as substrates, providing electrons for the regeneration of different types of antioxidant chloroplast enzymes including peroxiredoxins (PRXs) (Dietz, 2011), glutathione peroxidases (GPXs) (Navrot, Gelhaye, Jacquot, & Rouhier, 2006), and methionine sulfoxide reductases (MSRs) (Tarrago et al., 2009). In these cases, TRXs function as a substrate since the target enzymes use the electrons and protons in the reaction that they catalyze. A TRX-related system named NADPH-TRX reductase C (NTRC) consists of a fusion protein containing a TRX domain and an NTR domain. NTRC plays an important role in the maintenance of chloroplast redox homeostasis by providing

electrons to antioxidant enzymes such as PRXs (Perez-Ruiz, Naranjo, Ojeda, Guinea, & Cejudo, 2017; Yoshida & Hisabori, 2016).

The TRX isoforms of the chloroplast (f, m, x, y, z) are each generally encoded by multiple nuclear genes (Chibani et al., 2009; Lemaire et al., 2007). This multiplicity is more limited in microorganisms, which make them, for these reasons among others, potentially simpler models to study TRXs. For example, *Synechocystis* sp. PCC 6803 has four TRXs (1 TRXm, 1 TRXx, 1 TRXy, and one that is atypical), *Ostreococcus lucimarinus* has five chloroplastic TRXs (2 TRXf, 1 TRXm, 1 TRXx, no TRXy, 1 TRXz), and *Chlamydomonas* has six chloroplastic TRXs (2 TRXf, 1 TRXm, 1 TRXx, 1 TRXy, 1 TRXz) (while Arabidopsis has 10 and poplar 13) (Chibani et al., 2009; Lemaire et al., 2007; Perez-Perez, Martin-Figueroa, & Florencio, 2009; Zaffagnini et al., 2019). All chloroplastic TRXs are reduced by FTR (Chibani et al., 2009; Yoshida & Hisabori, 2017) and some of them, such as TRXz, may be reduced by NTRC as well (Yoshida & Hisabori, 2016). Biochemical analyses suggest that CBC enzymes are preferentially regulated by f-type TRXs (Chibani, Couturier, Selles, Jacquot, & Rouhier, 2010; Lemaire et al., 2007; Michelet, Zaffagnini et al., 2013; Nee et al., 2009). TRXx and TRXy are the most efficient TRXs for the reduction of PRXs, GPXs, and MSRs (Chibani, Tarrago, Schurmann, Jacquot, & Rouhier, 2011; Collin et al., 2003; Collin et al., 2004). TRXz has been characterized as a subunit and regulator of the plastid encoded RNA polymerase (Arsova et al., 2010; Schroter, Steiner, Matthai, & Pfannschmidt, 2010) and thereby it plays an important role in chloroplast transcription and chloroplast development (Arsova et al., 2010; Diaz et al., 2018; Huang et al., 2013). The specificity of TRXm is less clear: it can replace TRXf for activation of metabolic enzymes, though less efficiently, and it was suggested to play a role in the transfer of reducing equivalents from the stroma to the thylakoid lumen or in the regulation of chloroplastic proteins involved in electron transfer pathways (Courteille et al., 2013).

Beyond established targets for which TRX reduction was confirmed biochemically, proteomic analyses based on TRX-affinity columns or in vitro TRX reduction revealed hundreds of putative TRX targets in diverse organisms ((Perez-Perez et al., 2017) and references therein).

8.4.2 The ferredoxin-thioredoxin system in *Chlamydomonas*

The FDX-TRX system has been extensively studied in *Chlamydomonas*. Several components of the system including FTR and TRXh, TRXf and TRXm were identified in the early 1990s (Huppe et al., 1990; Huppe, Picaud, Buchanan, & Miginiac-Maslow, 1991). After purification from *Chlamydomonas* cultures, the primary sequence of TRXm and TRXh1 were determined by Edman sequencing (Decottignies et al., 1990; Decottignies, Schmitter, Dutka, Jacquot, & Miginiac-Maslow, 1991), allowing cloning of the corresponding cDNA and genomic sequences, and initial characterizations of the proteins after purification of the TRXs expressed in *E. coli* (Jacquot, Stein, Hodges, & Miginiac-Maslow, 1992; Stein et al., 1995). Numerous structures of these two TRXs were solved by NMR or X-ray crystallography (Krimm et al., 1998; Lancelin et al., 2000; Lancelin, Stein, & Jacquot, 1993; Marchand et al., 2019; Menchise et al., 2000; Menchise et al., 2001; Mittard et al., 1995; Mittard et al., 1997). The biochemical and physico-chemical properties of these two TRXs were investigated extensively, primarily because they served as model proteins to study one-electron oxidation and protein stability and folding (Hirasawa et al., 1999; Lemaire et al., 2000; Lemaire et al., 2018; Lmoumene, Conte, Jacquot, & Houee-Levin, 2000; Richardson, Lemaire, Jacquot, & Makhatadze, 2000; Setterdahl et al., 2003; Sicard-Roselli et al., 2004).

The availability of genomic sequences led to the identification of new chloroplast thioredoxin isoforms, including a second TRXf and four new types of TRX proteins: 1 TRXo, 1 TRXx, 1 TRXy, and 1 TRXz (Le Moigne, Gurrieri, et al., 2021; Lemaire & Miginiac-Maslow, 2004; Lemaire, Collin, Keryer, Issakidis-Bourguet, et al., 2003; Lemaire, Collin, Keryer, Quesada, & Miginiac-Maslow, 2003). These TRXs exhibit properties and specificities comparable to those of land plant. While CBC enzymes are preferentially activated by TRXf and to a lesser extent by TRXm, TRXx and TRXy are more efficient for reducing antioxidant enzymes such as PRXs. The recently solved structures of *Chlamydomonas* TRXf2 (Lemaire et al., 2018) and TRXz (Le Moigne, Gurrieri, et al., 2021) indicate that the surface electrostatic charge distribution is a major determinant of TRX specificity. The role of TRX in regulating CBC enzymes, extensively studied in land plants and *Chlamydomonas*, is detailed in a section of this chapter.

Besides CBC regulation, *Chlamydomonas* TRXs participate in the maintenance of ROS homeostasis through reduction of PRXs and GPXs (Charoenwattanasatien et al., 2020; Dayer, Fischer, Eggen, & Lemaire, 2008; Goyer et al., 2002), and may also play a role in hydrogen peroxide signaling through regulation of catalase (Shao, Beck, Lemaire, & Krieger-Liszkay, 2008). In addition, TRXs regulate chloroplast redox homeostasis through redox-dependent activation of NADP-malate dehydrogenase (NADP-MDH). This enzyme is involved in the export of reducing power from the chloroplast to the cytosol through the malate shuttle (Selinski & Scheibe, 2019). Chloroplastic NADP-MDHs from land

plants are redox regulated through two disulfide bonds present in N- and C-terminal extensions (Issakidis, Lemaire, Decottignies, Jacquot, & Miginiac-Maslow, 1996). By contrast, *Chlamydomonas* NADP-MDH (MDH5) contains a single C-terminal TRX-regulated disulfide bond (Lemaire et al., 2005). The recently identified calredoxin (CRX) is a chloroplast-localized protein from *Chlamydomonas* that is able to integrate calcium and redox signals as it comprises a Ca^{2+}-binding CaM domain with four EF-hands, which controls a thioredoxin domain that exhibits a typical thioredoxin-fold and Ca^{2+}-dependent thioredoxin activity (Hochmal et al., 2016). The structural determinants of CRX underlying this calcium-dependent control of TRX activity were recently unraveled as well as the interaction and reduction of CRX with PRX1, a major chloroplastic PRX (Charoenwattanasatien et al., 2020). The *Chlamydomonas* genome also contains a gene encoding NTRC, which has not yet been studied (Table 8.1).

Many genes encoding components of the FDX-TRX system were shown to be regulated by light and the circadian clock (Lemaire, Stein et al., 1999; Strenkert et al., 2019), oxidative stress (Blaby et al., 2015; Terauchi et al., 2009), and heavy metals (Lemaire, Keryer et al., 1999). *Chlamydomonas* is well-adapted for genome-wide proteomic analyses (Rolland et al., 2009) (see Chapter 12), making it ideal for developing redox proteomic approaches aimed at identifying new TRX targets (Lemaire et al., 2004). The most comprehensive thioredoxome (thioredoxin interacting proteome) was established in *Chlamydomonas* and identified 1188 proteins and 1052 cysteines regulated by TRX (Perez-Perez et al., 2017). Considering the multiplicity of TRX isoforms and their multiple targets, dissecting their functions in vivo is a highly challenging task since alteration of the TRX system through genetic engineering will likely impact a multitude of cellular processes and pathways. Therefore in vivo engineering of TRX-regulation should rather focus on altering the redox properties of target enzymes (e.g., engineering of disulfide bonds through mutagenesis). This strategy was recently applied to show that autophagy is regulated by TRX in *Saccharomyces cerevisiae* and *Chlamydomonas* through oxidoreduction of a regulatory disulfide bond of the ATG4 cysteine protease (Perez-Perez, Lemaire, & Crespo, 2016; Perez-Perez, Zaffagnini, Marchand, Crespo, & Lemaire, 2014). The *Chlamydomonas* thioredoxome contains more than 350 chloroplastic proteins, showing again the multiple roles of TRXs for electron distribution in the stroma.

8.5 The Calvin-Benson cycle in *Chlamydomonas reinhardtii*

This section will focus on the CBC. We describe the functioning of this cardinal metabolic pathway in *Chlamydomonas*, highlight differences in the pathway among photosynthetic organisms, and detail what is known in *Chlamydomonas* about its regulation and structural organization.

8.5.1 Components and functioning of the Calvin-Benson cycle in *Chlamydomonas*

The CBC is a conserved cyclic loop of 13 chemical reactions that ensures the process of carbon fixation (Melvin Calvin and collaborators, Nobel Prize in Chemistry 1961). The fixation of CO_2 occurs by carboxylation of the acceptor pentose, ribulose-1,5-bisphosphate (RuBP), that is subsequently recycled through 12 reaction steps (Benson et al., 1952). The 13 CBC reactions are catalyzed by 11 enzymes that group into three phases: (i) ribulose-5-phosphate is phosphorylated by phosphoribulokinase (PRK) (Hurwitz, Weissbach, Horecker, & Smyrniotis, 1956; Moll & Levine, 1970), generating RuBP, which serves as the acceptor for CO_2 fixation in a reaction catalyzed by RuBP carboxylase/oxygenase (Rubisco); (ii) the 3-phosphoglycerate produced enters the reduction phase, which is catalyzed by phosphoglycerate kinase (PGK) and glyceraldehyde-3-phosphate dehydrogenase (GAPDH) to form glyceraldehyde-3-phosphate; (iii) ribulose-5-phosphate is then regenerated by the collective activities of triose phosphate isomerase (TPI), fructose-6-phosphate aldolase (FBA), fructose-1,6-bisphosphatase (FBPase), transketolase (TRK), sedoheptulose-1,7-bisphosphatase (SBPase), ribulose-5-phosphate epimerase (RPE), and ribose-5-phosphate isomerase (RPI). Three CO_2 molecules eventually yield one triose while the pool of RuBP acceptors is regenerated at each iteration of the cycle. For each fixed CO_2, the CBC consumes three ATP molecules (one by PRK and two by PGK) and oxidizes two NADPH molecules (GAPDH) (Fig. 8.2).

The CBC is present in all oxygenic photosynthetic eukaryotes and is highly conserved. All enzymes are present in *Chlamydomonas* and exhibit sequences and structures that are conserved with those of land plants (Table 8.2). CBC enzymes are highly abundant as determined by global or targeted proteomic approaches (Hammel et al., 2020; Mettler et al., 2014; Schroda, Hemme, & Muhlhaus, 2015; Wienkoop et al., 2010); Rubisco is the most abundant protein on Earth with 90% found in the leaves of land plants (Bar-On & Milo, 2019). In *Chlamydomonas*, the CBC enzymes were shown to collectively represent 11.9% of total cell proteins, with a 128-fold difference between the most abundant (RbcL, 268 μM) and the least abundant (TPI, 2 μM) (Hammel et al., 2020). This abundance combined with the measurements of CBC metabolites suggests that some CBC enzymes are near-saturated in vivo (Rubisco, PGK, FBPase,

TABLE 8.2 Enzymes of the Calvin-Benson cycle and their regulators in *Chlamydomonas*.

Protein name	Gene name	Locus ID	Uniprot	MW (kDa) Pre/mat	Length (aa) Pre/mat
Ribulose-1,5-bisphosphate carboxylase/oxygenase large subunit (RubisCO LSU)	*rbcL*	Cre.RbcL	P00877	52.47	475
Ribulose-1,5-bisphosphate carboxylase/oxygenase small subunit (RubisCO SSU)	*RBCS1*	Cre02.g120100	P00873	20.58 / 16.22	185 / 140
	RBCS2	Cre02.g120150	P08475	20.6 / 16.25	185 / 140
Phosphoglycerate kinase	*PGK1*	Cre11.g467770	Q548U3	48.96 / 42.58	462 / 402
Glyceraldehyde-3-phosphate dehydrogenase subunit A	*GAP3*	Cre01.g010900	P50362	40.24 / 36.82	374 /340
Triose phosphate isomerase	*TPIC1*	Cre01.g029300	Q5S7Y5	30.00 / 27.01	282 / 255
Fructose-1,6-bisphosphate aldolase	*ALDCHL*	Cre05.g234550	Q42690	40.92 / 38.11	377 / 350
Fructose-1,6-bisphosphatase	*FBP1*	Cre12.g510650	A8IKQ0	44.38 / 38.87	415 / 359
Transketolase	*TRK1*	Cre02.g080200	A8IAN1	77.55 / 73.85	718 / 683
Sedoheptulose-1,7-bisphosphatase	*SEBP1*	Cre03.g185550	P46284	41.38 / 35.00	385 / 323
Ribulose phosphate-3-epimerase	*RPE1*	Cre12.g511900	A8IKW6	28.35 / 25.54	265 / 238
Ribose-5-phosphate isomerase	*RPI1*	Cre03.g187450	A8IRQ1	28.77 / 26.58	269 / 248
Phosphoribulokinase	*PRK*	Cre12.g554800	P19824	48.96 / 42.58	462 / 402
Calvin cycle protein CP12	*CP12*	Cre08.g380250	A6Q0K5	11.40 / 8.44	107 / 80
RubisCO activase	*RCA1*	Cre04.g229300	P23489	44.97 / 41.58	408 / 376

pre, Premature protein MW; *mat*, mature protein MW.

SBPase) while the remainder operates at low substrate saturation (Mettler et al., 2014). In *Chlamydomonas*, RbcS is less abundant (182 μM) than RbcL, suggesting that the Rubisco holoenzyme represents less than 2% of total proteins (see Chapter 7). Indeed, Rubisco is much less abundant in *Chlamydomonas* than in land plants where it can account for several tens of percent of the proteome. The higher abundance of RbcL compared to RbcS in *Chlamydomonas* may be linked to its independent moonlighting functions in the control of mRNA homeostasis and gene expression (Zhan et al., 2015).

The expression of CBC genes (mRNA accumulation) is regulated by light and the circadian clock with maximal expression during the light phase and minimal during the dark phase of the diel cycle, while the protein abundances also show some oscillations, although less pronounced (Lemaire, Miginiac-Maslow, & Jacquot, 2002; Lemaire, Stein et al., 1999; Schmollinger et al., 2014; Strenkert et al., 2019). RbcS in plants and green algae is encoded in the nucleus and translated by cytosolic ribosomes before being imported into the chloroplast where it is processed to its mature form. In contrast, RbcL is the only CBC protein in these organisms encoded by the chloroplast genome.

One major difference in many algae and cyanobacteria compared to land plants is the presence of carbon concentration mechanisms (CCMs), which increases the CO_2 concentration in the vicinity of Rubisco to favor its carboxylation rate over its oxygenase activity (Lin, Occhialini, Andralojc, Parry, & Hanson, 2014; Rae et al., 2013; Raven, Giordano, Beardall, & Maberly, 2012). One feature of the CCM is the pyrenoid, a liquid-like microcompartment present in the chloroplasts of algae and hornworts which contains densely packed Rubisco (see Chapter 7). The pyrenoid is therefore functionally analogous to, though structurally different from, the carboxysomes of cyanobacteria (Kerfeld & Melnicki, 2016). The pyrenoid in conjunction with other components of the CCM mitigates the low catalytic efficiency of Rubisco and the dual substrate specificity of its active site for CO_2 and O_2 (Spreitzer & Salvucci, 2002). CO_2 is the substrate for the productive carbon-fixing step of the CBC, but the oxygenase activity of Rubisco leads to the production of glycolate, which is recycled by the nonproductive and energetically costly photorespiratory pathway (Foyer, Bloom, Queval, & Noctor, 2009; South, Cavanagh, Liu, & Ort, 2019). The CCM also mitigates the limited availability of CO_2 in aquatic environments where uptake is hampered by slower diffusion rates and the conversion of most CO_2 to the

bicarbonate anion, which cannot diffuse across the lipid bilayers of the plasma membrane and chloroplast envelope (Wang, Stessman, & Spalding, 2015). Rubisco is the only CBC enzyme present in the pyrenoid as revealed by proteomic studies, activity assays, and fluorescence microscopy (Kuken et al., 2018; Mackinder et al., 2016; Mackinder et al., 2017; Zhan et al., 2018). Therefore a high flux of RuBP and 3PGA between the pyrenoid interior or "matrix" containing Rubisco and the stroma containing all other CBC enzymes must occur. Computational modeling of *Chlamydomonas* CBC suggested that there is no major diffusional barrier to this cellular metabolic trafficking of RuBP and 3PGA, which might involve pyrenoid minitubules that connect the stroma to the interior of the pyrenoid (Engel et al., 2015; Kuken et al., 2018; Syeda et al., 2015). Due to the presence of the CCM, *Chlamydomonas* and most other photosynthetic aquatic microorganisms are efficient energy converters; their photorespiration is low, and they require less Rubisco (Raven, Beardall, & Sanchez-Baracaldo, 2017).

8.5.2 Regulation mediated by posttranslational modifications

8.5.2.1 Thioredoxin-dependent regulation of Calvin-Benson cycle enzymes

In land plants, four enzymes of the CBC (FBPase, SBPase, PRK, and A_2B_2-GAPDH) are activated by the FDX-TRX system, enabling light-dependent modulation of CBC activity. The light-dependent activation of SBPase, FBPase, and PRK was initially reported in the unicellular green alga Chlorella (Bassham, 1971; Pedersen, Kirk, & Bassham, 1966). Each of these four enzymes contains a regulatory disulfide reduced specifically or preferentially by TRXf and which upon reduction triggers a conformational change of the enzyme from a low to a high activity state (Michelet, Zaffagnini et al., 2013). Comparisons of the redox regulatory properties of enzymes from cyanobacteria, diatoms, algae, and higher plants suggest that the light-dependent regulation mediated by TRX has been progressively introduced during evolution by the addition of regulatory disulfides (Lemaire et al., 2007; Michelet, Zaffagnini et al., 2013; Ruelland & Miginiac-Maslow, 1999). The Synechocystis CBC enzymes are generally not regulated through TRX-dependent regulatory disulfides (Balsera et al., 2014; Tamoi, Murakami, Takeda, & Shigeoka, 1998) unlike their *Chlamydomonas* counterparts (Farr et al., 1994; Huppe & Buchanan, 1989; Huppe, Farr, & Turpin, 1994). By contrast with land plants that contain a TRX-dependent isoform of GAPDH (A_2B_2-GAPDH), this control is absent in *Chlamydomonas* where another enzyme, PGK, is instead regulated by TRX (Morisse, Michelet, et al., 2014). *Chlamydomonas* CBC contains four established targets of TRX: SBPase, FBPase, PRK, and PGK.

8.5.2.1.1 Glyceraldehyde-3-phosphate dehydrogenase

Land plants contain several isoforms of GAPDH encoded by the GAPA, GAPB, and GAPC genes. GAPC corresponds to the glycolytic type while GAPA and GAPB encode nearly identical photosynthetic GAPDH subunits, but GAPB contains a specific C-terminal extension containing the TRX-dependent regulatory disulfide responsible for the light/dark regulation of the enzyme (Baalmann, Scheibe, Cerff, & Martin, 1996; Sparla, Pupillo, & Trost, 2002). Two isoforms participate in the CBC: the major form is heterotetrameric A_2B_2-GAPDH and the minor form is homotetrameric A_4-GAPDH (Trost et al., 2006). By contrast with NAD(H)-specific glycolytic GAPDH (GAPC) (Zaffagnini, Fermani, Costa, Lemaire, & Trost, 2013), photosynthetic GAPDH uses both NAD(H) and NADP(H) as coenzymes (Melandri, Baccarini, & Pupillo, 1968). The NADPH-dependent activity of A_2B_2-GAPDH is specifically light regulated by TRXf while the A_4 isoform is not (Marri et al., 2009). Structural and kinetic analyses demonstrated that the C-terminal extension of GAPB acts as a redox-sensitive auto-inhibitory domain forming a bulky hairpin structure in the proximity of the NADP-binding site (Fermani et al., 2007; Sparla et al., 2005). The GAPB gene is only found in the genomes of Streptophytes (land plants and Charophytes (Petersen, Teich, Becker, Cerff, & Brinkmann, 2006)), and the Prasinophycean green algae (e.g., Ostreococcus (Robbens, Petersen, Brinkmann, Rouze, & Van de Peer, 2007)). It is absent in all other oxygenic phototrophs, which usually contain a single GAPA gene, except for the cryptomonads, diatoms, and chromalveolates in which chloroplast GAPDH is generally encoded by GAPC-type genes (Liaud, Brandt, Scherzinger, & Cerff, 1997). A_4-GAPDH is a minor GAPDH isoform in land plants (Howard, Lloyd, & Raines, 2011; Scagliarini, Trost, Pupillo, & Valenti, 1993) but is the only isoform of photosynthetic GAPDH in green algae, red algae, and cyanobacteria (Petersen et al., 2006). The *Chlamydomonas* genome contains a single GAPA gene (Table 8.2) and the CBC operates only with A_4-GAPDH, which lacks regulatory cysteines and is therefore not directly regulated by TRX. In all organisms, including *Chlamydomonas*, GAPDH is indirectly regulated by TRX through the formation of a complex with two TRX-regulated proteins, PRK and CP12 (Graciet, Lebreton, & Gontero, 2004; Trost et al., 2006; Wedel & Soll, 1998). This is the only known mechanism of light/dark regulation of GAPDH in *Chlamydomonas* and

all other GAPB-deficient species. This will be discussed further below in the section on the supramolecular organization of the CBC.

8.5.2.1.2 Phosphoglycerate kinase

PGK, a CBC enzyme that converts 3-PGA produced by the Rubisco reaction to 1,3-bisphosphoglycerate, the substrate of GAPDH, is not known to be redox regulated in land plants. By contrast, a TRX-dependent redox activation was reported in *Chlamydomonas*, *Synechocystis*, and *Phaeodactylum tricornutum* (Bosco, Aleanzi, & Iglesias, 2012; Morisse, Michelet, et al., 2014; Tsukamoto, Fukushima, Hara, & Hisabori, 2013). This may suggest that this regulatory mechanism has been lost in land plants after the invention of GAPB or that it is a recent innovation of some aquatic phototrophs. In *Chlamydomonas* chloroplastic PGK, the regulatory disulfide bond involves the two C-terminal cysteines, has a midpoint redox potential of −335 mV at pH 7.0, and its reduction, preferentially performed by TRXf, increases the enzyme turnover number but does not affect the enzyme affinities for its substrates (Morisse, Michelet, et al., 2014).

8.5.3 Phosphoribulokinase

PRK is a homodimer in eukaryotes (Gurrieri et al., 2019; Porter, Milanez, Stringer, & Hartman, 1986) and each monomer contains four strictly conserved cysteines. PRK is unique to the CBC and has therefore no cytosolic counterpart. It has a low activity in the oxidized form and is activated by TRX-dependent reduction of the N-terminal Cys16-Cys55 regulatory disulfide (Brandes, Larimer, & Hartman, 1996). Formation of the Cys16-Cys55 disulfide efficiently blocks the activity because Cys55 likely plays a role in catalysis through binding of the sugar phosphate substrate (Milanez, Mural, & Hartman, 1991; Porter & Hartman, 1990). As in the case of other CBC enzymes, TRXf is more efficient for activation of PRK compared to TRXm while no activation by TRXx and TRXy was observed in Arabidopsis (Marri et al., 2009). PRK was purified from *Chlamydomonas* and shown to be activated by TRXf through reduction of the conserved N-terminal disulfide (Farr et al., 1994; Lebreton, Graciet, & Gontero, 2003). Two C-terminal cysteines were shown to participate in a disulfide formation, which might alter the physical interaction of PRK with GAPDH and CP12 (Thieulin-Pardo, Remy, Lignon, Lebrun, & Gontero, 2015). Proteomic approaches also identified this disulfide as a target of TRX (Perez-Perez et al., 2017). *Chlamydomonas* PRK is preferentially activated by TRXf (Gurrieri et al., 2019) but can also be activated, to a lesser extent, by TRXz (Le Moigne, Gurrieri, et al., 2021).

8.5.4 Fructose-1,6-bisphosphatase

Oxidized land plant FBPase has a basal activity (20%−30%) and becomes fully activated upon disulfide reduction, which is strictly dependent on TRXf; all other TRX types are inefficient. The molecular mechanism of TRX-dependent activation of FBPase was initially unraveled for pea FBPase. Compared to cytosolic FBPase, which participates in gluconeogenesis and is not redox regulated by TRX, pea chloroplast FBPase contains two insertions containing cysteines that form the regulatory disulfide bond (Cys153-Cys178) (Chiadmi, Navaza, Miginiac-Maslow, Jacquot, & Cherfils, 1999; Jacquot et al., 1995; Jacquot, Lopez-Jaramillo, et al., 1997; Rodriguez-Suarez, Mora-Garcia, & Wolosiuk, 1997). The conformational changes linking the redox state of the regulatory cysteines and the level of activation of the enzyme have been established by comparing the structure of oxidized and reduced FBPase (Chiadmi et al., 1999; Jacquot et al., 1995; Jacquot, Lopez-Jaramillo, et al., 1997; Rodriguez-Suarez et al., 1997). Formation of the disulfide forces the sliding of a loop by 8−9 Å toward the active site, thereby disrupting the binding sites for the catalytic Mg^{2+} cations (Chiadmi et al., 1999). Therefore in contrast to other CBC enzymes, the conformational changes induced by the oxidation of the regulatory disulfide do not impact the active site or its proximity but stabilizes a general conformation in which the active site is almost nonfunctional. Chloroplastic FBPase was the first TRX (TRXf) target purified from *Chlamydomonas* (Chiadmi et al., 1999; Jacquot et al., 1995; Jacquot, Lopez-Jaramillo, et al., 1997; Rodriguez-Suarez et al., 1997).

8.5.5 Sedoheptulose-1,7-bisphosphatase

SBPase is a homodimeric enzyme that is unique to the CBC and has no cytosolic counterpart. SBPase contains a single regulatory disulfide that is preferentially reduced by TRXf (Dunford, Durrant, Catley, & Dyer, 1998; Gutle et al., 2016; Nishizawa & Buchanan, 1981). The regulatory cysteines are conserved in all photosynthetic eukaryotes including *Chlamydomonas*, but the algal enzyme has not been characterized biochemically.

8.5.6 Rubisco and Rubisco activase (see also Chapter 7)

Despite the finding that Rubisco was systematically identified among putative TRX targets in redox proteomic studies performed in photosynthetic cells (Michelet, Zaffagnini et al., 2013; Perez-Perez et al., 2017), a direct effect of TRX on Rubisco has not yet been reported. In the large subunit of *Chlamydomonas* Rubisco, seven of the twelve cysteines are highly conserved among photosynthetic eukaryotes (Moreno, Garcia-Murria, & Marin-Navarro, 2008), and among them, oxidation of Cys172, Cys192, Cys449, and Cys459 was reported to play a prominent role either in Rubisco inactivation and degradation through conformational modulation (Garcia-Murria et al., 2008; Garcia-Murria, Sudhani, Marin-Navarro, Sanchez Del Pino, & Moreno, 2018; Marin-Navarro & Moreno, 2006) or chloroplastic mRNA binding (Uniacke & Zerges, 2008; Yosef et al., 2004; Zhan et al., 2015). The Cys449-Cys459 pair was proposed to function as a redox sensor (Garcia-Murria et al., 2008) and Cys459 is reduced in the presence of TRX (Perez-Perez et al., 2017), but an experimental demonstration of a direct TRX-dependent regulation of Rubisco remains to be established. In some species, Rubisco may be indirectly regulated by TRX through Rubisco activase (RCA), an ATP-dependent molecular chaperone of the AAA^+ family required to release tight-binding inhibitors from the active site of Rubisco (Portis, 2003; Portis, Li, Wang, & Salvucci, 2008). The ATPase activity of RCA is controlled by the ADP/ATP ratio and/or by the FDX-TRX system. Two types of RCA have been identified: the short form (beta isoform), not regulated by TRX, and the long form (alpha isoform), which contains a TRXf-dependent regulatory disulfide (Zhang, Schurmann, & Portis, 2001). The extension contains negative charges that, upon oxidation of the disulfide, interact with the ATP-binding site and inhibits the enzyme while reduction by TRXf alleviates this inhibition (Portis et al., 2008; Wang & Portis, 2006). Some species, such as Arabidopsis, contain both alpha and beta isoforms while others such as tobacco, maize, and green algae only contain the short beta isoform, but they still exhibit light-dependent regulation of RCA activity due to a unique sensitivity to ADP/ATP ratios (Carmo-Silva & Salvucci, 2013; Salvucci, Werneke, Ogren, & Portis, 1987) and to light-dependent fluctuations of magnesium ions (Hazra, Henderson, Liles, Hilton, & Wachter, 2015).

8.5.6.1 *diversity of posttranslational modifications in* Chlamydomonas *Calvin-Benson cycle*

Proteome-wide analysis of posttranslationally modified proteins have considerably challenged our current models of CBC regulation, which has been focused on the activation by TRXf of four CBC enzymes plus CP12. In addition to TRX-regulation, two other types of redox modifications have been investigated in *Chlamydomonas* using proteomics: glutathionylation and nitrosylation. Glutathionylation results in the formation of a mixed disulfide bond between a protein cysteine and the thiol group of glutathione, the major nonprotein thiol in most organisms (Rouhier, Lemaire, & Jacquot, 2008; Zaffagnini et al., 2019; Zaffagnini, Bedhomme, Marchand, et al., 2012). Glutathionylation is a widespread oxidative modification involved in the modulation of protein function but also in the protection of protein Cys from irreversible oxidation. Nitrosylation results in the formation of nitrosothiols by the reaction of protein thiols with a nitric oxide (NO) moiety. It can be triggered chemically not only by reactive nitrogen species (RNS) such as NO and related species but also by transnitrosylation reactions mediated by small nitrosothiols (e.g., nitrosoglutathione, GSNO) or other nitrosylated proteins (Benhar, Forrester, & Stamler, 2009; Chen et al., 2020; Hess, Matsumoto, Kim, Marshall, & Stamler, 2005; Hogg, 2002; Zaffagnini et al., 2014). In *Chlamydomonas*, NO signaling participates in the regulation of nutrient acquisition, photosynthetic efficiency, and other processes including autophagy and programmed cell death (Calatrava et al., 2017; De Mia, Lemaire, Choquet, & Wollman, 2019; Kuo, Chang, Lin, & Lee, 2020; Sanz-Luque, Ocana-Calahorro, Llamas, Galvan, & Fernandez, 2013; Wei et al., 2014; Zalutskaya, Kochemasova, & Ermilova, 2018). Both nitrosylation and glutathionylation can be reversed by TRX and/or glutathione/glutaredoxins (GRXs) (Bedhomme et al., 2012; Zaffagnini et al., 2016; Zaffagnini, Bedhomme, Marchand, et al., 2012). As GSNO has been proposed to trigger both nitrosylation and glutathionylation, these two modifications could be dependent on GSNO homeostasis, which is under the control of a GSNO reductase that was recently characterized biochemically and structurally in *Chlamydomonas* (Tagliani et al., 2021).

In *Chlamydomonas*, proteomic studies identified 225 proteins regulated by glutathionylation (Michelet et al., 2008; Zaffagnini, Bedhomme, Groni, et al., 2012) and nearly 400 nitrosylated cysteines in 492 nitrosylated proteins (Morisse, Zaffagnini, Gao, Lemaire, & Marchand, 2014). The thioredoxome (TRX-interacting proteome) has also been investigated in *Chlamydomonas* and allowed the identification of 1188 proteins and 1052 cysteines regulated by TRX (Perez-Perez et al., 2017). Comparison of these datasets suggests the existence of a complex redox regulation network in *Chlamydomonas* and provides evidence of a tremendous selectivity of posttranslational redox modifications for specific cysteine residues, even within the same protein. These results indicate that the Cys proteome does not represent a small subset of highly reactive Cys residues that are modified through indiscriminate interaction with the molecules they encounter but represents a complex system of posttranslational modifications (PTMs) associated with redox conditions

that are specific for distinct interconnected protein networks (Perez-Perez et al., 2017). The CBC is a major target pathway within this complex network since all *Chlamydomonas* CBC enzymes were identified as potential targets of nitrosylation (Morisse, Zaffagnini, et al., 2014), glutathionylation (Michelet et al., 2008; Zaffagnini et al., 2014; Zaffagnini, Bedhomme, Groni, et al., 2012), and thioredoxin-mediated redox regulation (Lemaire et al., 2004; Morisse, Michelet, et al., 2014; Perez-Perez et al., 2017) (Table 8.3). Most of these modifications have been confirmed on the corresponding purified enzyme, with the modified cysteines mapped. However, the effect of the modification varies considerably between enzymes (Bedhomme et al., 2012; Zaffagnini et al., 2007; Zaffagnini et al., 2014; Zaffagnini, Bedhomme, Groni, et al., 2012; Zaffagnini, Fermani, et al., 2013; Zaffagnini, Morisse, et al., 2013). For example, TPI and A_4-GAPDH were both confirmed to undergo glutathionylation and nitrosylation, with PTMs fully inhibiting GAPDH activity but barely affecting TPI activity (Zaffagnini et al., 2014). Some modified enzymes may represent moonlighting proteins that, upon redox PTMs, are diverted to new functions unrelated to their metabolic role in carbon metabolism, as shown for cytosolic GAPDH in mammals (Zaffagnini, Fermani, et al., 2013). Among CBC enzymes, a moonlighting function has been reported for *Chlamydomonas* RbcL (Vol 2, Chapter 7). It binds chloroplast mRNAs and accumulates in chloroplast stress granules under oxidative stress conditions (Cohen, Sapir, & Shapira, 2006; Knopf & Shapira, 2005; Uniacke & Zerges, 2008; Yosef et al., 2004). RbcL undergoes numerous redox modifications that may participate in the regulation of this moonlighting function (Table 8.3).

Interestingly, all CBC enzymes except FBPase were also identified in the phosphoproteome of *Chlamydomonas* with multiple modified residues for most enzymes (McConnell, Werth, & Hicks, 2018; Wang et al., 2014). *Chlamydomonas* CBC enzymes likely undergo multiple other modifications that remain to be investigated in detail. For example, recent proteomic data showed that most if not all CBC enzymes of land plants can be crotonylated on multiple lysine residues (Liu et al., 2018; Sun et al., 2017; Sun, Qiu et al., 2019; Xu et al., 2021). The functional role of all these modifications is still unknown. Therefore it appears that CBC enzymes are regulated by an intricate network of PTMs, with different modifications that may not occur at the same time, at the same site, to the same extent, or under the same physiological/cellular conditions. Regulation by PTM may allow a tight coupling between the activity and function of CBC enzymes and environmental conditions.

8.5.7 Structure and supramolecular organization

8.5.7.1 Structural features of Calvin-Benson cycle enzymes

The CBC enzymes have been studied by biochemical and proteomic approaches, which have unraveled some of their functions, specificities, and mechanisms of regulation. To go further into the characterization of these enzymes, their structures were determined by X-ray crystallography. We will inventory the current knowledge on the structures of the 11 CBC enzymes and the small interacting protein CP12 (Erales, Lignon, & Gontero, 2009) from *Chlamydomonas* (Table 8.2). We focus on solvent-exposed regulatory cysteines that are susceptible to redox modification in the folded state of the protein, since they elucidate how CBC functioning is coupled to the redox state of the PET chain and thus to light. Structural information on *Chlamydomonas* CBC proteins is described and referenced using the Protein Data Bank (PDB) 4-character codes. Unless otherwise stated, residues are numbered according to the mature protein after cleavage of the transit peptide. The structure of each enzyme is represented in Fig. 8.3.

8.5.8 Rubisco

Rubisco is a heteromultimeric assembly of two gene products: a large subunit (LSU) and a small subunit (SSU). A complex set of chaperones (Aigner et al., 2017) guide eight LSU and eight SSU into a hexadecameric (LSU_8:SSU_8) working assembly (Andersson & Backlund, 2008) (Vol 2, Chapter 7). Rubisco is classified as a lyase because it catalyzes the formation of carbon–carbon bonds between RuBP and carbon dioxide (CO_2). When utilizing dioxygen (O_2) instead of CO_2, Rubisco will form 3-PGA and 2-phosphoglycolate; the latter is toxic and is detoxified at an energetic cost to the cell. *Chlamydomonas* Rubisco is a major constituent of the pyrenoid, which is a component of the CCM. This subcellular compartment becomes especially prominent under low CO_2 conditions and is the site at which CO_2 is concentrated in the vicinity of Rubisco; this organization allows for the more efficient fixation of CO_2. Additionally, the pyrenoid has interesting physical properties and undergoes liquid–liquid phase separation during cell division (Vol 2, Chapter 7).

Rubisco SSU folds as a two-layer α/β sandwich. Rubisco LSU is composed of two domains, the B domain is an α/β TIM barrel and the N domain is a ferredoxin-like $\alpha+\beta$ sandwich (Chapman et al., 1988). The structure, 1GK8 for *Chlamydomonas* Rubisco, was determined at atomic resolution by X-ray crystallography of the protein complexed with

TABLE 8.3 Main posttranslational modifications of Calvin-Benson cycle enzymes and their known sites.

Protein name	Targeted by thioredoxin[a]		Regulatory disulfide[a]	S-glutathionylation		S-nitrosylation[a]		Redox-modified cysteines[a]	Phosphorylation sites[a]
Rubisco (LSU)	yes[c,l]	C459[l]		yes[f]	C172[f]; C247[f]; C427[f]	yes[g]	C172[g]; C247[g]; C427[g]; C459[g]	C84[n]; C172[b,n,o]; C192[m,n,o]; C247[m,o]; C427[n,o]; C449[j,m,o,b,d]; C459[k,b,d,m,n]	T471[s]
Rubisco (SSU)	yes[c,l]	C110[l]; C128[l]; C141[l]		yes[f]		yes[g]	C110[g]	C86[m,n]; C110[j,m]; C128[j,m]; C141[j,m]	S98[s]; S107[s]
PGK	yes[h,l]	C159[l]; C412[l]	C278-C412[h]	yes[e,f]	C159[f]; C412[f]	yes[g]	C412[g]	C278[o]; C412[o]	S262[s]; S301[s]; S302[s]; T414[s]; S421[s]; T439[s]; S444[s]
GAPDH-A	yes[l]	C190[l]; C194[l]		yes[f]		yes[g]		C190[j,m,o]; C194[j,m,o]; C325[o]	T62[s]; S72[s]; S86[s,v]; T90[s]; S104[s]; S229[v]; T246[s]; T247[s]; S255[s]; S320[s,v]; S358[s]
TPI	yes[l]	C154[l]; C245[l]; C273[l]		yes[i]		yes[g,i]	C245[g]; C273[g]	C41[m,o]; C245[m,o]	S128[s,t]
FBA	yes[c,l]	C58[l]		yes[f]		yes[g]	C58[g]; C142[g]; C256[g]	C58[o]; C142[m,o]; C152[m,o]; C183[o]; C218[o]; C256[m,o]	S54[s]; T57[s]; S64[s,x]; S170[s]; S176[s]
FBPase	yes[l]	C109[l]; C228[l]; C233[l]; C362[l]		yes[f]	C109[f]	yes[g]	C233[g]	C109[m,o]; C152[m,o]; C156[m,o]; C228[m,o]; C233[m,o]; C362[m,o]	
TRK	yes[l]	C386[l]; C484[l]		yes[f]	C84[f]	yes[g]	C582[g]	C58[j]; C84[j,o]; C173[j]; C204[j]; C210[j]; C366[j]; C386[j,m,o]; C470[j,m,o]; C582[j,o]; C638[j]	S451[s]; S669[s]
SBPase	yes[c,l]	C218[l]; C227[l]; C351[l]; C358[l]		yes[f]		yes[g]	C351[g]; C358[g]	C111[m,o]; C116[m,o]; C218[m,o]; C227[m,o]; C351[m,o]; C358[m,o]	T108[w]; S110[s,w,x]; T114[q,s,w,x]; S119[s,v,w,x]; T306[s]; S307[s,w]; T309[s]
RPE	yes[l]			yes[f]		yes[g]		C68[m]	S50[s]; T220[s]; S239[s]
RPI	yes[c,l]	C149[l]; C175[l]		yes[e,f]		yes[g]		C149[m,o]; C175[m,o]	S87[s]
PRK	yes[c,l]	C274[l]; C280[l]	C47-C86[p] C274-C280[k]	yes[f]	C47[f]; C274[f]	yes[g]	C47[g]	C47[m,o]; C86[m,o]; C92[j,m,o]; C274[j,m,o]; C280[o]	T4[v]; T57[w]; S204[s]; S281[s,w]

CP12	yes[l]	C74[l];C82[l]; C117[l]; C126[l]						C74[j,m,o]; C82[m,o]; C117[j,m,o]; C126[m,o]	S52[s]; T78[s]; S79[s,v,w]; T88[s,w,u]; T108[s,w]; T110[s,w]
RCA	yes[l]	C148[l]; C196[l]; C255[l]; C289[l]		yes[f]		yes[g]	C196[g]; C289[g]	C148[m,o]; C196[j,m,o]; C255[j,m,o]; C289[o]	S45[s,t,u,v,w]; S53[r,s,t,u,v,w]; S85[s,v,w]; S86[s,v,w]; S96[s,v]; S163[s]; S390[s,v]; S400[s]; S401[s]; S407[s]

[a]*Amino acids numbering according to the full-length sequence of the v5.6 genome annotation. References are:*
[b]*Moreno and Spreitzer (1999)*.
[c]*Lemaire et al. (2004)*.
[d]*Marin-Navarro & Moreno (2006)*.
[e]*Michelet et al. (2008)*.
[f]*Zaffagnini, Bedhomme, Groni, et al. (2012)*.
[g]*Morisse, Zaffagnini, et al. (2014)*.
[h]*Morisse, Michelet, et al. (2014)*.
[i]*Zaffagnini et al. (2014)*.
[j]*Slade, Werth, McConnell, Alvarez, and Hicks (2015)*.
[k]*Thieulin-Pardo et al. (2015)*.
[l]*Perez-Perez et al. (2017)*.
[m]*McConnell et al. (2018)*.
[n]*Garcia-Murria et al. (2018)*.
[o]*Ford et al. (2019)*.
[p]*Gurrieri et al. (2019)*.
[q]*Wagner et al. (2006)*.
[r]*Lemeille, Turkina, Vener, and Rochaix (2010)*.
[s]*H. Wang et al. (2014)*.
[t]*Werth et al. (2017)*.
[u]*Roustan, Bakhtiari, Roustan, and Weckwerth (2017)*.
[v]*Roustan and Weckwerth (2018)*.
[w]*McConnell et al. (2018)*.
[x]*Werth et al. (2019)*.

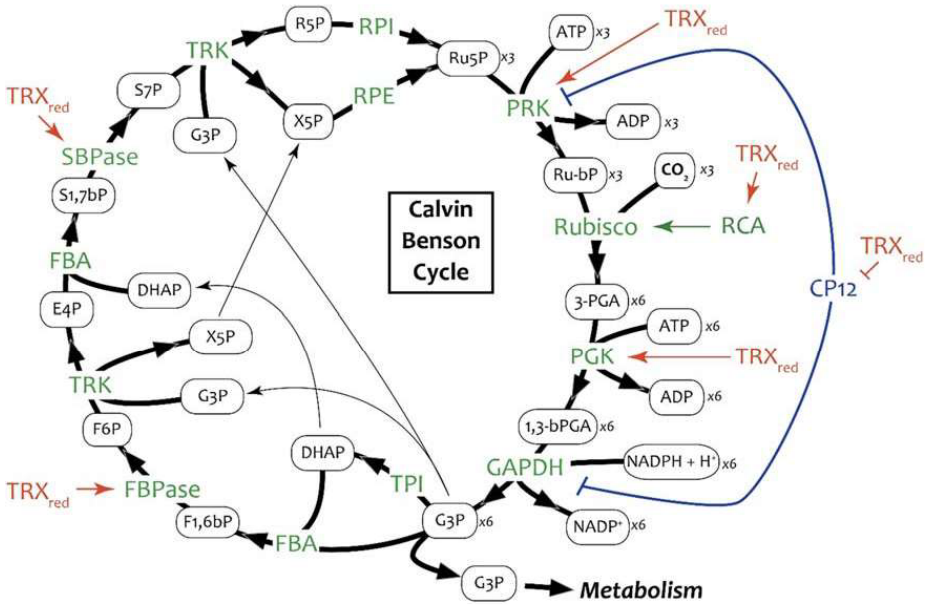

FIGURE 8.2 The Calvin-Benson cycle in *Chlamydomonas reinhardtii*. The 11 enzymes of the CBC are indicated in green. Four enzymes are activated in the light by reduced thioredoxin (TRXred), CP12 activity is bracketed by a blue line. Metabolites are indicated in black ellipses with their global stoichiometry. The carbon input (CO_2 in bold) and output (G3P) toward metabolism are indicated. **Enzymes**: *Rubisco*, ribulose-1,5-bisphosphate carboxylase/oxygenase; *PGK*, phosphoglycerate kinase; *GAPDH*, glyceraldehyde-3-phosphate dehydrogenase; *TPI*, triose phosphate isomerase; *FBA*, fructose-1,6-bisphosphate aldolase; *FBPase*, fructose-1,6-bisphosphatase; *TRK*, transketolase; *SBPase*, sedoheptulose-1,7-bisphosphatase; *RPE*, ribulose-5-phosphate 3-epimerase; *RPI*, ribose-5-phosphate isomerase; *PRK*, phosphoribulokinase. **Metabolites:** *Ru-bP*, ribulose-1,5-bisphosphate; *3-PGA*, 3-phosphoglycerate; *1,3-bPGA*, 1,3-bisphosphoglycerate; *G3P*, glyceraldehyde-3-phosphate; *DHAP*, dihydroxyacetone phosphate; *F1,6bP*, fructose-1,6-bisphosphate; *F6P*, fructose-6-phosphate; *X5P*, xylulose-5-phosphate; *E4P*, erythrose-4-phosphate; *S1,7bP*, sedoheptulose-1,7-bisphosphate; *S7P*, sedoheptulose-7-phosphate; *R5P*, ribose-5-phosphate; *RuP*, ribulose-5-phosphate.

the RuBP analog 2-carboxyarabinitol-1,5-diphosphate (CAP) and magnesium (Taylor, Backlund, Bjorhall, Spreitzer, & Andersson, 2001). CAP is bound by the B domain of one LSU through residues Lys175, Lys177, His294, Arg295, His327, Lys334, Leu335, Ser379, Gly380, Gly381, Gly403, and Gly404 and by the N domain of a neighboring LSU through residues Glu60, Thr65, Trp66, and Asn123. Thr173, carbamylated Lys201, Asp203, and Glu204 interact with magnesium. The betaA-betaB loop is different in the algal structure compared to its spinach ortholog (1RCX), and the residues of the loop are important for the holoenzyme function.

8.5.9 Phosphoglycerate kinase

An in silico three-dimensional model of reduced *Chlamydomonas* PGK1 was built from the ortholog crystal structure from *Bacillus stearothermophilus*, which has the highest sequence identity in the structural database (Morisse, Michelet, et al., 2014). PGK is composed of two domains adopting the Rossman fold and connected by a hinge containing a long α-helix. Consistent with most reported PGK structures, *Chlamydomonas* PGK is a monomer in solution. Its oxidation was evaluated by energy minimization. Molecular dynamics suggested that redox control of *Chlamydomonas* PGK is exerted by the modulation of domain—domain contacts through the hinge dynamics. The Cys227-Cys361 disulfide bridge of oxidized PGK rigidifies the enzyme, preventing it from attaining the optimal closed conformation.

8.5.10 Glyceraldehyde-3-phosphate dehydrogenase

No experimental structure is yet available for *Chlamydomonas* A_4-GAPDH, but the ortholog from Arabidopsis is a proxy of high sequence identity (>80%). *Chlamydomonas* A_4-GAPDH is most probably folded as Arabidopsis 3K2B (Fermani et al., 2010) that is itself highly similar to spinach 1JN0 (Fermani et al., 2001) and 1RM4

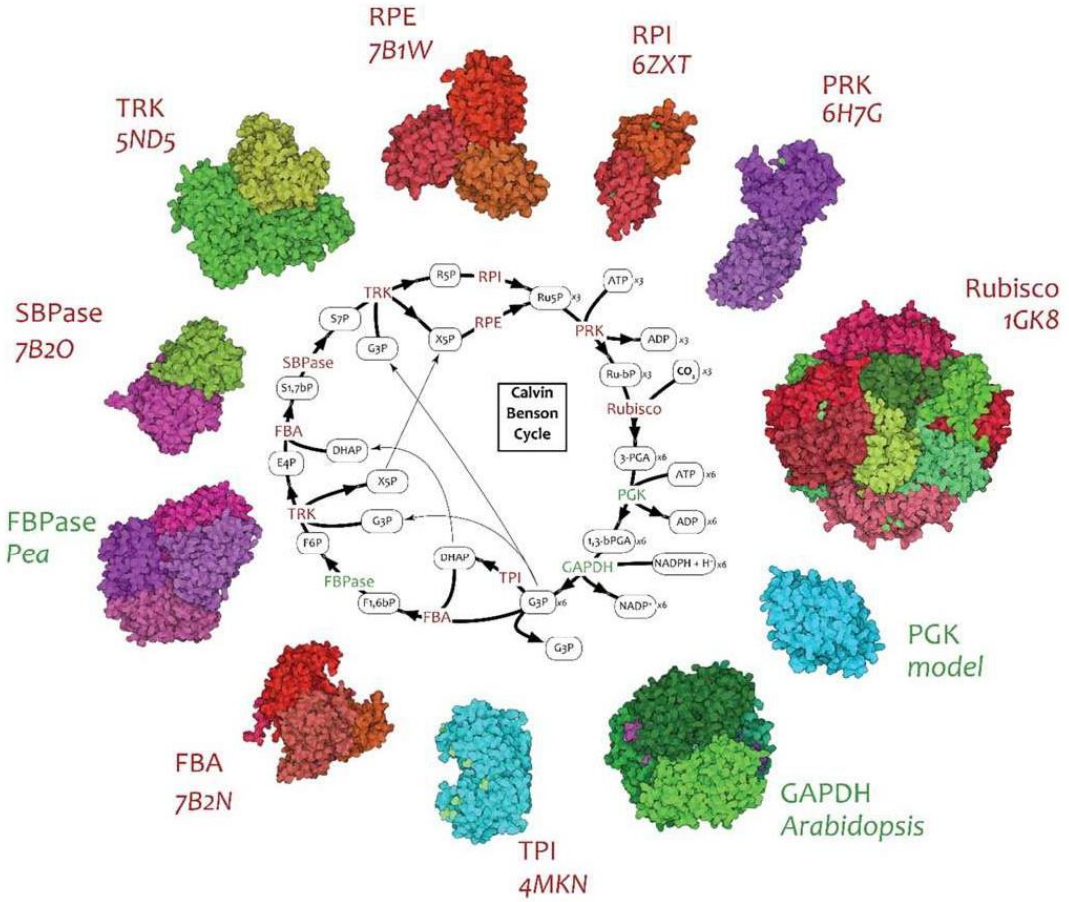

FIGURE 8.3 Structural components of the Calvin-Benson cycle. Metabolites are indicated in black with stoichiometric ratio for the fixation of $3 \times CO_2$ into $1 \times$ glyceraldehyde. Metabolites and enzymes are identified as in Fig. 8.2. Known experimental structures (red) or models (green) of the Calvin-Benson enzymes in *Chlamydomonas* are represented with Illustrate software (Goodsell, Autin, & Olson, 2019). Protein Data Bank (PDB) identifiers 1GK8 (Rubisco), 4MKN (TPI), 7B2N (FBA), 5ND5 (TRK), 7B1W (RPE), 6H7G (PRK), 7B2O (SBPase), and 6ZXT (RPI) are indicated near their respective representation.

(Sparla et al., 2004). The GAPDH monomer is composed of two domains: an amino-terminal NADP-coenzyme binding domain with an α/β Rossman fold into which is inserted a catalytic domain folded as an eight-stranded antiparallel β-sheet and two α-helices. An S-loop protrudes from the β-sheet and contacts NADP nicotinamide. GAPDH monomers assemble into a tetrameric dimer of dimers. The structure of the higher-order redox-controlled assemblies of GAPDH with PRK will be discussed in the next section.

8.5.11 Triose phosphate isomerase

The crystal structure 4MKN of *Chlamydomonas* TPI was determined at 1.1 Å resolution (Zaffagnini et al., 2014). TPI folds as an α/β barrel typical of the TIM topology. The alternance of eight α-helices and eight β-strands defines a core parallel β-barrel surrounded by α-helices. TIM barrels are among the most abundant folds in proteins (Jansen & Gerstein, 2000). *Chlamydomonas* TPI is homodimeric, with the enzymatic site located near the dimer interface and the catalytic residues at the carboxy-pole of the β-barrel from each protomer. Because it is the most exposed to solvent

among the five cysteines of TPI, Cys219 is the most probable site of glutathionylation and nitrosylation, although these modifications barely affected catalytic properties in vitro (Zaffagnini et al., 2014).

8.5.12 Fructose-1,6-bisphosphate aldolase

The crystal structure 7B2N of *Chlamydomonas* FBA was recently determined by the authors (Le Moigne, Sarti, et al., 2021). FBA folds as an α/β TIM barrel supplemented by a β-sheet of two antiparallel strands and a pair of carboxy-terminal α-helices. The active site residues sit at the carboxy-pole of the β-barrel, where they contribute an electropositive cleft adapted to the binding of the phosphates of the substrates. *Chlamydomonas* FBA is a homotetramer with one dimer interface at the opposite side of the active site and the other dimer interface involving the additional two-strand β-sheet. The contacting subunit is located 18 Å away from the active site, with the additional β-sheet likely controlling accessibility to the catalytic pocket. All six cysteine residues of FBA have been reported to be redox modified (Table 8.3). Cys256 is the most exposed to solvent, in comparison to Cys58 and Cys142 whose reported susceptibility to nitrosylation may result from conformational changes or local unfolding. Arabidopsis cytosolic Ald2 is irreversibly inactivated by the cysteine nitrosylating agent GSNO, while GSSG partially and reversibly inactivated the enzyme (van der Linde et al., 2011). Disulfide bridge formation rearranges the active site of a metazoan aldolase into an inactive conformation (Heyduk, Michalczyk, & Kochman, 1991).

8.5.13 Fructose-1,6-bisphosphatase

No experimental crystal structure is available for *Chlamydomonas* FBPase, but a faithful homology model can be assumed from spinach or pea photosynthetic orthologs, 1SPI and 1D9Q, respectively (Chiadmi et al., 1999; Villeret, Huang, Zhang, Xue, & Lipscomb, 1995). FBPases fold into two domains, each composed of an antiparallel β-sheet surrounded by α-helices; these monomers assemble into a dimer of dimers. As mentioned in the previous section, a regulatory disulfide bridge between Cys153 and Cys173 of pea FBPase stabilizes a disordered 20-amino acid peptide segment into an ordered α-helix, displacing two β-strands that eventually disrupt the binding of the catalytic Mg^{2+} in the catalytic pocket located 20 Å away. Reduction of the regulatory disulfide bridge restores the disordered character of the peptidic segment and Mg^{2+} binding. FBPase is exclusively reduced by TRXf due to complementary FBPase-TRXf interaction surfaces. Electrostatic potential appears to be the main driver of this selectivity, with a marked electropositive potential around the TRXf redox site that mirrors an electronegative potential around the FBPase redox regulatory site (Lemaire et al., 2018).

8.5.14 Sedoheptulose-1,7-bisphosphatase

A photosynthetic SBPase structure 5IZ3 was first reported for the moss Physcomitrella (Gutle et al., 2016). We recently solved the crystal structure 7B2O of the *Chlamydomonas* ortholog. SBPase shares the same fold and has high structural similarity to FBPase, with an average distance of 1.241 Å between equivalent residues for the alignment of *Chlamydomonas* SBPase with pea FBPase. Meanwhile, the peptidic extension bearing the regulatory disulfide Cys153-Cys173 in the pea FBPase is shorter and devoid of cysteine in SBPase. Conversely, disulfide bridged Cys115 and Cys120 are located in a distinct β-hairpin motif in *Chlamydomonas* FBPase. The unique structural features of the redox regulatory disulfides in each enzyme argues in favor of a distinct phylogenetic origin between SBPase (archeal ancestry) and FBPase (bacterial ancestry) (Gutle et al., 2016).

8.5.15 Transketolase

The crystal structures 5ND6 and 5ND5 of *Chlamydomonas* TRK were respectively determined in the apo state or bound to the cofactor thiamine pyrophosphate (TPP) and Mg^{2+} (Pasquini et al., 2017). TRK is composed of three α/β domains, each centered on a five-stranded β-sheet interspersed by α-helices; the monomer assembles into an intricate homodimer. The amino-terminal domain binds Mg^{2+} and the TPP pyrophosphate (PP) moiety. The middle domain binds the TPP pyrimidine (Pyr) moiety. The PP domain of one dimer subunit and the Pyr domain of the other subunit both participate in the formation of one active site. By comparison with the apoprotein structure, the binding of TPP-Mg^{2+} appears to stabilize an ordered conformation on two peptidic segments of the active site. The C-terminal domain is neither involved in cofactor interaction nor dimerization. Oxidation of TRK-TPP-Mg^{2+} bears no catalytic consequence even though the cysteine pairs Cys173-Cys220, Cys204-Cys210, and Cys470-Cys484 are within disulfide

bonding distance. However, TRK-TPP is reversibly inactivated by oxidized dithiothreitol (DTTox) treatment with a sensitivity that depends on the Mg^{2+} concentration. Indeed, >80% TRK activity is preserved from DTTox-mediated inactivation in the presence of 2 mmol/L Mg^{2+} while the same oxidative treatment inactivates >50% of the enzyme at Mg^{2+} concentrations lower than 0.05 mmol/L (Pasquini et al., 2017). Illumination of chloroplasts causes an increase in the stroma Mg^{2+} concentration above the TRK-protection threshold value of 1–3 mmol/L (Portis & Heldt, 1976), which helps coordinate photosystem activity with the activity of the CBC.

8.5.16 Ribose-5-phosphate isomerase

The crystal structure 6ZXT of *Chlamydomonas* RPI was determined at 1.40 Å resolution (Le Moigne, Crozet, Lemaire, & Henri, 2020). RPI is a homodimer and each subunit folds as two domains: a Rossman fold at the amino-terminus and an ACT domain at the carboxy-terminus. The ACT (Aspartate kinase, Chorismate mutase, and TyrA) domain is composed of a four-stranded antiparallel β-sheet and two α-helices and determines the dimeric quaternary state. The active site is remote from the dimerization interface and 13 residues contribute to an electropositive pocket of ideal dimensions to accommodate the ribose-5-phosphate substrate. At the opposite side of the protein, an extended electronegative surface runs along both protomers and is a candidate platform to interact with electropositive partner proteins. Among four cysteines of *Chlamydomonas* RPI, the most solvent-exposed is Cys175, located near the dimer interface. Moreover, Thr61 and Ser87 were suggested to be phosphorylated in *Chlamydomonas* protein extracts (McConnell et al., 2018; Wang et al., 2014). The Thr61 side chain hydroxyl sits inside the enzymatic pocket and phosphorylation of this residue would prevent substrate binding.

8.5.17 Ribulose-5-phosphate 3-epimerase

The authors recently determined the high-resolution crystal structure 7B1W of *Chlamydomonas* RPE. RPE folds as an α/β TIM barrel with a metal ion at the carboxy-pole of the barrel. His72, Asp74, His105, and Asp216 (full-length sequence numbering) coordinate the metal that was identified as Zn^{2+} in the ortholog structures 1H1Z and 2FLI. Three loops, A, B, and C, project from strands 1, 2, and 6 and delimit the active site cavity around the Zn^{2+}. Ser50, Ser239, and Thr220 were reported to be phosphorylated (McConnell et al., 2018; Wang et al., 2014). Their side chains are located at 10–17 Å from the Zn^{2+}, at the entrance of the catalytic pocket where their phosphorylation would decrease the affinity for ribulose-5-phosphate by steric and charge repulsion effects. RPE assembles as a homohexamer composed of a trimer of dimers. The trimer neighbor of each protomer pushes the aforementioned loop C toward the catalytic site, reducing its accessibility for substrate. Hence, homohexamerization is likely to increase the Michaelis constant of *Chlamydomonas* RPE. An extra α-helix caps the amino-pole of the barrel. This cap, bearing the *Chlamydomonas*-specific Cys37 residue, is in a solvent-exposed environment. Cys68, Cys150, and Cys204 are each located 10–18 Å from Cys37 and may form disulfide bridges if Cys37 is given enough flexibility. All four of these cysteines may also be modified, for example, by nitrosylation or glutathionylation, given their accessibility in the model. The effect of such redox modifications is, however, hard to rationalize because all cysteines are >18 Å from the active site, separated from it by the depth of the barrel.

8.5.18 Phosphoribulokinase

Experimental structures of oxygenic photosynthetic PRKs were reported for *Chlamydomonas* (6H7G), Arabidopsis (6H7H, 6KEW, 6KEX), and Synechococcus (6KEV, 6HZK, 6HZL) (Gurrieri et al., 2019; Wilson, Hayer-Hartl, & Bracher, 2019; Yu et al., 2020). PRK is an elongated homodimer with a subunit-to-subunit continuous mixed β-sheet of 20 strands (10 strands per subunit), defining a rod-like molecular shape. The active site lies at the extremities of the rod in a shallow cleft. The phosphate group of the substrate is expected to bind Arg64, Arg67, Tyr103, and His105 that bind a sulfate in the crystal structure. Two cysteine pairs are amenable to disulfide bonding: Cys16-Cys55 in the catalytic cleft and Cys243-Cys249 near the dimerization surface. The formation of the Cys16-Cys55 disulfide would reduce catalytic efficiency (A. Yu et al., 2020) while the redox effect of the disulfide near the dimer interface may modify the flexibility of the assembly.

No experimental structures of PGK, GAPDH, FBPase, CP12, and RCA from *Chlamydomonas reinhardtii* have been reported at the date of this review. Although computational homology models predict the structure of globular proteins aligned onto models from other organisms or cytosolic pathways, these predictions may contain local erroneous predictions that are hard to discriminate. A complete understanding of photosynthetic carbon fixation thus requires a

description of the remaining structures at high resolution. When X-ray crystallography proves difficult for disordered, dynamic, or generally hard to crystallize objects, the other structural tools such as single-particle cryo-electron microscopy (cryo-EM) or nuclear magnetic resonance (NMR) will likely provide solutions. To achieve complete modeling of the carbon flow in the cycle, the exact catalytic mechanisms of each step of the CBC will need to be investigated. This includes but is not limited to; the type of catalysis, multiple substrate/product reaction orders, allosteric effects, affinity constants, and catalytic constants. Supplementary controls over enzymes such as excess product or excess substrate inhibition are likely to occur. Suborganellar protein localization in the pyrenoid, in translational T-zones (Sun, Valente-Paterno et al., 2019) or at the thylakoid membranes (Zerges, Wang, & Rochaix, 2002) may be analyzed by in situ cryogenic electron tomography. Nevertheless, supramolecular assembly of CBC enzymes is likely an important determinant of the rate of carbon fixation, as reviewed in the next section.

8.5.18.1 Supramolecular organization of the Calvin-Benson cycle

Past work in vivo and in vitro repeatedly suggested that CBC enzymes form higher-order complexes (Anderson et al., 1995; Gontero, Mulliert, Rault, Giudici-Orticoni, & Ricard, 1993; Jebanathirajah & Coleman, 1998; Rault, Giudici-Orticoni, Gontero, & Ricard, 1993; Romanova, Semenova, Ignat'ev, Novichkova, & Fomina, 2016; Sainis & Harris, 1986; Suss, Arkona, Manteuffel, & Adler, 1993; Teige, Melzer, & Suss, 1998), either for allosteric control of reaction rates (Ricard, Giudici-Orticoni, & Buc, 1990; Ricard, Giudici-Orticoni, & Gontero, 1994), for controlling the geometry of active sites (Avilan, Gontero, Lebreton, & Ricard, 1997b; Graciet et al., 2004; Graciet, Lebreton, Camadro, & Gontero, 2002; Lebreton et al., 2003) or for partitioning the enzymes into catalytically optimized assemblies (H. Wang et al., 2019; Wunder, Cheng, Lai, Li, & Mueller-Cajar, 2018). However, only the structures of PRK-CP12-GAPDH complex (6GVE and 6KEZ) and Rubisco condensates (6HBC, 7JFO, and 7JSX) are available as samples of the supramolecular organization of the CBC (McFarlane et al., 2019; Wang et al., 2019; Yu et al., 2020).

In the pyrenoid, Rubisco–Rubisco interaction is mediated by the intrinsically disordered protein EPYC1, which contains five Rubisco small-subunit (RbcS) sequence-repeated binding regions (He et al., 2020; Mackinder et al., 2016) (Vol 2, Chapter 7). In the 7JFO complex, EPYC1 repeat 1, folds as an α-helix that binds RbcS via three salt bridges (EPYC1-RbcS) Arg64-Glu24, Glu66-Arg91, Arg71-Asp23, and a hydrophobic interface composed of EPYC1 residues Trp63, Leu67, and Leu70, and RbcS residues Met87, Leu90, and Val94. Each EPYC1 region has a millimolar affinity for Rubisco along with a high dissociation constant, accounting for the dynamic character of the pyrenoid matrix.

PRK homodimers and GAPDH homotetramers form a supramolecular complex with the small, intrinsically disordered proteins CP12, which act as connectors (Avilan et al., 2012; Gontero & Avilan, 2011; Graciet et al., 2003; Graciet et al., 2004; Launay et al., 2016; Lebreton, Andreescu, Graciet, & Gontero, 2006). The formation of the PRK-CP12-GAPDH complex allows for fine regulation of PRK and A_4-GAPDH activities (reviewed in Trost et al., 2006). CP12 is an intrinsically disordered protein, especially when fully reduced, and upon oxidation, the formation of two disulfide bonds within the polypeptide decreases this disorder (Graciet et al., 2003; Marri et al., 2008; Marri et al., 2010). In Arabidopsis, the C-terminal disulfide has a redox potential comparable to GAPB ($E_m = -352$ mV at pH 7.9 (Marri et al., 2008)) allowing reduction of CP12 disulfides by TRXs, although with no strict specificity (Marri et al., 2009). In both Arabidopsis (Fermani et al., 2012; Marri et al., 2008) and *Chlamydomonas* (Kaaki, Woudstra, Gontero, & Halgand, 2013), A_4-GAPDH binds two CP12 molecules. However, while this binding is very strong in *Chlamydomonas* (K_D 0.4 nM) and leads to inhibition of GAPDH activity (Erales, Mekhalfi, Woudstra, & Gontero, 2011), it is much weaker in Arabidopsis (K_D 0.2 μM, (Marri et al., 2008)) and barely affects GAPDH activity (Marri et al., 2008; Marri, Trost, Pupillo, & Sparla, 2005). Nevertheless, binding of two PRK molecules to the GAPDH/CP12 complex results in strong inhibition of both enzymes (Marri et al., 2005). PRK is also inhibited in the supercomplex because catalytic Arg64 residue is mobilized for CP12–GAPDH interaction (Avilan, Gontero, Lebreton, & Ricard, 1997a). Therefore PRK-CP12-GAPDH complexes accumulate in the dark and lead to inhibition of PRK and GAPDH activities, while upon illumination, TRX reduction causes rapid dissociation of the complex and recovery of enzyme activities (Marri et al., 2009). Experimental structures of GAPDH-CP12-PRK were determined from Thermosynechococcus (6GVE) and Arabidopsis (6KEZ) (McFarlane et al., 2019; Yu et al., 2020); the Arabidopsis structure is likely to resemble that of *Chlamydomonas*. In the crystal asymmetric unit, GAPDH-CP12-PRK is modeled with two oxidized PRK dimers, four oxidized CP12, and two GAPDH tetramers. In this complex, CP12 bears two TRX-dependent disulfides at Cys22-Cys31 and Cys64-Cys73 and is folded into three α-helices. CP12 is inserted in the PRK catalytic cleft on one side and in between two GAPDH subunits on the other side (Fig. 8.4). In GAPDH, five residues from helix 254–269, two loop residues at positions 252–253, and one at position 305 come into contact with seven residues of PRK at positions 248, 283, 286, 299–301, and 308. They reinforce the stability of the ensemble.

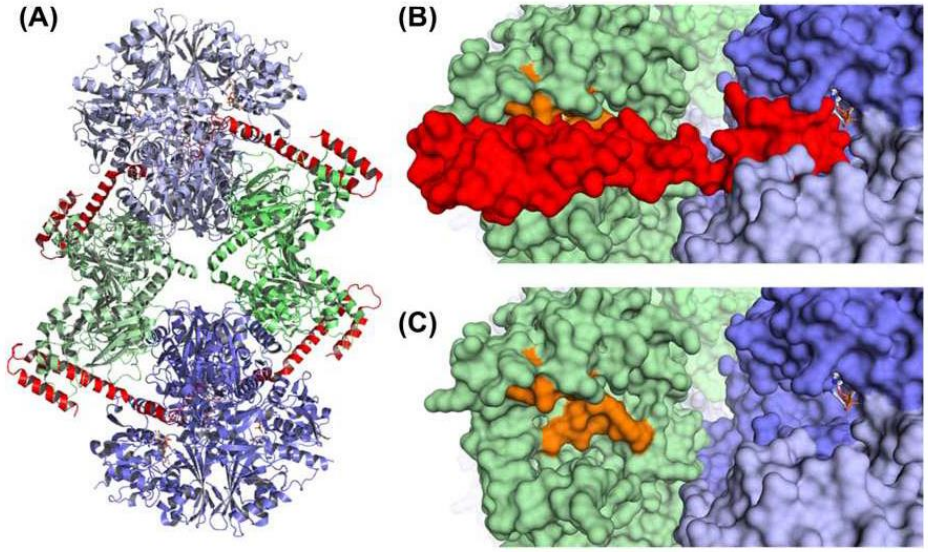

FIGURE 8.4 Crystal structure of GAPDH-CP12-PRK complex. (A) Cartoon representation of the crystal structure of *Arabidopsis thaliana* GAPDH-CP12-PRK complex (PDB ID: 6KEZ (Yu et al., 2020)) with GAPDH tetramers colored in blue, CP12 in red, and PRK dimers in green. (B) Surface representation of the insertion site of CP12 protein colored in red in the GAPDH and PRK active pockets. PRK is colored as in (A) with residues involved in the fixation of phosphate and ATP in orange. Two GAPDH subunits are colored in shades of blue with NAD in white. (C) Same representation as in (B) without CP12.

8.6 Energetic considerations and the dual purpose of NADPH turnover

8.6.1 NADPH and ATP: the assimilatory power duo

Photoreduction of $NADP^+$ to generate NADPH serves an important dual purpose, firstly, to provide assimilatory power for the CBC and secondly, to maintain linear electron flow. With three rounds of the CBC, NADPH donates 12 hydrogens of "reducing power" during the reductive phase to produce 6 glyceraldehyde-3-phosphate (GAP) from the 6 3-phosphoglyceric acid (3-PGA) molecules generated by the carboxylation reaction. $NADP^+$ regenerated as a consequence of the use of reductant in CO_2 assimilation is required to maintain linear electron flow because photosynthetic electron transfer and water oxidation cannot proceed without a terminal electron acceptor. Thus oxidation of the primary electron donor for photosynthesis, water, renews the NADPH pool, while the CBC consumes the NADPH produced by electron transport, re-establishing the $NADP^+$ pool. A limitation in $NADP^+$ can be observed at the onset of illumination, in high light, in fluctuating light, in a transition from dark to light under anaerobic conditions, and under nutrient deprivation (see references in the rest of this section). This situation creates a high NADPH/$NADP^+$ ratio and ultimately results in the production of ROS and damage to PSI. However, in contrast to PSII photoinhibition, this is rarely witnessed for *Chlamydomonas* under physiological conditions (Chaux, Peltier, & Johnson, 2015). Pathways that contribute to the NADPH/$NADP^+$ balance have been identified using forward and reverse genetics combined with photosynthetic physiology and metabolite measurements. In recent years, this knowledge has been enhanced by transcriptomic, proteomic, and metabolomic studies.

ATP is the other component of the electron transport-derived, assimilatory "power duo." Three cycles of the CBC require high energy injection of 18 phosphates (from ATP), into two separate reactions of the reductive phase. ATP limitation induces a different set of regulatory pathways in the light than that of an elevated NADPH/$NADP^+$ ratio, including photoprotective heat dissipation at the level of PSII (nonphotochemical quenching). ATP production is not a redox reaction; its synthesis is fueled by the proton gradient generated by both linear and cyclic electron flows and is also strongly dependent on the levels of its substrates, ADP and Pi (for a comprehensive discussion, see Walker, (1992)). Furthermore, although NADPH regeneration is often treated separately from ATP production and limitation, the two are intertwined. NADPH in balance with $NADP^+$ facilitates cyclic electron flow that produces a proton gradient and

ATP synthesis (Alric, 2010). Additionally, ATP and NADPH are required in stoichiometric quantities (3 ATP for 2 NADPH) for CO_2 assimilation by the CBC, with more ATP required under CO_2 limiting conditions (Allen, 2003; Lucker & Kramer, 2013), which means that an ATP deficiency will have a direct effect on the consumption and turnover of NADPH. Thus it can be difficult to separate the outcome of ATP limitation from those of NADPH overproduction in a "chicken-and-egg" scenario.

8.6.2 Pathways that contribute to maintenance of optimal NADPH/NADP$^+$ pools in the light

8.6.2.1 Detoxification pathways

A sustained increase in the NADPH/NADP$^+$ ratio leads to overreduction of PSI donor side electron carriers. Oxygen radicals, principally hydrogen peroxide (H_2O_2) and the superoxide anion ($O_2^{\bullet-}$), are formed in the iron-sulfur centers of PSI, FDX, and stromal flavodehydrogenases via nonenzymatic O_2 photoreduction. These reactions occur at all light intensities but increase with elevated light intensity; water–water pathways (considering the first H_2O to be the primary electron donor to PSII and oxygen the electron acceptor to regenerate H_2O) have evolved for detoxification of the ROS hydrogen peroxide and superoxide anion radical that may be formed by the Mehler (O_2 to H_2O_2 to H_2O) or Asada (O_2 to $O_2^{\bullet-}$ to H_2O_2 to H_2O) reactions (Fig. 8.5). These pathways are highly conserved in oxygenic phototrophs and the major detoxification enzymes for these reactions have been characterized in *Chlamydomonas* chloroplast: Fe-superoxide dismutase (Fe-SOD1 of three isoforms) (Kitayama, Kitayama, Osafune, & Togasaki, 1999), Mn-SOD3

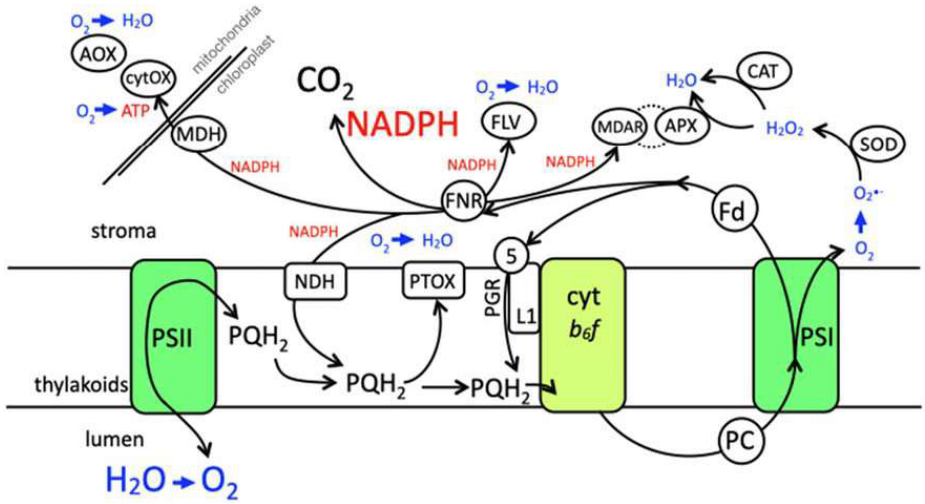

FIGURE 8.5 The photosynthetic electron transport chain and the pathways that consume and maintain NADPH and its homeostasis. In the chloroplast, electrons are provided for the first charge separation through Photosystem II (PSII) by the water-splitting reaction giving rise to oxygen (O_2) as a side product. Plastoquinol (PQH_2), cytochrome b_6f complex (cytb_6f), and plastocyanin (PC) are intersystem electron carriers that deliver electrons for a second charge separation through Photosystem I (PSI) in the thylakoid membrane. This linear electron flow passes to the stromal electron carriers, ferredoxins (Fd) and Ferredoxin NADP Reductase (FNR), to reduce the terminal electron acceptor NADP$^+$ and produce NADPH. The major consumer of NADPH is the CBC for CO_2 fixation. When NADPH:NADP$^+$ ratios are high, Fd is redirected toward a recycling of electrons around cytb_6f and PSI via the Proton Gradient Regulation (PGR5/PGRL1) pathway, referred to as cyclic electron flow. NADPH can also be directly recycled via the type 2 NADPH Reductase (NDH) and the PQ pool also by a cyclic electron flow around PSI. Plastid terminal oxidase (PTOX) is an oxygen valve that controls the equilibrium between the PQH_2 pool and NADPH (stromal redox poise) between dark and light. At the onset of light, the Flavodiiron (FLV) proteins catalyze a rapid O_2 valve for NADPH oxidation at the acceptor side of PSI that transfers electrons to make H_2O. The malate NADP dehydrogenase (MDH) can also rapidly metabolize NADPH in exchange for a transportable organic acid to transfer reducing power to the mitochondria for consumption of O_2 to drive ATP production (cytochrome oxidase pathway, cytOX) or, more likely during active photosynthesis under saturating light, the alternative oxidase (AOX) pathway to complete a water–water cycle. When PSI and the PSI stromal carriers have no acceptors, the redox-active iron-centers spontaneously react with oxygen to produce superoxide anion radical ($O_2^{\bullet-}$). Superoxide dismutase detoxifies $O_2^{\bullet-}$ to H_2O_2 followed by further detoxification to water via catalase (CAT) and the ascorbate peroxidase (APX)/monodehydroascorbate reductase pathway (MDAR) that consumes NADPH. The size of the font represents the importance of the pathway, the black lines with arrows represent electron flows and the discontinuous lines represent multiple enzymatic reactions.

(of five isoforms) under Fe limiting conditions (Page et al., 2012), catalase (CAT1 of two isoforms) (Michelet, Roach et al., 2013), and ascorbate peroxidase 4 (APX4 of five isoforms) (Kuo, Cai, & Lee, 2020), which uses an iron and an ascorbate to reduce H_2O_2 to H_2O. Monodehydroascorbate reductase (MDAR1) (Yeh et al., 2019) recycles oxidized ascorbate back to its reduced form at the expense of NADPH. In the *Chlamydomonas* genome, homologs for both dehydroascorbate reductase (one isoform) and gluthathione reductase (two isoforms) are found but remain uncharacterized. H_2O_2 can block redox activation of CBC enzymes, so its detoxification is vital to maintain CO_2 fixation (Charles & Halliwell, 1981). However, in *Chlamydomonas*, catalase is downregulated by light and is only activated after APX4, allowing for a threshold level of H_2O_2 accumulation, which is required to activate retrograde protection pathways (Shao et al., 2008). The deletion of the aforementioned genes results in high light photosensitive phenotypes in *Chlamydomonas*.

8.6.2.2 Interactions between photosynthesis and respiration

In steady state mixotrophic or phototrophic conditions, O_2 photoreduction by mitochondrial respiration due to the exchange of reductant and photosynthate between the chloroplast and mitochondria is observed. The relationship between photosynthesis and respiration is dependent on light intensity; at low light intensities, there is a break in the net O_2 exchange rate that has been confirmed as an inhibition of respiration by photosynthesis in the light known as the Kok effect (Kok, 1949). In different algal species, the Kok effect is enhanced by preferential excitation of PSI at 695 nm (Hoch, Owens, & Kok, 1963; Jones & Myers, 1963). The implications of the control of the Kok effect by PSI activity have not yet been fully understood, but the ADP:ATP ratio and cyclic electron flow were ruled out as the controlling factors (Healey & Myers, 1971; Peltier & Thibault, 1985). The preferred hypothesis to explain the inhibition of respiration at low light intensities is that there is an import of reductant toward the chloroplast and photosynthetic electron transport and away from mitochondrial reactions. This would occur through an exchange of NADH for NADPH via a metabolite transport mechanism, such as the malate shuttle (see section below).

As light intensities increase and in the presence of an active CBC, respiration increases in accord with the light, which is known as light-enhanced dark respiration (LEDR). Measures of respiration after a light treatment show a good correlation with CO_2 uptake in the light (Peltier & Thibault, 1985; Xue, Gauthier, Turpin, & Weger, 1996). This increase in respiration is due to the export of photosynthate in the form of triose phosphate to the mitochondria as well as an increase in alternative oxidase (AOX) activity. The minimum rate of respiration in the light is set by the requirement for carbon skeletons for amino acid biosynthesis (Raven & Beardall, 2003). A respiratory-defective mutant cannot grow in the dark on acetate, but is however viable in the light, just as the inverse is true for nonphotosynthetic mutants, which are able to grow on acetate in the dark but not in the light with CO_2 (Levine, 1960; Matagne, Michel-Wolwertz, Munaut, Duyckaerts, & Sluse, 1989). The interdependence between these two energetic organelles is not critical for survival but serves to optimize and conserve energy in *Chlamydomonas*.

Inhibiting mitochondrial activity affects the chloroplast redox poise. This is observed under anaerobic light conditions (Kessler, 1973) or via the addition of mitochondrial electron transport inhibitors. Myxothiazole and Antimycin A inhibit the cytochrome *bc1* complex and salicylhydroxamic acid (SHAM) inhibits the alternative oxidase in *Chlamydomonas* (Gans & Rebeille, 1990; Rebeille & Gans, 1988). AOX (two mitochondrial isoforms) has a strong activity in *Chlamydomonas* (Weger, Guy, & Turpin, 1990), and its uncoupling effect in mitochondrial respiration has been shown to modulate the redox state of both plastoquinone and ubiquinone under high light conditions (Kaye et al., 2019; Mathy et al., 2010). The reducing effect on the PQ pool when mitochondrial respiration is inhibited is due to ATP depletion in the cell, which results in the stimulation of the upper half of glycolysis and the loss of consumption of NADH by oxidative phosphorylation. A reduced PQ pool results in a photoprotective shift toward State 2 (LHCII antennae attach to PSI) (Allen, Bennett, Steinback, & Arntzen, 1981), while, interestingly, cells trapped in state I cannot evolve oxygen when respiration is inhibited by low oxygen concentrations (Forti, 2008). Numerous studies have shown that state transitions modulate the capacity for NADPH and ATP production in the chloroplast in response to both respiratory status and nitrogen metabolism (Bulté, Gans, Rebéillé, & Wollman, 1990; Cardol et al., 2009; Forti, Furia, Bombelli, & Finazzi, 2003; Turpin, 1991). Active NH_4 metabolism increases the NADPH/$NADP^+$ ratio and the cells are maintained in State 2; under these conditions, the ATP/NADPH ratio in the chloroplast increases dramatically, with a resulting decrease in CO_2 fixation and an increase in AOX activity (Gauthier and Turpin, 1997).

8.6.2.3 Starch, oxidative pentose phosphate pathway, and glycolysis in plastid metabolism

In *Chlamydomonas* chloroplasts, proteomic studies confirm that the upper half of glycolysis is compartmentalized to the plastid (Terashima et al., 2011). In conditions where NADPH is forcibly depleted from the plastid using inhibitors

of photosynthesis and anaerobic incubation, measurements of PSI P_{700} oxidation prove that NADPH can be provided by the conversion of G3P to 3PGA in glycolysis (Johnson & Alric, 2012). The chloroplast-localized OPPP can be considered an alternative pathway to this "upper half" of glycolysis: G6P can be converted to F6P by phosphoglucose isomerase in the case of glycolysis or oxidized to 6-phosphoglucolactone by G6P-dehydrogenase as a part of the OPPP, yielding two molecules of NADPH. The activity of glycolysis under phototrophic or mixotrophic conditions was found to be seven times greater than that of the OPPP (Klein, 1986). G6P-dehydrogenase activity is inhibited by high levels of NADPH and RuBP (Lendzian & Bassham, 1975) and subject to light-driven redox modulation in *Chlamydomonas* (Farr et al., 1994). In Arabidopsis, reduction of the Cys99-Cys107 disulfide bond of chloroplastic G6PDH isoform P1, mediated by TRXf, causes inactivation of the enzyme (Nee et al., 2009). The cysteine pair is conserved in the *Chlamydomonas* G6PDH sequence, supporting a similar mechanism for redox regulation.

Starch accumulation provides another means to favorably adjust the NADPH/$NADP^+$ to avoid oxidative stress and maintain metabolites for the CBC. The *sta6* mutant that lacks ADP-glucose pyrophosphorylase activity (Zabawinski et al., 2001), and thus is unable to accumulate starch, has been extensively used to understand NADPH turnover in a genetic background devoid of the starch sink (see Chapter 1). In *sta6* grown phototrophically, CO_2 assimilation rates are gradually attenuated and an elevated NADPH/$NADP^+$ results in redirection of reducing equivalents that favors mitochondrial respiration (myxothiazole sensitive pathway) over carbon fixation and eventually leads to photoinhibition (Krishnan et al., 2015). In *sta6* under N-deficient mixotrophic conditions, NADPH imbalance is further accentuated and results in shunting fixed carbon toward the accumulation of soluble lipid as a reserve material (Li et al., 2010; Wang, Ullrich, Joo, Waffenschmidt, & Goodenough, 2009). As linear electron flow is downregulated, the source of NADPH for lipid synthesis is derived from the activity of the OPPP, for example transaldolase is significantly transcriptionally upregulated (Goodenough et al., 2014). Under N-deficient conditions, upregulated enzymes outside of the chloroplast include the glyoxylate cycle enzymes, Malate Synthase 1 and Isocitrate Lyase 1 for sustained acetate uptake as the cell transitions from mixotrophic to heterotrophic metabolism, as well as Phosphoenolpyruvate Carboxykinase 1 and Fructose Bisphosphatase1 (chloroplastic), which are implicated in the gluconeogenic flow of carbon toward starch; in the *sta6* mutant, carbon is shunted toward OPPP, presumably for NADPH generation in the light when linear electron flow and CBC cycle are downregulated (Blaby et al., 2013).

8.6.2.4 NADP Malate dehydrogenase

A high NADPH/$NADP^+$ ratio is linked to thioredoxin activation and redox regulation. A reduced stromal redox poise can be balanced by the transfer of reducing equivalents between compartments (Selinski & Scheibe, 2019) through the activities of enzymes like the chloroplast MDY, which is only found in the green lineage. The malate shunt operates in two directions, excess NADPH is consumed by the mitochondria to re-equilibrate the NADPH/$NADP^+$ ratio in phototrophic conditions or reductant is supplied to the chloroplast by the mitochondria in mixotrophic conditions (Boyle & Morgan, 2009; Chapman, Paget, Johnson, & Schwartz, 2015; Xue et al., 1996). The *Chlamydomonas* NADP-Malate Dehydrogenase 1 and 5 (MDY1 and MDY5 of five isoforms) are plastidial isoforms that reversibly reduces oxaloacetate to malate and oxidizes NADPH. The chloroplast MDY5 of *Chlamydomonas* is more rapidly activated than the analogous enzyme in higher plants, and this property is conserved in other green algal homologs of MDY5 (Lemaire et al., 2005). Malate is then transported via chloroplast envelope localized transporters to shunt reducing power to the cytosol/mitochondria (MDY3 cytosolic and MDY4 mitochondrial). *Chlamydomonas* has three homologs of Arabidopsis 2-oxoglutarate/malate transporter (Weber et al., 1995): one of them, the LCI20 (low-CO_2-inducible) protein, occurs in the chloroplast proteome (Terashima et al., 2011) and is significantly upregulated under mixotrophic conditions (Puzanskiy, Romanyuk, Kirpichnikova, & Shishova, 2020). In glyoxysomes, NAD-Malate Dehydrogenase (MDY2) has a secondary effect on NADPH consumption in the chloroplast under nitrogen-deprivation conditions in the light (Kong et al., 2018).

8.6.2.5 Chloroplastic NAD(P)H dehydrogenase, NDA-2

This monomeric type-2 NAD(P)H dehydrogenase enzyme is anchored to the thylakoid membrane and reduces plastoquinone at the expense of NAD(P)H (Desplats et al., 2009). Of the six NDA isoforms in *Chlamydomonas*, only NDA-2 and NDA-3 are found in chloroplasts (Terashima et al., 2011), the others all have predicted or characterized (NDA-1) localization to mitochondria (Lecler, Vigeolas, Emonds-Alt, Cardol, & Remacle, 2012). NDA-2 has a significantly higher affinity for NADH than NADPH, and it is hypothesized that a transhydrogenase may be required for its activity (Peltier, Aro, & Shikanai, 2016). NDA-2 is also considered the most probable enzyme for cycling electrons around PSI under mixotrophic or phototrophic aerobic light conditions, where PSII photochemistry is active and PGR5/PGRL1 are not activated (Alric, 2010). NDA-2 is considered nonphotochemical and nonelectrogenic, active in the dark in

chlororespiration (in tandem with the plastid terminal oxidase 2) (Jans et al., 2008), and in the light under sulfur and nitrogen deprivation to modulate the redox poise of the plastoquinone pool (Mignolet, Lecler, Ghysels, Remacle, & Franck, 2012; Saroussi, Wittkopp, & Grossman, 2016). Under N-deficient phototrophic conditions, a condition in which the plastid must receive reducing power from the mitochondria, NADPH recycling via NDA-2 is the main pathway to increase cyclic electron transfer around PSI to generate housekeeping ATP and maintain PSII quenching. Here, NADPH would be primarily generated by metabolic reactions, plastidial glycolysis as well as triose phosphate and malate import, rather than generated by linear electron flow (Saroussi et al., 2016).

8.6.2.6 Flavodiiron proteins and Mehler reaction

A rapid change in light conditions produces the chlorophyll fluorescence signature called the Kautsky effect that attests to a rapid accumulation followed by a consumption of reductant that feeds back along the whole of the electron transport chain. Mutants devoid of FLV proteins lose this transient kinetic and chlorophyll fluorescence proceeds directly to F_{max} (Chaux et al., 2017). This is driven by a light intensity starting around 100 μmol/m^2/s, suggesting that the process relies on a threshold of substrate to be activated. FLV proteins in a number of species function in oxygen photoreduction at the acceptor side of PSI to oxidize NADPH and donate the hydrogens to oxygen to yield water (Allahverdiyeva et al., 2013). FLVA/B are soluble proteins that form heterodimers and bind flavin and nonheme Fe cofactors, and their activity is transiently observed during an initial shift from the dark to the light but is no longer measurable after 5 min in the light (Chaux et al., 2017). The physiological relevance of this transient expression, in agreement with work in cyanobacteria, *Marchantia* and *Physcomitrella*, is to prime or oxidize the electron transfer carriers of the photosynthetic electron transfer chain until CBC enzymes are redox activated, creating a proton motive force (*pmf*) for ATP synthesis and rapidly providing a renewed source of $NADP^+$ (Allahverdiyeva et al., 2013; Chaux et al., 2017; Gerotto et al., 2016; Shimakawa et al., 2017). The deactivation of this process remains to be understood but may be associated with differences in affinity for NADPH between FLV and CBC enzymes (Yamamoto, Takahashi, Badger, & Shikanai, 2016). FLV proteins gradually replace hydrogenases (H^+ reduction) during a dark to light transition in anaerobic conditions and both enable *Chlamydomonas* cells to reoxidize the electron transport chain in the light (Burlacot et al., 2018; Ghysels, Godaux, Matagne, Cardol, & Franck, 2013).

In an absence of the FLV pathway, over the course of a fluctuating light treatment, an alternative O_2 photoreduction pathway is stimulated to a much greater extent than in wild-type cells. The Mehler/Asada reactions are highly stimulated in an *flv* mutant, but their associated detoxification reactions must be exceeded because destruction of oxidizable P_{700} and a loss of PSI complex proteins are observed (Chaux et al., 2017). A second function of the FLV proteins is to reduce the amplitude of Mehler/Asada type reactions in fluctuating light in *Chlamydomonas*. In prolonged high light, $O_2^{\bullet -}$ to H_2O_2 production is constitutive and catalase, FE-SOD, APX, and MDAR (consumer of NADPH) are required for cell survival via ROS detoxification (Ledford & Niyogi, 2005). In the regulation of NADPH photoproduction, these prolonged water–water cycles should not be ignored and would replace $NADP^+$ photoreduction and act as terminal electron acceptors, so their activity contributes to maintenance of *pmf* (Forti & Elli, 1996) and recycling NADPH to $NADP^+$ (Fig. 8.5).

8.6.2.7 NADPH-controlled interplay between cyclic electron flow and oxygen photoreduction

Photosynthetic O_2 uptake in algae is stimulated by light exciting PSII and diminished when most of the light excites PSI (Setlik, Ried, & Berkova, 1973). Mutants without the *pgr5/pgrl1* pathway mimic the PSII stimulation experiment, with both linear electron flow and O_2 photoreduction being highly induced (Dang et al., 2014; Johnson et al., 2014). A strong O_2 uptake is due to reoxidation of NADPH via FLV proteins as well as activation of respiratory pathways. When NADPH accumulates, for instance in PSI light or in a mutant lacking Rubisco, it causes inhibition of linear electron transport, observed by a marked increase in cyclic electron flow and less O_2 photoreduction (Alric, Lavergne, & Rappaport, 2010; Johnson et al., 2014). Increased light-induced O_2 uptake is associated with a state of increased demand for ATP in the chloroplast (Setlik et al., 1973), and O_2 photoreduction pathways release the restriction on linear electron transport/water–water pathways. Conversely, PSI-mediated cyclic electron transport, by raising the ATP level, will inhibit light-induced oxygen uptake (Evans & Carr, 1979).

8.7 New avenues for the future: *Chlamydomonas* as a chassis for engineering carbon fixation pathways

The studies discussed so far are based on established analytical approaches that have deepened our understanding of the CBC and its regulation, but this knowledge could be complemented by synthetic biology methods. Biology is indeed

currently facing a revolution through its transition from analytic to synthetic biology approaches (Cameron, Bashor, & Collins, 2014). Synthesis is a forward biological engineering discipline, a powerful methodology to understand by building rather than by deconstruction (Endy, 2011). It relies on the capacity to design and build a biological system from standardized simple DNA bricks, to test it in a systematic way, and to gain new knowledge to allow optimization of the design. These DESIGN, BUILD, TEST, and LEARN cycles can then be iterated as many times as necessary to cumulate the improvements required for process optimization (Petzold, Chan, Nhan, & Adams, 2015). Synthetic biology offers new possibilities to answer fundamental questions using new approaches and concepts or to create artificial systems that have potential biotechnological applications (Képès, 2011).

The rise of green synthetic biology presents researchers with the potential to tackle the challenge of improving photosynthetic efficiency through engineering of microalgae, cyanobacteria, and plants. With its photosynthetic apparatus very similar to that of land plants, its dispensable photosynthesis allowing growth of photosynthetic mutants by supplementation with organic carbon (acetate), and our long-term knowledge of its genetics and physiology, *Chlamydomonas* appears as an ideal chassis to enable and accelerate the green synthetic revolution. This will take advantage of standardized synthetic biology tools developed during recent years for engineering *Chlamydomonas* including a Modular Cloning (MoClo) toolkit comprising 119 bricks allowing fast and easy generation of any multigenic assembly (Crozet et al., 2018). New standardized MoClo parts, including new antibiotic resistance modules (de Carpentier et al., 2020) and riboswitches (Mehrshahi et al., 2020), are regularly expanding engineering possibilities using *Chlamydomonas*.

Synthetic biology approaches aimed at improving carbon fixation fall into four major categories: (i) engineering synthetic photorespiration bypasses; (ii) improving the working conditions of Rubisco through carbon-concentrating mechanisms (CCM); (iii) engineering respiration; (iv) engineering redesigned or synthetic CO_2 fixation pathways (Erb & Zarzycki, 2016; Kubis & Bar-Even, 2019; Long, Marshall-Colon, & Zhu, 2015; Ort et al., 2015; Simkin, Lopez-Calcagno, & Raines, 2019). Numerous possibilities exist to rewire photorespiration, several of which have been implemented with great success in cyanobacteria, microalgae, and plants (Bar-Even, 2018; Betti et al., 2016; Kubis & Bar-Even, 2019; Simkin et al., 2019; South et al., 2019; Trudeau et al., 2018; Yu, Li, Duchoud, Chuang, & Liao, 2018). Many organisms have developed carbon concentrating mechanisms (Raven, Cockell, & De La Rocha, 2008) that could be engineered in CCM-free crops to boost their yield, although the functions of many components associated with the CCM remain to be determined (Atkinson, Mao, Chan, & McCormick, 2020; Hibberd, Sheehy, & Langdale, 2008; Long, Rae, Rolland, Forster, & Price, 2016; Rae et al., 2017; Schuler, Mantegazza, & Weber, 2016) (Vol 2, Chapter 7). Multiple engineering strategies have also been proposed to boost crop productivity by cutting respiratory carbon loss (Amthor et al., 2019; Long et al., 2015).

Major energy losses during photosynthesis, that reduce the overall light conversion efficiency, can be directly attributed to kinetic bottlenecks within the CBC (Raines, 2011; Stitt, Lunn, & Usadel, 2010). The limitation of photosynthesis is due to the slow turnover of the CBC compared to PET capacity at moderate to high light intensities (Marcus, Altman-Gueta, Wolff, & Gurevitz, 2011; Wobbe & Remacle, 2015). Under these conditions, the excess of excitation energy can be dissipated as heat through nonphotochemical quenching, fluorescence, or increased production of harmful ROS. Since the CBC bottlenecks lead to overreduction of PET components and threatens cell survival, photosynthetic organisms have evolved sophisticated mechanisms to limit PET such as downregulation of antenna size and inactivation of key photosynthetic complexes (Nawrocki et al., 2019; Pinnola & Bassi, 2018). For these reasons, cell growth (biomass production) can sometimes be increased by lowering either light intensities or the size of antennae (Mussgnug et al., 2007; Ort & Melis, 2011). Engineering quenching pathways to accelerate relaxation during shading increased carbon fixation and plant dry matter by about 15% in tobacco under fluctuating light (Kromdijk et al., 2016). However, another way to optimize photosynthesis and increase production yields would be to enhance the efficiency of carbon fixation rather than to decrease light harvesting capacity.

As slow turnover of the CBC is the most important limiting factor in photosynthetic efficiency under optimal conditions, any improvement of this carbon fixation pathway will result directly in higher photosynthetic efficiency and increase the photoproduction of biomass and engineered products at moderate to high light intensities. At light saturation, the CBC is typically colimited in vivo by the capacity for regeneration of the acceptor molecule for carboxylation, RuBP, and the capacity for carboxylation by the notoriously inefficient Rubisco (Long, Ainsworth, Rogers, & Ort, 2004; Zhu, de Sturler, & Long, 2007). The catalytic rate of Rubisco is indeed one of the slowest of any enzyme-catalyzed reaction, and the enzyme's low specificity for CO_2 versus O_2 further detracts from carbon fixation (Bar-Even et al., 2011; Parry et al., 2013; Tcherkez, 2013; Zhu, Portis, & Long, 2004). Engineering strategies to improve Rubisco catalytic efficiency or specificity have generally failed (Kubis & Bar-Even, 2019). The enzyme appears trapped in a trade-off between catalytic rate and specificity. Several studies suggested that improvement of its CO_2 fixation rate comes at the expense of CO_2 affinity and that, despite its inefficiency, the enzyme might already be optimized through

natural evolution (Erb & Zarzycki, 2016; Galmes et al., 2014; Savir, Noor, Milo, & Tlusty, 2010; Tcherkez, Farquhar, & Andrews, 2006), although several recent studies challenge this finding (Cummins, Kannappan, & Gready, 2018; Durao et al., 2015; Young et al., 2016) (Vol 2, Chapter 7). For example, Synechocystis Rubisco was improved using directed evolution (threefold increase of carboxylation efficiency) (Durao et al., 2015) and overproduction of Rubisco in cyanobacteria was shown to increase production of biomass and carbon-based chemicals (Atsumi, Higashide, & Liao, 2009; Iwaki et al., 2006; Liang & Lindblad, 2016, 2017; Rosgaard, de Porcellinis, Jacobsen, Frigaard, & Sakuragi, 2012).

However, Rubisco is not the only enzyme limiting CBC turnover. Indeed, metabolic flux control analyses and modeling of the CBC suggested that more effective enzymatic partitioning/stoichiometry could significantly improve photosynthetic efficiency (Mettler et al., 2014; Raines, 2003, 2006, 2011; Simkin, McAusland, Headland, Lawson, & Raines, 2015; Stitt & Schulze, 1994; Stitt et al., 2010; Trudeau et al., 2018; Zhu et al., 2007). These studies predicted that SBPase could limit the CBC and, consistently, the overproduction of this enzyme increased CO_2 fixation and biomass production in several species (Ding, Wang, Zhang, & Ai, 2016; Driever et al., 2017; Fang et al., 2012; Lefebvre et al., 2005; Liang & Lindblad, 2016; Miyagawa, Tamoi, & Shigeoka, 2001; Ogawa et al., 2015; Rosenthal et al., 2011; Simkin et al., 2017; Suzuki, Kondo, & Makino, 2017; Tamoi, Nagaoka, Miyagawa, & Shigeoka, 2006). In *Chlamydomonas*, SBPase overexpression of up to threefold (0.3% of total cell protein) resulted in a significant increase of both the photosynthetic rate and growth under high light and elevated CO_2 conditions (Hammel et al., 2020). Other enzymes such as FBPase, PGK, TRK, or FBA are also potential targets for improvement (Liang & Lindblad, 2016; Liang, Englund, Lindberg, & Lindblad, 2018; Mettler et al., 2014; Simkin et al., 2015; Simkin et al., 2017; Uematsu, Suzuki, Iwamae, Inui, & Yukawa, 2012). Indeed, under low light or elevated CO_2 concentrations, the rate of Rubisco becomes less limiting and carbon fixation is mostly constrained by RuBP regeneration (Kubis & Bar-Even, 2019). Engineering in cyanobacteria to increase metabolic sinks has also proved efficient for improving photosynthetic capacity and PSI oxidation (Santos-Merino et al., 2021).

An alternative approach to improving natural CBC would be to build artificial CO_2-fixing synthetic cycles more efficient than naturally occurring ones, such as the MOG pathways (Malonyl-CoA-oxaloacetate-glyoxylate) (Bar-Even, Noor, Lewis, & Milo, 2010), the CETCH cycle (crotonyl−coenzyme A (CoA)/ethylmalonyl-CoA/hydroxybutyryl-CoA) (Schwander, Schada von Borzyskowski, Burgener, Cortina, & Erb, 2016), or the GED cycle (Gnd−Entner−Doudoroff) (Satanowski et al., 2020). New pathways using one carbon metabolism (Gleizer et al., 2019) or nonnatural reactions (Bar-Even, 2018) have also been proposed but are hardly practically feasible since they would require challenging de novo enzyme design and complete metabolism rewiring, which are not possible with our current knowledge and technologies. Hence, many possibilities exist to improve the efficiency of the CBC, either through redesign of natural CBC or through replacement of CBC by more efficient synthetic CO_2 fixation pathways.

References

Aigner, H., Wilson, R. H., Bracher, A., Calisse, L., Bhat, J. Y., Hartl, F. U., ... Hayer-Hartl, M. (2017). Plant RuBisCo assembly in *E. coli* with five chloroplast chaperones including BSD2. *Science*, *358*(6368), 1272−1278. Available from https://doi.org/10.1126/science.aap9221.

Allahverdiyeva, Y., Mustila, H., Ermakova, M., Bersanini, L., Richaud, P., Ajlani, G., ... Aro, E. M. (2013). Flavodiiron proteins Flv1 and Flv3 enable cyanobacterial growth and photosynthesis under fluctuating light. *Proceedings of the National Academy of Sciences of the United States of America*, *110*(10), 4111−4116. Available from https://doi.org/10.1073/pnas.1221194110.

Allen, J. F. (2003). Cyclic, pseudocyclic and noncyclic photophosphorylation: New links in the chain. *Trends in Plant Science*, *8*(1), 15−19. Available from https://doi.org/10.1016/s1360-1385(02)00006-7.

Allen, J. F., Bennett, J., Steinback, K. E., & Arntzen, C. J. (1981). Chloroplast protein phosphorylation couples plastoquinone redox state to distribution of excitation energy between photosystems. *Nature*, *291*(5810), 25−29.

Alric, J. (2010). Cyclic electron flow around photosystem I in unicellular green algae. *Photosynthesis Research*, *106*(1−2), 47−56. Available from https://doi.org/10.1007/s11120-010-9566-4.

Alric, J., Lavergne, J., & Rappaport, F. (2010). Redox and ATP control of photosynthetic cyclic electron flow in *Chlamydomonas reinhardtii* (I) aerobic conditions. *Biochimica et Biophysica Acta*, *1797*(1), 44−51. Available from https://doi.org/10.1016/j.bbabio.2009.07.009.

Amthor, J. S., Bar-Even, A., Hanson, A. D., Millar, A. H., Stitt, M., Sweetlove, L. J., ... Tyerman, S. D. (2019). Engineering strategies to boost crop productivity by cutting respiratory carbon loss. *The Plant Cell*, *31*(2), 297−314. Available from https://doi.org/10.1105/tpc.18.00743.

Anderson, L. E., Goldhaber-Gordon, I. M., Li, D., Tang, X. Y., Xiang, M., & Prakash, N. (1995). Enzyme-enzyme interaction in the chloroplast: Glyceraldehyde-3-phosphate dehydrogenase, triose phosphate isomerase and aldolase. *Planta*, *196*(2), 245−255. Available from https://doi.org/10.1007/BF00201381.

Andersson, I., & Backlund, A. (2008). Structure and function of Rubisco. *Plant Physiology and Biochemistry*, *46*(3), 275−291. Available from https://doi.org/10.1016/j.plaphy.2008.01.001.

Arsova, B., Hoja, U., Wimmelbacher, M., Greiner, E., Ustun, S., Melzer, M., ... Bornke, F. (2010). Plastidial thioredoxin z interacts with two fructokinase-like proteins in a thiol-dependent manner: Evidence for an essential role in chloroplast development in *Arabidopsis* and *Nicotiana benthamiana*. *The Plant Cell*, *22*(5), 1498–1515. Available from https://doi.org/10.1105/tpc.109.071001.

Aslund, F., Berndt, K. D., & Holmgren, A. (1997). Redox potentials of glutaredoxins and other thiol-disulfide oxidoreductases of the thioredoxin superfamily determined by direct protein-protein redox equilibria. *The Journal of Biological Chemistry*, *272*(49), 30780–30786. Available from https://doi.org/10.1074/jbc.272.49.30780.

Atkinson, N., Mao, Y., Chan, K. X., & McCormick, A. J. (2020). Condensation of Rubisco into a proto-pyrenoid in higher plant chloroplasts. *Nature Communications*, *11*(1), 6303. Available from https://doi.org/10.1038/s41467-020-20132-0.

Atsumi, S., Higashide, W., & Liao, J. C. (2009). Direct photosynthetic recycling of carbon dioxide to isobutyraldehyde. *Nature Biotechnology*, *27*(12), 1177–1180. Available from https://doi.org/10.1038/nbt.1586.

Avilan, L., Gontero, B., Lebreton, S., & Ricard, J. (1997a). Information transfer in multienzyme complexes–2. The role of Arg64 of *Chlamydomonas reinhardtii* phosphoribulokinase in the information transfer between glyceraldehyde-3-phosphate dehydrogenase and phosphoribulokinase. *European Journal of Biochemistry*, *250*(2), 296–302. Available from https://doi.org/10.1111/j.1432-1033.1997.0296a.x.

Avilan, L., Gontero, B., Lebreton, S., & Ricard, J. (1997b). Memory and imprinting effects in multienzyme complexes–I. Isolation, dissociation, and reassociation of a phosphoribulokinase-glyceraldehyde-3-phosphate dehydrogenase complex from *Chlamydomonas reinhardtii* chloroplasts. *European Journal of Biochemistry*, *246*(1), 78–84. Available from https://doi.org/10.1111/j.1432-1033.1997.00078.x.

Avilan, L., Puppo, C., Erales, J., Woudstra, M., Lebrun, R., & Gontero, B. (2012). CP12 residues involved in the formation and regulation of the glyceraldehyde-3-phosphate dehydrogenase-CP12-phosphoribulokinase complex in *Chlamydomonas reinhardtii*. *Molecular Biosystems*, *8*(11), 2994–3002. Available from https://doi.org/10.1039/c2mb25244a.

Baalmann, E., Scheibe, R., Cerff, R., & Martin, W. (1996). Functional studies of chloroplast glyceraldehyde-3-phosphate dehydrogenase subunits A and B expressed in *Escherichia coli*: Formation of highly active A4 and B4 homotetramers and evidence that aggregation of the B4 complex is mediated by the B subunit carboxy terminus. *Plant Molecular Biology*, *32*(3), 505–513. Available from https://doi.org/10.1007/BF00019102.

Ballicora, M. A., Frueauf, J. B., Fu, Y., Schurmann, P., & Preiss, J. (2000). Activation of the potato tuber ADP-glucose pyrophosphorylase by thioredoxin. *The Journal of Biological Chemistry*, *275*(2), 1315–1320. Available from https://doi.org/10.1074/jbc.275.2.1315.

Balsera, M., Uberegui, E., Schurmann, P., & Buchanan, B. B. (2014). Evolutionary development of redox regulation in chloroplasts. *Antioxidants & Redox Signaling*, *21*(9), 1327–1355. Available from https://doi.org/10.1089/ars.2013.5817.

Bar-Even, A. (2018). Daring metabolic designs for enhanced plant carbon fixation. *Plant Science*, *273*, 71–83. Available from https://doi.org/10.1016/j.plantsci.2017.12.007.

Bar-Even, A., Noor, E., Lewis, N. E., & Milo, R. (2010). Design and analysis of synthetic carbon fixation pathways. *Proceedings of the National Academy of Sciences of the United States of America*, *107*(19), 8889–8894. Available from https://doi.org/10.1073/pnas.0907176107.

Bar-Even, A., Noor, E., Savir, Y., Liebermeister, W., Davidi, D., Tawfik, D. S., ... Milo, R. (2011). The moderately efficient enzyme: Evolutionary and physicochemical trends shaping enzyme parameters. *Biochemistry*, *50*(21), 4402–4410. Available from https://doi.org/10.1021/bi2002289.

Bar-On, Y. M., & Milo, R. (2019). The global mass and average rate of rubisco. *Proceedings of the National Academy of Sciences of the United States of America*, *116*(10), 4738–4743. Available from https://doi.org/10.1073/pnas.1816654116.

Bassham, J. A. (1971). Photosynthetic carbon metabolism. *Proceedings of the National Academy of Sciences of the United States of America*, *68*(11), 2877–2882. Available from https://doi.org/10.1073/pnas.68.11.2877.

Bedhomme, M., Adamo, M., Marchand, C. H., Couturier, J., Rouhier, N., Lemaire, S. D., ... Trost, P. (2012). Glutathionylation of cytosolic glyceraldehyde-3-phosphate dehydrogenase from the model plant *Arabidopsis thaliana* is reversed by both glutaredoxins and thioredoxins in vitro. *The Biochemical Journal*, *445*(3), 337–347. Available from https://doi.org/10.1042/BJ20120505.

Benhar, M., Forrester, M. T., & Stamler, J. S. (2009). Protein denitrosylation: Enzymatic mechanisms and cellular functions. *Nature Reviews. Molecular Cell Biology*, *10*(10), 721–732. Available from https://doi.org/10.1038/nrm2764.

Benson, A. A., Bassham, J. A., Calvin, M., Hall, A. G., Hirsch, H. E., Kawaguchi, S., ... Tolbert, N. E. (1952). The path of carbon in photosynthesis. XV. Ribulose and sedoheptulose. *The Journal of Biological Chemistry*, *196*(2), 703–716. Available from https://doi.org/10.2172/915054.

Bergner, S. V., Scholz, M., Trompelt, K., Barth, J., Gabelein, P., Steinbeck, J., ... Hippler, M. (2015). STATE TRANSITION7-dependent phosphorylation is modulated by changing environmental conditions, and its absence triggers remodeling of photosynthetic protein complexes. *Plant Physiology*, *168*(2), 615–634. Available from https://doi.org/10.1104/pp.15.00072.

Betti, M., Bauwe, H., Busch, F. A., Fernie, A. R., Keech, O., Levey, M., ... Weber, A. P. (2016). Manipulating photorespiration to increase plant productivity: recent advances and perspectives for crop improvement. *Journal of Experimental Botany*, *67*(10), 2977–2988. Available from https://doi.org/10.1093/jxb/erw076.

Blaby, I. K., Blaby-Haas, C. E., Perez-Perez, M. E., Schmollinger, S., Fitz-Gibbon, S., Lemaire, S. D., ... Merchant, S. S. (2015). Genome-wide analysis on *Chlamydomonas reinhardtii* reveals the impact of hydrogen peroxide on protein stress responses and overlap with other stress transcriptomes. *The Plant Journal*, *84*(5), 974–988. Available from https://doi.org/10.1111/tpj.13053.

Blaby, I. K., Glaesener, A. G., Mettler, T., Fitz-Gibbon, S. T., Gallaher, S. D., Liu, B., ... Merchant, S. S. (2013). Systems-level analysis of nitrogen starvation-induced modifications of carbon metabolism in a *Chlamydomonas reinhardtii* starchless mutant. *The Plant Cell*, *25*(11), 4305–4323. Available from https://doi.org/10.1105/tpc.113.117580.

Boehm, M., Alahuhta, M., Mulder, D. W., Peden, E. A., Long, H., Brunecky, R., ... Dubini, A. (2016). Crystal structure and biochemical characterization of *Chlamydomonas* FDX2 reveal two residues that, when mutated, partially confer FDX2 the redox potential and catalytic properties of FDX1. *Photosynthesis Research*, *128*(1), 45–57. Available from https://doi.org/10.1007/s11120-015-0198-6.

Bosco, M. B., Aleanzi, M. C., & Iglesias, A. A. (2012). Plastidic phosphoglycerate kinase from *Phaeodactylum tricornutum*: On the critical role of cysteine residues for the enzyme function. *Protist*, *163*(2), 188–203. Available from https://doi.org/10.1016/j.protis.2011.07.001.

Boyle, N. R., & Morgan, J. A. (2009). Flux balance analysis of primary metabolism in *Chlamydomonas reinhardtii*. *BMC Systems Biology*, *3*(1), 4. Available from https://doi.org/10.1186/1752-0509-3-4.

Brandes, H. K., Larimer, F. W., & Hartman, F. C. (1996). The molecular pathway for the regulation of phosphoribulokinase by thioredoxin f. *The Journal of Biological Chemistry*, *271*(7), 3333–3335. Available from https://doi.org/10.1074/jbc.271.7.3333.

Buchanan, B. B. (2016). The path to thioredoxin and redox regulation in chloroplasts. *Annual Review of Plant Biology*, *67*, 1–24. Available from https://doi.org/10.1146/annurev-arplant-043015-111949.

Buchanan, B. B., Holmgren, A., Jacquot, J. P., & Scheibe, R. (2012). Fifty years in the thioredoxin field and a bountiful harvest. *Biochimica et Biophysica Acta*, *1820*(11), 1822–1829. Available from https://doi.org/10.1016/j.bbagen.2012.07.006.

Buchert, F., Bailleul, B., & Hisabori, T. (2017). A gamma-subunit point mutation in *Chlamydomonas reinhardtii* chloroplast F1Fo-ATP synthase confers tolerance to reactive oxygen species. *Biochimica et Biophysica Acta - Bioenergetics*, *1858*(12), 966–974. Available from https://doi.org/10.1016/j.bbabio.2017.09.001.

Bulté, L., Gans, P., Rebéillé, F., & Wollman, F. A. (1990). ATP control on state transitions in vivo in *Chlamydomonas reinhardtii*. *Biochimica et Biophysica Acta (BBA)-Bioenergetics*, *1020*(1), 72–80.

Burlacot, A., Sawyer, A., Cuine, S., Auroy-Tarrago, P., Blangy, S., Happe, T., … Peltier, G. (2018). Flavodiiron-mediated O_2 photoreduction links H_2 production with CO_2 fixation during the anaerobic induction of photosynthesis. *Plant Physiology*, *177*(4), 1639–1649. Available from https://doi.org/10.1104/pp.18.00721.

Calatrava, V., Chamizo-Ampudia, A., Sanz-Luque, E., Ocana-Calahorro, F., Llamas, A., Fernandez, E., … Galvan, A. (2017). How *Chlamydomonas* handles nitrate and the nitric oxide cycle. *Journal of Experimental Botany*, *68*(10), 2593–2602. Available from https://doi.org/10.1093/jxb/erw507.

Cameron, D. E., Bashor, C. J., & Collins, J. J. (2014). A brief history of synthetic biology. *Nature Reviews. Microbiology*, *12*(5), 381–390. Available from https://doi.org/10.1038/nrmicro3239.

Cardol, P., Alric, J., Girard-Bascou, J., Franck, F., Wollman, F. A., & Finazzi, G. (2009). Impaired respiration discloses the physiological significance of state transitions in *Chlamydomonas*. *Proceedings of the National Academy of Sciences of the United States of America*, *106*(37), 15979–15984. Available from https://doi.org/10.1073/pnas.0908111106.

Carmo-Silva, A. E., & Salvucci, M. E. (2013). The regulatory properties of Rubisco activase differ among species and affect photosynthetic induction during light transitions. *Plant Physiology*, *161*(4), 1645–1655. Available from https://doi.org/10.1104/pp.112.213348.

Chapman, M. S., Suh, S. W., Curmi, P. M., Cascio, D., Smith, W. W., & Eisenberg, D. S. (1988). Tertiary structure of plant RuBisCO: Domains and their contacts. *Science*, *241*(4861), 71–74. Available from https://doi.org/10.1126/science.3133767.

Chapman, S. P., Paget, C. M., Johnson, G. N., & Schwartz, J. M. (2015). Flux balance analysis reveals acetate metabolism modulates cyclic electron flow and alternative glycolytic pathways in *Chlamydomonas reinhardtii*. *Frontiers in Plant Science*, *6*, 474. Available from https://doi.org/10.3389/fpls.2015.00474.

Charles, S. A., & Halliwell, B. (1981). Light activation of fructose bisphosphatase in isolated spinach chloroplasts and deactivation by hydrogen peroxide: A physiological role for the thioredoxin system. *Planta*, *151*(3), 242–246. Available from https://doi.org/10.1007/BF00395175.

Charoenwattanasatien, R., Zinzius, K., Scholz, M., Wicke, S., Tanaka, H., Brandenburg, J. S., … Kurisu, G. (2020). Calcium sensing via EF-hand 4 enables thioredoxin activity in the sensor-responder protein calredoxin in the green alga *Chlamydomonas reinhardtii*. *The Journal of Biological Chemistry*, *295*(1), 170–180. Available from https://doi.org/10.1074/jbc.RA119.008735.

Chaux, F., Burlacot, A., Mekhalfi, M., Auroy, P., Blangy, S., Richaud, P., … Peltier, G. (2017). Flavodiiron proteins promote fast and transient O_2 photoreduction in *Chlamydomonas*. *Plant Physiology*, *174*(3), 1825–1836. Available from https://doi.org/10.1104/pp.17.00421.

Chaux, F., Peltier, G., & Johnson, X. (2015). A security network in PSI photoprotection: Regulation of photosynthetic control, NPQ and O_2 photoreduction by cyclic electron flow. *Frontiers in Plant Science*, *6*, 875. Available from https://doi.org/10.3389/fpls.2015.00875.

Chen, L., Wu, R., Feng, J., Feng, T., Wang, C., Hu, J., … Zuo, J. (2020). Transnitrosylation mediated by the non-canonical catalase ROG1 regulates nitric oxide signaling in plants. *Developmental Cell*, *53*(4), 444–457. Available from https://doi.org/10.1016/j.devcel.2020.03.020, e445.

Chiadmi, M., Navaza, A., Miginiac-Maslow, M., Jacquot, J. P., & Cherfils, J. (1999). Redox signalling in the chloroplast: Structure of oxidized pea fructose-1,6-bisphosphate phosphatase. *The EMBO Journal*, *18*(23), 6809–6815. Available from https://doi.org/10.1093/emboj/18.23.6809.

Chibani, K., Couturier, J., Selles, B., Jacquot, J. P., & Rouhier, N. (2010). The chloroplastic thiol reducing systems: Dual functions in the regulation of carbohydrate metabolism and regeneration of antioxidant enzymes, emphasis on the poplar redoxin equipment. *Photosynthesis Research*, *104*(1), 75–99. Available from https://doi.org/10.1007/s11120-009-9501-8.

Chibani, K., Tarrago, L., Schurmann, P., Jacquot, J. P., & Rouhier, N. (2011). Biochemical properties of poplar thioredoxin z. *FEBS Letters*, *585*(7), 1077–1081. Available from https://doi.org/10.1016/j.febslet.2011.03.006.

Chibani, K., Wingsle, G., Jacquot, J. P., Gelhaye, E., & Rouhier, N. (2009). Comparative genomic study of the thioredoxin family in photosynthetic organisms with emphasis on *Populus trichocarpa*. *Molecular Plant*, *2*(2), 308–322. Available from https://doi.org/10.1093/mp/ssn076.

Cohen, I., Sapir, Y., & Shapira, M. (2006). A conserved mechanism controls translation of Rubisco large subunit in different photosynthetic organisms. *Plant Physiology*, *141*(3), 1089–1097. Available from https://doi.org/10.1104/pp.106.079046.

Collin, V., Issakidis-Bourguet, E., Marchand, C., Hirasawa, M., Lancelin, J. M., Knaff, D. B., … Miginiac-Maslow, M. (2003). The Arabidopsis plastidial thioredoxins: New functions and new insights into specificity. *The Journal of Biological Chemistry*, *278*(26), 23747–23752. Available from https://doi.org/10.1074/jbc.M302077200.

Collin, V., Lamkemeyer, P., Miginiac-Maslow, M., Hirasawa, M., Knaff, D. B., Dietz, K. J., ... Issakidis-Bourguet, E. (2004). Characterization of plastidial thioredoxins from Arabidopsis belonging to the new y-type. *Plant Physiology*, *136*(4), 4088–4095. Available from https://doi.org/10.1104/pp.104.052233.

Courteille, A., Vesa, S., Sanz-Barrio, R., Cazale, A. C., Becuwe-Linka, N., Farran, I., ... Rumeau, D. (2013). Thioredoxin m4 controls photosynthetic alternative electron pathways in Arabidopsis. *Plant Physiology*, *161*(1), 508–520. Available from https://doi.org/10.1104/pp.112.207019.

Crozet, P., Navarro, F. J., Willmund, F., Mehrshahi, P., Bakowski, K., Lauersen, K. J., ... Lemaire, S. D. (2018). Birth of a photosynthetic chassis: A MoClo toolkit enabling synthetic biology in the microalga *Chlamydomonas reinhardtii*. *ACS Synthetic Biology*, *7*(9), 2074–2086. Available from https://doi.org/10.1021/acssynbio.8b00251.

Cummins, P. L., Kannappan, B., & Gready, J. E. (2018). Directions for optimization of photosynthetic carbon fixation: RuBisCO's efficiency may not be so constrained after all. *Frontiers in Plant Science*, *9*, 183. Available from https://doi.org/10.3389/fpls.2018.00183.

Dai, S., Friemann, R., Glauser, D. A., Bourquin, F., Manieri, W., Schurmann, P., ... Eklund, H. (2007). Structural snapshots along the reaction pathway of ferredoxin-thioredoxin reductase. *Nature*, *448*(7149), 92–96. Available from https://doi.org/10.1038/nature05937.

Dai, S., Johansson, K., Miginiac-Maslow, M., Schurmann, P., & Eklund, H. (2004). Structural basis of redox signaling in photosynthesis: Structure and function of ferredoxin:thioredoxin reductase and target enzymes. *Photosynthesis Research*, *79*(3), 233–248. Available from https://doi.org/10.1023/B:PRES.0000017194.34167.6d.

Dang, K. V., Plet, J., Tolleter, D., Jokel, M., Cuine, S., Carrier, P., ... Peltier, G. (2014). Combined increases in mitochondrial cooperation and oxygen photoreduction compensate for deficiency in cyclic electron flow in *Chlamydomonas reinhardtii*. *The Plant Cell*, *26*(7), 3036–3050. Available from https://doi.org/10.1105/tpc.114.126375.

Dayer, R., Fischer, B. B., Eggen, R. I., & Lemaire, S. D. (2008). The peroxiredoxin and glutathione peroxidase families in *Chlamydomonas reinhardtii*. *Genetics*, *179*(1), 41–57. Available from https://doi.org/10.1534/genetics.107.086041.

de Carpentier, F., Le Peillet, J., Boisset, N. D., Crozet, P., Lemaire, S. D., & Danon, A. (2020). Blasticidin S deaminase: A new efficient selectable marker for *Chlamydomonas reinhardtii*. *Frontiers in Plant Science*, *11*, 242. Available from https://doi.org/10.3389/fpls.2020.00242.

De Mia, M., Lemaire, S. D., Choquet, Y., & Wollman, F. A. (2019). Nitric oxide remodels the photosynthetic apparatus upon S-starvation in *Chlamydomonas reinhardtii*. *Plant Physiology*, *179*(2), 718–731. Available from https://doi.org/10.1104/pp.18.01164.

Decottignies, P., Schmitter, J. M., Dutka, S., Jacquot, J. P., & Miginiac-Maslow, M. (1991). Characterization and primary structure of a second thioredoxin from the green alga, *Chlamydomonas reinhardtii*. *European Journal of Biochemistry*, *198*(2), 505–512. Available from https://doi.org/10.1111/j.1432-1033.1991.tb16043.x.

Decottignies, P., Schmitter, J. M., Jacquot, J. P., Dutka, S., Picaud, A., & Gadal, P. (1990). Purification, characterization, and complete amino acid sequence of a thioredoxin from a green alga, *Chlamydomonas reinhardtii*. *Archives of Biochemistry and Biophysics*, *280*(1), 112–121. Available from https://doi.org/10.1016/0003-9861(90)90525-4.

Desplats, C., Mus, F., Cuine, S., Billon, E., Cournac, L., & Peltier, G. (2009). Characterization of Nda2, a plastoquinone-reducing type II NAD(P)H dehydrogenase in chlamydomonas chloroplasts. *The Journal of Biological Chemistry*, *284*(7), 4148–4157. Available from https://doi.org/10.1074/jbc.M804546200.

Diaz, M. G., Hernandez-Verdeja, T., Kremnev, D., Crawford, T., Dubreuil, C., & Strand, A. (2018). Redox regulation of PEP activity during seedling establishment in *Arabidopsis thaliana*. *Nature Communications*, *9*(1), 50. Available from https://doi.org/10.1038/s41467-017-02468-2.

Dietz, K. J. (2011). Peroxiredoxins in plants and cyanobacteria. *Antioxidants & Redox Signaling*, *15*(4), 1129–1159. Available from https://doi.org/10.1089/ars.2010.3657.

Ding, F., Wang, M., Zhang, S., & Ai, X. (2016). Changes in SBPase activity influence photosynthetic capacity, growth, and tolerance to chilling stress in transgenic tomato plants. *Scientific Reports*, *6*, 32741. Available from https://doi.org/10.1038/srep32741.

Driever, S. M., Simkin, A. J., Alotaibi, S., Fisk, S. J., Madgwick, P. J., Sparks, C. A., ... Raines, C. A. (2017). Increased SBPase activity improves photosynthesis and grain yield in wheat grown in greenhouse conditions. *Philosophical Transactions of the Royal Society of London. Series B, Biological Sciences*, *372*(1730). Available from https://doi.org/10.1098/rstb.2016.0384.

Dunford, R. P., Durrant, M. C., Catley, M. A., & Dyer, T. A. (1998). Location of the redox-active cysteines in chloroplast sedoheptulose-1,7-bisphosphatase indicates that its allosteric regulation is similar but not identical to that of fructose-1,6-bisphosphatase. *Photosynthesis Research*, *58*(3), 221–230. Available from https://doi.org/10.1023/a:1006178826976.

Durao, P., Aigner, H., Nagy, P., Mueller-Cajar, O., Hartl, F. U., & Hayer-Hartl, M. (2015). Opposing effects of folding and assembly chaperones on evolvability of Rubisco. *Nature Chemical Biology*, *11*(2), 148–155. Available from https://doi.org/10.1038/nchembio.1715.

Endy, D. (2011). Building a new biology. *Comptes Rendus Chimie*, *14*(4), 424–428. Available from https://doi.org/10.1016/j.crci.2010.11.013.

Engel, B. D., Schaffer, M., Kuhn Cuellar, L., Villa, E., Plitzko, J. M., & Baumeister, W. (2015). Native architecture of the *Chlamydomonas* chloroplast revealed by in situ cryo-electron tomography. *Elife*, *4*. Available from https://doi.org/10.7554/eLife.04889.

Erales, J., Lignon, S., & Gontero, B. (2009). CP12 from *Chlamydomonas reinhardtii*, a permanent specific "chaperone-like" protein of glyceraldehyde-3-phosphate dehydrogenase. *The Journal of Biological Chemistry*, *284*(19), 12735–12744. Available from https://doi.org/10.1074/jbc.M808254200.

Erales, J., Mekhalfi, M., Woudstra, M., & Gontero, B. (2011). Molecular mechanism of NADPH-glyceraldehyde-3-phosphate dehydrogenase regulation through the C-terminus of CP12 in *Chlamydomonas reinhardtii*. *Biochemistry*, *50*(14), 2881–2888. Available from https://doi.org/10.1021/bi1020259.

Erb, T. J., & Zarzycki, J. (2016). Biochemical and synthetic biology approaches to improve photosynthetic CO_2-fixation. *Current Opinion in Chemical Biology*, *34*, 72–79. Available from https://doi.org/10.1016/j.cbpa.2016.06.026.

Evans, E. H., & Carr, N. G. (1979). The interaction of respiration and photosynthesis in microalgae. In M. Gibbs, & E. Latzko (Eds.), *Photosynthesis II* (pp. 163–173). Berlin, Heidelberg: Springer Berlin Heidelberg.

Fang, L., Lin, H. X., Low, C. S., Wu, M. H., Chow, Y., & Lee, Y. K. (2012). Expression of the *Chlamydomonas reinhardtii* sedoheptulose-1,7-bisphosphatase in *Dunaliella bardawil* leads to enhanced photosynthesis and increased glycerol production. *Plant Biotechnology Journal*, *10*(9), 1129–1135. Available from https://doi.org/10.1111/pbi.12000.

Farr, T. J., Huppe, H. C., & Turpin, D. H. (1994). Coordination of chloroplastic metabolism in N-limited *Chlamydomonas reinhardtii* by redox modulation (I. The activation of phosphoribulosekinase and glucose-6-phosphate dehydrogenase is relative to the photosynthetic supply of electrons). *Plant Physiology*, *105*(4), 1037–1042. Available from https://doi.org/10.1104/pp.105.4.1037.

Fermani, S., Ripamonti, A., Sabatino, P., Zanotti, G., Scagliarini, S., Sparla, F., ... Pupillo, P. (2001). Crystal structure of the non-regulatory A(4) isoform of spinach chloroplast glyceraldehyde-3-phosphate dehydrogenase complexed with NADP. *Journal of Molecular Biology*, *314*(3), 527–542. Available from https://doi.org/10.1006/jmbi.2001.5172.

Fermani, S., Sparla, F., Falini, G., Martelli, P. L., Casadio, R., Pupillo, P., ... Trost, P. (2007). Molecular mechanism of thioredoxin regulation in photosynthetic A2B2-glyceraldehyde-3-phosphate dehydrogenase. *Proceedings of the National Academy of Sciences of the United States of America*, *104*(26), 11109–11114. Available from https://doi.org/10.1073/pnas.0611636104.

Fermani, S., Sparla, F., Marri, L., Thumiger, A., Pupillo, P., Falini, G., ... Trost, P. (2010). Structure of photosynthetic glyceraldehyde-3-phosphate dehydrogenase (isoform A4) from *Arabidopsis thaliana* in complex with NAD. *Acta Crystallographica. Section F, Structural Biology and Crystallization Communications*, *66*(Pt 6), 621–626. Available from https://doi.org/10.1107/S1744309110013527.

Fermani, S., Trivelli, X., Sparla, F., Thumiger, A., Calvaresi, M., Marri, L., ... Trost, P. (2012). Conformational selection and folding-upon-binding of intrinsically disordered protein CP12 regulate photosynthetic enzymes assembly. *The Journal of Biological Chemistry*, *287*(25), 21372–21383. Available from https://doi.org/10.1074/jbc.M112.350355.

Ford, M. M., Smythers, A. L., McConnell, E. W., Lowery, S. C., Kolling, D. R. J., & Hicks, L. M. (2019). Inhibition of TOR in *Chlamydomonas reinhardtii* leads to rapid cysteine oxidation reflecting sustained physiological changes. *Cells*, *8*(10). Available from https://doi.org/10.3390/cells8101171.

Forti, G. (2008). The role of respiration in the activation of photosynthesis upon illumination of dark adapted *Chlamydomonas reinhardtii*. *Biochimica et Biophysica Acta*, *1777*(11), 1449–1454. Available from https://doi.org/10.1016/j.bbabio.2008.08.011.

Forti, G., & Elli, G. (1996). Stimulation of photophosphorylation by ascorbate as a function of light intensity. *Plant Physiology*, *112*(4), 1509–1511. Available from https://doi.org/10.1104/pp.112.4.1509.

Forti, G., Furia, A., Bombelli, P., & Finazzi, G. (2003). In vivo changes of the oxidation-reduction state of NADP and of the ATP/ADP cellular ratio linked to the photosynthetic activity in *Chlamydomonas reinhardtii*. *Plant Physiology*, *132*(3), 1464–1474. Available from https://doi.org/10.1104/pp.102.018861.

Foyer, C. H., & Noctor, G. (2005). Redox homeostasis and antioxidant signaling: A metabolic interface between stress perception and physiological responses. *The Plant Cell*, *17*(7), 1866–1875. Available from https://doi.org/10.1105/tpc.105.033589.

Foyer, C. H., Bloom, A. J., Queval, G., & Noctor, G. (2009). Photorespiratory metabolism: Genes, mutants, energetics, and redox signaling. *Annual Review of Plant Biology*, *60*, 455–484. Available from https://doi.org/10.1146/annurev.arplant.043008.091948.

Galmes, J., Kapralov, M. V., Andralojc, P. J., Conesa, M. A., Keys, A. J., Parry, M. A., ... Flexas, J. (2014). Expanding knowledge of the Rubisco kinetics variability in plant species: environmental and evolutionary trends. *Plant, Cell & Environment*, *37*(9), 1989–2001. Available from https://doi.org/10.1111/pce.12335.

Gans, P., & Rebeille, F. (1990). Control in the dark of the plastoquinone redox state by mitochondrial activity in *Chlamydomonas reinhardtii*. *Biochimica et Biophysica Acta (BBA)-Bioenergetics*, *1015*(1), 150–155.

Garcia-Murria, M. J., Karkehabadi, S., Marin-Navarro, J., Satagopan, S., Andersson, I., Spreitzer, R. J., ... Moreno, J. (2008). Structural and functional consequences of the replacement of proximal residues Cys(172) and Cys(192) in the large subunit of ribulose-1,5-bisphosphate carboxylase/oxygenase from *Chlamydomonas reinhardtii*. *The Biochemical Journal*, *411*(2), 241–247. Available from https://doi.org/10.1042/BJ20071422.

Garcia-Murria, M. J., Sudhani, H. P. K., Marin-Navarro, J., Sanchez Del Pino, M. M., & Moreno, J. (2018). Dissecting the individual contribution of conserved cysteines to the redox regulation of RubisCO. *Photosynthesis Research*, *137*(2), 251–262. Available from https://doi.org/10.1007/s11120-018-0497-9.

Garcia-Sanchez, M. I., Gotor, C., Jacquot, J. P., Stein, M., Suzuki, A., & Vega, J. M. (1997). Critical residues of *Chlamydomonas reinhardtii* ferredoxin for interaction with nitrite reductase and glutamate synthase revealed by site-directed mutagenesis. *European Journal of Biochemistry*, *250*(2), 364–368. Available from https://doi.org/10.1111/j.1432-1033.1997.0364a.x.

Gauthier, D. A., & Turpin, D. H. (1997). Interactions between inorganic phosphate (Pi) assimilation, photosynthesis and respiration in the Pi-limited green alga *Selenastrum minutum*. *Plant, Cell & Environment*, *20*(1), 12–24.

Geigenberger, P., Kolbe, A., & Tiessen, A. (2005). Redox regulation of carbon storage and partitioning in response to light and sugars. *Journal of Experimental Botany*, *56*(416), 1469–1479. Available from https://doi.org/10.1093/jxb/eri178.

Gerotto, C., Alboresi, A., Meneghesso, A., Jokel, M., Suorsa, M., Aro, E. M., ... Morosinotto, T. (2016). Flavodiiron proteins act as safety valve for electrons in *Physcomitrella patens*. *Proceedings of the National Academy of Sciences of the United States of America*, *113*(43), 12322–12327. Available from https://doi.org/10.1073/pnas.1606685113.

Ghysels, B., Godaux, D., Matagne, R. F., Cardol, P., & Franck, F. (2013). Function of the chloroplast hydrogenase in the microalga *Chlamydomonas*: The role of hydrogenase and state transitions during photosynthetic activation in anaerobiosis. *PLoS One*, *8*(5), e64161. Available from https://doi.org/10.1371/journal.pone.0064161.

Gleizer, S., Ben-Nissan, R., Bar-On, Y. M., Antonovsky, N., Noor, E., Zohar, Y., ... Milo, R. (2019). Conversion of *Escherichia coli* to generate all biomass carbon from CO_2. *Cell*, *179*(6), 1255–1263. Available from https://doi.org/10.1016/j.cell.2019.11.009, e1212.

Gontero, B., & Avilan, L. (2011). Creating order out of disorder: Structural imprint of GAPDH on CP12. *Structure*, *19*(12), 1728–1729. Available from https://doi.org/10.1016/j.str.2011.11.004.

Gontero, B., Mulliert, G., Rault, M., Giudici-Orticoni, M. T., & Ricard, J. (1993). Structural and functional properties of a multi-enzyme complex from spinach chloroplasts. 2. Modulation of the kinetic properties of enzymes in the aggregated state. *European Journal of Biochemistry*, *217*(3), 1075–1082. Available from https://doi.org/10.1111/j.1432-1033.1993.tb18339.x.

Goodenough, U., Blaby, I., Casero, D., Gallaher, S. D., Goodson, C., Johnson, S., ... Wulan, T. (2014). The path to triacylglyceride obesity in the sta6 strain of *Chlamydomonas reinhardtii*. *Eukaryotic Cell*, *13*(5), 591–613. Available from https://doi.org/10.1128/EC.00013-14.

Goodsell, D. S., Autin, L., & Olson, A. J. (2019). Illustrate: Software for biomolecular illustration. *Structure*, *27*(11), 1716–1720. Available from https://doi.org/10.1016/j.str.2019.08.011, e1711.

Gorman, D. S., & Levine, R. P. (1966). Photosynthetic electron transport chain of *Chlamydomonas reinhardi*. V. Purification and properties of cytochrome 553 and ferredoxin. *Plant Physiology*, *41*(10), 1643–1647. Available from https://doi.org/10.1104/pp.41.10.1643.

Goyer, A., Haslekas, C., Miginiac-Maslow, M., Klein, U., Le Marechal, P., Jacquot, J. P., ... Decottignies, P. (2002). Isolation and characterization of a thioredoxin-dependent peroxidase from *Chlamydomonas reinhardtii*. *European Journal of Biochemistry*, *269*(1), 272–282. Available from https://doi.org/10.1046/j.0014-2956.2001.02648.x.

Graciet, E., Gans, P., Wedel, N., Lebreton, S., Camadro, J. M., & Gontero, B. (2003). The small protein CP12: A protein linker for supramolecular complex assembly. *Biochemistry*, *42*(27), 8163–8170. Available from https://doi.org/10.1021/bi034474x.

Graciet, E., Lebreton, S., & Gontero, B. (2004). Emergence of new regulatory mechanisms in the Benson-Calvin pathway via protein-protein interactions: A glyceraldehyde-3-phosphate dehydrogenase/CP12/phosphoribulokinase complex. *Journal of Experimental Botany*, *55*(400), 1245–1254. Available from https://doi.org/10.1093/jxb/erh107.

Graciet, E., Lebreton, S., Camadro, J. M., & Gontero, B. (2002). Thermodynamic analysis of the emergence of new regulatory properties in a phosphoribulokinase-glyceraldehyde 3-phosphate dehydrogenase complex. *The Journal of Biological Chemistry*, *277*(15), 12697–12702. Available from https://doi.org/10.1074/jbc.M111121200.

Gurrieri, L., Del Giudice, A., Demitri, N., Falini, G., Pavel, N. V., Zaffagnini, M., ... Fermani, S. (2019). *Arabidopsis* and *Chlamydomonas* phosphoribulokinase crystal structures complete the redox structural proteome of the Calvin-Benson cycle. *Proceedings of the National Academy of Sciences of the United States of America*, *116*(16), 8048–8053. Available from https://doi.org/10.1073/pnas.1820639116.

Gutle, D. D., Roret, T., Muller, S. J., Couturier, J., Lemaire, S. D., Hecker, A., ... Jacquot, J. P. (2016). Chloroplast FBPase and SBPase are thioredoxin-linked enzymes with similar architecture but different evolutionary histories. *Proceedings of the National Academy of Sciences of the United States of America*, *113*(24), 6779–6784. Available from https://doi.org/10.1073/pnas.1606241113.

Hammel, A., Sommer, F., Zimmer, D., Stitt, M., Muhlhaus, T., & Schroda, M. (2020). Overexpression of sedoheptulose-1,7-bisphosphatase enhances photosynthesis in *Chlamydomonas reinhardtii* and has no effect on the abundance of other calvin-benson cycle enzymes. *Frontiers in Plant Science*, *11*, 868. Available from https://doi.org/10.3389/fpls.2020.00868.

Hanke, G., & Mulo, P. (2013). Plant type ferredoxins and ferredoxin-dependent metabolism. *Plant, Cell & Environment*, *36*(6), 1071–1084. Available from https://doi.org/10.1111/pce.12046.

Hanschmann, E. M., Godoy, J. R., Berndt, C., Hudemann, C., & Lillig, C. H. (2013). Thioredoxins, glutaredoxins, and peroxiredoxins–molecular mechanisms and health significance: From cofactors to antioxidants to redox signaling. *Antioxidants & Redox Signaling*, *19*(13), 1539–1605. Available from https://doi.org/10.1089/ars.2012.4599.

Hazra, S., Henderson, J. N., Liles, K., Hilton, M. T., & Wachter, R. M. (2015). Regulation of ribulose-1,5-bisphosphate carboxylase/oxygenase (rubisco) activase: product inhibition, cooperativity, and magnesium activation. *The Journal of Biological Chemistry*, *290*(40), 24222–24236. Available from https://doi.org/10.1074/jbc.M115.651745.

He, S., Chou, H. T., Matthies, D., Wunder, T., Meyer, M. T., Atkinson, N., ... Jonikas, M. C. (2020). The structural basis of Rubisco phase separation in the pyrenoid. *Nature Plants*, *6*(12), 1480–1490. Available from https://doi.org/10.1038/s41477-020-00811-y.

Healey, F. P., & Myers, J. (1971). The Kok effect in *Chlamydomonas reinhardi*. *Plant Physiology*, *47*(3), 373–379. Available from https://doi.org/10.1104/pp.47.3.373.

Hertle, A. P., Blunder, T., Wunder, T., Pesaresi, P., Pribil, M., Armbruster, U., ... Leister, D. (2013). PGRL1 is the elusive ferredoxin-plastoquinone reductase in photosynthetic cyclic electron flow. *Molecular Cell*, *49*(3), 511–523. Available from https://doi.org/10.1016/j.molcel.2012.11.030.

Hess, D. T., Matsumoto, A., Kim, S. O., Marshall, H. E., & Stamler, J. S. (2005). Protein S-nitrosylation: Purview and parameters. *Nature Reviews. Molecular Cell Biology*, *6*(2), 150–166. Available from https://doi.org/10.1038/nrm1569.

Heyduk, T., Michalczyk, R., & Kochman, M. (1991). Long-range effects and conformational flexibility of aldolase. *The Journal of Biological Chemistry*, *266*(24), 15650–15655. Available from https://doi.org/10.1016/S0021-9258(18)98456-5.

Hibberd, J. M., Sheehy, J. E., & Langdale, J. A. (2008). Using C4 photosynthesis to increase the yield of rice-rationale and feasibility. *Current Opinion in Plant Biology*, *11*(2), 228–231. Available from https://doi.org/10.1016/j.pbi.2007.11.002.

Hirasawa, M., Schurmann, P., Jacquot, J. P., Manieri, W., Jacquot, P., Keryer, E., ... Knaff, D. B. (1999). Oxidation-reduction properties of chloroplast thioredoxins, ferredoxin:thioredoxin reductase, and thioredoxin f-regulated enzymes. *Biochemistry*, *38*(16), 5200–5205. Available from https://doi.org/10.1021/bi982783v.

Hirasawa, M., Tripathy, J. N., Sommer, F., Somasundaram, R., Chung, J. S., Nestander, M., ... Knaff, D. B. (2010). Enzymatic properties of the ferredoxin-dependent nitrite reductase from *Chlamydomonas reinhardtii*. Evidence for hydroxylamine as a late intermediate in ammonia production. *Photosynthesis Research*, *103*(2), 67–77. Available from https://doi.org/10.1007/s11120-009-9512-5.

Hoch, G., Owens, O. V., & Kok, B. (1963). Photosynthesis and respiration. *Archives of Biochemistry and Biophysics*, *101*, 171–180. Available from https://doi.org/10.1016/0003-9861(63)90547-2.

Hochmal, A. K., Zinzius, K., Charoenwattanasatien, R., Gabelein, P., Mutoh, R., Tanaka, H., ... Hippler, M. (2016). Calredoxin represents a novel type of calcium-dependent sensor-responder connected to redox regulation in the chloroplast. *Nature Communications*, *7*, 11847. Available from https://doi.org/10.1038/ncomms11847.

Hogg, N. (2002). The biochemistry and physiology of S-nitrosothiols. *Annual Review of Pharmacology and Toxicology*, *42*, 585–600. Available from https://doi.org/10.1146/annurev.pharmtox.42.092501.104328.

Howard, T. P., Lloyd, J. C., & Raines, C. A. (2011). Inter-species variation in the oligomeric states of the higher plant Calvin cycle enzymes glyceraldehyde-3-phosphate dehydrogenase and phosphoribulokinase. *Journal of Experimental Botany*, *62*(11), 3799–3805. Available from https://doi.org/10.1093/jxb/err057.

Huang, C., Yu, Q. B., Lv, R. H., Yin, Q. Q., Chen, G. Y., Xu, L., ... Yang, Z. N. (2013). The reduced plastid-encoded polymerase-dependent plastid gene expression leads to the delayed greening of the Arabidopsis fln2 mutant. *PLoS One*, *8*(9), e73092. Available from https://doi.org/10.1371/journal.pone.0073092.

Huppe, H. C., & Buchanan, B. B. (1989). Activation of a chloroplast type of fructose bisphosphatase from *Chlamydomonas reinhardtii* by light-mediated agents. *Journal of Biosciences*, *44*(5-6), 487–494. Available from https://doi.org/10.1515/znc-1989-5-624.

Huppe, H. C., de Lamotte-Guery, F., Jacquot, J. P., & Buchanan, B. B. (1990). The ferredoxin-thioredoxin system of a green alga, *Chlamydomonas reinhardtii*: Identification and characterization of thioredoxins and ferredoxin-thioredoxin reductase components. *Planta*, *180*, 341–351. Available from https://doi.org/10.1007/BF00198785.

Huppe, H. C., Farr, T. J., & Turpin, D. H. (1994). Coordination of chloroplastic metabolism in N-limited *Chlamydomonas reinhardtii* by redox modulation (II. Redox modulation activates the oxidative pentose phosphate pathway during photosynthetic nitrate assimilation). *Plant Physiology*, *105* (4), 1043–1048. Available from https://doi.org/10.1104/pp.105.4.1043.

Huppe, H. C., Picaud, A., Buchanan, B. B., & Miginiac-Maslow, M. (1991). Identification of an NADP/thioredoxin system in *Chlamydomonas reinhardtii*. *Planta*, *186*, 115–121. Available from https://doi.org/10.1007/BF00201506.

Hurwitz, J., Weissbach, A., Horecker, B. L., & Smyrniotis, P. Z. (1956). Spinach phosphoribulokinase. *The Journal of Biological Chemistry*, *218*(2), 769–783. Available from https://doi.org/10.1016/S0021-9258(18)65841-7.

Issakidis, E., Lemaire, M., Decottignies, P., Jacquot, J. P., & Miginiac-Maslow, M. (1996). Direct evidence for the different roles of the N- and C-terminal regulatory disulfides of sorghum leaf NADP-malate dehydrogenase in its activation by reduced thioredoxin. *FEBS Letters*, *392*(2), 121–124. Available from https://doi.org/10.1016/0014-5793(96)00801-0.

Iwaki, T., Haranoh, K., Inoue, N., Kojima, K., Satoh, R., Nishino, T., ... Wadano, A. (2006). Expression of foreign type I ribulose-1,5-bisphosphate carboxylase/ oxygenase (EC 4.1.1.39) stimulates photosynthesis in cyanobacterium Synechococcus PCC7942 cells. *Photosynthesis Research*, *88* (3), 287–297. Available from https://doi.org/10.1007/s11120-006-9048-x.

Jacobs, J., Pudollek, S., Hemschemeier, A., & Happe, T. (2009). A novel, anaerobically induced ferredoxin in *Chlamydomonas reinhardtii*. *FEBS Letters*, *583*(2), 325–329. Available from https://doi.org/10.1016/j.febslet.2008.12.018.

Jacquot, J. P., Eklund, H., Rouhier, N., & Schurmann, P. (2009). Structural and evolutionary aspects of thioredoxin reductases in photosynthetic organisms. *Trends in Plant Science*, *14*(6), 336–343. Available from https://doi.org/10.1016/j.tplants.2009.03.005.

Jacquot, J. P., Lopez-Jaramillo, J., Chueca, A., Cherfils, J., Lemaire, S., Chedozeau, B., ... Lopez-Gorge, J. (1995). High-level expression of recombinant pea chloroplast fructose-1,6-bisphosphatase and mutagenesis of its regulatory site. *European Journal of Biochemistry*, *229*(3), 675–681. Available from https://doi.org/10.1111/j.1432-1033.1995.tb20513.x.

Jacquot, J. P., Lopez-Jaramillo, J., Miginiac-Maslow, M., Lemaire, S., Cherfils, J., Chueca, A., ... Lopez-Gorge, J. (1997). Cysteine-153 is required for redox regulation of pea chloroplast fructose-1,6-bisphosphatase. *FEBS Letters*, *401*(2-3), 143–147. Available from https://doi.org/10.1016/s0014-5793(96)01459-7.

Jacquot, J. P., Stein, M., Suzuki, A., Liottet, S., Sandoz, G., & Miginiac-Maslow, M. (1997). Residue Glu-91 of *Chlamydomonas reinhardtii* ferredoxin is essential for electron transfer to ferredoxin-thioredoxin reductase. *FEBS Letters*, *400*(3), 293–296. Available from https://doi.org/10.1016/s0014-5793(96)01407-x.

Jacquot, J. P., Stein, M., Hodges, M., & Miginiac-Maslow, M. (1992). PCR cloning of a nucleotidic sequence coding for the mature part of *Chlamydomonas reinhardtii* thioredoxin Ch2. *Nucleic Acids Research*, *20*(3), 617. Available from https://doi.org/10.1093/nar/20.3.617.

Jans, F., Mignolet, E., Houyoux, P. A., Cardol, P., Ghysels, B., Cuine, S., ... Franck, F. (2008). A type II NAD(P)H dehydrogenase mediates light-independent plastoquinone reduction in the chloroplast of *Chlamydomonas*. *Proceedings of the National Academy of Sciences of the United States of America*, *105*(51), 20546–20551. Available from https://doi.org/10.1073/pnas.0806896105.

Jansen, R., & Gerstein, M. (2000). Analysis of the yeast transcriptome with structural and functional categories: Characterizing highly expressed proteins. *Nucleic Acids Research*, *28*(6), 1481–1488. Available from https://doi.org/10.1093/nar/28.6.1481.

Jebanathirajah, J. A., & Coleman, J. R. (1998). Association of carbonic anhydrase with a Calvin cycle enzyme complex in *Nicotiana tabacum*. *Planta*, *204*(2), 177–182. Available from https://doi.org/10.1007/s004250050244.

Johnson, X., & Alric, J. (2012). Interaction between starch breakdown, acetate assimilation, and photosynthetic cyclic electron flow in *Chlamydomonas reinhardtii*. *Journal of Biological Chemistry*, *287*(31), 26445–26452.

Johnson, X., Steinbeck, J., Dent, R. M., Takahashi, H., Richaud, P., Ozawa, S., … Alric, J. (2014). Proton gradient regulation 5-mediated cyclic electron flow under ATP- or redox-limited conditions: A study of DeltaATpase pgr5 and DeltarbcL pgr5 mutants in the green alga *Chlamydomonas reinhardtii*. *Plant Physiology*, *165*(1), 438–452. Available from https://doi.org/10.1104/pp.113.233593.

Jones, L. W., & Myers, J. (1963). A common link between photosynthesis and respiration in a blue-green alga. *Nature*, *199*, 670–672. Available from https://doi.org/10.1038/199670a0.

Kaaki, W., Woudstra, M., Gontero, B., & Halgand, F. (2013). Exploration of CP12 conformational changes and of quaternary structural properties using electrospray ionization traveling wave ion mobility mass spectrometry. *Rapid Communications in Mass Spectrometry*, *27*(1), 179–186. Available from https://doi.org/10.1002/rcm.6442.

Kaye, Y., Huang, W., Clowez, S., Saroussi, S., Idoine, A., Sanz-Luque, E., … Grossman, A. R. (2019). The mitochondrial alternative oxidase from *Chlamydomonas reinhardtii* enables survival in high light. *The Journal of Biological Chemistry*, *294*(4), 1380–1395. Available from https://doi.org/10.1074/jbc.RA118.004667.

Képès, F. (2011). Biologie synthétique et intégrative. *Comptes Rendus Chimie*, *14*(4), 420–423. Available from https://doi.org/10.1016/j.crci.2010.11.012.

Kerfeld, C. A., & Melnicki, M. R. (2016). Assembly, function and evolution of cyanobacterial carboxysomes. *Current Opinion in Plant Biology*, *31*, 66–75. Available from https://doi.org/10.1016/j.pbi.2016.03.009.

Keryer, E., Collin, V., Lavergne, D., Lemaire, S., & Issakidis-Bourguet, E. (2004). Characterization of Arabidopsis mutants for the variable subunit of ferredoxin:thioredoxin reductase. *Photosynthesis Research*, *79*(3), 265–274. Available from https://doi.org/10.1023/B:PRES.0000017173.46185.3e.

Kessler, E. (1973). Effect of anaerobiosis on photosynthetic reactions and nitrogen metabolism of algae with and without hydrogenase. *Archiv Für Mikrobiologie*, *93*(2), 91–100.

Kitayama, K., Kitayama, M., Osafune, T., & Togasaki, R. K. (1999). Subcellular localization of iron and manganese superoxide dismutase in *Chlamydomonas reinhardtii* (Chlorophyceae). *Journal of Phycology*, *35*(1), 136–142.

Klein, U. (1986). Compartmentation of glycolysis and of the oxidative pentose-phosphate pathway in *Chlamydomonas reinhardii*. *Planta*, *167*(1), 81–86. Available from https://doi.org/10.1007/BF00446372.

Knopf, J. A., & Shapira, M. (2005). Degradation of Rubisco SSU during oxidative stress triggers aggregation of Rubisco particles in *Chlamydomonas reinhardtii*. *Planta*, *222*(5), 787–793. Available from https://doi.org/10.1007/s00425-005-0023-0.

Kok, B. (1949). On the interrelation of respiration and photosynthesis in green plants. *Biochimica et Biophysica Acta*, *3*, 625–631. Available from https://doi.org/10.1016/0006-3002(49)90136-5.

Kong, F., Burlacot, A., Liang, Y., Légeret, B., Alseekh, S., Brotman, Y., … Peltier, G. (2018). Interorganelle communication: Peroxisomal MALATE DEHYDROGENASE2 connects lipid catabolism to photosynthesis through redox coupling in *Chlamydomonas*. *The Plant Cell*, *30*(8), 1824–1847.

Krimm, I., Lemaire, S., Ruelland, E., Miginiac-Maslow, M., Jaquot, J. P., Hirasawa, M., … Lancelin, J. M. (1998). The single mutation Trp35– > Ala in the 35-40 redox site of *Chlamydomonas reinhardtii* thioredoxin h affects its biochemical activity and the pH dependence of C36-C39 1H-13C NMR. *European Journal of Biochemistry*, *255*(1), 185–195. Available from https://doi.org/10.1046/j.1432-1327.1998.2550185.x.

Krishnan, A., Kumaraswamy, G. K., Vinyard, D. J., Gu, H., Ananyev, G., Posewitz, M. C., … Dismukes, G. C. (2015). Metabolic and photosynthetic consequences of blocking starch biosynthesis in the green alga *Chlamydomonas reinhardtii* sta6 mutant. *The Plant Journal*, *81*(6), 947–960.

Kromdijk, J., Glowacka, K., Leonelli, L., Gabilly, S. T., Iwai, M., Niyogi, K. K., … Long, S. P. (2016). Improving photosynthesis and crop productivity by accelerating recovery from photoprotection. *Science*, *354*(6314), 857–861. Available from https://doi.org/10.1126/science.aai8878.

Kubis, A., & Bar-Even, A. (2019). Synthetic biology approaches for improving photosynthesis. *Journal of Experimental Botany*, *70*(5), 1425–1433. Available from https://doi.org/10.1093/jxb/erz029.

Kuken, A., Sommer, F., Yaneva-Roder, L., Mackinder, L. C., Hohne, M., Geimer, S., … Mettler-Altmann, T. (2018). Effects of microcompartmentation on flux distribution and metabolic pools in *Chlamydomonas reinhardtii* chloroplasts. *Elife*, *7*. Available from https://doi.org/10.7554/eLife.37960.

Kuo, E. Y., Cai, M. S., & Lee, T. M. (2020). Ascorbate peroxidase 4 plays a role in the tolerance of *Chlamydomonas reinhardtii* to photo-oxidative stress. *Scientific Reports*, *10*(1), 13287. Available from https://doi.org/10.1038/s41598-020-70247-z.

Kuo, E. Y., Chang, H. L., Lin, S. T., & Lee, T. M. (2020). High light-induced nitric oxide production induces autophagy and cell death in *Chlamydomonas reinhardtii*. *Frontiers in Plant Science*, *11*, 772. Available from https://doi.org/10.3389/fpls.2020.00772.

Lancelin, J. M., Guilhaudis, L., Krimm, I., Blackledge, M. J., Marion, D., & Jacquot, J. P. (2000). NMR structures of thioredoxin m from the green alga *Chlamydomonas reinhardtii*. *Proteins*, *41*(3), 334–349. Available from https://doi.org/10.1002/1097-0134(20001115)41:3 < 334::aid-prot60 > 3.3.co;2-d.

Lancelin, J. M., Stein, M., & Jacquot, J. P. (1993). Secondary structure and protein folding of recombinant chloroplastic thioredoxin Ch2 from the green alga *Chlamydomonas reinhardtii* as determined by 1H NMR. *Journal of Biochemistry*, *114*(3), 421–431. Available from https://doi.org/10.1093/oxfordjournals.jbchem.a124192.

Launay, H., Barre, P., Puppo, C., Manneville, S., Gontero, B., & Receveur-Brechot, V. (2016). Absence of residual structure in the intrinsically disordered regulatory protein CP12 in its reduced state. *Biochemical and Biophysical Research Communications*, *477*(1), 20–26. Available from https://doi.org/10.1016/j.bbrc.2016.06.014.

Laurent, T. C., Moore, E. C., & Reichard, P. (1964). Enzymatic synthesis of deoxyribonucleotides. Iv. Isolation and characterization of thioredoxin, the hydrogen donor from *Escherichia coli* B. *The Journal of Biological Chemistry*, *239*, 3436–3444. Available from https://doi.org/10.1016/S0021-9258(18)97742-2.

Le Moigne, T., Crozet, P., Lemaire, S. D., & Henri, J. (2020). High-resolution crystal structure of chloroplastic ribose-5-phosphate isomerase from *Chlamydomonas reinhardtii* – An enzyme involved in the photosynthetic Calvin-Benson cycle. *International Journal of Molecular Sciences*, *21* (20). Available from https://doi.org/10.3390/ijms21207787.

Le Moigne, T., Gurrieri, L., Crozet, P., Marchand, C. H., Zaffagnini, M., Sparla, F., … Henri, J. (2021). Crystal structure of chloroplastic thioredoxin z defines a type-specific target recognition. *The Plant Journal*, *107*(2), 434–447. Available from https://doi.org/10.1111/tpj.15300.

Le Moigne, T., Sarti, E., Nourisson, A., Carbone, A., Lemaire, S. D., & Henri, J. (2022). Crystal structure of chloroplast fructose-1,6-bisphosphate aldolase from the green alga *Chlamydomonas reinhardtii*. *Journal of Structural Biology*, *214*(3), 107873. Available from https://doi.org/10.1016/j.jsb.2022.107873.

Lebreton, S., Andreescu, S., Graciet, E., & Gontero, B. (2006). Mapping of the interaction site of CP12 with glyceraldehyde-3-phosphate dehydrogenase from *Chlamydomonas reinhardtii*. Functional consequences for glyceraldehyde-3-phosphate dehydrogenase. *The FEBS Journal*, *273*(14), 3358–3369. Available from https://doi.org/10.1111/j.1742-4658.2006.05342.x.

Lebreton, S., Graciet, E., & Gontero, B. (2003). Modulation, via protein-protein interactions, of glyceraldehyde-3-phosphate dehydrogenase activity through redox phosphoribulokinase regulation. *The Journal of Biological Chemistry*, *278*(14), 12078–12084. Available from https://doi.org/10.1074/jbc.M213096200.

Lecler, R., Vigeolas, H., Emonds-Alt, B., Cardol, P., & Remacle, C. (2012). Characterization of an internal type-II NADH dehydrogenase from *Chlamydomonas reinhardtii* mitochondria. *Current Genetics*, *58*(4), 205–216. Available from https://doi.org/10.1007/s00294-012-0378-2.

Ledford, H. K., & Niyogi, K. K. (2005). Singlet oxygen and photo-oxidative stress management in plants and algae. *Plant, Cell & Environment*, *28* (8), 1037–1045. Available from https://doi.org/10.1111/j.1365-3040.2005.01374.x.

Lee, S., Kim, S. M., & Lee, R. T. (2013). Thioredoxin and thioredoxin target proteins: From molecular mechanisms to functional significance. *Antioxidants & Redox Signaling*, *18*(10), 1165–1207. Available from https://doi.org/10.1089/ars.2011.4322.

Lefebvre, S., Lawson, T., Zakhleniuk, O. V., Lloyd, J. C., Raines, C. A., & Fryer, M. (2005). Increased sedoheptulose-1,7-bisphosphatase activity in transgenic tobacco plants stimulates photosynthesis and growth from an early stage in development. *Plant Physiology*, *138*(1), 451–460. Available from https://doi.org/10.1104/pp.104.055046.

Lemaire, S. D., & Miginiac-Maslow, M. (2004). The thioredoxin superfamily in *Chlamydomonas reinhardtii*. *Photosynthesis Research*, *82*(3), 203–220. Available from https://doi.org/10.1007/s11120-004-1091-x.

Lemaire, S. D., Collin, V., Keryer, E., Issakidis-Bourguet, E., Lavergne, D., & Miginiac-Maslow, M. (2003). *Chlamydomonas reinhardtii*: A model organism for the study of the thioredoxin family. *Plant Physiology and Biochemistry*, *41*(6-7), 513–521. Available from https://doi.org/10.1016/s0981-9428(03)00079-2.

Lemaire, S. D., Collin, V., Keryer, E., Quesada, A., & Miginiac-Maslow, M. (2003). Characterization of thioredoxin y, a new type of thioredoxin identified in the genome of *Chlamydomonas reinhardtii*. *FEBS Letters*, *543*(1-3), 87–92. Available from https://doi.org/10.1016/s0014-5793(03)00416-2.

Lemaire, S. D., Guillon, B., Le Marechal, P., Keryer, E., Miginiac-Maslow, M., & Decottignies, P. (2004). New thioredoxin targets in the unicellular photosynthetic eukaryote *Chlamydomonas reinhardtii*. *Proceedings of the National Academy of Sciences of the United States of America*, *101*(19), 7475–7480. Available from https://doi.org/10.1073/pnas.0402221101.

Lemaire, S. D., Michelet, L., Zaffagnini, M., Massot, V., & Issakidis-Bourguet, E. (2007). Thioredoxins in chloroplasts. *Current Genetics*, *51*(6), 343–365. Available from https://doi.org/10.1007/s00294-007-0128-z.

Lemaire, S. D., Miginiac-Maslow, M., & Jacquot, J. P. (2002). Plant thioredoxin gene expression: Control by light, circadian clock, and heavy metals. *Methods in Enzymology*, *347*, 412–421. Available from https://doi.org/10.1016/s0076-6879(02)47041-3.

Lemaire, S. D., Quesada, A., Merchan, F., Corral, J. M., Igeno, M. I., Keryer, E., … Miginiac-Maslow, M. (2005). NADP-malate dehydrogenase from unicellular green alga *Chlamydomonas reinhardtii*. A first step toward redox regulation? *Plant Physiology*, *137*(2), 514–521. Available from https://doi.org/10.1104/pp.104.052670.

Lemaire, S. D., Richardson, J. M., Goyer, A., Keryer, E., Lancelin, J. M., Makhatadze, G. I., … Jacquot, J. P. (2000). Primary structure determinants of the pH- and temperature-dependent aggregation of thioredoxin. *Biochimica et Biophysica Acta*, *1476*(2), 311–323. Available from https://doi.org/10.1016/s0167-4838(99)00235-6.

Lemaire, S. D., Stein, M., Issakidis-Bourguet, E., Keryer, E., Benoit, V. V., Pineau, B., … Jacquot, J. P. (1999). The complex regulation of ferredoxin/thioredoxin-related genes by light and the circadian clock. *Planta*, *209*(2), 221–229. Available from https://doi.org/10.1007/s004250050626.

Lemaire, S. D., Tedesco, D., Crozet, P., Michelet, L., Fermani, S., Zaffagnini, M., … Henri, J. (2018). Crystal structure of chloroplastic thioredoxin f2 from *Chlamydomonas reinhardtii* reveals distinct surface properties. *Antioxidants*, *7*(12). Available from https://doi.org/10.3390/antiox7120171.

Lemaire, S., Keryer, E., Stein, M., Schepens, I. I., Issakidis-Bourguet, E. C. G., … Jacquot, J. P. (1999). Heavy-metal regulation of thioredoxin gene expression in *Chlamydomonas reinhardtii*. *Plant Physiology*, *120*(3), 773–778. Available from https://doi.org/10.1104/pp.120.3.773.

Lemeille, S., Turkina, M. V., Vener, A. V., & Rochaix, J. D. (2010). Stt7-dependent phosphorylation during state transitions in the green alga *Chlamydomonas reinhardtii*. *Molecular & Cellular Proteomics*, *9*(6), 1281–1295. Available from https://doi.org/10.1074/mcp.M000020-MCP201.

Lendzian, K., & Bassham, J. A. (1975). Regulation of glucose-6-phosphate dehydrogenase in spinach chloroplasts by ribulose 1,5-diphosphate and NADPH/NADP+ ratios. *Biochimica et Biophysica Acta*, *396*(2), 260–275. Available from https://doi.org/10.1016/0005-2728(75)90040-7.

Levine, R. P. (1960). A screening technique for photosynthetic mutants in unicellular algae. *Nature*, *188*(4747), 339–340. Available from https://doi.org/10.1038/188339b0.

Li, Y., Han, D., Hu, G., Dauvillee, D., Sommerfeld, M., Ball, S., … Hu, Q. (2010). Chlamydomonas starchless mutant defective in ADP-glucose pyrophosphorylase hyper-accumulates triacylglycerol. *Metabolic Engineering*, *12*(4), 387–391. Available from https://doi.org/10.1016/j.ymben.2010.02.002.

Liang, F., & Lindblad, P. (2016). Effects of overexpressing photosynthetic carbon flux control enzymes in the cyanobacterium Synechocystis PCC 6803. *Metabolic Engineering*, *38*, 56–64. Available from https://doi.org/10.1016/j.ymben.2016.06.005.

Liang, F., & Lindblad, P. (2017). Synechocystis PCC 6803 overexpressing RuBisCO grow faster with increased photosynthesis. *Metabolic Engineering Communications*, *4*, 29–36. Available from https://doi.org/10.1016/j.meteno.2017.02.002.

Liang, F., Englund, E., Lindberg, P., & Lindblad, P. (2018). Engineered cyanobacteria with enhanced growth show increased ethanol production and higher biofuel to biomass ratio. *Metabolic Engineering*, *46*, 51–59. Available from https://doi.org/10.1016/j.ymben.2018.02.006.

Liaud, M. F., Brandt, U., Scherzinger, M., & Cerff, R. (1997). Evolutionary origin of cryptomonad microalgae: Two novel chloroplast/cytosol-specific GAPDH genes as potential markers of ancestral endosymbiont and host cell components. *Journal of Molecular Evolution*, *44*(Suppl 1), S28–S37. Available from https://doi.org/10.1007/pl00000050.

Lin, M. T., Occhialini, A., Andralojc, P. J., Parry, M. A., & Hanson, M. R. (2014). A faster Rubisco with potential to increase photosynthesis in crops. *Nature*, *513*(7519), 547–550. Available from https://doi.org/10.1038/nature13776.

Liu, K., Yuan, C., Li, H., Chen, K., Lu, L., Shen, C., … Zheng, X. (2018). A qualitative proteome-wide lysine crotonylation profiling of papaya (*Carica papaya* L.). *Scientific Reports*, *8*(1), 8230. Available from https://doi.org/10.1038/s41598-018-26676-y.

Lmoumene, C. E., Conte, D., Jacquot, J. P., & Houee-Levin, C. (2000). Redox properties of protein disulfide bond in oxidized thioredoxin and lysozyme: A pulse radiolysis study. *Biochemistry*, *39*(31), 9295–9301. Available from https://doi.org/10.1021/bi000468e.

Long, B. M., Rae, B. D., Rolland, V., Forster, B., & Price, G. D. (2016). Cyanobacterial CO_2-concentrating mechanism components: Function and prospects for plant metabolic engineering. *Current Opinion in Plant Biology*, *31*, 1–8. Available from https://doi.org/10.1016/j.pbi.2016.03.002.

Long, S. P., Ainsworth, E. A., Rogers, A., & Ort, D. R. (2004). Rising atmospheric carbon dioxide: Plants FACE the future. *Annual Review of Plant Biology*, *55*, 591–628. Available from https://doi.org/10.1146/annurev.arplant.55.031903.141610.

Long, S. P., Marshall-Colon, A., & Zhu, X. G. (2015). Meeting the global food demand of the future by engineering crop photosynthesis and yield potential. *Cell*, *161*(1), 56–66. Available from https://doi.org/10.1016/j.cell.2015.03.019.

Lucker, B., & Kramer, D. M. (2013). Regulation of cyclic electron flow in *Chlamydomonas reinhardtii* under fluctuating carbon availability. *Photosynthesis Research*, *117*(1-3), 449–459. Available from https://doi.org/10.1007/s11120-013-9932-0.

Mackinder, L. C. M., Chen, C., Leib, R. D., Patena, W., Blum, S. R., Rodman, M., … Jonikas, M. C. (2017). A spatial interactome reveals the protein organization of the algal CO_2-concentrating mechanism. *Cell*, *171*(1), 133–147. Available from https://doi.org/10.1016/j.cell.2017.08.044, e114.

Mackinder, L. C., Meyer, M. T., Mettler-Altmann, T., Chen, V. K., Mitchell, M. C., Caspari, O., … Jonikas, M. C. (2016). A repeat protein links Rubisco to form the eukaryotic carbon-concentrating organelle. *Proceedings of the National Academy of Sciences of the United States of America*, *113*(21), 5958–5963. Available from https://doi.org/10.1073/pnas.1522866113.

Marchand, C. H., Fermani, S., Rossi, J., Gurrieri, L., Tedesco, D., Henri, J., … Zaffagnini, M. (2019). Structural and biochemical insights into the reactivity of thioredoxin h1 from *Chlamydomonas reinhardtii*. *Antioxidants*, *8*(1). Available from https://doi.org/10.3390/antiox8010010.

Marco, P., Elman, T., & Yacoby, I. (2019). Binding of ferredoxin NADP(+) oxidoreductase (FNR) to plant photosystem I. *Biochimica et Biophysica Acta - Bioenergetics*, *1860*(9), 689–698. Available from https://doi.org/10.1016/j.bbabio.2019.07.007.

Marco, P., Kozuleva, M., Eilenberg, H., Mazor, Y., Gimeson, P., Kanygin, A., … Yacoby, I. (2018). Binding of ferredoxin to algal photosystem I involves a single binding site and is composed of two thermodynamically distinct events. *Biochimica et Biophysica Acta - Bioenergetics*, *1859*(4), 234–243. Available from https://doi.org/10.1016/j.bbabio.2018.01.001.

Marcus, Y., Altman-Gueta, H., Wolff, Y., & Gurevitz, M. (2011). Rubisco mutagenesis provides new insight into limitations on photosynthesis and growth in Synechocystis PCC6803. *Journal of Experimental Botany*, *62*(12), 4173–4182. Available from https://doi.org/10.1093/jxb/err116.

Marin-Navarro, J., & Moreno, J. (2006). Cysteines 449 and 459 modulate the reduction-oxidation conformational changes of ribulose 1.5-bisphosphate carboxylase/oxygenase and the translocation of the enzyme to membranes during stress. *Plant, Cell & Environment*, *29*(5), 898–908. Available from https://doi.org/10.1111/j.1365-3040.2005.01469.x.

Marri, L., Pesaresi, A., Valerio, C., Lamba, D., Pupillo, P., Trost, P., … Sparla, F. (2010). In vitro characterization of Arabidopsis CP12 isoforms reveals common biochemical and molecular properties. *Journal of Plant Physiology*, *167*(12), 939–950. Available from https://doi.org/10.1016/j.jplph.2010.02.008.

Marri, L., Trost, P., Pupillo, P., & Sparla, F. (2005). Reconstitution and properties of the recombinant glyceraldehyde-3-phosphate dehydrogenase/CP12/phosphoribulokinase supramolecular complex of Arabidopsis. *Plant Physiology*, *139*(3), 1433–1443. Available from https://doi.org/10.1104/pp.105.068445.

Marri, L., Trost, P., Trivelli, X., Gonnelli, L., Pupillo, P., & Sparla, F. (2008). Spontaneous assembly of photosynthetic supramolecular complexes as mediated by the intrinsically unstructured protein CP12. *The Journal of Biological Chemistry*, *283*(4), 1831–1838. Available from https://doi.org/10.1074/jbc.M705650200.

Marri, L., Zaffagnini, M., Collin, V., Issakidis-Bourguet, E., Lemaire, S. D., Pupillo, P., … Trost, P. (2009). Prompt and easy activation by specific thioredoxins of calvin cycle enzymes of *Arabidopsis thaliana* associated in the GAPDH/CP12/PRK supramolecular complex. *Molecular Plant*, *2*(2), 259–269. Available from https://doi.org/10.1093/mp/ssn061.

Matagne, R. F., Michel-Wolwertz, M. R., Munaut, C., Duyckaerts, C., & Sluse, F. (1989). Induction and characterization of mitochondrial DNA mutants in *Chlamydomonas reinhardtii*. *The Journal of Cell Biology*, *108*(4), 1221–1226. Available from https://doi.org/10.1083/jcb.108.4.1221.

Mathy, G., Cardol, P., Dinant, M., Blomme, A., Gerin, S., Cloes, M., ... Sluse, F. E. (2010). Proteomic and functional characterization of a *Chlamydomonas reinhardtii* mutant lacking the mitochondrial alternative oxidase 1. *Journal of Proteome Research*, *9*(6), 2825–2838. Available from https://doi.org/10.1021/pr900866e.

McConnell, E. W., Werth, E. G., & Hicks, L. M. (2018). The phosphorylated redox proteome of *Chlamydomonas reinhardtii*: Revealing novel means for regulation of protein structure and function. *Redox Biology*, *17*, 35–46. Available from https://doi.org/10.1016/j.redox.2018.04.003.

McFarlane, C. R., Shah, N. R., Kabasakal, B. V., Echeverria, B., Cotton, C. A. R., Bubeck, D., ... Murray, J. W. (2019). Structural basis of light-induced redox regulation in the Calvin-Benson cycle in cyanobacteria. *Proceedings of the National Academy of Sciences of the United States of America*, *116*(42), 20984–20990. Available from https://doi.org/10.1073/pnas.1906722116.

Mehrshahi, P., Nguyen, G. T. D. T., Gorchs Rovira, A., Sayer, A., Llavero-Pasquina, M., Lim Huei Sin, M., ... Smith, A. G. (2020). Development of novel riboswitches for synthetic biology in the green alga *Chlamydomonas*. *ACS Synthetic Biology*, *9*(6), 1406–1417. Available from https://doi.org/10.1021/acssynbio.0c00082.

Melandri, B. A., Baccarini, A., & Pupillo, P. (1968). Glyceraldehyde-3-phosphate dehydrogenase in photosynthetic tissues: Kinetic evidence for competitivity between NADP and NAD. *Biochemical and Biophysical Research Communications*, *33*(1), 160–164. Available from https://doi.org/10.1016/0006-291x(68)90272-6.

Menchise, V., Corbier, C., Didierjean, C., Jacquot, J. P., Benedetti, E., Saviano, M., ... Aubry, A. (2000). Crystal structure of the W35A mutant thioredoxin h from *Chlamydomonas reinhardtii*: The substitution of the conserved active site Trp leads to modifications in the environment of the two catalytic cysteines. *Biopolymers*, *56*(1), 1–7. Available from https://doi.org/10.1002/1097-0282(2000)56:1<1::AID-BIP1036>3.0.CO;2-5.

Menchise, V., Corbier, C., Didierjean, C., Saviano, M., Benedetti, E., Jacquot, J. P., ... Aubry, A. (2001). Crystal structure of the wild-type and D30A mutant thioredoxin h of *Chlamydomonas reinhardtii* and implications for the catalytic mechanism. *Biochemical Journal*, *359*(Pt 1), 65–75. Available from https://doi.org/10.1042/0264-6021:3590065.

Mettler, T., Muhlhaus, T., Hemme, D., Schottler, M. A., Rupprecht, J., Idoine, A., ... Stitt, M. (2014). Systems analysis of the response of photosynthesis, metabolism, and growth to an increase in irradiance in the photosynthetic model organism *Chlamydomonas reinhardtii*. *The Plant Cell*, *26*(6), 2310–2350. Available from https://doi.org/10.1105/tpc.114.124537.

Meyer, Y., Belin, C., Delorme-Hinoux, V., Reichheld, J. P., & Riondet, C. (2012). Thioredoxin and glutaredoxin systems in plants: Molecular mechanisms, crosstalks, and functional significance. *Antioxidants & Redox Signaling*, *17*(8), 1124–1160. Available from https://doi.org/10.1089/ars.2011.4327.

Michelet, L., Zaffagnini, M., Morisse, S., Sparla, F., Perez-Perez, M. E., Francia, F., ... Lemaire, S. D. (2013). Redox regulation of the Calvin-Benson cycle: Something old, something new. *Frontiers in Plant Science*, *4*, 470. Available from https://doi.org/10.3389/fpls.2013.00470.

Michelet, L., Roach, T., Fischer, B. B., Bedhomme, M., Lemaire, S. D., & Krieger-Liszkay, A. N. J. A. (2013). Down-regulation of catalase activity allows transient accumulation of a hydrogen peroxide signal in *Chlamydomonas reinhardtii*. *Plant, Cell & Environment*, *36*(6), 1204–1213.

Michelet, L., Zaffagnini, M., Vanacker, H., Le Marechal, P., Marchand, C., Schroda, M., ... Decottignies, P. (2008). In vivo targets of S-thiolation in *Chlamydomonas reinhardtii*. *The Journal of Biological Chemistry*, *283*(31), 21571–21578. Available from https://doi.org/10.1074/jbc.M802331200.

Mignolet, E., Lecler, R., Ghysels, B., Remacle, C., & Franck, F. (2012). Function of the chloroplastic NAD(P)H dehydrogenase Nda2 for H(2) photoproduction in sulphur-deprived *Chlamydomonas reinhardtii*. *Journal of Biotechnology*, *162*(1), 81–88. Available from https://doi.org/10.1016/j.jbiotec.2012.07.002.

Mikkelsen, R., Mutenda, K. E., Mant, A., Schurmann, P., & Blennow, A. (2005). Alpha-glucan, water dikinase (GWD): A plastidic enzyme with redox-regulated and coordinated catalytic activity and binding affinity. *Proceedings of the National Academy of Sciences of the United States of America*, *102*(5), 1785–1790. Available from https://doi.org/10.1073/pnas.0406674102.

Milanez, S., Mural, R. J., & Hartman, F. C. (1991). Roles of cysteinyl residues of phosphoribulokinase as examined by site-directed mutagenesis. *The Journal of Biological Chemistry*, *266*(16), 10694–10699. Available from https://doi.org/10.1016/S0021-9258(18)99279-3.

Mittard, V., Blackledge, M. J., Stein, M., Jacquot, J. P., Marion, D., & Lancelin, J. M. (1997). NMR solution structure of an oxidised thioredoxin h from the eukaryotic green alga *Chlamydomonas reinhardtii*. *European Journal of Biochemistry*, *243*(1-2), 374–383. Available from https://doi.org/10.1111/j.1432-1033.1997.0374a.x.

Mittard, V., Morelle, N., Brutscher, B., Simorre, J. P., Marion, D., Stein, M., ... Lancelin, J. M. (1995). 1H, 13C, 15N-NMR resonance assignments of oxidized thioredoxin h from the eukaryotic green alga *Chlamydomonas reinhardtii* using new methods based on two-dimensional triple-resonance NMR spectroscopy and computer-assisted backbone assignment. *European Journal of Biochemistry*, *229*(2), 473–485. Available from https://doi.org/10.1111/j.1432-1033.1995.tb20488.x.

Miyagawa, Y., Tamoi, M., & Shigeoka, S. (2001). Overexpression of a cyanobacterial fructose-1,6-/sedoheptulose-1,7-bisphosphatase in tobacco enhances photosynthesis and growth. *Nature Biotechnology*, *19*(10), 965–969. Available from https://doi.org/10.1038/nbt1001-965.

Moll, B., & Levine, R. P. (1970). Characterization of a photosynthetic mutant strain of *Chlamydomonas reinhardi* deficient in phosphoribulokinase activity. *Plant Physiology*, *46*(4), 576–580. Available from https://doi.org/10.1104/pp.46.4.576.

Montrichard, F., Alkhalfioui, F., Yano, H., Vensel, W. H., Hurkman, W. J., & Buchanan, B. B. (2009). Thioredoxin targets in plants: The first 30 years. *Journal of Proteomics*, *72*(3), 452–474. Available from https://doi.org/10.1016/j.jprot.2008.12.002.

Moreno, J., & Spreitzer, R. J. (1999). C172S substitution in the chloroplast-encoded large subunit affects stability and stress-induced turnover of ribulose-1,5-bisphosphate carboxylase/oxygenase. *The Journal of Biological Chemistry*, *274*(38), 26789–26793. Available from https://doi.org/10.1074/jbc.274.38.26789.

Moreno, J., Garcia-Murria, M. J., & Marin-Navarro, J. (2008). Redox modulation of Rubisco conformation and activity through its cysteine residues. *Journal of Experimental Botany*, *59*(7), 1605–1614. Available from https://doi.org/10.1093/jxb/erm310.

Morisse, S., Michelet, L., Bedhomme, M., Marchand, C. H., Calvaresi, M., Trost, P., … Lemaire, S. D. (2014). Thioredoxin-dependent redox regulation of chloroplastic phosphoglycerate kinase from *Chlamydomonas reinhardtii*. *The Journal of Biological Chemistry*, *289*(43), 30012–30024. Available from https://doi.org/10.1074/jbc.M114.597997.

Morisse, S., Zaffagnini, M., Gao, X. H., Lemaire, S. D., & Marchand, C. H. (2014). Insight into protein S-nitrosylation in *Chlamydomonas reinhardtii*. *Antioxidants & Redox Signaling*, *21*(9), 1271–1284. Available from https://doi.org/10.1089/ars.2013.5632.

Mosebach, L., Heilmann, C., Mutoh, R., Gabelein, P., Steinbeck, J., Happe, T., … Hippler, M. (2017). Association of Ferredoxin:NADP(+) oxidoreductase with the photosynthetic apparatus modulates electron transfer in *Chlamydomonas reinhardtii*. *Photosynthesis Research*, *134*(3), 291–306. Available from https://doi.org/10.1007/s11120-017-0408-5.

Mussgnug, J. H., Thomas-Hall, S., Rupprecht, J., Foo, A., Klassen, V., McDowall, A., … Hankamer, B. (2007). Engineering photosynthetic light capture: impacts on improved solar energy to biomass conversion. *Plant Biotechnology Journal*, *5*(6), 802–814. Available from https://doi.org/10.1111/j.1467-7652.2007.00285.x.

Navrot, N., Gelhaye, E., Jacquot, J. P., & Rouhier, N. (2006). Identification of a new family of plant proteins loosely related to glutaredoxins with four CxxC motives. *Photosynthesis Research*, *89*(2-3), 71–79. Available from https://doi.org/10.1007/s11120-006-9083-7.

Nawrocki, W. J., Bailleul, B., Picot, D., Cardol, P., Rappaport, F., Wollman, F. A., … Joliot, P. (2019). The mechanism of cyclic electron flow. *Biochimica et Biophysica Acta - Bioenergetics*, *1860*(5), 433–438. Available from https://doi.org/10.1016/j.bbabio.2018.12.005.

Nee, G., Zaffagnini, M., Trost, P., & Issakidis-Bourguet, E. (2009). Redox regulation of chloroplastic glucose-6-phosphate dehydrogenase: A new role for f-type thioredoxin. *FEBS Letters*, *583*(17), 2827–2832. Available from https://doi.org/10.1016/j.febslet.2009.07.035.

Nikolova, D., Heilmann, C., Hawat, S., Gabelein, P., & Hippler, M. (2018). Absolute quantification of selected photosynthetic electron transfer proteins in *Chlamydomonas reinhardtii* in the presence and absence of oxygen. *Photosynthesis Research*, *137*(2), 281–293. Available from https://doi.org/10.1007/s11120-018-0502-3.

Nishizawa, A. N., & Buchanan, B. B. (1981). Enzyme regulation in C4 photosynthesis. Purification and properties of thioredoxin-linked fructose bisphosphatase and sedoheptulose bisphosphatase from corn leaves. *The Journal of Biological Chemistry*, *256*(12), 6119–6126. Available from https://doi.org/10.1016/S0021-9258(19)69136-2.

Ogawa, T., Tamoi, M., Kimura, A., Mine, A., Sakuyama, H., Yoshida, E., … Shigeoka, S. (2015). Enhancement of photosynthetic capacity in *Euglena gracilis* by expression of cyanobacterial fructose-1,6-/sedoheptulose-1,7-bisphosphatase leads to increases in biomass and wax ester production. *Biotechnology for Biofuels*, *8*, 80. Available from https://doi.org/10.1186/s13068-015-0264-5.

Ort, D. R., & Melis, A. (2011). Optimizing antenna size to maximize photosynthetic efficiency. *Plant Physiology*, *155*(1), 79–85. Available from https://doi.org/10.1104/pp.110.165886.

Ort, D. R., Merchant, S. S., Alric, J., Barkan, A., Blankenship, R. E., Bock, R., … Zhu, X. G. (2015). Redesigning photosynthesis to sustainably meet global food and bioenergy demand. *Proceedings of the National Academy of Sciences of the United States of America*, *112*(28), 8529–8536. Available from https://doi.org/10.1073/pnas.1424031112.

Page, M. D., Allen, M. D., Kropat, J., Urzica, E. I., Karpowicz, S. J., Hsieh, S. I., … Merchant, S. S. (2012). Fe sparing and Fe recycling contribute to increased superoxide dismutase capacity in iron-starved *Chlamydomonas reinhardtii*. *The Plant Cell*, *24*(6), 2649–2665. Available from https://doi.org/10.1105/tpc.112.098962.

Parry, M. A., Andralojc, P. J., Scales, J. C., Salvucci, M. E., Carmo-Silva, A. E., Alonso, H., … Whitney, S. M. (2013). Rubisco activity and regulation as targets for crop improvement. *Journal of Experimental Botany*, *64*(3), 717–730. Available from https://doi.org/10.1093/jxb/ers336.

Pasquini, M., Fermani, S., Tedesco, D., Sciabolini, C., Crozet, P., Naldi, M., … Francia, F. (2017). Structural basis for the magnesium-dependent activation of transketolase from *Chlamydomonas reinhardtii*. *Biochimica et Biophysica Acta - General Subjects*, *1861*(8), 2132–2145. Available from https://doi.org/10.1016/j.bbagen.2017.05.021.

Peden, E. A., Boehm, M., Mulder, D. W., Davis, R., Old, W. M., King, P. W., … Dubini, A. (2013). Identification of global ferredoxin interaction networks in *Chlamydomonas reinhardtii*. *The Journal of Biological Chemistry*, *288*(49), 35192–35209. Available from https://doi.org/10.1074/jbc.M113.483727.

Pedersen, T. A., Kirk, M., & Bassham, J. A. (1966). Light-dark transients in levels of intermediate compounds during photosynthesis in air-adapted chlorella. *Physiologia Plantarum*, *19*(1), 219–231. Available from https://doi.org/10.1111/j.1399-3054.1966.tb09094.x.

Peltier, G., & Thibault, P. (1985). O_2 uptake in the light in chlamydomonas: Evidence for persistent mitochondrial respiration. *Plant Physiology*, *79*(1), 225–230. Available from https://doi.org/10.1104/pp.79.1.225.

Peltier, G., Aro, E. M., & Shikanai, T. (2016). NDH-1 and NDH-2 plastoquinone reductases in oxygenic photosynthesis. *Annual Review of Plant Biology*, *67*, 55–80. Available from https://doi.org/10.1146/annurev-arplant-043014-114752.

Perez-Perez, M. E., Lemaire, S. D., & Crespo, J. L. (2016). Control of autophagy in Chlamydomonas is mediated through redox-dependent inactivation of the ATG4 protease. *Plant Physiology*, *172*(4), 2219–2234. Available from https://doi.org/10.1104/pp.16.01582.

Perez-Perez, M. E., Martin-Figueroa, E., & Florencio, F. J. (2009). Photosynthetic regulation of the cyanobacterium *Synechocystis* sp. PCC 6803 thioredoxin system and functional analysis of TrxB (Trx x) and TrxQ (Trx y) thioredoxins. *Molecular Plant*, *2*(2), 270–283. Available from https://doi.org/10.1093/mp/ssn070.

Perez-Perez, M. E., Mauries, A., Maes, A., Tourasse, N. J., Hamon, M., Lemaire, S. D., … Marchand, C. H. (2017). The deep thioredoxome in *Chlamydomonas reinhardtii*: New insights into redox regulation. *Molecular Plant*, *10*(8), 1107–1125. Available from https://doi.org/10.1016/j.molp.2017.07.009.

Perez-Perez, M. E., Zaffagnini, M., Marchand, C. H., Crespo, J. L., & Lemaire, S. D. (2014). The yeast autophagy protease Atg4 is regulated by thioredoxin. *Autophagy*, *10*(11), 1953–1964. Available from https://doi.org/10.4161/auto.34396.

Perez-Ruiz, J. M., Naranjo, B., Ojeda, V., Guinea, M., & Cejudo, F. J. (2017). NTRC-dependent redox balance of 2-Cys peroxiredoxins is needed for optimal function of the photosynthetic apparatus. *Proceedings of the National Academy of Sciences of the United States of America*, *114*(45), 12069–12074. Available from https://doi.org/10.1073/pnas.1706003114.

Petersen, J., Teich, R., Becker, B., Cerff, R., & Brinkmann, H. (2006). The GapA/B gene duplication marks the origin of Streptophyta (charophytes and land plants). *Molecular Biology and Evolution*, *23*(6), 1109–1118. Available from https://doi.org/10.1093/molbev/msj123.

Petzold, C. J., Chan, L. J., Nhan, M., & Adams, P. D. (2015). Analytics for metabolic engineering. *Frontiers in Bioengineering and Biotechnology*, *3*, 135. Available from https://doi.org/10.3389/fbioe.2015.00135.

Pinnola, A., & Bassi, R. (2018). Molecular mechanisms involved in plant photoprotection. *Biochemical Society Transactions*, *46*(2), 467–482. Available from https://doi.org/10.1042/BST20170307.

Porter, M. A., & Hartman, F. C. (1990). Exploration of the function of a regulatory sulfhydryl of phosphoribulokinase from spinach. *Archives of Biochemistry and Biophysics*, *281*(2), 330–334. Available from https://doi.org/10.1016/0003-9861(90)90452-5.

Porter, M. A., Milanez, S., Stringer, C. D., & Hartman, F. C. (1986). Purification and characterization of ribulose-5-phosphate kinase from spinach. *Archives of Biochemistry and Biophysics*, *245*(1), 14–23. Available from https://doi.org/10.1016/0003-9861(86)90185-2.

Portis, A. R., Jr. (2003). Rubisco activase – Rubisco's catalytic chaperone. *Photosynthesis Research*, *75*(1), 11–27. Available from https://doi.org/10.1023/A:1022458108678.

Portis, A. R., Jr., & Heldt, H. W. (1976). Light-dependent changes of the Mg^{2+} concentration in the stroma in relation to the Mg^{2+} dependency of CO_2 fixation in intact chloroplasts. *Biochimica et Biophysica Acta*, *449*(3), 434–436. Available from https://doi.org/10.1016/0005-2728(76)90154-7.

Portis, A. R., Jr., Li, C., Wang, D., & Salvucci, M. E. (2008). Regulation of Rubisco activase and its interaction with Rubisco. *Journal of Experimental Botany*, *59*(7), 1597–1604. Available from https://doi.org/10.1093/jxb/erm240.

Puzanskiy, R. K., Romanyuk, D. A., Kirpichnikova, A. A., & Shishova, M. F. (2020). Alteration in the expression of genes encoding primary metabolism enzymes and plastid transporters during the culture growth of *Chlamydomonas reinhardtii*. *Molecular Biology*, *54*(4), 562–579. Available from https://doi.org/10.31857/S0026898420040151.

Rae, B. D., Long, B. M., Forster, B., Nguyen, N. D., Velanis, C. N., Atkinson, N., ... McCormick, A. J. (2017). Progress and challenges of engineering a biophysical CO_2-concentrating mechanism into higher plants. *Journal of Experimental Botany*, *68*(14), 3717–3737. Available from https://doi.org/10.1093/jxb/erx133.

Rae, B. D., Long, B. M., Whitehead, L. F., Forster, B., Badger, M. R., & Price, G. D. (2013). Cyanobacterial carboxysomes: Microcompartments that facilitate CO_2 fixation. *Journal of Molecular Microbiology and Biotechnology*, *23*(4-5), 300–307. Available from https://doi.org/10.1159/000351342.

Raines, C. A. (2003). The Calvin cycle revisited. *Photosynthesis Research*, *75*(1), 1–10. Available from https://doi.org/10.1023/A:1022421515027.

Raines, C. A. (2006). Transgenic approaches to manipulate the environmental responses of the C3 carbon fixation cycle. *Plant, Cell & Environment*, *29*(3), 331–339. Available from https://doi.org/10.1111/j.1365-3040.2005.01488.x.

Raines, C. A. (2011). Increasing photosynthetic carbon assimilation in C3 plants to improve crop yield: Current and future strategies. *Plant Physiology*, *155*(1), 36–42. Available from https://doi.org/10.1104/pp.110.168559.

Rault, M., Giudici-Orticoni, M. T., Gontero, B., & Ricard, J. (1993). Structural and functional properties of a multi-enzyme complex from spinach chloroplasts. 1. Stoichiometry of the polypeptide chains. *European Journal of Biochemistry*, *217*(3), 1065–1073. Available from https://doi.org/10.1111/j.1432-1033.1993.tb18338.x.

Raven, J. A., Beardall, J., & Sanchez-Baracaldo, P. (2017). The possible evolution and future of CO_2-concentrating mechanisms. *Journal of Experimental Botany*, *68*(14), 3701–3716. Available from https://doi.org/10.1093/jxb/erx110.

Raven, J. A., Cockell, C. S., & De La Rocha, C. L. (2008). The evolution of inorganic carbon concentrating mechanisms in photosynthesis. *Philosophical Transactions of the Royal Society of London. Series B, Biological Sciences*, *363*(1504), 2641–2650. Available from https://doi.org/10.1098/rstb.2008.0020.

Raven, J. A., Giordano, M., Beardall, J., & Maberly, S. C. (2012). Algal evolution in relation to atmospheric CO_2: Carboxylases, carbon-concentrating mechanisms and carbon oxidation cycles. *Philosophical Transactions of the Royal Society of London. Series B, Biological Sciences*, *367*(1588), 493–507. Available from https://doi.org/10.1098/rstb.2011.0212.

Raven, John A., & Beardall, J. (2003). Carbohydrate metabolism and respiration in algae. In A. W. D. Larkum, S. E. Douglas, & J. A. R (Eds.), *Photosynthesis in algae* (14, pp. 205–224). Dordrecht: Springer.

Rebeille, F., & Gans, P. (1988). Interaction between chloroplasts and mitochondria in microalgae: Role of glycolysis. *Plant Physiology*, *88*(4), 973–975.

Ricard, J., Giudici-Orticoni, M. T., & Buc, J. (1990). Thermodynamics of information transfer between subunits in oligomeric enzymes and kinetic cooperativity. 1. Thermodynamics of subunit interactions, partition functions and enzyme reaction rate. *European Journal of Biochemistry*, *194*(2), 463–473. Available from https://doi.org/10.1111/j.1432-1033.1990.tb15640.x.

Ricard, J., Giudici-Orticoni, M. T., & Gontero, B. (1994). The modulation of enzyme reaction rates within multi-enzyme complexes. 1. Statistical thermodynamics of information transfer through multi-enzyme complexes. *European Journal of Biochemistry*, *226*(3), 993–998. Available from https://doi.org/10.1111/j.1432-1033.1994.00993.x.

Richardson, J. M., 3rd, Lemaire, S. D., Jacquot, J. P., & Makhatadze, G. I. (2000). Difference in the mechanisms of the cold and heat induced unfolding of thioredoxin h from *Chlamydomonas reinhardtii*: Spectroscopic and calorimetric studies. *Biochemistry*, *39*(36), 11154–11162. Available from https://doi.org/10.1021/bi000610b.

Robbens, S., Petersen, J., Brinkmann, H., Rouze, P., & Van de Peer, Y. (2007). Unique regulation of the Calvin cycle in the ultrasmall green alga Ostreococcus. *Journal of Molecular Evolution*, *64*(5), 601–604. Available from https://doi.org/10.1007/s00239-006-0159-y.

Rodriguez-Suarez, R. J., Mora-Garcia, S., & Wolosiuk, R. A. (1997). Characterization of cysteine residues involved in the reductive activation and the structural stability of rapeseed (*Brassica napus*) chloroplast fructose-1,6-bisphosphatase. *Biochemical and Biophysical Research Communications*, *232*(2), 388–393. Available from https://doi.org/10.1006/bbrc.1997.6242.

Rolland, N., Atteia, A., Decottignies, P., Garin, J., Hippler, M., Kreimer, G., … Wagner, V. (2009). Chlamydomonas proteomics. *Current Opinion in Microbiology*, *12*(3), 285–291. Available from https://doi.org/10.1016/j.mib.2009.04.001.

Romanova, A. K., Semenova, G. A., Ignat'ev, A. R., Novichkova, N. S., & Fomina, I. R. (2016). Biochemistry and cell ultrastructure changes during senescence of *Beta vulgaris* L. leaf. *Protoplasma*, *253*(3), 719–727. Available from https://doi.org/10.1007/s00709-015-0923-1.

Rosenthal, D. M., Locke, A. M., Khozaei, M., Raines, C. A., Long, S. P., & Ort, D. R. (2011). Over-expressing the C(3) photosynthesis cycle enzyme Sedoheptulose-1-7 Bisphosphatase improves photosynthetic carbon gain and yield under fully open air CO(2) fumigation (FACE). *BMC Plant Biology*, *11*, 123. Available from https://doi.org/10.1186/1471-2229-11-123.

Rosgaard, L., de Porcellinis, A. J., Jacobsen, J. H., Frigaard, N. U., & Sakuragi, Y. (2012). Bioengineering of carbon fixation, biofuels, and biochemicals in cyanobacteria and plants. *Journal of Biotechnology*, *162*(1), 134–147. Available from https://doi.org/10.1016/j.jbiotec.2012.05.006.

Rouhier, N., Lemaire, S. D., & Jacquot, J. P. (2008). The role of glutathione in photosynthetic organisms: Emerging functions for glutaredoxins and glutathionylation. *Annual Review of Plant Biology*, *59*, 143–166. Available from https://doi.org/10.1146/annurev.arplant.59.032607.092811.

Roustan, V., & Weckwerth, W. (2018). Quantitative phosphoproteomic and system-level analysis of TOR Inhibition unravel distinct organellar acclimation in *Chlamydomonas reinhardtii*. *Frontiers in Plant Science*, *9*, 1590. Available from https://doi.org/10.3389/fpls.2018.01590.

Roustan, V., Bakhtiari, S., Roustan, P. J., & Weckwerth, W. (2017). Quantitative in vivo phosphoproteomics reveals reversible signaling processes during nitrogen starvation and recovery in the biofuel model organism *Chlamydomonas reinhardtii*. *Biotechnology for Biofuels*, *10*, 280. Available from https://doi.org/10.1186/s13068-017-0949-z.

Ruelland, E., & Miginiac-Maslow, M. (1999). Regulation of chloroplast enzyme activities by thioredoxins: Activation or relief from inhibition? *Trends in Plant Science*, *4*(4), 136–141. Available from https://doi.org/10.1016/s1360-1385(99)01391-6.

Sainis, J. K., & Harris, G. C. (1986). The association of ribulose-1,5-bisphosphate carboxylase with phosphoriboisomerase and phosphoribulokinase. *Biochemical and Biophysical Research Communications*, *139*(3), 947–954. Available from https://doi.org/10.1016/s0006-291x(86)80269-8.

Salvucci, M. E., Werneke, J. M., Ogren, W. L., & Portis, A. R. (1987). Purification and species distribution of rubisco activase. *Plant Physiology*, *84*(3), 930–936. Available from https://doi.org/10.1104/pp.84.3.930.

Santos-Merino, M., Torrado, A., Davis, G. A., Rottig, A., Bibby, T. S., Kramer, D. M., … Ducat, D. C. (2021). Improved photosynthetic capacity and photosystem I oxidation via heterologous metabolism engineering in cyanobacteria. *Proceedings of the National Academy of Sciences of the United States of America*, *118*(11). Available from https://doi.org/10.1073/pnas.2021523118.

Sanz-Luque, E., Ocana-Calahorro, F., Llamas, A., Galvan, A., & Fernandez, E. (2013). Nitric oxide controls nitrate and ammonium assimilation in *Chlamydomonas reinhardtii*. *Journal of Experimental Botany*, *64*(11), 3373–3383. Available from https://doi.org/10.1093/jxb/ert175.

Saroussi, S. I., Wittkopp, T. M., & Grossman, A. R. (2016). The type II NADPH dehydrogenase facilitates cyclic electron flow, energy-dependent quenching, and chlororespiratory metabolism during acclimation of *Chlamydomonas reinhardtii* to nitrogen deprivation. *Plant Physiology*, *170*(4), 1975–1988. Available from https://doi.org/10.1104/pp.15.02014.

Sasaki, Y., Kozaki, A., & Hatano, M. (1997). Link between light and fatty acid synthesis: thioredoxin-linked reductive activation of plastidic acetyl-CoA carboxylase. *Proceedings of the National Academy of Sciences of the United States of America*, *94*(20), 11096–11101. Available from https://doi.org/10.1073/pnas.94.20.11096.

Satanowski, A., Dronsella, B., Noor, E., Vogeli, B., He, H., Wichmann, P., … Bar-Even, A. (2020). Awakening a latent carbon fixation cycle in *Escherichia coli*. *Nature Communications*, *11*(1), 5812. Available from https://doi.org/10.1038/s41467-020-19564-5.

Savir, Y., Noor, E., Milo, R., & Tlusty, T. (2010). Cross-species analysis traces adaptation of Rubisco toward optimality in a low-dimensional landscape. *Proceedings of the National Academy of Sciences of the United States of America*, *107*(8), 3475–3480. Available from https://doi.org/10.1073/pnas.0911663107.

Sawyer, A., & Winkler, M. (2017). Evolution of *Chlamydomonas reinhardtii* ferredoxins and their interactions with [FeFe]-hydrogenases. *Photosynthesis Research*, *134*(3), 307–316. Available from https://doi.org/10.1007/s11120-017-0409-4.

Scagliarini, S., Trost, P., Pupillo, P., & Valenti, V. (1993). Light activation and molecular-mass changes of NAD(P)-glyceraldehyde 3-phosphate dehydrogenase of spinach and maize leaves. *Planta*, *190*(3), 313–319. Available from https://doi.org/10.1007/bf00196959.

Schmollinger, S., Muhlhaus, T., Boyle, N. R., Blaby, I. K., Casero, D., Mettler, T., … Merchant, S. S. (2014). Nitrogen-sparing mechanisms in Chlamydomonas affect the transcriptome, the proteome, and photosynthetic metabolism. *The Plant Cell*, *26*(4), 1410–1435. Available from https://doi.org/10.1105/tpc.113.122523.

Schroda, M., Hemme, D., & Muhlhaus, T. (2015). The Chlamydomonas heat stress response. *The Plant Journal*, *82*(3), 466–480. Available from https://doi.org/10.1111/tpj.12816.

Schroter, Y., Steiner, S., Matthai, K., & Pfannschmidt, T. (2010). Analysis of oligomeric protein complexes in the chloroplast sub-proteome of nucleic acid-binding proteins from mustard reveals potential redox regulators of plastid gene expression. *Proteomics*, *10*(11), 2191–2204. Available from https://doi.org/10.1002/pmic.200900678.

Schuler, M. L., Mantegazza, O., & Weber, A. P. (2016). Engineering C4 photosynthesis into C3 chassis in the synthetic biology age. *The Plant Journal*, *87*(1), 51–65. Available from https://doi.org/10.1111/tpj.13155.

Schurmann, P. (2002). Ferredoxin-dependent thioredoxin reductase: A unique iron-sulfur protein. *Methods in Enzymology*, *347*, 403–411. Available from https://doi.org/10.1016/s0076-6879(02)47040-1.

Schurmann, P., & Buchanan, B. B. (2008). The ferredoxin/thioredoxin system of oxygenic photosynthesis. *Antioxidants & Redox Signaling*, *10*(7), 1235–1274. Available from https://doi.org/10.1089/ars.2007.1931.

Schwander, T., Schada von Borzyskowski, L., Burgener, S., Cortina, N. S., & Erb, T. J. (2016). A synthetic pathway for the fixation of carbon dioxide in vitro. *Science*, *354*(6314), 900–904. Available from https://doi.org/10.1126/science.aah5237.

Sekiguchi, T., Yoshida, K., Okegawa, Y., Motohashi, K., Wakabayashi, K. I., & Hisabori, T. (2020). Chloroplast ATP synthase is reduced by both f-type and m-type thioredoxins. *Biochimica et Biophysica Acta - Bioenergetics*, *1861*(11), 148261. Available from https://doi.org/10.1016/j.bbabio.2020.148261.

Selinski, J., & Scheibe, R. (2019). Malate valves: Old shuttles with new perspectives. *Plant Biology*, *21*(Suppl 1), 21–30. Available from https://doi.org/10.1111/plb.12869.

Sengupta, R., & Holmgren, A. (2014). Thioredoxin and glutaredoxin-mediated redox regulation of ribonucleotide reductase. *World Journal of Biological Chemistry*, *5*(1), 68–74. Available from https://doi.org/10.4331/wjbc.v5.i1.68.

Serrato, A. J., Fernandez-Trijueque, J., Barajas-Lopez, J. D., Chueca, A., & Sahrawy, M. (2013). Plastid thioredoxins: A "one-for-all" redox-signaling system in plants. *Frontiers in Plant Science*, *4*, 463. Available from https://doi.org/10.3389/fpls.2013.00463.

Setlik, I., Ried, A., & Berkova, E. (1973). *Czech. Acad. Sci. Inst. Microbiol. Annu. Rep. Lab. Algol.*

Setterdahl, A. T., Chivers, P. T., Hirasawa, M., Lemaire, S. D., Keryer, E., Miginiac-Maslow, M., … Knaff, D. B. (2003). Effect of pH on the oxidation-reduction properties of thioredoxins. *Biochemistry*, *42*(50), 14877–14884. Available from https://doi.org/10.1021/bi0302088.

Shao, N., Beck, C. F., Lemaire, S. D., & Krieger-Liszkay, A. (2008). Photosynthetic electron flow affects H_2O_2 signaling by inactivation of catalase in *Chlamydomonas reinhardtii*. *Planta*, *228*(6), 1055–1066. Available from https://doi.org/10.1007/s00425-008-0807-0.

Shimakawa, G., Ishizaki, K., Tsukamoto, S., Tanaka, M., Sejima, T., & Miyake, C. (2017). The liverwort, marchantia, drives alternative electron flow using a flavodiiron protein to protect PSI. *Plant Physiology*, *173*(3), 1636–1647. Available from https://doi.org/10.1104/pp.16.01038.

Sicard-Roselli, C., Lemaire, S., Jacquot, J. P., Favaudon, V., Marchand, C., & Houee-Levin, C. (2004). Thioredoxin Ch1 of *Chlamydomonas reinhardtii* displays an unusual resistance toward one-electron oxidation. *European Journal of Biochemistry*, *271*(17), 3481–3487. Available from https://doi.org/10.1111/j.1432-1033.2004.04279.x.

Simkin, A. J., Lopez-Calcagno, P. E., & Raines, C. A. (2019). Feeding the world: Improving photosynthetic efficiency for sustainable crop production. *Journal of Experimental Botany*, *70*(4), 1119–1140. Available from https://doi.org/10.1093/jxb/ery445.

Simkin, A. J., Lopez-Calcagno, P. E., Davey, P. A., Headland, L. R., Lawson, T., Timm, S., … Raines, C. A. (2017). Simultaneous stimulation of sedoheptulose 1,7-bisphosphatase, fructose 1,6-bisphophate aldolase and the photorespiratory glycine decarboxylase-H protein increases CO_2 assimilation, vegetative biomass and seed yield in Arabidopsis. *Plant Biotechnology Journal*, *15*(7), 805–816. Available from https://doi.org/10.1111/pbi.12676.

Simkin, A. J., McAusland, L., Headland, L. R., Lawson, T., & Raines, C. A. (2015). Multigene manipulation of photosynthetic carbon assimilation increases CO_2 fixation and biomass yield in tobacco. *Journal of Experimental Botany*, *66*(13), 4075–4090. Available from https://doi.org/10.1093/jxb/erv204.

Slade, W. O., Werth, E. G., McConnell, E. W., Alvarez, S., & Hicks, L. M. (2015). Quantifying reversible oxidation of protein thiols in photosynthetic organisms. *Journal of the American Society for Mass Spectrometry*, *26*(4), 631–640. Available from https://doi.org/10.1007/s13361-014-1073-y.

South, P. F., Cavanagh, A. P., Liu, H. W., & Ort, D. R. (2019). Synthetic glycolate metabolism pathways stimulate crop growth and productivity in the field. *Science*, *363*(6422). Available from https://doi.org/10.1126/science.aat9077.

Sparla, F., Costa, A., Lo Schiavo, F., Pupillo, P., & Trost, P. (2006). Redox regulation of a novel plastid-targeted beta-amylase of Arabidopsis. *Plant Physiology*, *141*(3), 840–850. Available from https://doi.org/10.1104/pp.106.079186.

Sparla, F., Fermani, S., Falini, G., Zaffagnini, M., Ripamonti, A., Sabatino, P., … Trost, P. (2004). Coenzyme site-directed mutants of photosynthetic A4-GAPDH show selectively reduced NADPH-dependent catalysis, similar to regulatory AB-GAPDH inhibited by oxidized thioredoxin. *Journal of Molecular Biology*, *340*(5), 1025–1037. Available from https://doi.org/10.1016/j.jmb.2004.06.005.

Sparla, F., Pupillo, P., & Trost, P. (2002). The C-terminal extension of glyceraldehyde-3-phosphate dehydrogenase subunit B acts as an autoinhibitory domain regulated by thioredoxins and nicotinamide adenine dinucleotide. *The Journal of Biological Chemistry*, *277*(47), 44946–44952. Available from https://doi.org/10.1074/jbc.M206873200.

Sparla, F., Zaffagnini, M., Wedel, N., Scheibe, R., Pupillo, P., & Trost, P. (2005). Regulation of photosynthetic GAPDH dissected by mutants. *Plant Physiology*, *138*(4), 2210–2219. Available from https://doi.org/10.1104/pp.105.062117.

Spreitzer, R. J., & Salvucci, M. E. (2002). Rubisco: structure, regulatory interactions, and possibilities for a better enzyme. *Annual Review of Plant Biology*, *53*, 449–475. Available from https://doi.org/10.1146/annurev.arplant.53.100301.135233.

Stein, M., Jacquot, J. P., Jeannette, E., Decottignies, P., Hodges, M., Lancelin, J. M., … Miginiac-Maslow, M. (1995). *Chlamydomonas reinhardtii* thioredoxins: Structure of the genes coding for the chloroplastic m and cytosolic h isoforms; expression in *Escherichia coli* of the recombinant proteins, purification and biochemical properties. *Plant Molecular Biology*, *28*(3), 487–503. Available from https://doi.org/10.1007/BF00020396.

Stitt, M., & Schulze, D. (1994). Does Rubisco control the rate of photosynthesis and plant growth? An exercise in molecular ecophysiology. *Plant, Cell and Environment*, *17*(5), 465–487. Available from https://doi.org/10.1111/j.1365-3040.1994.tb00144.x.

Stitt, M., Lunn, J., & Usadel, B. (2010). Arabidopsis and primary photosynthetic metabolism – More than the icing on the cake. *The Plant Journal*, *61*(6), 1067–1091. Available from https://doi.org/10.1111/j.1365-313X.2010.04142.x.

Strenkert, D., Schmollinger, S., Gallaher, S. D., Salome, P. A., Purvine, S. O., Nicora, C. D., … Merchant, S. S. (2019). Multiomics resolution of molecular events during a day in the life of *Chlamydomonas*. *Proceedings of the National Academy of Sciences of the United States of America*, *116*(6), 2374–2383. Available from https://doi.org/10.1073/pnas.1815238116.

Subramanian, V., Wecker, M. S. A., Gerritsen, A., Boehm, M., Xiong, W., Wachter, B., … Ghirardi, M. L. (2019). Ferredoxin5 deletion affects metabolism of algae during the different phases of sulfur deprivation. *Plant Physiology*, *181*(2), 426–441. Available from https://doi.org/10.1104/pp.19.00457.

Sun, H., Liu, X., Li, F., Li, W., Zhang, J., Xiao, Z., … Yang, J. (2017). First comprehensive proteome analysis of lysine crotonylation in seedling leaves of *Nicotiana tabacum*. *Scientific Reports*, *7*(1), 3013. Available from https://doi.org/10.1038/s41598-017-03369-6.

Sun, J., Qiu, C., Qian, W., Wang, Y., Sun, L., Li, Y., … Ding, Z. (2019). Ammonium triggered the response mechanism of lysine crotonylome in tea plants. *BMC Genomics*, *20*(1), 340. Available from https://doi.org/10.1186/s12864-019-5716-z.

Sun, Y., Valente-Paterno, M., Bakhtiari, S., Law, C., Zhan, Y., & Zerges, W. (2019). Photosystem biogenesis is localized to the translation zone in the chloroplast of *Chlamydomonas*. *The Plant Cell*, *31*(12), 3057–3072. Available from https://doi.org/10.1105/tpc.19.00263.

Suss, K. H., Arkona, C., Manteuffel, R., & Adler, K. (1993). Calvin cycle multienzyme complexes are bound to chloroplast thylakoid membranes of higher plants in situ. *Proceedings of the National Academy of Sciences of the United States of America*, *90*(12), 5514–5518. Available from https://doi.org/10.1073/pnas.90.12.5514.

Suzuki, Y., Kondo, E., & Makino, A. (2017). Effects of co-overexpression of the genes of Rubisco and transketolase on photosynthesis in rice. *Photosynthesis Research*, *131*(3), 281–289. Available from https://doi.org/10.1007/s11120-016-0320-4.

Syeda, R., Xu, J., Dubin, A. E., Coste, B., Mathur, J., Huynh, T., … Patapoutian, A. (2015). Chemical activation of the mechanotransduction channel Piezo1. *Elife*, *4*. Available from https://doi.org/10.7554/eLife.07369.

Tagliani, A., Rossi, J., Marchand, C. H., De Mia, M., Tedesco, D., Gurrieri, L., … Zaffagnini, M. (2021). Structural and functional insights into nitrosoglutathione reductase from *Chlamydomonas reinhardtii*. *Redox Biology*, *38*, 101806. Available from https://doi.org/10.1016/j.redox.2020.101806.

Tamoi, M., Murakami, A., Takeda, T., & Shigeoka, S. (1998). Lack of light/dark regulation of enzymes involved in the photosynthetic carbon reduction cycle in cyanobacteria, Synechococcus PCC 7942 and Synechocystis PCC 6803. *Bioscience, Biotechnology, and Biochemistry*, *62*(2), 374–376. Available from https://doi.org/10.1271/bbb.62.374.

Tamoi, M., Nagaoka, M., Miyagawa, Y., & Shigeoka, S. (2006). Contribution of fructose-1,6-bisphosphatase and sedoheptulose-1,7-bisphosphatase to the photosynthetic rate and carbon flow in the Calvin cycle in transgenic plants. *Plant & Cell Physiology*, *47*(3), 380–390. Available from https://doi.org/10.1093/pcp/pcj004.

Tarrago, L., Laugier, E., Zaffagnini, M., Marchand, C., Le Marechal, P., Rouhier, N., … Rey, P. (2009). Regeneration mechanisms of *Arabidopsis thaliana* methionine sulfoxide reductases B by glutaredoxins and thioredoxins. *The Journal of Biological Chemistry*, *284*(28), 18963–18971. Available from https://doi.org/10.1074/jbc.M109.015487.

Taylor, T. C., Backlund, A., Bjorhall, K., Spreitzer, R. J., & Andersson, I. (2001). First crystal structure of Rubisco from a green alga, *Chlamydomonas reinhardtii*. *The Journal of Biological Chemistry*, *276*(51), 48159–48164. Available from https://doi.org/10.1074/jbc.M107765200.

Tcherkez, G. (2013). Modelling the reaction mechanism of ribulose-1,5-bisphosphate carboxylase/oxygenase and consequences for kinetic parameters. *Plant, Cell & Environment*, *36*(9), 1586–1596. Available from https://doi.org/10.1111/pce.12066.

Tcherkez, G. G., Farquhar, G. D., & Andrews, T. J. (2006). Despite slow catalysis and confused substrate specificity, all ribulose bisphosphate carboxylases may be nearly perfectly optimized. *Proceedings of the National Academy of Sciences of the United States of America*, *103*(19), 7246–7251. Available from https://doi.org/10.1073/pnas.0600605103.

Teige, M., Melzer, M., & Suss, K. H. (1998). Purification, properties and in situ localization of the amphibolic enzymes D-ribulose 5-phosphate 3-epimerase and transketolase from spinach chloroplasts. *European Journal of Biochemistry*, *252*(2), 237–244. Available from https://doi.org/10.1046/j.1432-1327.1998.2520237.x.

Terashima, M., Specht, M., & Hippler, M. (2011). The chloroplast proteome: A survey from the *Chlamydomonas reinhardtii* perspective with a focus on distinctive features. *Current Genetics*, *57*(3), 151–168. Available from https://doi.org/10.1007/s00294-011-0339-1.

Terauchi, A. M., Lu, S. F., Zaffagnini, M., Tappa, S., Hirasawa, M., Tripathy, J. N., … Merchant, S. S. (2009). Pattern of expression and substrate specificity of chloroplast ferredoxins from *Chlamydomonas reinhardtii*. *The Journal of Biological Chemistry*, *284*(38), 25867–25878. Available from https://doi.org/10.1074/jbc.M109.023622.

Thieulin-Pardo, G., Remy, T., Lignon, S., Lebrun, R., & Gontero, B. (2015). Phosphoribulokinase from *Chlamydomonas reinhardtii*: A Benson-Calvin cycle enzyme enslaved to its cysteine residues. *Molecular Biosystems*, *11*(4), 1134–1145. Available from https://doi.org/10.1039/c5mb00035a.

Toledano, M. B., Delaunay-Moisan, A., Outten, C. E., & Igbaria, A. (2013). Functions and cellular compartmentation of the thioredoxin and glutathione pathways in yeast. *Antioxidants & Redox Signaling*, *18*(13), 1699–1711. Available from https://doi.org/10.1089/ars.2012.5033.

Trost, P., Fermani, S., Marri, L., Zaffagnini, M., Falini, G., Scagliarini, S., … Sparla, F. (2006). Thioredoxin-dependent regulation of photosynthetic glyceraldehyde-3-phosphate dehydrogenase: Autonomous vs. CP12-dependent mechanisms. *Photosynthesis Research*, *89*(2-3), 263–275. Available from https://doi.org/10.1007/s11120-006-9099-z.

Trudeau, D. L., Edlich-Muth, C., Zarzycki, J., Scheffen, M., Goldsmith, M., Khersonsky, O., … Bar-Even, A. (2018). Design and in vitro realization of carbon-conserving photorespiration. *Proceedings of the National Academy of Sciences of the United States of America*, *115*(49), E11455–E11464. Available from https://doi.org/10.1073/pnas.1812605115.

Tsukamoto, Y., Fukushima, Y., Hara, S., & Hisabori, T. (2013). Redox control of the activity of phosphoglycerate kinase in *Synechocystis* sp. PCC6803. *Plant & Cell Physiology*, *54*(4), 484–491. Available from https://doi.org/10.1093/pcp/pct002.

Turpin, D. H. (1991). Effects of inorganic N availability on algal photosynthesis and carbon metabolism. *Journal of Phycology*, *27*(1), 14–20. Available from https://doi.org/10.1111/j.0022-3646.1991.00014.x.

Uematsu, K., Suzuki, N., Iwamae, T., Inui, M., & Yukawa, H. (2012). Increased fructose 1,6-bisphosphate aldolase in plastids enhances growth and photosynthesis of tobacco plants. *Journal of Experimental Botany*, *63*(8), 3001–3009. Available from https://doi.org/10.1093/jxb/ers004.

Uniacke, J., & Zerges, W. (2008). Stress induces the assembly of RNA granules in the chloroplast of *Chlamydomonas reinhardtii*. *The Journal of Cell Biology*, *182*(4), 641–646. Available from https://doi.org/10.1083/jcb.200805125.

van der Linde, K., Gutsche, N., Leffers, H. M., Lindermayr, C., Muller, B., Holtgrefe, S., … Scheibe, R. (2011). Regulation of plant cytosolic aldolase functions by redox-modifications. *Plant Physiology and Biochemistry*, *49*(9), 946–957. Available from https://doi.org/10.1016/j.plaphy.2011.06.009.

Villeret, V., Huang, S., Zhang, Y., Xue, Y., & Lipscomb, W. N. (1995). Crystal structure of spinach chloroplast fructose-1,6-bisphosphatase at 2.8 A resolution. *Biochemistry*, *34*(13), 4299–4306. Available from https://doi.org/10.1021/bi00013a019.

Wagner, V., Gessner, G., Heiland, I., Kaminski, M., Hawat, S., Scheffler, K., … Mittag, M. (2006). Analysis of the phosphoproteome of *Chlamydomonas reinhardtii* provides new insights into various cellular pathways. *Eukaryotic Cell*, *5*(3), 457–468. Available from https://doi.org/10.1128/EC.5.3.457-468.2006.

Walker, D. (1992). *Energy, plants and man*. Univ Science Books.

Wang, D., & Portis, A. R., Jr. (2006). Increased sensitivity of oxidized large isoform of ribulose-1,5-bisphosphate carboxylase/oxygenase (rubisco) activase to ADP inhibition is due to an interaction between its carboxyl extension and nucleotide-binding pocket. *The Journal of Biological Chemistry*, *281*(35), 25241–25249. Available from https://doi.org/10.1074/jbc.M604756200.

Wang, H., Gau, B., Slade, W. O., Juergens, M., Li, P., & Hicks, L. M. (2014). The global phosphoproteome of *Chlamydomonas reinhardtii* reveals complex organellar phosphorylation in the flagella and thylakoid membrane. *Molecular & Cellular Proteomics*, *13*(9), 2337–2353. Available from https://doi.org/10.1074/mcp.M114.038281.

Wang, H., Yan, X., Aigner, H., Bracher, A., Nguyen, N. D., Hee, W. Y., … Hayer-Hartl, M. (2019). Rubisco condensate formation by CcmM in beta-carboxysome biogenesis. *Nature*, *566*(7742), 131–135. Available from https://doi.org/10.1038/s41586-019-0880-5.

Wang, Y., Stessman, D. J., & Spalding, M. H. (2015). The CO_2 concentrating mechanism and photosynthetic carbon assimilation in limiting CO_2: How *Chlamydomonas* works against the gradient. *The Plant Journal*, *82*(3), 429–448. Available from https://doi.org/10.1111/tpj.12829.

Wang, Z. T., Ullrich, N., Joo, S., Waffenschmidt, S., & Goodenough, U. (2009). Algal lipid bodies: Stress induction, purification, and biochemical characterization in wild-type and starchless *Chlamydomonas reinhardtii*. *Eukaryotic Cell*, *8*(12), 1856–1868. Available from https://doi.org/10.1128/EC.00272-09.

Weber, A., Menzlaff, E., Arbinger, B., Gutensohn, M., Eckerskorn, C., & Flugge, U. I. (1995). The 2-oxoglutarate/malate translocator of chloroplast envelope membranes: Molecular cloning of a transporter containing a 12-helix motif and expression of the functional protein in yeast cells. *Biochemistry*, *34*(8), 2621–2627. Available from https://doi.org/10.1021/bi00008a028.

Wedel, N., & Soll, J. (1998). Evolutionary conserved light regulation of Calvin cycle activity by NADPH-mediated reversible phosphoribulokinase/CP12/ glyceraldehyde-3-phosphate dehydrogenase complex dissociation. *Proceedings of the National Academy of Sciences of the United States of America*, *95*(16), 9699–9704. Available from https://doi.org/10.1073/pnas.95.16.9699.

Weger, H. G., Guy, R. D., & Turpin, D. H. (1990). Cytochrome and alternative pathway respiration in green algae: Measurements using inhibitors and o(2) discrimination. *Plant Physiology*, *93*(1), 356–360. Available from https://doi.org/10.1104/pp.93.1.356.

Wei, L., Derrien, B., Gautier, A., Houille-Vernes, L., Boulouis, A., Saint-Marcoux, D., … Wollman, F. A. (2014). Nitric oxide-triggered remodeling of chloroplast bioenergetics and thylakoid proteins upon nitrogen starvation in *Chlamydomonas reinhardtii*. *The Plant Cell*, *26*(1), 353–372. Available from https://doi.org/10.1105/tpc.113.120121.

Wenderoth, I., Scheibe, R., & von Schaewen, A. (1997). Identification of the cysteine residues involved in redox modification of plant plastidic glucose-6-phosphate dehydrogenase. *The Journal of Biological Chemistry*, *272*(43), 26985–26990. Available from https://doi.org/10.1074/jbc.272.43.26985.

Werth, E. G., McConnell, E. W., Couso Lianez, I., Perrine, Z., Crespo, J. L., Umen, J. G., … Hicks, L. M. (2019). Investigating the effect of target of rapamycin kinase inhibition on the *Chlamydomonas reinhardtii* phosphoproteome: From known homologs to new targets. *The New Phytologist*, *221*(1), 247–260. Available from https://doi.org/10.1111/nph.15339.

Werth, E. G., McConnell, E. W., Gilbert, T. S., Couso Lianez, I., Perez, C. A., Manley, C. K., … Hicks, L. M. (2017). Probing the global kinome and phosphoproteome in *Chlamydomonas reinhardtii* via sequential enrichment and quantitative proteomics. *The Plant Journal*, *89*(2), 416–426. Available from https://doi.org/10.1111/tpj.13384.

Wienkoop, S., Weiss, J., May, P., Kempa, S., Irgang, S., Recuenco-Munoz, L., … Weckwerth, W. (2010). Targeted proteomics for *Chlamydomonas reinhardtii* combined with rapid subcellular protein fractionation, metabolomics and metabolic flux analyses. *Molecular Biosystems*, *6*(6), 1018–1031. Available from https://doi.org/10.1039/b920913a.

Wilson, R. H., Hayer-Hartl, M., & Bracher, A. (2019). Crystal structure of phosphoribulokinase from *Synechococcus* sp. strain PCC 6301. *Acta Crystallographica Section F: Structural Biology Communications*, *75*(Pt 4), 278–289. Available from https://doi.org/10.1107/S2053230X19002693.

Winkler, M., Hemschemeier, A., Jacobs, J., Stripp, S., & Happe, T. (2010). Multiple ferredoxin isoforms in *Chlamydomonas reinhardtii* – Their role under stress conditions and biotechnological implications. *European Journal of Cell Biology*, *89*(12), 998–1004. Available from https://doi.org/10.1016/j.ejcb.2010.06.018.

Wobbe, L., & Remacle, C. (2015). Improving the sunlight-to-biomass conversion efficiency in microalgal biofactories. *Journal of Biotechnology*, *201*, 28–42. Available from https://doi.org/10.1016/j.jbiotec.2014.08.021.

Wunder, T., Cheng, S. L. H., Lai, S. K., Li, H. Y., & Mueller-Cajar, O. (2018). The phase separation underlying the pyrenoid-based microalgal Rubisco supercharger. *Nature Communications*, *9*(1), 5076. Available from https://doi.org/10.1038/s41467-018-07624-w.

Xu, M., Luo, J., Li, Y., Shen, L., Zhang, X., Yu, J., … Yang, J. (2021). First comprehensive proteomics analysis of lysine crotonylation in leaves of peanut (*Arachis hypogaea* L.). *Proteomics*, *21*(5), e2000156. Available from https://doi.org/10.1002/pmic.202000156.

Xue, X., Gauthier, D. A., Turpin, D. H., & Weger, H. G. (1996). Interactions between photosynthesis and respiration in the green alga *Chlamydomonas reinhardtii* (characterization of light-enhanced dark respiration). *Plant Physiology*, *112*(3), 1005–1014. Available from https://doi.org/10.1104/pp.112.3.1005.

Yacoby, I., Pochekailov, S., Toporik, H., Ghirardi, M. L., King, P. W., & Zhang, S. (2011). Photosynthetic electron partitioning between [FeFe]-hydrogenase and ferredoxin:NADP + -oxidoreductase (FNR) enzymes in vitro. *Proceedings of the National Academy of Sciences of the United States of America*, *108*(23), 9396–9401. Available from https://doi.org/10.1073/pnas.1103659108.

Yamamoto, H., Takahashi, S., Badger, M. R., & Shikanai, T. (2016). Artificial remodelling of alternative electron flow by flavodiiron proteins in Arabidopsis. *Nature Plants*, *2*, 16012. Available from https://doi.org/10.1038/nplants.2016.12.

Yang, W., Wittkopp, T. M., Li, X., Warakanont, J., Dubini, A., Catalanotti, C., … Grossman, A. R. (2015). Critical role of *Chlamydomonas reinhardtii* ferredoxin-5 in maintaining membrane structure and dark metabolism. *Proceedings of the National Academy of Sciences of the United States of America*, *112*(48), 14978–14983. Available from https://doi.org/10.1073/pnas.1515240112.

Yeh, H. L., Lin, T. H., Chen, C. C., Cheng, T. X., Chang, H. Y., & Lee, T. M. (2019). Monodehydroascorbate reductase plays a role in the tolerance of *Chlamydomonas reinhardtii* to photooxidative stress. *Plant & Cell Physiology*, *60*(10), 2167–2179. Available from https://doi.org/10.1093/pcp/pcz110.

Yosef, I., Irihimovitch, V., Knopf, J. A., Cohen, I., Orr-Dahan, I., Nahum, E., … Shapira, M. (2004). RNA binding activity of the ribulose-1,5-bisphosphate carboxylase/oxygenase large subunit from *Chlamydomonas reinhardtii*. *The Journal of Biological Chemistry*, *279*(11), 10148–10156. Available from https://doi.org/10.1074/jbc.M308602200.

Yoshida, K., & Hisabori, T. (2016). Two distinct redox cascades cooperatively regulate chloroplast functions and sustain plant viability. *Proceedings of the National Academy of Sciences of the United States of America*, *113*(27), E3967–E3976. Available from https://doi.org/10.1073/pnas.1604101113.

Yoshida, K., & Hisabori, T. (2017). Distinct electron transfer from ferredoxin-thioredoxin reductase to multiple thioredoxin isoforms in chloroplasts. *The Biochemical Journal*, *474*(8), 1347–1360. Available from https://doi.org/10.1042/BCJ20161089.

Young, J. N., Heureux, A. M., Sharwood, R. E., Rickaby, R. E., Morel, F. M., & Whitney, S. M. (2016). Large variation in the Rubisco kinetics of diatoms reveals diversity among their carbon-concentrating mechanisms. *Journal of Experimental Botany*, *67*(11), 3445–3456. Available from https://doi.org/10.1093/jxb/erw163.

Yu, A., Xie, Y., Pan, X., Zhang, H., Cao, P., Su, X., … Li, M. (2020). Photosynthetic phosphoribulokinase structures: Enzymatic mechanisms and the redox regulation of the Calvin-Benson-Bassham cycle. *The Plant Cell*, *32*(5), 1556–1573. Available from https://doi.org/10.1105/tpc.19.00642.

Yu, H., Li, X., Duchoud, F., Chuang, D. S., & Liao, J. C. (2018). Augmenting the Calvin-Benson-Bassham cycle by a synthetic malyl-CoA-glycerate carbon fixation pathway. *Nature Communications*, *9*(1), 2008. Available from https://doi.org/10.1038/s41467-018-04417-z.

Zabawinski, C., Van Den Koornhuyse, N., d'Hulst, C., Schlichting, R., Giersch, C., Delrue, B., … Ball, S. (2001). Starchless mutants of Chlamydomonas reinhardtii lack the small subunit of a heterotetrameric ADP-glucose pyrophosphorylase. *Journal of Bacteriology*, *183*(3), 1069–1077.

Zaffagnini, M., Bedhomme, M., Groni, H., Marchand, C. H., Puppo, C., Gontero, B., … Lemaire, S. D. (2012). Glutathionylation in the photosynthetic model organism *Chlamydomonas reinhardtii*: A proteomic survey. *Molecular & Cellular Proteomics*, *11*(2). Available from https://doi.org/10.1074/mcp.M111.014142.

Zaffagnini, M., Bedhomme, M., Marchand, C. H., Morisse, S., Trost, P., & Lemaire, S. D. (2012). Redox regulation in photosynthetic organisms: Focus on glutathionylation. *Antioxidants & Redox Signaling*, *16*(6), 567–586. Available from https://doi.org/10.1089/ars.2011.4255.

Zaffagnini, M., De Mia, M., Morisse, S., Di Giacinto, N., Marchand, C. H., Maes, A., … Trost, P. (2016). Protein S-nitrosylation in photosynthetic organisms: A comprehensive overview with future perspectives. *Biochimica et Biophysica Acta*, *1864*(8), 952–966. Available from https://doi.org/10.1016/j.bbapap.2016.02.006.

Zaffagnini, M., Fermani, S., Costa, A., Lemaire, S. D., & Trost, P. (2013). Plant cytoplasmic GAPDH: Redox post-translational modifications and moonlighting properties. *Frontiers in Plant Science*, *4*, 450. Available from https://doi.org/10.3389/fpls.2013.00450.

Zaffagnini, M., Fermani, S., Marchand, C. H., Costa, A., Sparla, F., Rouhier, N., … Trost, P. (2019). Redox homeostasis in photosynthetic organisms: Novel and established thiol-based molecular mechanisms. *Antioxidants & Redox Signaling*, *31*(3), 155–210. Available from https://doi.org/10.1089/ars.2018.7617.

Zaffagnini, M., Michelet, L., Marchand, C., Sparla, F., Decottignies, P., Le Marechal, P., … Lemaire, S. D. (2007). The thioredoxin-independent isoform of chloroplastic glyceraldehyde-3-phosphate dehydrogenase is selectively regulated by glutathionylation. *The FEBS Journal*, *274*(1), 212–226. Available from https://doi.org/10.1111/j.1742-4658.2006.05577.x.

Zaffagnini, M., Michelet, L., Sciabolini, C., Di Giacinto, N., Morisse, S., Marchand, C. H., … Lemaire, S. D. (2014). High-resolution crystal structure and redox properties of chloroplastic triosephosphate isomerase from *Chlamydomonas reinhardtii*. *Molecular Plant*, *7*(1), 101–120. Available from https://doi.org/10.1093/mp/sst139.

Zaffagnini, M., Morisse, S., Bedhomme, M., Marchand, C. H., Festa, M., Rouhier, N., … Trost, P. (2013). Mechanisms of nitrosylation and denitrosylation of cytoplasmic glyceraldehyde-3-phosphate dehydrogenase from *Arabidopsis thaliana*. *The Journal of Biological Chemistry*, *288*(31), 22777–22789. Available from https://doi.org/10.1074/jbc.M113.475467.

Zalutskaya, Z., Kochemasova, L., & Ermilova, E. (2018). Dual positive and negative control of *Chlamydomonas* PII signal transduction protein expression by nitrate/nitrite and NO via the components of nitric oxide cycle. *BMC Plant Biology*, *18*(1), 305. Available from https://doi.org/10.1186/s12870-018-1540-x.

Zerges, W., Wang, S., & Rochaix, J. D. (2002). Light activates binding of membrane proteins to chloroplast RNAs in *Chlamydomonas reinhardtii*. *Plant Molecular Biology*, *50*(3), 573–585. Available from https://doi.org/10.1023/a:1020246007858.

Zhan, Y., Dhaliwal, J. S., Adjibade, P., Uniacke, J., Mazroui, R., & Zerges, W. (2015). Localized control of oxidized RNA. *Journal of Cell Science*, *128*(22), 4210–4219. Available from https://doi.org/10.1242/jcs.175232.

Zhan, Y., Marchand, C. H., Maes, A., Mauries, A., Sun, Y., Dhaliwal, J. S., ... Zerges, W. (2018). Pyrenoid functions revealed by proteomics in *Chlamydomonas reinhardtii*. *PLoS One*, *13*(2), e0185039. Available from https://doi.org/10.1371/journal.pone.0185039.

Zhang, N., Schurmann, P., & Portis, A. R., Jr. (2001). Characterization of the regulatory function of the 46-kDa isoform of Rubisco activase from Arabidopsis. *Photosynthesis Research*, *68*(1), 29–37. Available from https://doi.org/10.1023/A:1011845506196.

Zhu, X. G., de Sturler, E., & Long, S. P. (2007). Optimizing the distribution of resources between enzymes of carbon metabolism can dramatically increase photosynthetic rate: A numerical simulation using an evolutionary algorithm. *Plant Physiology*, *145*(2), 513–526. Available from https://doi.org/10.1104/pp.107.103713.

Zhu, X. G., Portis, A. R., & Long, S. P. (2004). Would transformation of C3 crop plants with foreign Rubisco increase productivity? A computational analysis extrapolating from kinetic properties to canopy photosynthesis. *Plant, Cell and Environment*, *27*(2), 155–165. Available from https://doi.org/10.1046/j.1365-3040.2004.01142.x.

1.5.3 Notion d'enzyme limitante du CBBC

Il est communément admis que l'efficacité photosynthétique est limitée par des goulets d'étranglement cinétiques au sein du CBBC. En effet, un des objectifs majeurs dans le domaine de la recherche sur la photosynthèse est de trouver quels sont les points limitants pour essayer d'augmenter l'efficacité de la photosynthèse et donc la production de biomasse (Ort et al., 2015; Kubis et Bar-Even, 2019; Simkin et al., 2019). La Rubisco, en raison de son activité oxydase et de sa faible activité carboxylase, est le principal facteur limitant l'efficacité de la fixation du carbone par le CBBC (Harpel et Hartman, 1994). Cependant, la Rubisco n'est pas la seule enzyme limitante. Au total, la limitation imposée par sept des 11 enzymes du CBBC a été étudiée, ce qui a révélé que d'autres enzymes que la Rubisco limitent le flux du CBBC (Raines, 2003, 2022; Janasch et al., 2019; Simkin et al., 2019). En faisant varier la quantité d'enzyme individuellement, il est possible d'évaluer le contrôle que celle-ci peut avoir sur le flux du CBBC. Ces études ont pu identifier plusieurs autres enzymes limitantes telles que la sédoheptulose-1,7-bisphosphatase (SBPase), la fructose-1,6-bisphosphatase (FBPase), la fructose-1,6-bisphosphate aldolase (FBA) et la transketolase (TRK) (Simkin et al., 2019; Raines, 2022). Une analyse métabolique basée sur l'activité enzymatique permettant une mesure quantitative de l'impact d'une variation de l'abondance de l'enzyme sur la fixation du carbone a été décrite (Fell and Fell, 1997). Cette mesure est fondée sur la formule de l'équation 1.

Équation 1 :

$$C = \frac{\frac{\delta J}{J}}{\frac{\delta E}{E}}$$

Où C est le coefficient de contrôle du flux, J et δJ sont respectivement le flux et sa variation, et E et δE correspondent à l'activité enzymatique normale et sa variation, respectivement.

Plus C se rapproche de 1, plus l'enzyme contrôle le flux de la voie métabolique et, inversement, plus C tend vers zéro, moins elle le limite.

Les données publiées ont été synthétisées dans le Tableau 1 (Liang et al., 2018).

Enzyme	Organisms	Conditions	Effects or flux control coefficient	Reference
RuBisCO	Tobacco (*Nicotiana tabacum* L.)	15 h/9 h light/dark cycle (25 °C/20 °C), 300 μmol photons m^{-2} s^{-1}	Antisense lines (20% RuBisCO left) have longer senescence phase	14
	Tobacco (*Nicotiana tabacum* L.)	500 μmol photons m^{-2} s^{-1} irradiance (12 h light/12 h dark)	Decreased photosynthesis and nitrogen metabolism especially under higher nitrate (12 mM) or ammonium nitrate (6 mM) conditions with less than 60% RuBisCO left	15
	Tobacco (*Nicotiana tabacum* L.)	Lower than 1000 μmol m^{-2} s^{-1} irradiance, ambient CO_2	>0.2 flux control coefficient; 0.01–0.03 flux control coefficient with 100 μmol m^{-2} s^{-1} irradiance	16
		Higher than 1500 μmol m^{-2} s^{-1} irradiance, ambient CO_2	0.8–0.9 flux control coefficient	
		Limited inorganic nitrogen	0.5 flux control coefficient; photosynthesis was largely reduced while growth was hardly affected	
	Tobacco (*Nicotiana tabacum* L.)	12 h day/12 h night cycle (irradiance 340 μmol m^{-2} s^{-1}, 20 °C, 65% relative humidity)	Reduced growth and photosynthesis, increased leaf area ratio and increased shoot-to-root ratio when less than 50% RuBisCO is left	17
	Rice (*Oryza sativa* L.)	Saturated light conditions	Strains with 65% RuBisCO activity showed a 20% lower photosynthesis rate in ambient CO_2 and a 5% to 15% higher photosynthesis rate in 100–115 Pa CO_2	18
	Rice (*Oryza sativa* L.)	16–22 °C and 28 Pa intercellular CO_2	Flux control coefficient (>0.88) detected	19
	Flaveria bidentis	Day/night growth temperatures were 28/15 °C	With less than 40% RuBisCO left, CO_2 assimilation and photosynthesis was reduced at high light irradiance but unaffected under low light condition (less than 100 μmol m^{-2} s^{-1}) on a wide range of CO_2 concentration	20
	Tobacco (*Nicotiana tabacum*)	1000 μmol m^{-2} s^{-1}, 350 microbars CO_2, and 25 °C	With 18% RuBisCO left, soluble protein content reduced the same level as RuBisCO, little change on other photosynthesis proteins. 63% reduction of CO_2 assimilation	21
	Arabidopsis thaliana	Low (200 μmol m^{-2} s^{-1}) and high (600 μmol m^{-2} s^{-1})	With 30 to 40% RuBisCo activity, photosynthesis, growth and above ground biomass are all reduced	22
	Flaveria bidentis	28/20 °C day/night temperature, 700 μmol m^{-2} s^{-1}, and a 16 h photoperiod or a naturally lit greenhouse	With 40% RuBisCO activity left, photosynthesis decreased but the H_2O exchange rate was similar to that of the wild type	23
	Flaveria bidentis	28/20 °C day/night temperature, 700 μmol m^{-2} s^{-1}, and a 16 h photoperiod or a naturally lit greenhouse	Quantum yield of PSI to PSII, PSI to CO_2 fixation and PSII to CO_2 fixation increased with enhanced irradiance in the RuBisCO decreased plant	24
SBPase	Tobacco (*Nicotiana tabacum*)	14 h light/10 h dark, 26 °C/18 °C, 600–1200 μmol m^{-2} s^{-1}	With less than 20% SBPase left, there were no changes in other CBB cycle enzymes but starch accumulation was reduced. With 57% SBPase left, the CO_2 assimilation and quantum yield of PSII reduced	25
	Tobacco (*Nicotiana tabacum*)	Saturated light conditions	Flux control coefficient: 0.31 under ambient CO_2 conditions and 0.54 under saturated CO_2 conditions	26
	Tobacco (*Nicotiana tabacum*)	Greenhouse in light levels between 400 and 1500 μmol m^{-2} s^{-1}, a 16 h photoperiod at a minimum of 25 °C light/18 °C dark and a maximum of 35 °C light/25 °C dark	Reduced growth and shoot biomass with 75% SBPase activity. SBPase decreased resulting in a shorter plant	27

Enzyme	Organisms	Conditions	Effects or flux control coefficient	Reference
	Tobacco (*Nicotiana tabacum* L.)	Greenhouse with a 14 h photoperiod at 25 °C light/18 °C dark, 700 to 1200 μmol m^{-2} s^{-1}	−0.2 flux control coefficient in the youngest developing leaves, 0.3–0.5 flux control coefficient in mature leaves, and decreased photosynthesis and starch accumulation in mature leaves	28
	Tobacco (*Nicotiana tabacum* L.)	Greenhouse 14 h/10 h (26 °C/18 °C) light/dark period, 1000–1400 μmol m^{-2} s^{-1}	Reductions in SBPase activity between 9% and 60%, maximum RuBP regeneration capacity declined linearly ($r^2 = 0.79$) and no significant change in Rubisco activity	29
	Rice (*Oryza sativa* L. *ssp. japonica*)	Greenhouse at 25 ± 2 °C with a photosynthetic photon flux density of 300 μmol m^{-2} s^{-1}, a relative humidity of 70% to 80%, and a photoperiod of 14 h/10 h light/dark	Stronger effects on reducing growth, photosynthesis and starch accumulation under low N than high N conditions when SBPase was deduced	30
Chloroplast FBPase	Potato (*Solanum tuberosum*)	16 h light (250 μmol m^{-2} s^{-1}, 22 °C)/8 h dark (15 °C) under greenhouse conditions	Unchanged tuber yield and reduced photosynthetic rate when FBPase activity decreased to 36% of that of the wild type. Reduced growth and photosynthetic rate when FBPase activity is below 15% of that of the wild type. <0.2 flux control coefficient	31
PRK	Tobacco (*Nicotiana tabacum* L.)	330 μmol photons m^{-2} s^{-1}, 350 ppm CO_2, 25 °C	With less than 85% PRK activities left, CO_2 assimilation was reduced. Almost 0 flux control coefficient under low light conditions	32
	Tobacco (*Nicotiana tabacum* L.)	330 μmol photons m^{-2} s^{-1}, 350 μmol CO_2 mol^{-1}, 25 °C	94% decrease in PRK has stronger inhibition on photosynthesis (by 35%) with 0.4 mM NH_4NO_3 than with 0.5 mM NH_4NO_3 (by 20%)	33
	Tobacco (*Nicotiana tabacum* L.)	330 μmol photons m^{-2} s^{-1}	0.25 flux control coefficient to CO_2 assimilation	34
		800 μmol photons m^{-2} s^{-1}	0 flux control coefficient to CO_2 assimilation	
GAPDH	Tobacco (*Nicotiana tabacum* L.)	Ambient CO_2	With less than 35% GAPDH left, photosynthesis was inhibited (900 and 1500 μmol m^{-2} s^{-1}). RuBP was reduced linearly with reduction of GAPDH. <0.2 flux control coefficient	35
TK	Tobacco (*Nicotiana tabacum* L.)	170 μmol m^{-2} s^{-1}, ambient CO_2	0.07 flux control coefficient	36
		700 μmol m^{-2} s^{-1}, ambient CO_2	0.32 flux control coefficient	
		Saturating light and CO_2	Almost 1 flux control coefficient	
FBA	Potato (*Solanum tuberosum*)	70 μmol m^{-2} s^{-1} or 390 μmol m^{-2} s^{-1}, ambient CO_2 or 800 ppm CO_2	Decrease of FBA has stronger inhibition on photosynthesis and growth under higher light and CO_2 conditions than lower light and CO_2 conditions	37
	Potato (*Solanum tuberosum*)	70 μmol m^{-2} s^{-1}, ambient CO_2	0.15 flux control coefficient	38
		390 μmol m^{-2} s^{-1} light and 400 ppm CO_2	0.21 flux control coefficient	
		390 μmol m^{-2} s^{-1} light and 800 ppm CO_2	0.55 flux control coefficient	

Tableau 1. Caractéristiques physiologiques des plantes présentant une réduction de l'abondance d'enzymes du CBBC et coefficient de contrôle de flux des enzymes du CBBC sous différentes conditions de culture (Liang et al., 2018). *References citées : 14* (Asim et al., 2022) 15 (Matt et al., 2002), 16 (Stitt et Schulze, 1994), 17 (Quick et al., 1991), 18 (Makino et al., 1997), 19 (Makino et Sage, 2007), 20 (Furbank et al., 1996), 21 (Hudson et al., 1992), 22 (Eckardt et al., 1997), 23 (Von Caemmerer et al., 1997), 24 (Siebke et al., 1997), 25 (Harrison et al., 1997), 26 (Raines et al., 2000), 27 (Lawson et al., 2006), 28 (Ölçer et al., 2001), 29 (Harrison et al., 2001), 30 (Feng et al., 2009), 31 (Kobmann, Sonnewald et

Willmitzer 1994), 32 (Paul et al., 1995a), 33(Banks et al., 1999a) , 34 (Paul et al., 2000), 35 (Badger and Price, 1994), 36 (Henkes et al., 2001), 37 (Haake et al., 1999), 38 (Haake et al., 1998).

Ces études ont montré l'importance qu'une seule enzyme peut avoir sur le contrôle du flux métabolique du CBBC, permettant de mettre en évidence de potentielles cibles d'ingénierie afin d'améliorer ce flux. Cependant il est important de noter qu'en fonction des conditions de culture, ce coefficient peut être variable, en particulier pour la Rubisco (Liang et al., 2018). Même si la quantité d'une enzyme peut être une intégration de différents facteurs (production, stabilité, régulations…), le fait de la faire varier n'exclut pas l'impact des conditions environnementales. En effet, l'intensité lumineuse, la température, ou la source de nitrate peuvent également influer sur ce coefficient (Liang et al., 2018). C'est pourquoi il est important de prendre ce coefficient comme une indication. De plus, tel qu'il a été défini, il peut représenter l'importance de la stœchiométrie d'une enzyme sur l'activité du cycle. Néanmoins, il ne peut prendre en compte à lui seul tous les facteurs. De plus, si ces coefficients doivent être comparés, il est nécessaire de les mesurer dans le même organisme. Par exemple, un mécanisme de concentration du carbone *(cf*. 1.5.4.1) peut, logiquement, fortement influencer ce paramètre pour la Rubisco. De même, les activités spécifiques des enzymes peuvent fortement varier d'un organisme à l'autre (Raines, 2022).

Dans l'objectif d'identifier les enzymes limitant la fixation du carbone, une étude de la variation *in vivo* des enzymes du CBBC constitue néanmoins une très bonne approche pour mieux comprendre comment améliorer l'efficacité photosynthétique.

1.5.4 Améliorer la fixation photosynthétique du carbone

Comme décrit dans le chapitre précédent, nous avons une certaine connaissance de l'ensemble des enzymes du cycle de Calvin Benson Bassham, en particulier chez Chlamydomonas. Nous savons notamment que c'est le CBBC, et en particulier la Rubisco, qui est le facteur majeur limitant l'efficacité photosynthétique. La présence de la photorespiration, l'inefficacité catalytique et la mauvaise spécificité de la Rubisco en font une cible prioritaire pour l'amélioration du CBBC *(cf*.

1.5.4.4 ci-après).

Il existe quatre grandes approches d'ingénierie envisagées pour améliorer la fixation du carbone (Figure 14). Nous allons les décrire.

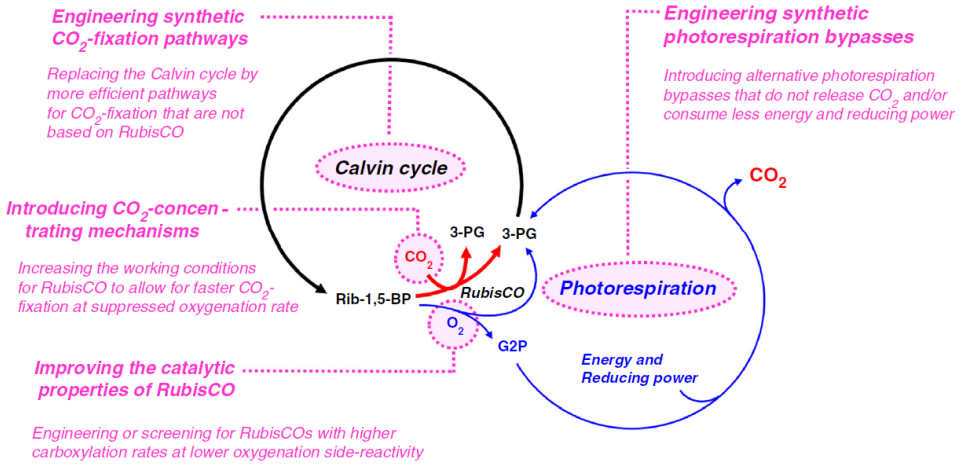

Figure 14. Quatre approches d'amélioration de la fixation du carbone. Tiré de (Erb and Zarzycki, 2016)

Nous considérerons l'axe « improving catalytic properties of Rubisco » de façon plus intégrée au niveau de l'ensemble du CBBC (*cf.* 1.5.4.4).

1.5.4.1 Utilisation des mécanismes de concentration du carbone

Les microalgues vertes et les cyanobactéries, possèdent un mécanisme de concentration du carbone (CCM). Chez les cyanobactéries, le CCM implique un compartiment spécifique appelé carboxysome (Kerfeld and Melnicki, 2016). C'est une structure protéique encapsulant la Rubisco et une anhydrase carbonique catalysant la conversion du bicarbonate en CO_2, augmentant ainsi la concentration de CO_2 à l'intérieur du carboxysome (Figure 15a). Le CCM permet ainsi d'augmenter la concentration du CO_2 à proximité de la Rubisco, favorisant ainsi son efficacité de carboxylation par rapport à son activité oxygénase.

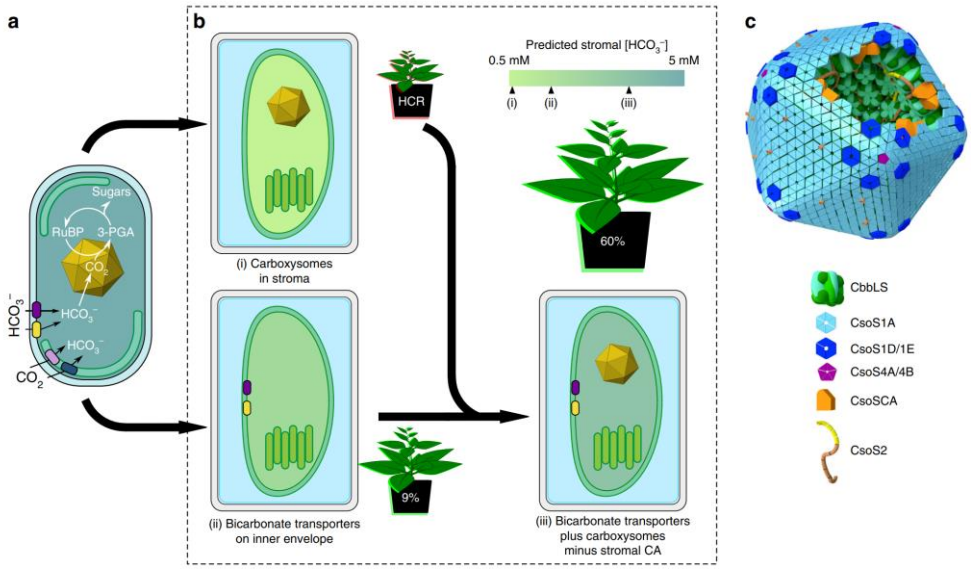

Figure 15. Composants du CCM cyanobactérien pour une photosynthèse améliorée. (A) Transport du carbone inorganique vers le carboxysome où le HCO_3^- est converti en CO_2 par une anhydrase carbonique (CA) et s'accumule. Le carboxysome encapsule la Rubisco à haut taux catalytique de la cellule. (B) Accumulation prédite du CO_2 dans le carboxyme. (C) Les carboxysomes de Cyanobium PCC7001, utilisés dans cette étude, sont composés de plusieurs milliers de polypeptides, disposés dans une structure icosaédrique. Dans ce modèle, une seule couche de Rubisco liée à la coque (CbbLS, vert) est montrée, avec une CA carboxysomale (orange). CsoS2 (jaune/marron) relie Rubisco et la coque principalement constituée (B. M. Long et al. 2018).

Chez Chlamydomonas, un mécanisme similaire de concentration du carbone se produit à l'intérieur d'un microcompartiment situé dans le chloroplaste et appelé pyrénoïde (Figure 16) (Barrett et al., 2021; Adler et al., 2022). Le pool de Rubisco est condensé en une matrice à l'intérieur du pyrénoide dans lequel le CO_2 est concentré *via* l'action de transporteurs de carbone inorganique (C_i) et d'anhydrases carboniques situés dans différents compartiments cellulaires. Le pyrénoïde a le même rôle que le carboxysome des cyanobactéries : concentrer le CO_2 à proximité de la Rubisco.

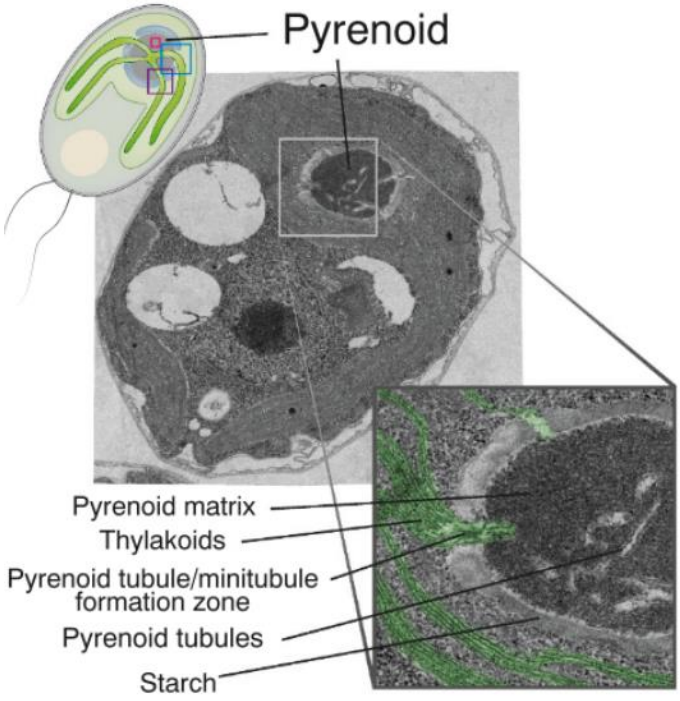

Figure 16. Image TEM du pyrénoïde de Chlamydomonas. Chlamydomonas reinhardtii *cultivée sous lumière et sous des niveaux de CO_2 atmosphérique où un pyrénoïde complet est assemblé. Le zoom met en évidence les parties structurales clés du pyrénoïde. Les thylakoïdes sont faussement colorés en vert pour plus de clarté.* (Barrett et al., 2021)

Des efforts sont en cours visant à utiliser des approches de biologie synthétique pour intégrer ces mécanismes de concentration dans les plantes terrestres, afin d'augmenter la fixation du carbone et donc les rendements (Fei et al., 2022). Les modèles suggèrent qu'implanter un CCM chez une plante en C3 pourrait potentiellement améliorer les rendements de 60% (Dean Price et al., 2011; McGrath et Long, 2014). Dans une étude de 2018, menée par Long *et al.,* un carboxysome synthétique a été reconstitué dans le chloroplaste du tabac, ce qui a démontré la faisabilité d'une telle approche (Long et al., 2018) (Figure 15). De même, un proto-pyrénoïde a également été implanté chez la plante modèle *Arabidopsis thaliana* (Atkinson et al., 2020). De nombreuses autres étapes seront cependant nécessaires pour que ce compartiment soit fonctionnel, notamment les éléments permettant de concentrer le carbone dans ces compartiments artificiels (Fei et al., 2022).

1.5.4.2 Contournement de la photorespiration

La photorespiration est la voie de régénération du 2-phosphoglycolate, généré à partir du RuBP par l'activité oxygénase de la Rubisco. Cette voie complexe implique 4 compartiments cellulaires :

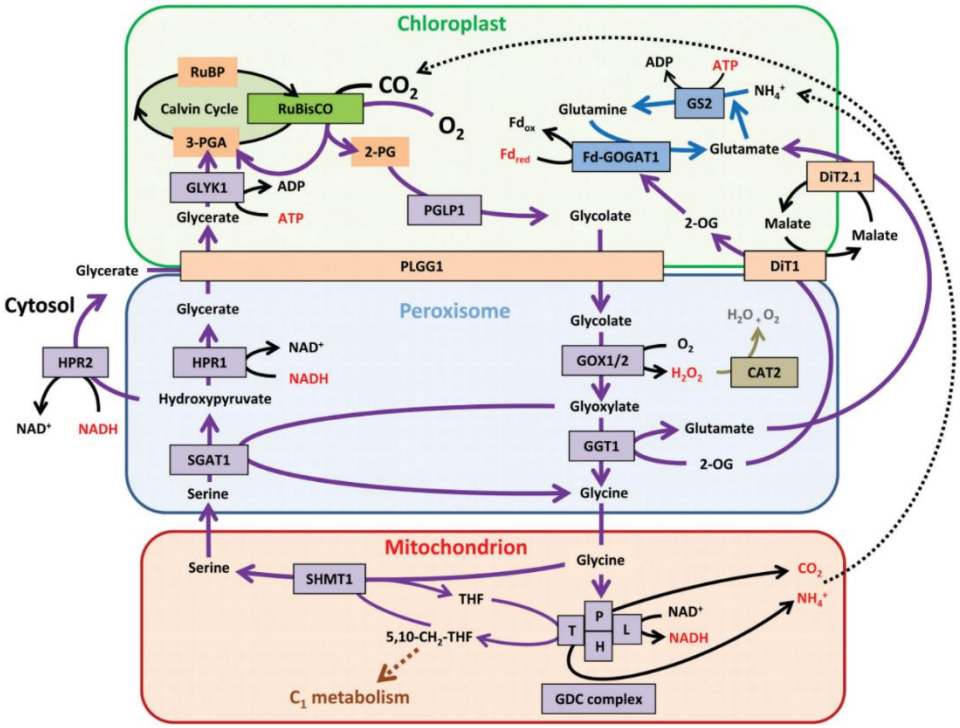

Figure 17. Le cycle photorespiratoire et son interaction avec le CBBC, l'assimilation de l'ammonium et le métabolisme C1. Abréviations : CAT2, catalase 2 ; DiT1, transporteur plastidial 2-OG/malate 1 ; DiT2, transporteur plastidial glutamate-malate 1 ; Fd-GOGAT1, glutamate synthase 1 dépendante de la ferredoxine ; GGT1, glutamate:glyoxylate aminotransférase 1 ; Complexe GDC, complexe de la glycine décarboxylase (composé des protéines P, T, L, H) ; GLYK1, glycérate kinase 1 ; GOX1/2, glycolate oxydase 1/2 ; GS2, glutamine synthétase plastidiale ; HPR1/2, hydroxypyruvate réductase 1/2 ; PGLP1, phosphatase 2-PG 1 ; PLGG1, transporteur plastidial glycolate/glycérate 1 ; RuBisCO, RuBP carboxylase/oxygénase ; RuBP, ribulose-1,5-bisphosphate ; SGAT1, sérine:glyoxylate aminotransférase 1 ; SHMT1, sérine hydroxyméthyl transférase 1 ; THF, tétrahydrofolate ; 2-OG, 2-oxoglutarate ; 2-PG, 2-phosphoglycolate ; 3-PGA, 3-phosphoglycérate (Hodges et al., 2016).

le chloroplaste, le cytosol, le peroxysome et la mitochondrie (Figure 17). Elle a comme bilan la perte d'un CO_2 ainsi qu'une molécule d'ammonium, qui doit être activement transportée de la mitochondrie au chloroplaste pour être fixée, à nouveau, par la GS/GOGAT (Glutamine Synthase/Glutamate OxoGlutarate AminoTransferase). Elle produit également une forme active de l'oxygène, l'H_2O_2, qui doit être détoxifié par la catalase (Hodges et al., 2016).

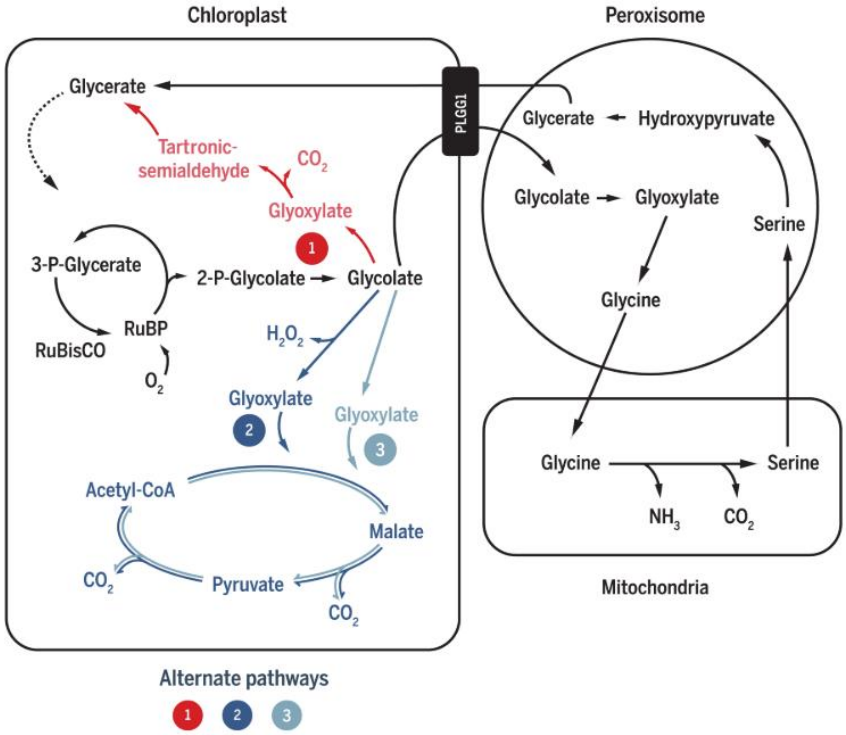

Figure 18. Chemins photorespiratoires alternatifs chez le tabac. Trois voies alternatives [1 (rouge), 2 (bleu foncé) et 3 (bleu clair)] ont été introduites dans les chloroplastes du tabac pour un recyclage plus efficace du glycolate. L'ARNi supprime le transporteur de glycolate/glycérate natif PLGG1 pour empêcher le glycolate de sortir du chloroplaste et d'entrer dans la voie native (gris). La stratégie 3 a été celle utilisée en champs. (South et al., 2019).

Pendant de nombreuses années, le doute a subsisté sur l'aspect bénéfique de la photorespiration pour la croissance des végétaux. Une approche de biologie synthétique consisterait à modifier le métabolisme afin de détoxifier le 2-phosphoglycolate par une voie alternative plus efficace énergétiquement que la photorespiration (Jin et al., 2023). Par exemple, il a été montré qu'en créant un raccourci métabolique (Figure 18) (Kebeish et al., 2007; Maier et al., 2012; Aboelmy et Peterhansel, 2014), les rendements des cultures de tabac en champs pouvaient être augmentés d'environ 40% (South et al., 2019).

1.5.4.3 Création *de novo* de voies de fixation du carbone artificielles

Les limitations du CBBC, et de la Rubisco en particulier, ont poussé de nombreuses équipes à proposer des voies métaboliques alternatives et totalement synthétiques. La motivation est en général de remplacer le CBBC par ces voies théoriquement plus efficaces. Nous pouvons citer par exemple les MOG *pathways* (Bar-Even et al., 2010) ou le CETCH (Schwander et al., 2016). D'autres cycles, existants dans le vivant mais utilisant une fixation du carbone dite en C1 (*via* le formate) sont aussi étudiées, tel le GED (Gnd–Entner–Doudoroff) *pathway* (Satanowski et al., 2020a).

Le CETCH (crotonyl-CoA/ethylmalonyl-CoA/hydroxybutyryl-CoA) *pathway* présente un intérêt particulier puisqu'il s'agit du seul cycle artificiel jamais reconstitué *in vitro* (Schwander et al., 2016; Miller et al., 2020), les autres ayant seulement été testés *in silico*, démontrant sa fonctionnalité. Il s'agit d'un cycle de 17 enzymes sélectionnées, issues de 9 organismes différents (Figure 19).

Une approche récente de biologie computationnelle a combiné les meilleurs aspects d'un ensemble de ces cycles pour proposer une nouvelle version d'un cycle de fixation du CO_2 ainsi qu'une autre version pour les cycles dits en « C1 » (Löwe and Kremling, 2021).

Bien que cette approche de *de novo design* soit particulièrement élégante, elle demeure encore très préliminaire puisqu'aucune de ces voies métaboliques potentielles n'a jamais été implémentée *in vivo*.

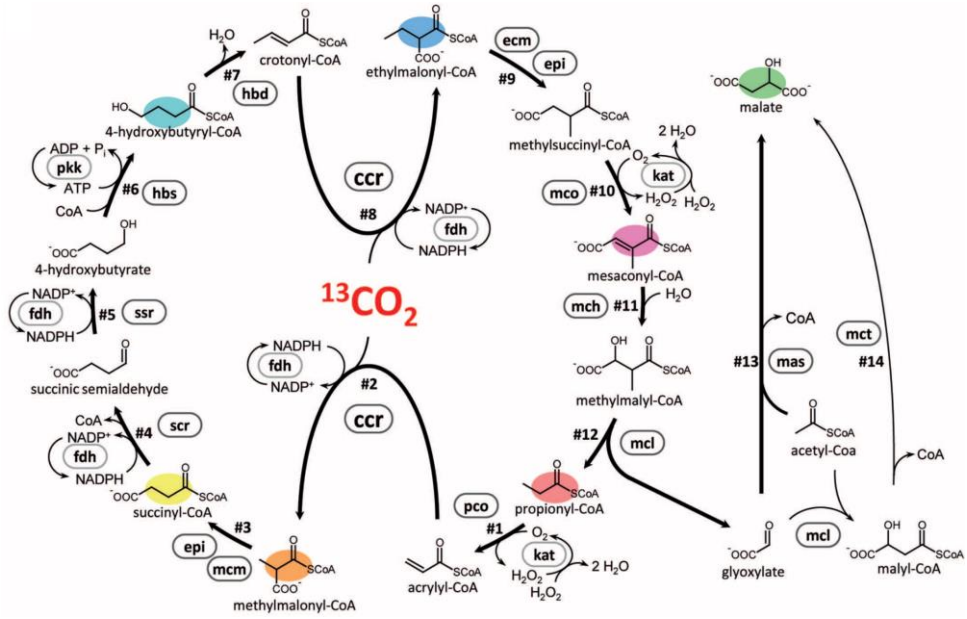

Figure 19. Représentation du cycle artificiel crotonyl-CoA/ethylmalonyl-CoA/hydroxybutyryl-CoA (CETCH) tiré de l'article (Schwander et al., 2016).

1.5.4.4 Amélioration du cycle de Calvin Benson Bassham

Le dernier axe qui me concerne plus particulièrement, car il fait l'objet de mon travail de thèse, est l'augmentation de l'efficacité du cycle de Calvin Benson Bassham. La compréhension de l'importance de la stœchiométrie des enzymes du cycle représente un axe important pour comprendre son fonctionnement et améliorer son efficacité (Raines 2006; Stitt, Lunn, and Usadel 2010; Zhu, De Sturler, and Long 2007).

De multiples études ont montré qu'il était possible d'augmenter la fixation photosynthétique du carbone et la production de biomasse en augmentant la quantité d'une ou plusieurs enzymes du CBBC. En effet, en surexprimant la Rubisco dans le maïs et le riz, une augmentation de biomasse de 30% pour ces deux espèces a été rapportée *(Wang et al. 2020 ; Salesee-Smith et al. 2020)*. Chez les cyanobactéries, la surexpression de la Rubisco a aussi eu un effet positif sur l'efficacité photosynthétique (Liang et al., 2018). Chez le Tabac et *Arabidopsis thaliana,* une surexpression de la SBPase conjointement à la FBA a permis une augmentation de la biomasse de 62% et 71%,

respectivement (*Simkin et al. 2017; Simkin et al. 2015)*. Chez le blé et *Chlamydomonas reinhardtii*, une surexpression de la SBPase a entrainé une augmentation de la biomasse de 40% et 38%, respectivement (Driever et al., 2017; Hammel et al., 2020). La surexpression de la SBPase a également amélioré l'efficacité photosynthétique chez le Tabac, Arabidopsis et le riz (Miyagawa et al., 2001; Liang et al., 2018). Ces résultats apparaissent transférables en termes de méthodologie puisqu'ils ont eu un grand succès sur plusieurs organismes. Il faut cependant nuancer cette remarque puisque la surexpression de la SBPase, dont les résultats ont été particulièrement intéressants, n'a pas été transposable chez une plante de type C4, *Setaria viridis* (Ermakova et al., 2023).

Parmi les trois enzymes spécifiques du CBBC (PRK, SBPase, Rubisco), l'importance de l'abondance de la PRK a été très peu étudiée. En effet, depuis les études chez le tabac de M. Paul dans les années 1990 (Badger et Price, 1994; Paul et al., 1995; Banks et al., 1999), aucune étude sur le contrôle de la PRK sur le flux du CBBC n'a été menée. De plus, aucun essai de surexpression de la PRK n'a jamais été réalisé.

1.5.5 La phosphoribulokinase (PRK)

La phosphoribulokinase (PRK, E.C. 2.7.1.19) est l'enzyme qui catalyse la réaction de phosphorylation du ribulose-5-phosphate en ribulose-1,5-bisphosphate en utilisant l'ATP généré par la chaine de transfert d'électrons (Figure 20).

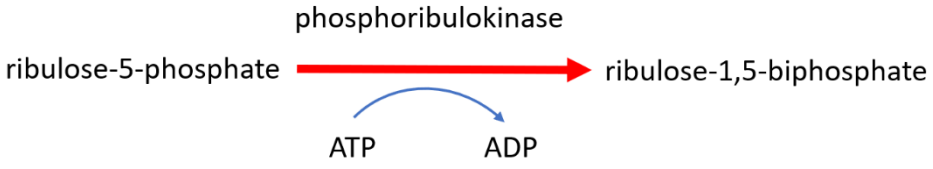

Figure 20. Conversion du ribulose-5-phosphate en ribulose-1,5-bisphosphate par la phosphoribulokinase en utilisant l'ATP.

Elle procure à la Rubisco son substrat, et c'est la seule enzyme connue capable de catalyser cette réaction (Le Moigne et al., 2023). Chez Chlamydomonas, elle est codée par un seul gène (Cre12.g554800) et

cette protéine comprend 376 résidus. Elle se présente sous la forme d'un homodimère de 70 kDa (Figure 21). Sa structure tridimensionnelle montre un long feuillet β mixte de neuf brins entourés par des hélices alpha et de 4 autres petits brins β. Ce grand feuillet est symétrique à celui du second monomère. L'interface d'homo-dimérisation est un motif à deux brins β antiparallèles. Chaque monomère contient 4 cystéines conservées (Figure 22 et 23).

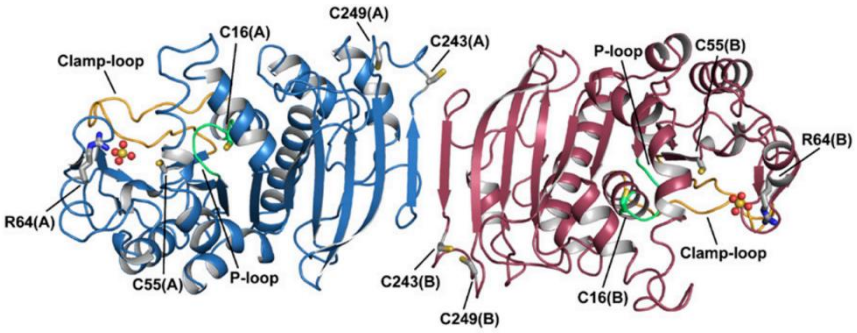

Figure 21. Représentation de la structure de la phosphorilubokinase. Tiré de Gurrieri et al, 2013

A

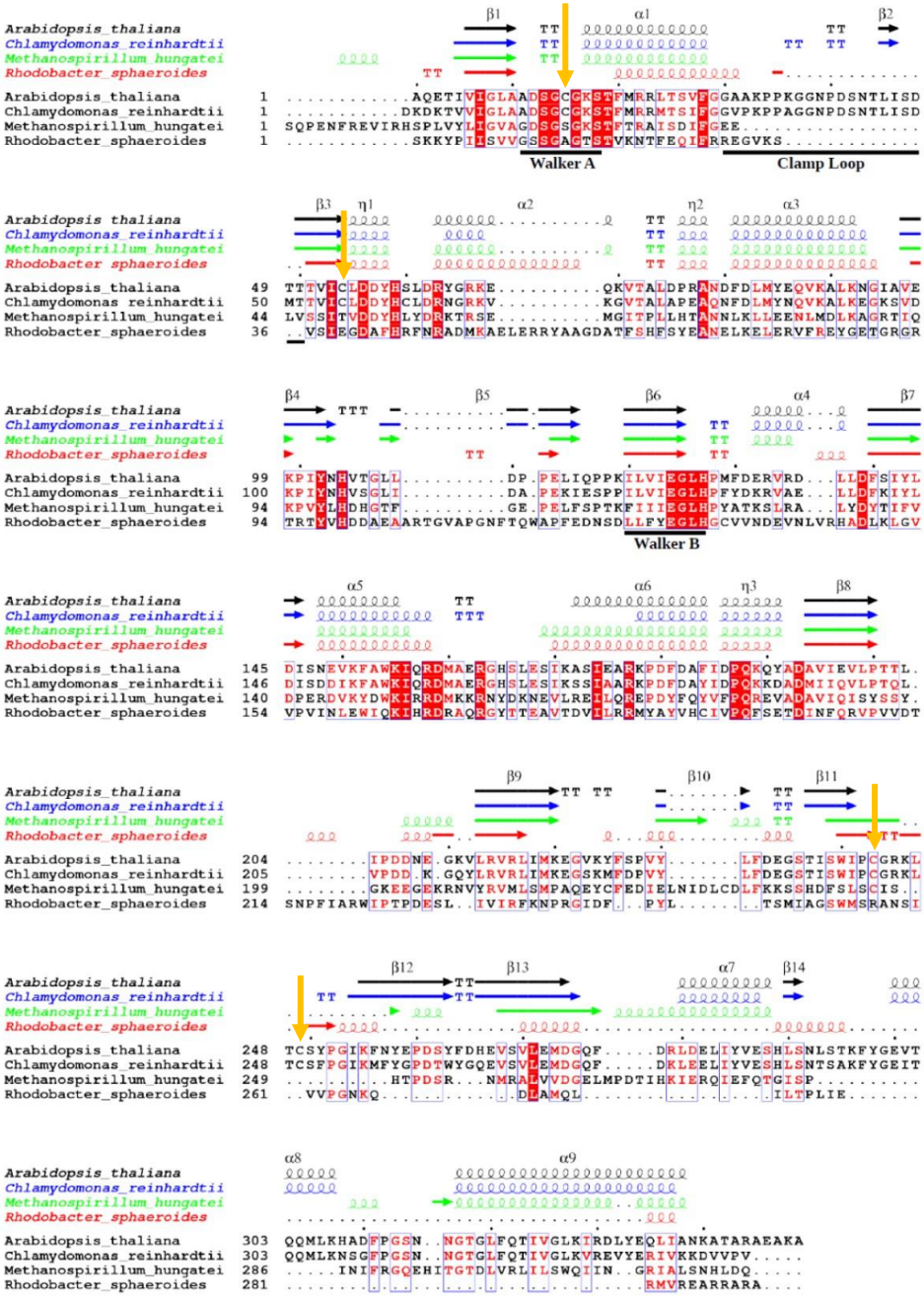
Arabidopsis_thaliana
Chlamydomonas_reinhardtii
Methanospirillum_hungatei
Rhodobacter_sphaeroides
Walker A
Clamp Loop
Walker B

B

Residue (*Cr*/*At*)	ASA (Å²)*			
	*Cr*PRK		*At*PRK	
	A	B	A	B
Cys16/15	14.5	8.5	7.6	10.6
Cys55/54	10.6	10.6	6.3	9.5
Cys61	55.9	58.7	/	/
Cys243	26.6	37.8	53.4	14.8
Cys249	42.4	31.1	14.8	50.6
Arg64/63	51.4	88.7	82.6	88.2

*Radius of the probe solvent molecule 1.4 Å

Figure 22. Conservation des cystéines des PRK, (Gurrieri et al., 2019).

(A) Alignement de séquence et de structure des quatre PRK connues structuralement. L'alignement a été effectué avec Espript (http://espript.ibcp.fr) en utilisant la séquence et la structure d'AtPRK (Uniprot P25697, PDB 6H7H) ; CrPRK (Uniprot P19824, PDB 6H7G) ; RsPRK (Uniprot P12033, PDB 1A7J) (31), MhPRK (Uniprot Q2FUB5, PDB 5B3F). Les séquences des deux PRK photosynthétiques sont plus longues (349 et 344 résidus pour AtPRK et CrPRK, respectivement) que les PRK bactériennes (290 résidus) et Archae (323 résidus). Les identités de séquence entre les PRK considérées sont : 75% pour AtPRK vs CrPRK ; 35% pour AtPRK vs MhPRK ; 32% pour CrPRK vs MhPRK ; 22% pour AtPRK vs RsPRK ; 24% pour CrPRK vs RsPRK. Les identités de séquence ont été calculées par Clustal Omega. Les fléches jaunes indiquent les cystéines des deux ponts disulfures régulateurs. (B) Valeurs d'accessibilité (ASA) pour les résidus cystéine et une arginine strictement conservée.

Son activité est régulée par les thiorédoxines. Sous sa forme oxydée, cette enzyme présente une faible activité alors qu'elle est activée par réduction. Le pont disulfure Cys16-Cys55 (potentiel rédox -330 mV à pH 7,9) en N-terminal est TRX-dépendant et est responsable de l'inhibition de l'enzyme par oxydation puisque la cystéine 55 est impliquée dans le mécanisme catalytique (Milanez et al., 1991; Marri et al., 2005).

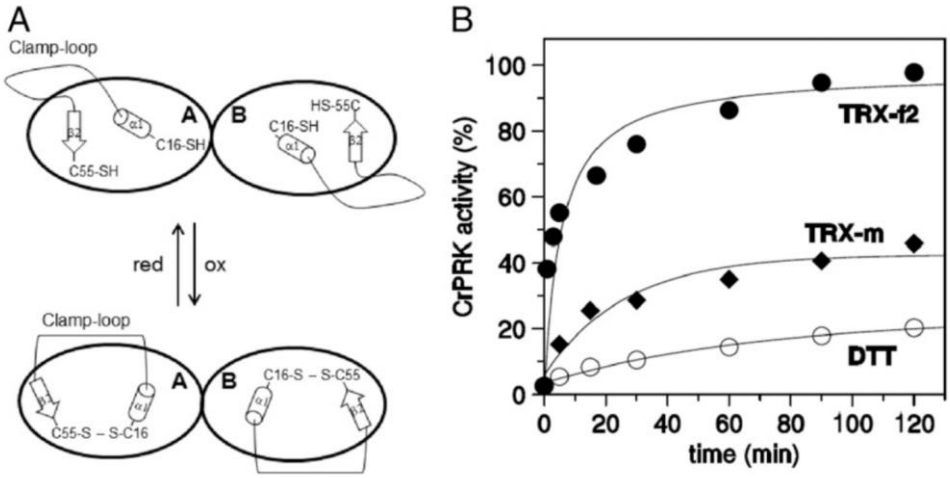

Figure 23. Clamp-loop et régulation TRX-dépendante de la PRK de Chlamydomonas. (A) Une représentation schématique du rôle proposé pour la « clamp loop *» et les changements conformationnels survenant dans la PRK chloroplastique lors de la réduction par la TRX. (B) Cinétique d'activation de la PRK par la TRX-f2, la TRX-m et le DTT* (Gurrieri et al., 2019).

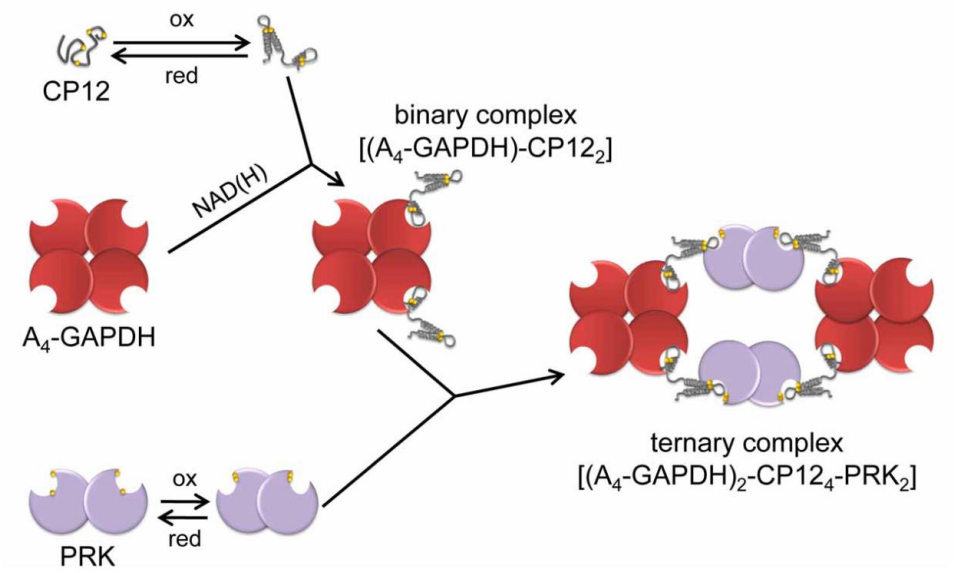

Figure 24. Représentation schématique de la formation du complexe GAPDH-CP12-PRK (Michelet et al, 2013)

En C-terminal, il existe un autre pont disulfure, impliquant les Cys243 et Cys249. Il est proche de la surface de dimérisation et jouerait un rôle dans la flexibilité de l'assemblage du complexe GAPDH/CP12/PRK (Moparthi et al., 2015). La formation de ce complexe inhibe l'activité de l'enzyme (*cf*. 1.5.2.2, Article 1) (Figure 24).

Plusieurs thiorédoxines ont été identifiées comme pouvant réduire la PRK. Elle peut être activée par les TRX chloroplastiques de type *f* et de type *m*. Notre équipe a récemment montré que la TRX*z* est aussi capable de réduire la PRK *in vitro* (Le Moigne et al., 2021). C'est cependant la TRX*f* qui est la plus efficace pour réduire et donc activer la PRK *in vitro* (Figure 23).

Si la PRK a été beaucoup étudiée *in vitro*, peu d'études ont été réalisées *in vivo*. Matthew J. Paul et ses collaborateurs ont publié trois articles sur l'impact d'une diminution de la quantité de PRK chez le tabac (Badger and Price, 1994; Paul et al., 1995; Banks et al., 1999). Dans différentes conditions de nutrition azotée et à différentes intensités lumineuses, ils ont pu montrer qu'une réduction de 85% de la quantité de PRK est nécessaire pour affecter la photosynthèse. La conclusion est que, dans les conditions testées par cette équipe, la PRK ne serait pas une enzyme limitante du CBBC chez le tabac.

Chez Chlamydomonas, un mutant de la PRK a été caractérisé en 1970. L'absence d'activité de la PRK ainsi que de croissance en milieu minimum ont été rapportées pour cette souche mutante, nommée F60 (Moll and Levine, 1970). Cependant, les techniques de caractérisation moléculaire n'étaient pas encore disponibles à cette époque. Quinze ans plus tard, un article rapportait que la protéine PRK était présente dans le mutant F60, sans doute en raison d'une réversion (Salvucci and Ogren, 1985), ce qui fut démontré en 2000 (Smith, 2000). Plus récemment, un criblage phénotypique à large échelle de la banque de mutants CLiP (Li et al., 2015, 2019) a été mené pour identifier des phénotypes intéressants, comme l'impossibilité de croitre en conditions phototrophiques strictes (Fauser et al., 2022). Des mutants alléliques pour le gène PRK ont été identifiés au cours de ce criblage, suggérant que la PRK est bien essentielle à la croissance dans ces conditions.

Un mutant knock-out de la banque CliP pourrait constituer un excellent outil pour étudier l'importance de l'abondance de la PRK sur l'efficacité de la fixation du carbone chez Chlamydomonas. Il pourrait également permettre d'explorer *in vivo* le rôle des régulations démontrées *in vitro*, notamment celles impliquant les thiorédoxines, en complémentant le mutant par des versions non régulées de la PRK.

1.6 Objectifs de la thèse

L'objectif principal de notre équipe est de comprendre et d'améliorer l'efficacité de la photosynthèse chez Chlamydomonas en employant des approches de biologie synthétique pour manipuler le CBBC *in vivo*. Etant donné que le CBBC est un facteur majeur limitant l'efficacité de la photosynthèse dans des conditions optimales de culture, toute amélioration de cette voie de fixation du carbone se traduira directement par une amélioration de l'efficacité photosynthétique et augmentera la photoproduction de biomasse et de bioproduits carbonés à des intensités lumineuses modérées à élevées. Comme détaillé dans l'introduction, la modification de la stœchiométrie des enzymes du CBBC, principalement par la surexpression d'enzymes spécifiques, s'est avérée efficace pour améliorer la fixation du carbone. En outre, toutes les enzymes du CBBC sont finement régulées par l'état redox intracellulaire, qui dépend de l'éclairage et des conditions environnementales, grâce à de multiples régulations post-traductionnelles. Le rôle exact de la plupart des modifications post-traductionnelles des enzymes du CBBC reste inconnu, à l'exception de l'activation dépendante de la lumière par les TRX qui a été largement étudiée *in vitro*. Chez *C. reinhardtii*, quatre enzymes du CBBC, à savoir PRK, PGK, FBPase et SBPase, sont activées à la lumière par la réduction TRX-dépendante de ponts disulfures régulateurs.

L'objectif à moyen terme de notre laboratoire est de modifier ces régulations *in vivo* en utilisant des approches de biologie synthétique basées sur les connaissances acquises précédemment *in vitro*. Cela permettrait d'approfondir notre compréhension de l'importance fonctionnelle de la régulation TRX-dépendante du CBBC *in vivo* dans diverses conditions de croissance. Cela pourrait également fournir des stratégies efficaces pour améliorer la fixation du carbone en modifiant les régulations en plus de l'abondance des enzymes. En effet, la modulation dépendante de la lumière des enzymes du CBBC par les

TRX permet un ajustement fin de l'activité du CBBC probablement nécessaire pour une croissance et une survie optimale dans la nature sous des cycles lumière/obscurité photopériodiques naturels et dans un large éventail de conditions environnementales. Les microalgues ne sont cependant pas optimisées pour la croissance dans les conditions spécifiques des photobioréacteurs industriels, en particulier les alternances lumière/obscurité provoquées par le mélange à haute fréquence de cultures à haute densité. Dans ces conditions, l'existence de l'activation dépendante de la lumière par les TRX pourrait limiter l'efficacité du CBBC en raison de l'activation/désactivation constante des enzymes dépendantes des TRX. Ainsi, la conception d'enzymes du CBBC modifiées quant à leur régulation dépendante des TRX pourrait avoir un impact important sur la production de biomasse et l'efficacité de la fixation du carbone pour les cultures de Chlamydomonas cultivées dans des conditions industrielles pertinentes. Mon projet de thèse visait à initier de telles approches en se concentrant sur la manipulation *in vivo* de la phosphoribulokinase.

L'objectif général de mon travail de thèse fut donc de caractériser un mutant knock-out de la PRK, de le complémenter avec différentes constructions de la PRK et d'étudier l'importance de son abondance sur l'efficacité du CBBC en modulant son expression. Les résultats obtenus seront présentés dans la première partie des résultats. Des résultats préliminaires sur l'utilisation de ce mutant pour étudier la régulation redox de la PRK *in vivo* seront également présentés.

Mon deuxième objectif était de contribuer au développement de nouveaux outils de biologie synthétique chez *C. reinhardtii*. Dans ce cadre, j'ai pu concevoir, construire et caractériser de nouvelles briques génétiques, dont certaines sont présentées dans la première partie. J'ai également contribué à l'adaptation du gène de résistance à la blasticidine chez *Chlamydomonas reinhardtii*. Dans le cas d'une étude où l'on aurait besoin de transformations successives, l'utilisation de plusieurs marqueurs de sélection est nécessaire. L'objectif était donc de développer une nouvelle brique de résistance à un antibiotique pour le kit Moclo. Cette brique devait être compatible avec d'autres marqueurs de sélection, ne devait pas affecter la croissance de Chlamydomonas et ne devait pas conférer de résistance à un autre antibiotique.

2 RÉSULTATS

2.1 Étude de la phosphoribulokinase *in vivo* chez *Chlamydomonas reinhardtii*

2.1.1 Introduction

Pour pouvoir étudier la phosphoribulokinase *in vivo* chez Chlamydomonas, il était nécessaire de mettre en place une méthodologie pour pouvoir contrôler l'abondance de la PRK et pour pouvoir remplacer la PRK native par une version modifiée, par exemple dépourvue d'une ou plusieurs cystéines régulatrices. Pour cela, il nous fallait disposer d'un mutant knock-out de la PRK afin de pouvoir le complémenter avec des formes sauvages ou modifiées. Il était également nécessaire de caractériser les briques génétiques pour contrôler l'expression de la PRK.

L'étude présentée ci-après porte sur la caractérisation du mutant ΔPRK et sa complémentation fonctionnelle. Cette étude a permis de montrer que la PRK est essentielle à la phototrophie. La complémentation fonctionnelle de ce mutant permet de restaurer la phototrophie. Néanmoins, en utilisant des éléments génétiques standard, l'expression de la PRK était limitée à 40% du niveau de référence dans les souches complémentées et ne pouvait pas rétablir une croissance normale en conditions photoautotrophes, suggérant que le CBBC était limité. Nous avons ensuite réussi à surmonter cette limitation initiale en améliorant la conception de l'unité de transcription exprimant la PRK, notamment en utilisant le promoteur endogène de la PRK et la séquence codante de la PRK contenant ses introns. Cela nous a permis d'atteindre le niveau élevé de PRK présent dans la souche WT et même de surexprimer l'enzyme. Une collection de souches présentant des niveaux de PRK compris entre 16% et 250% des niveaux de PRK WT a été générée et caractérisée. Nous avons pu montrer qu'un contenu en PRK de 86% est suffisant pour rétablir complètement la croissance photoautotrophe et qu'une surexpression de l'enzyme ne permet pas d'améliorer la production de biomasse. La PRK est donc en excès chez Chlamydomonas mais cet excès est plus limité que chez le tabac où

seulement 15% du niveau sauvage suffit à restaurer une croissance normale (Badger and Price, 1994; Paul et al., 1995; Banks et al., 1999).

Mon rôle dans ces travaux a consisté à concevoir et expérimenter la méthodologie d'étude de la PRK chez Chlamydomonas, caractériser le mutant PRK et les souches complémentées. J'ai également mis en place les stratégies pour la forte expression de la PRK et construit les briques nécessaires à partir du gène PRK.

2.1.2 Article 2

L'article intitulé « Phosphoribulokinase abundance is not limiting the Calvin-Benson-Bassham cycle in *Chlamydomonas reinhardtii* » par Nicolas D. Boisset, Giusi Favoino, Maria Meloni, Lucile Jomat, Corinne Cassier-Chauvat, Mirko Zaffagnini, Stéphane D. Lemaire et Pierre Crozet est présenté sous la forme d'un manuscrit actuellement soumis pour publication.

frontiers

Phosphoribulokinase abundance is not limiting the Calvin-Benson-Bassham cycle in *Chlamydomonas reinhardtii*

Nicolas D. Boisset[1,2,3,*], Giusi Favoino[1,*,†], Maria Meloni[4], Lucile Jomat[1], Corinne Cassier-Chauvat[5], Mirko Zaffagnini[4], Stéphane D. Lemaire[1,2,‡] and Pierre Crozet[1,2,6,‡]

[1]Laboratoire de Biologie Computationnelle et Quantitative, Institut de Biologie Parie-Seine, Sorbonne Université, CNRS, UMR 7238, Paris, France
[2]Laboratoire de Biologie Moléculaire et Cellulaire des Eucaryotes, Institut de Biologie Physico-Chimique, Sorbonne Université, CNRS, UMR 8226, Paris France
[3]Doctoral School of Plant Sciences, Université Paris-Saclay, Saint-Aubin, France
[4]Department of Pharmacy and Biotechnology, Bologna, Italy
[5]Université Paris-Saclay, CEA, CNRS, Institute for Integrative Biology of the Cell (I2BC), UMR 9198, Gif-sur-Yvette, France
[6]Polytech-Sorbonne, Sorbonne Université, Paris, France

[*]**authors participated equally to this work**

[‡] **Correspondence:**

Pierre Crozet pierre.crozet@sorbonne-universite.fr

Stéphane D. Lemaire, stephane.lemaire@sorbonne-universite.fr

†present address:

Keywords: Phosphoribulokinase, Synthetic biology, Carbon fixation, *Chlamydomonas reinhardtii,* Calvin-Benson-Bassham cycle.

Abstract

Improving photosynthetic efficiency in plants and microalgae is of utmost importance to support the growing world population and to enable the bioproduction of energy and chemicals. Limitations in photosynthetic light conversion efficiency can be directly attributed to kinetic bottlenecks within the Calvin-Benson-Bassham cycle (CBBC) responsible for carbon fixation. A better understanding of these bottlenecks *in vivo* is crucial to overcome these limiting factors through bio-engineering. The present study is focused on the analysis of phosphoribulokinase (PRK) in the unicellular green alga *Chlamydomonas reinhardtii*. We have characterized a PRK knock-out mutant strain and showed that in the absence of PRK, Chlamydomonas cannot grow photoautotrophically while functional complementation with a synthetic construct allowed restoration of photoautotrophy. Nevertheless,

using standard genetic elements, the expression of PRK was limited to 40% of the reference level in complemented strains and could not restore normal growth in photoautotrophic conditions suggesting that the CBBC is limited. We were subsequently able to overcome this initial limitation by improving the design of the transcriptional unit expressing PRK using diverse combinations of DNA parts including PRK endogenous promoter and introns. This enabled us to obtain strains with PRK levels comparable to the reference strain and even overexpressing strains. A collection of strains with PRK levels between 16% and 250% of WT PRK levels was generated and characterized. Immunoblot and growth assays revealed that a PRK content of ≈86% is sufficient to fully restore photoautotrophic growth. This result suggests that PRK is present in moderate excess in Chlamydomonas. Consistently, the overexpression of PRK did not increase photosynthetic growth indicating that that the endogenous level of PRK in Chlamydomonas is not limiting the Calvin-Benson-Bassham cycle under optimal conditions.

1. Introduction

The irreversible depletion of traditional sources of fossil fuels coupled with the accumulation of greenhouse gases produced by their combustion has created an urgent need to develop alternative forms of eco-responsible processes for large scale CO_2 sequestration and new sources of reduced carbon for the production of fuels and chemicals needed by our society (Eckardt et al., 2023). Photoautotrophic microorganisms such as green microalgae and cyanobacteria, are regarded as promising platforms for the development of innovative concepts based on their inherent ability to fix CO_2, thereby producing various organic molecules *via* a sunlight-driven and sustainable process. Simultaneously, the global crop production needs to double by 2050 to meet the demand of a growing population, especially considering the use of arable lands to feed bio-refineries, deleterious effects of climate change, and continuous erosion of agricultural land (Godfray et al., 2010; Tilman et al., 2011; Ort et al., 2015; Simkin et al., 2019). The remarkable gains in productivity of the Green Revolution of the late 20th century have largely been achieved by increasing the light capture efficiency and the harvest index (*i.e.* the fraction of biomass that is captured in the harvested part); but these two factors approach their practical limits (Long et al., 2006). Improved solar energy conversion efficiency (*i.e.*, photosynthetic efficiency) has so far played little role in improving yield potential, yet photosynthesis is the only determinant that is not close to its biological limits (Zhu et al., 2010).

In order to face the challenge of improving photosynthetic efficiency, new methodologies are required to allow success (Erb and Zarzycki, 2016; Kubis and Bar-Even, 2019; da Fonseca-Pereira et al., 2022). Biology is currently facing a revolution through its transition from analytic to synthetic biology approaches. The rise of green synthetic biology offers the potential to tackle the challenge of improving photosynthetic efficiency through engineering of microalgae, cyanobacteria and plants. Different strategies have shown the potential of synthetic approaches aimed at improving carbon fixation through rewiring of photorespiration (Trudeau et al., 2018; South et al., 2019; Wang et al.,

2020; Roell et al., 2021; Jin et al., 2023), engineering of carbon concentration mechanisms (Long et al., 2016; Long et al., 2018; Mackinder, 2018; Atkinson et al., 2020; Hennacy and Jonikas, 2020; Adler et al., 2022) or cutting respiratory carbon losses (Long et al., 2015; Amthor et al., 2019; Garcia et al., 2023). One of the strategies with the highest potential consists in engineering redesigned or synthetic CO_2 fixation pathways (Long et al., 2015). In the light, the photosynthetic electron transfer (PET) chain produces both energy (ATP) and reducing power (NADPH), which are mainly used by the Calvin-Benson-Bassham cycle (CBBC) to fix atmospheric CO_2 thereby generating triose phosphate as an immediate product (Vecchi et al., 2020; Raines, 2022). The CBBC comprises 11 enzymes catalyzing 13 reactions and three enzymes are specific to the cycle: ribulose-1,5-bisphosphate carboxylase oxygenase (Rubisco), sedoheptulose-1,7-bisphosphatase (SBPase) and phosphoribulokinase (PRK) (Michelet et al., 2013; Le Moigne et al., 2023; Meloni et al., 2023).

Limitations in photosynthetic light conversion efficiency can be directly attributed to kinetic bottlenecks within the CBBC (Stitt et al., 2010; Raines, 2011). At moderate to high light intensities, the slow turnover of the CBBC leads to overreduction of the PET and results in the dissipation of the excess energy as heat, fluorescence or increased production of reactive oxygen species (Marcus et al., 2011; Wobbe and Remacle, 2015). Therefore, improving the CBBC turnover through synthetic biology approaches is a major avenue to enhance photosynthetic efficiency and increase production of biomass and chemicals. An innovative approach would be to replace the natural CBBC by a more efficient artificial synthetic carbon fixation pathway. Several cycles, which are theoretically more efficient than the CBBC have been proposed or even tested *in vitro* but remain to be validated *in vivo* (Bar-Even et al., 2010; Schwander et al., 2016; Bar-Even, 2018; Gleizer et al., 2019; Satanowski et al., 2020).

The green microalga *Chlamydomonas reinhardtii* (hereafter Chlamydomonas) has a photosynthetic apparatus very similar to that of land plants, and our long-term knowledge of its genetics and physiology make it a good model system to study the CBBC (Salome and Merchant, 2019; Le Moigne et al., 2023). Notably, it is able to grow fast either photoautotrophically or heterotrophically in the presence of a reduced carbon source (acetate), allowing growth of photosynthetic mutants. Moreover, Chlamydomonas is a suitable chassis for synthetic biology approaches (Vavitsas et al., 2019). Diverse key enabling technologies are available including a Chlamydomonas modular cloning toolkit comprising 120 bricks allowing fast and easy generation of any multigenic assembly (Crozet et al., 2018; de Carpentier et al., 2020), CRISPR/Cas9 genome editing techniques (Shin et al., 2016; Ferenczi et al., 2017; Greiner et al., 2017; Kim et al., 2020), and a collection of mapped insertional mutants covering 83% of the nuclear genes (Li et al., 2019). Hence, Chlamydomonas appears as a very good chassis to explore *in vivo* the synthetic redesign of the CBBC and its potential to improve biomass and bioproduct production.

Under saturating light, the CBBC is co-limited by the low catalytic efficiency of Rubisco-dependent carboxylation and by the capacity for regeneration of the Rubisco substrate ribulose-1,5-

bisphosphate (RuBP). Strategies for rationally redesigning Rubisco in order to improve its catalytic features or its substrate specificity have generally failed (Kubis and Bar-Even, 2019), although some directed evolution or overexpression strategies were shown to have some potential in several species (Iwaki et al., 2006; Durao et al., 2015; Liang and Lindblad, 2016; 2017; Salesse-Smith et al., 2018; Yoon et al., 2020). Other enzymes also limit CBBC turnover as suggested by modeling and metabolic flux control analyses (Stitt and Schulze, 1994; Raines, 2003; Zhu et al., 2007; Janasch et al., 2019; Raines, 2022). The overexpression of SBPase was shown to improve biomass production and carbon fixation in numerous species (Lefebvre et al., 2005; Tamoi et al., 2006; Rosenthal et al., 2011; Fang et al., 2012; Ding et al., 2016; Liang and Lindblad, 2016; Driever et al., 2017). Similarly, in *Chlamydomonas*, a 3-fold increase of SBPase content increased both photosynthetic rate and growth under high-light and high CO_2 (Hammel et al., 2020). Besides Rubisco and SBPase, the limitations imposed by the third CBBC specific enzyme, PRK, remain largely unexplored. This enzyme catalyzes the phosphorylation of ribulose-5-phosphate into RuBP, the substrate of Rubisco. The biochemical properties of PRK have been extensively studied *in vitro* (Michelet et al., 2013; Le Moigne et al., 2023; Meloni et al., 2023). These studies showed that, *in vitro*, this enzyme is tightly regulated by light through oxidoreduction of specific disulfides by thioredoxins. PRK activity is regulated both autonomously through reduction of an intramolecular disulfide by thioredoxin that couples PRK activity to light intensity, and non-autonomously through formation in the dark of an inhibitory supramolecular complex with the CP12 protein and the CBBC enzyme glyceraldehyde-3-phosphate dehydrogenase (Gurrieri et al., 2021; Gurrieri et al., 2023). The formation and dissociation of the complex is under the control of thioredoxins through reduction of disulfides on CP12 and PRK (Marri et al., 2008; Marri et al., 2009; Thieulin-Pardo et al., 2015). The structure of oxygenic photosynthetic PRK has been solved for Chlamydomonas, *Arabidopsis thaliana*, and *Synechococcus elongatus* (Gurrieri et al., 2019; Wilson et al., 2019; Yu et al., 2020), as well as the structure of the GAPDH-CP12-PRK complex (McFarlane et al., 2019; Yu et al., 2020). Altering the level of PRK in tobacco using antisense RNA approaches revealed that only plants with a PRK activity below 15% showed decreased carbon fixation (Paul et al., 1995; Banks et al., 1999). This suggests that PRK content might not be limiting the CBBC in tobacco although this was not confirmed by measuring PRK protein content or by overexpression of PRK. In Chlamydomonas, a strain lacking PRK activity was reported to be inefficient for photosynthetic carbon fixation (Moll and Levine, 1970) but this mutant was later found to revert spontaneously precluding its use for engineering approaches ((Smith, 2000) and personal observation of the authors).

In the present study, we characterized a PRK knock-out mutant strain and demonstrated that, Chlamydomonas cannot grow photoautotrophically in the absence of PRK, while functional complementation with a synthetic construct allowed the restoration of photoautotrophy. However, using standard genetic elements, PRK expression was limited to 16-40% of the reference level in complemented strains. By improving the design of the transcriptional unit expressing PRK using various combinations of DNA parts, including the endogenous PRK promoter and introns, we overcame this initial limitation. This enabled us to obtain strains with PRK levels comparable to the

reference strain and even overexpressing strains. We generated and characterized a collection of strains with PRK levels between 16% and 250% of WT PRK levels.

2. Materials and Methods

2.1. Strains, media and growth conditions

The strains used in this study originate from the CLiP library (Li et al., 2019): the reference strain (CC-4533) and ΔPRK (LMJ.RY0402.119555), both obtained from the Chlamydomonas Resource Center. Chlamydomonas cells were grown on agar plates or liquid medium, using Tris-acetate-phosphate (TAP) medium (Gorman and Levine, 1965) or High salt medium (HSM) (Sueoka, 1960) at 25°C, under continuous light (40-60 µmol photons m^{-2} s^{-1}) or dark (in particular for the ΔPRK strain), and shaking for liquid cultures (130 rpm). Antibiotics used were hygromycin B (10 µg/mL) and paromomycin (15 µg/mL). Growth analyses were performed in the Algem® labscale double photobioreactor systems (Algenuity, Stewartby, UK) for large volume cultures (400 mL) or in the Algem® HT-24 (Algenuity) photobioreactor for small volume cultures (25 mL). All chemicals were obtained from Sigma-Aldrich unless otherwise specified.

2.2. Plasmid construction

Protein and nucleic acid designs were performed *in silico* using Serial Cloner 2.6.1 software. All recipient plasmids are derived from the MoClo original toolkit (Weber et al., 2011).
Phosphoribulokinase PRK cDNA sequence (Cre12.g554800; Uniprot accession P19824) was obtained by PCR on reverse translated mRNA extracts from a D66 strain (Schnell and Lefebvre, 1993) using primers TTGAAGACTTAATGGCTTTCACTATGCGCGC and TTGAAGACAACGAACCCACGGGCACAACGTCC. The resulting PRK coding sequence was designed for the position B3-B4 of the Chlamydomonas MoClo toolkit (Crozet et al., 2018), and cloned into the plasmid pAGM1287 (Weber et al., 2011). Two other constructs were obtained by PCR on genomic DNA of CC-4533 strain using the following primers:
TTGAAGACTTCTCAGGAGGCCCTGGGCTTTAGCCCC and AAGAAGACAACTCGAGTACATGATGCATGTAACAGCAGCAATGAT for the PRK promoter,
TTGAAGACTTCTCATACTGCGTCTTGGGTCGGTGCGCT and CAGAAGACAACTCGCATTGGTTGCTAACAGCTCGACGC for the PRK 5'UTR, and
TTGAAGACTTCTCAAATGGCTTTCACTATGCGCGC and TTGAAGACTTCTCAAATGGCTTTCACTATGCGCGC for the PRK CDS with introns.
Each part was cloned into the plasmid pAGM9121 (Patron et al., 2015). The level 1 plasmids were built in pICH47742 with the endogenous promoter and 5'UTR of PRK and the 3'UTR/Terminator of PSAD controlling the expression of the PRK CDS with or without its endogenous introns. Level M plasmids were built in pAGM8031 combining p1-013 (hygromycin resistance gene) (de Carpentier et al., 2020) with the PRK transcriptional unit resulting in pCMM-24 (P_{PSAD}-PRK_{CDS}), pCMM-25 (P_{PRK}-PRK_{CDS}) and pCMM-26 (P_{PRK}-$PRK_{(i)}$).

2.3. Chlamydomonas transformation

Transformations were performed as previously described (Crozet et al., 2018), using 55 fmol of purified cassette after *Bbs*I-HF (for photoautotrophy screening with p1 plasmids) or *Bsa*I-HF (for

antibiotic screening with pM plasmids) digestion (New England Biolabs) of the corresponding plasmid. Transformants were selected on HSM-agar medium or TAP-agar containing hygromycin B (20 mg/L), Plates and transformants were analyzed after 5 to 7 days of growth in medium light (50 µmol photons m^{-2} s^{-1}).

2.4. Chlamydomonas genotyping

Cells were grown in TAP medium up to 4-5 x 10^6 cells mL^{-1}, harvested by centrifugation at 2500 *g* for 5 min at room temperature (RT), and lysed in 400 µL of extraction buffer (0.2 M Tris-HCl pH 7.5, 200 mM NaCl; 25 mM EDTA; 0.5% SDS) for 10 min at 37°C under agitation (1400 rpm). After centrifugation at 17000 *g* for 3 min at RT, the genomic DNA contained in the supernatant was precipitated with one volume of isopropanol for 10 min at room temperature and collected by centrifugation at 17000 *g* for 10 min at RT. The pellet DNA was then washed with 70% ethanol, spinned (17000 *g* for 3 min at RT) and the pellet was air-dried prior to resuspension in water. PCR was performed using the Quick-LoadR©Taq2×Master Mix (New England Biolabs) according to the manufacturer's instructions. Primers used were Plex5: AAGGACGCTGACATG, Plm1: CCTGATGGATGGTTC, PLPSAD: TTGAAGACAATCATCTCAATGGGTGTG and Plen3U: AGGTGCCAAAGCAAC.

2.5. Protein extraction

Cells were grown in TAP medium up to 4-5 x 10^6 cells mL^{-1}, harvested by centrifugation at 5000 *g* for 10 min at 4°C, resuspended in 500 µL of Buffer B (30 mM Tris-HCl pH 7.9, 0.5 mM EDTA, antiprotease complete tablets (Roche)), and lysed twice by using glass beads and vortexing (30 sec vortex, 1 min on ice). The total extract was then clarified by centrifugation (2x10 min at 21000 *g*) and the concentration of the total soluble protein was determined by BCA Protein Assay using bovine serum albumin (BSA) as standard.

2.6. Western blot

Total soluble proteins were analyzed by western blotting with a custom rabbit polyclonal primary antibody raised against Chlamydomonas PRK (Covalab, Bron, France) subsequently detected by secondary anti-rabbit antibody coupled to horseradish peroxidase (Sigma-Aldrich reference A9169, Saint Louis, USA). Detection was done with commercial ECL peroxidase assay (GE Healthcare, Chicago IL USA) with a Chemidoc (Bio-Rad, Hercules CA USA).

2.7. Spot tests

Cells were grown until exponential phase (2-6 x 10^6 cells mL^{-1}) and serial dilutions in TAP or HSM media were made. The dilution was spotted (10 µL) onto TAP and HSM agar plates at different light intensities. The plates were then scanned after 7 days using a Perfection V800 Photo scanner (Epson). This analysis was automatized using an Opentrons OT-2.

2.8. Growth analysis in photobioreactor

Growth analyses were performed using the Algem® labscale double photobioreactor system (Algenuity, Stewartby, United Kingdom) under continuous light (100 µmol photons m^{-2} s^{-1}) and 120 rpm agitation in TAP or high salt medium (HSM). The absorbance at 740 nm was recorded every 10 min using the built-in sensor. The maximal growth rate was determined as the maximal slope of the growth curve (ΔAbs/Δtime). Growth curves obtained with the AlgemHT24 photobioreactor were performed in autotrophic conditions and with three different light intensities, *i.e.* low light at 38 µmol.m^{-2}.s^{-1}, medium light at 100 µmol.m^{-2}.s^{-1}, and high light at 300 µmol.m^{-2}.s^{-1}. The resulting growth curves were analyzed using GraphPad Prism software, and in particular a fit was made with the Gompertz growth equation (Y = YM*(Y0/YM)^(exp(-K*X))) to obtain an accurate value of lag phase and µmax, the maximum specific growth rate.

2.9. Enzymatic activity

To eliminate metabolites that could interfere with enzymatic activity measurements, the crude extract was desalted in Sephadex G-25 Columns (GE Healthcare) and reduced with 20 mM DTT in 50 mM Tris-HCl (pH 7.5) for 30 min at 30°C. The PRK activity was measured as previously described (Gurrieri et al., 2019). Briefly, the reaction mixture contained 50 mM Tris-HCl (pH 7.5), 1 mM EDTA, 40 mM KCl, 10 mM $MgCl_2$, 5 U/mL Pyruvate kinase, 6 U/mL Lactate dehydrogenase, 2.5 mM phosphoenolpyruvate, 2 mM ATP, and 0.2 mM NADH. The desalted crude extract was added and the background was recorded for 1-2 min. PRK activity was then measured by adding 0.5 mM ribulose-5-phosphate and monitoring the oxidation of NADH at 340 nm.

3. Results and discussion

3.1. The absence of PRK impacts the growth of Chlamydomonas

Phosphoribulokinase is an enzyme unique to the CBBC encoded by a single gene (Cre12.g554800_4532) in *Chlamydomonas reinhardtii*. To comprehensively investigate the function of the PRK-encoding gene, we used the mutant LMJ.RY0402.119555 (hereafter named ΔPRK) from the Clip Library, generated by random insertion of the paromomycin resistance gene (Li et al., 2019). This mutant strain harbors an insertion (named CIB1) in the exon 7 of the PRK gene (Figure 1A) as identified by junction sequencing with a 95% confidence (Li et al., 2019). In the mutant strain, the position of the CIB insertion in exon 7 was verified by PCR analysis with primer couples allowing specific detection of a single band related to either the WT PRK gene or the disrupted PRK gene containing the CIB1 insertion (Figure 1B). To determine the impact of the CIB1 insertion on PRK protein expression, total protein extracts from the mutant strain and the reference strain were analyzed by western blotting. The PRK signal was very strong in the reference strain, while no signal could be detected in the mutant strain (Figure 1C). To evaluate the detection threshold of our custom made anti-PRK polyclonal antibody, a gradient of total protein from the reference strain CC-4533 was utilized and a PRK signal could be still be detected using 5% of the total protein extract (Figure 1C).

This finding indicates that the mutant strain has a PRK content lower than 5% of that in CC-4533, strongly suggesting that the presence of the CIB insertion disrupts PRK protein expression. Since PRK activity is unique in Chlamydomonas, the absence of the PRK protein should correlate with a loss of the corresponding enzymatic activity. As PRK is activated by reduction (Marri et al., 2008), we treated the total soluble protein extract from each strain with the strong reducing agent DTT to obtain maximal PRK activity. Consistently, no PRK activity was detected in the mutant strain compared to the reference strain (Figure 1D). Consequently, the LMJ.RY0402.119555 strain is a knock-out strain with undetectable levels of both PRK protein and activity.

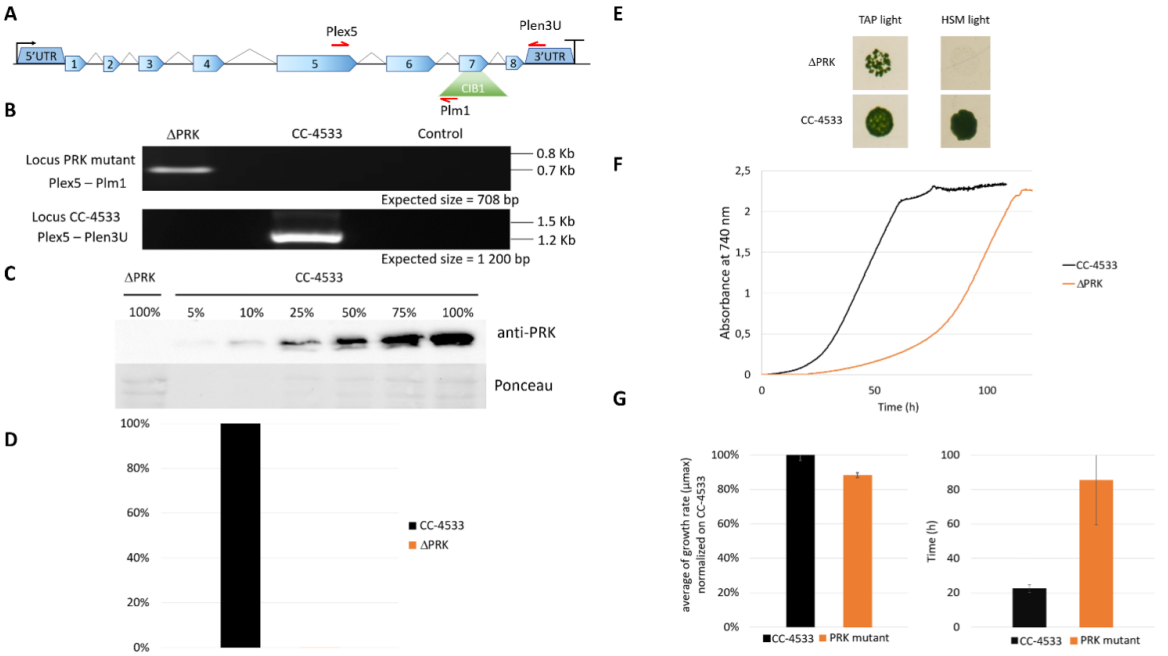

Figure 1: Characterization of the PRK mutant. (A) Representation of the PRK genomic locus in the Clip mutant with the CIB1 insertion (containing the paromomycin resistance gene) positioned in exon 7. (B) PCR on genomic DNA to confirm the presence of the CIB1 insertion in the PRK gene in the mutant strain (Locus PRK mutant) and the presence of the intact PRK locus (Locus CC-4533) in the reference strain. (C) Anti-PRK western blot on total soluble protein extracts of CC-4533 and ΔPRK strains (100% corresponds to 12 µg of total protein). (D) Total activity of reduced PRK. Desalted crude extracts of CC-4533 and ΔPRK were reduced with 20 mM DTT prior to activity measurement. (E) Spot test in TAP and minimal (HSM) media under continuous light (25°C, 100 µmol photons m^{-2} s^{-1}). The reference strain CC-4533 was used as a control. 10^6 cells were spotted and incubated for 7 days prior to observation. (F) Growth profile comparison between ΔPRK and CC-4533. Cultures were inoculated at 10^5 cells/mL and incubated in TAP under light (25°C and 100 µmol photons m^{-2} s^{-1}). (G) Kinetic parameters of growth for ΔPRK and CC-4533 strains, calculated from the data in panel F. Left graph: mean of the maximal growth rate (μ_{max}), Right graph: mean of the lag phase duration. Error bars represent the standard deviation on a biological triplicate. B, C, E and F are one representative experiment out of 3 biological replicates.

To examine the functional consequences of PRK deficiency in Chlamydomonas we analyzed the growth phenotype of the ΔPRK mutant under various conditions. Since PRK is central to the CBBC, we

tested the ability of this mutant to grow in the presence of light and acetate as a carbon source (TAP light, mixotrophic conditions) or in the presence of light in a minimal medium without acetate (HSM light, strictly photoautotrophic conditions). In solid media, the ΔPRK mutant could not grow photoautotrophically but was able to grow in the presence of light and acetate, albeit more slowly than the reference strain (Figure 1E). To further characterize the growth phenotype of the ΔPRK strain in mixotrophic conditions, we monitored its growth over time in a photobioreactor in TAP liquid medium, compared with the CC-4533 reference strain (Figure 1F). The growth profiles revealed a pronounced difference between the two strains. Indeed, the mutant grew much slower than CC-4533, explaining the difference observed on solid media. This growth defect of the PRK mutant is characterized by an extended lag phase (Figure 1G) and a reduced maximum growth rate (μ_{max}) compared to the reference strain (Figure 1G). These data indicate that the ΔPRK strain is non-photoautotrophic and strongly imply that the PRK gene is essential for photosynthetic carbon fixation, and that the absence of the CBBC limits the growth of the knock-out strain. To demonstrate that this phenotype is due to the absence of PRK, we sought to functionally complement the ΔPRK strain.

3.2. Complementation of the *PRK* mutant shows that PRK is essential for photoautotrophy

To verify whether the loss of photoautotrophic growth is due to the absence of PRK in the mutant, we functionally complemented the ΔPRK strain with a synthetic construct designed to restore PRK expression. This construct was built using the intron-less coding sequence (CDS) of the PRK gene, obtained from cDNA, fused to a triple HA tag under the control of the promoter, 5'UTR and 3'UTR/Terminator of PSAD gene. This transcriptional unit was coupled to a hygromycin resistance gene (Figure 2A). The PSAD genetic elements were previously shown to allow strong constitutive expression of a reporter gene (Crozet et al., 2018). The synthetic construct containing the two transcriptional units was introduced into Chlamydomonas nuclear genome by transformation. Multiple clones from the transformation were selected in the light on TAP solid medium supplemented with hygromycin and named C_x, for complemented strain X. The C_x strains were genotyped by PCR using primer couples allowing specific detection of either the CIB insertion characteristic of the ΔPRK strain background or of the synthetic transgene (Figure 2B). All five chosen C_x and the mutant were found to contain the CIB1 insertion confirming the ΔPRK background. All selected clones also displayed the presence of the synthetic PRK transgene that was absent in the ΔPRK strain. We performed anti-PRK western blots to confirm the expression of the transgenic PRK. As shown in Figure 2C, 3xHA tagged PRK, which has a higher molecular weight than endogenous PRK, is present in all C_x complemented strains. In comparison with the gradient of CC-4533 total protein extract, we observed that the expression of the transgenic PRK-3HA is much lower than the endogenous PRK and shows some variability between C_x clones. This may be due to the design of the synthetic PRK construct and/or to position effects due to insertion of the transgene in distinct genomic sites.

If the loss of PRK in the mutant is responsible for its growth phenotype, a functional complementation restoring photoautotrophic growth in minimal medium should be observed in the C_x strains. The growth phenotype of the different strains was assessed using a spot test analysis on solid media (Figure 2D).

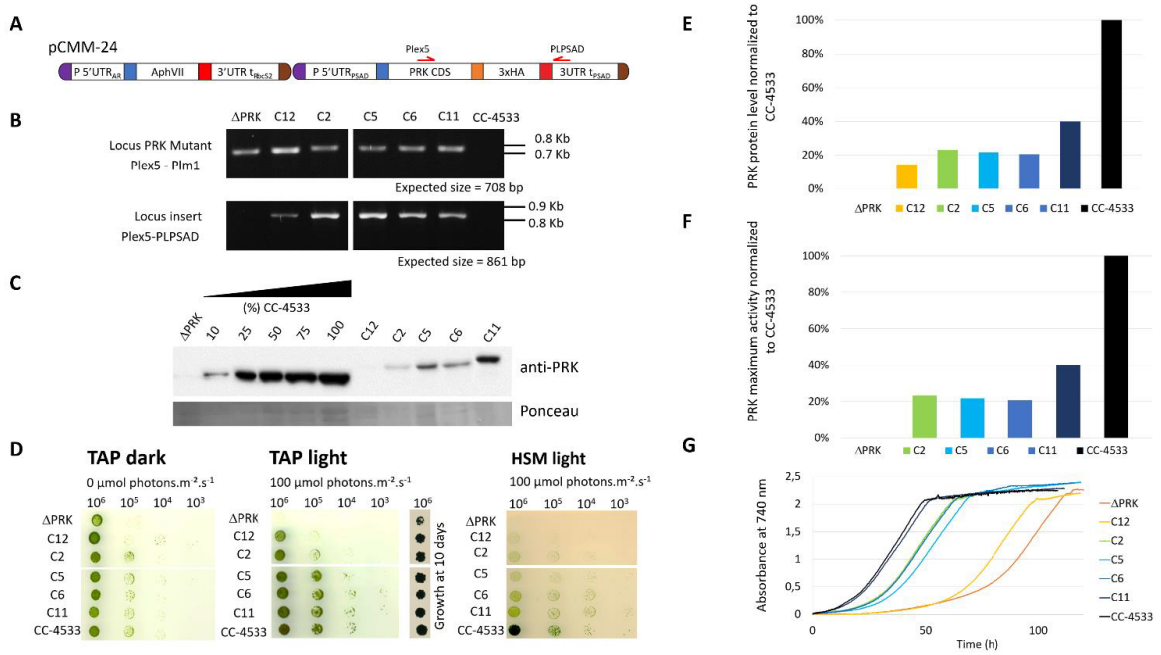

Figure 2: Functional complementation of the PRK mutant. (A) Design of the pCMM-24 construct used for PRK mutant complementation. (B) PCR on genomic DNA to confirm the presence of the CIB1 insertion in the PRK gene in the ΔPRK strain (Locus PRK mutant) and the presence of the pCMM-24 insertion in the complemented strains (Locus insert) in the complemented strains (C_x strains). (C) Anti-PRK western blot on total soluble protein extracts of the CC-4533, ΔPRK and C_x strains (100% corresponds to 12 µg of total protein). (D) Spot test in TAP and HSM minimal media after 5 days growth at 25°C in the dark or in the light (100 µmol photons m^{-2} s^{-1}). The number of cells spotted is indicated above the spot test image. To show the growth of the ΔPRK strain in TAP light conditions, the growth after 10 days is shown. (E) Relative quantification of the PRK protein content in the C_x strains compared to CC-4533, calculated from the data in panel C. (F) Total activity of reduced PRK in the different strains. Desalted crude extracts of WT, C_x and ΔPRK were reduced with 20 mM DTT prior to activity measurement. (G) Growth profile of selected strains. Cultures were inoculated at 10^5 cells/mL and incubated in TAP under light (25°C and 100 µmol photons m^{-2} s^{-1}).

In TAP medium in the dark, Chlamydomonas grows heterotrophically and all C_x strains grew like the reference strain. In TAP medium in the light, the complemented strains C_x grew similarly to CC-4533 although C_{12} appeared to grow significantly more slowly. By contrast the ΔPRK strain grew much more slowly than all other strains, as shown previously (Figure 1E). Nevertheless, after 10 days the growth the ΔPRK strain was clearly visible (Figure 2D). In HSM medium in the light, a restoration of the photoautotrophic growth was observed in the C_x strains. This demonstrates that PRK is essential for photoautotrophy in Chlamydomonas. However, the growth of C_x strains appeared slower compared to CC-4533 suggesting a partial functional complementation. To assess whether this phenotype was caused by a lower level of PRK protein, the relative quantity of PRK expressed in the complemented

strains was determined. All the C_x strains showed a relatively low expression of the PRK enzyme, with a maximum of 40% of the PRK content compared to the reference strain (Figure 2E). The C_{12} strain that has a barely detectable level of PRK still partially restored photoautotrophy. PRK activity measurements fully correlated with the PRK levels estimated by western blot (Figure 2F). To quantitatively assess the growth limitation imposed by decreased PRK contents, we performed growth kinetics in a controlled photobioreactor. The C_x strains grew in TAP liquid medium in accordance with their PRK content (Figure 2G), as observed in the spot test assays (Figure 2D). Importantly, the strain with 40% of PRK content (C_{11}) behaved as the reference strain in TAP medium but not in minimal medium (Figure 2D). This suggests that 40% of PRK content compared to the reference strain is limiting the CBBC in Chlamydomonas. In tobacco, the content of PRK leading to a phenotype was below 15% of the reference (Paul et al., 1995; Banks et al., 1999). Therefore, the excess of PRK may be more limited in Chlamydomonas than in tobacco. In order to determine more precisely the PRK content limiting the CBBC and to test whether overexpression of PRK may increase the CBBC turnover, a higher level of expression of the transgene needs to be achieved.

Although position effect may account for the variations observed between transformants, the limitation is more likely due to the design of the synthetic transgene (Figure 2A). Indeed, we screened hundreds of transformants and never found any clone with a PRK level above 40% of the level of the endogenous PRK, as exemplified in Figure 2. This suggested that the genetic elements controlling PRK expression may not be appropriate to ensure an expression level comparable to the reference strain.

3.3. New synthetic construct designs for enhanced PRK expression

The limitation to about 40% of the protein level found in the reference strain when expressing PRK from the synthetic construct may stem from various factors. PRK, like numerous other CBBC enzymes, is highly abundant and is estimated to represent 0.25% of total cellular proteins in Chlamydomonas (Hammel et al., 2020). Although the strong constitutive PSAD promoter and 5'UTR were employed to drive PRK expression in the synthetic pCMM-24 construct, it is plausible that the endogenous PRK promoter is significantly stronger and would ensure a higher expression level. The absence of introns in the synthetic gene may also be partly responsible for the low expression. Indeed, it is now well-established that the presence of introns in the synthetic construct is frequently required to ensure high-level expression of a transgene in Chlamydomonas (Lumbreras and Purton, 1998; Fuhrmann et al., 1999; Baier et al., 2018). The presence of introns could boost gene expression due to the presence of a transcriptional enhancer, through a process called Intron-mediated enhancement that stimulates directly transcription or through interaction with the spliceosome (Schroda, 2019; Baier et al., 2020). An online tool has been developed to design Chlamydomonas transgenes with artificial introns (Jaeger et al., 2019). The fusion of the recombinant PRK with a triple HA-tag may also impact expression, potentially by destabilizing the protein or affecting its activity.

To investigate the significance of the promoter strength and of the presence of introns we have designed new synthetic constructs that incorporate the endogenous PRK promoter and its 5'UTR to

drive either expression of the PRK CDS devoid of introns and also lacking triple HA-tag or the native PRK coding sequence containing natural introns (Figure 3A). The PRK promoter and the native PRK gene coding sequences were amplified by PCR from Chlamydomonas CC-4533 genomic DNA and cloned as level 0 MoClo parts. These parts were then used to build the two transcriptional units later on coupled to the hygromycin resistance gene to generate pCMM-25 and pCMM-26 (Figure 3A). Each of these synthetic constructs were introduced in the nuclear genome of the ΔPRK strain. The original synthetic gene (pCMM-24) containing the PSAD promoter and PRK CDS was also transformed again in the ΔPRK strain as a control. The transformants were selected on photoautotrophic growth restoration in minimal medium. It was observed that more colonies were obtained for transformations with pCMM-26 than with pCMM-25 or pCMM-24, suggesting that the presence of introns had a positive effect on the number of functionally complemented strains. For each transformation, roughly 50 colonies were selected for further analysis.

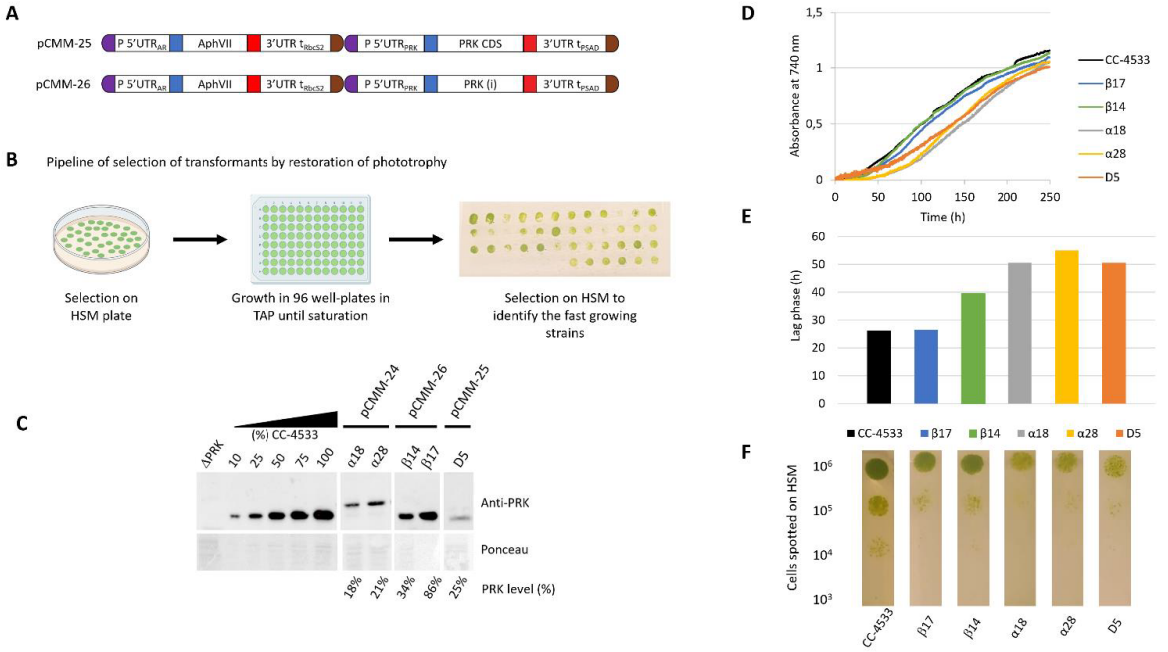

Figure 3. New designs to achieve higher PRK expression. (A) Design of the pCMM-25 and pCMM-26 constructs. (B) Pipeline for the identification of strains with high PRK content by selection of transformants on HSM plates, followed by growth to saturation in 96-well plates in TAP medium, and re-plating on HSM agar plates. The strains with the fastest growth on the plate were selected for further analysis. (C) Anti-PRK western blot on total soluble protein extracts of the ΔPRK, CC-4533, and complemented strains obtained by transforming the ΔPRK strain with the pCMM-24 (α strains), pCMM-26 (β strains) or pCMMM-25 (D5 strain) constructs. 100% corresponds to 12 µg of total protein. A gradient of the total protein extract of the strain CC-4533 was used for the quantification of the PRK content in the different complemented strains, indicated as PRK level (%). (D) Growth profile of CC-4533 and complemented strains. Cultures were inoculated at 10^5 cells/mL and incubated in HSM at 25°C under continuous light (100 µmol photons m^{-2} s^{-1}). (E) Lag phase measured for CC-4533 and complemented strains, calculated from the data in panel D. (F) Spot test on HSM minimal medium after 5 days of growth at 25°C in the light (50 µmol photons m^{-2} s^{-1}). The number of cells spotted is indicated on the left and the strain is indicated below each spot test line.

As we previously observed with the first synthetic construct that in the ΔPRK background cell growth is directly correlated with PRK expression level (Figure 2), we selected the fastest growers to increase the probability to select strains with higher PRK levels through spot test assays on HSM medium after growth to saturation in TAP medium (Figure 3B). For several representative fast growers, we analyzed the PRK content by immunoblot (Figure 3C) and the growth properties in liquid HSM medium in a photobioreactor (Figure 3D, 3E) or in solid HSM medium (Figure 3F). As previously shown (Figure 2), the pCMM-24 construct (α strains) only allowed partial complementation of the ΔPRK phenotype. The level of PRK was limited to 21% in the best case and photoautotrophic growth was only partially restored compared to CC-4533. Comparable results were obtained with the pCMM-25 construct as exemplified by the best growing strain D5 which PRK level was limited to 25% of the reference strain CC-4533 and consistently showed partial complementation of photoautotrophic growth. This indicates that neither the expression without the triple-HA tag nor the use of the PRK promoter to drive PRK CDS expression resulted in increased PRK expression level. Conversely, the pCMM-26 construct expressing the intron-containing PRK endogenous coding sequence allowed to fully complement the phenotype of the ΔPRK strain (Figure 3) and even overexpress the protein (Figure 4). This indicates that the presence of introns in the PRK coding sequence is crucial for high level expression of the transgene. This result is consistent with previous studies (Lumbreras and Purton, 1998; Fuhrmann et al., 1999; Baier et al., 2018; Lauersen et al., 2018; Schroda, 2019; Baier et al., 2020). It would be interesting in future studies to determine whether the high-level expression is linked to a specific PRK intron. Even with the pCMM-26 intron containing construct, a range of PRK expression levels (34%-250% relative to CC-4533) was observed in the transformants. This variability is most likely attributable to random insertion of the construct in regions of the genome with a variable ability to drive gene expression. This position effect is classically observed in Chlamydomonas and can be exploited to generate strains with diverse levels of expression of a given transgene. In our case, immunoblot and growth assays revealed that a PRK content of 86% is sufficient to fully restore photoautotrophic growth with kinetics comparable to the reference strain CC-4533 (Figure 3). This result suggests that PRK may be present in excess in Chlamydomonas. Nevertheless, this excess appears much more limited than previously reported in tobacco where PRK limitation was only observed below 15% of the WT level (Paul et al., 1995; Banks et al., 1999). To confirm that PRK endogenous level does not limit the CBBC we analyzed strains overexpressing PRK.

3.4. Overexpression of PRK does not affect cell growth

To analyze the impact of PRK overexpression in Chlamydomonas, we examined strains transformed with the pCMM-26 construct either in the ΔPRK or the CC-4533 backgrounds (Figure 4A). The growth of strains overexpressing PRK 1.5-fold (A2 strain) or 2.5-fold (β3 strain) (Figure 4B) was analyzed in a photobioreactor in liquid HSM medium under three different light intensities (Figure 4C-E). Strains expressing 100% (CC-4533) or 25% (D5) of PRK were used as controls. The growth of the two overexpressor strains was comparable to the CC-4533 strain. At high light intensity (300 µmol m^{-2} s^{-1}) growth of the overexpressor was similar to CC-4533 while at lower light intensities the 1.5-fold

overexpressor showed a marginally slower growth kinetics compared to the two other strains. The cause of this slower growth in low light of the A2 strain is not known but could be related to the site of insertion of the transgene. Nonetheless, these results clearly show that overexpression of PRK does not lead to an increased growth. This suggests that the endogenous level of PRK in Chlamydomonas is not limiting the Calvin-Benson-Bassham cycle under optimal growth conditions.

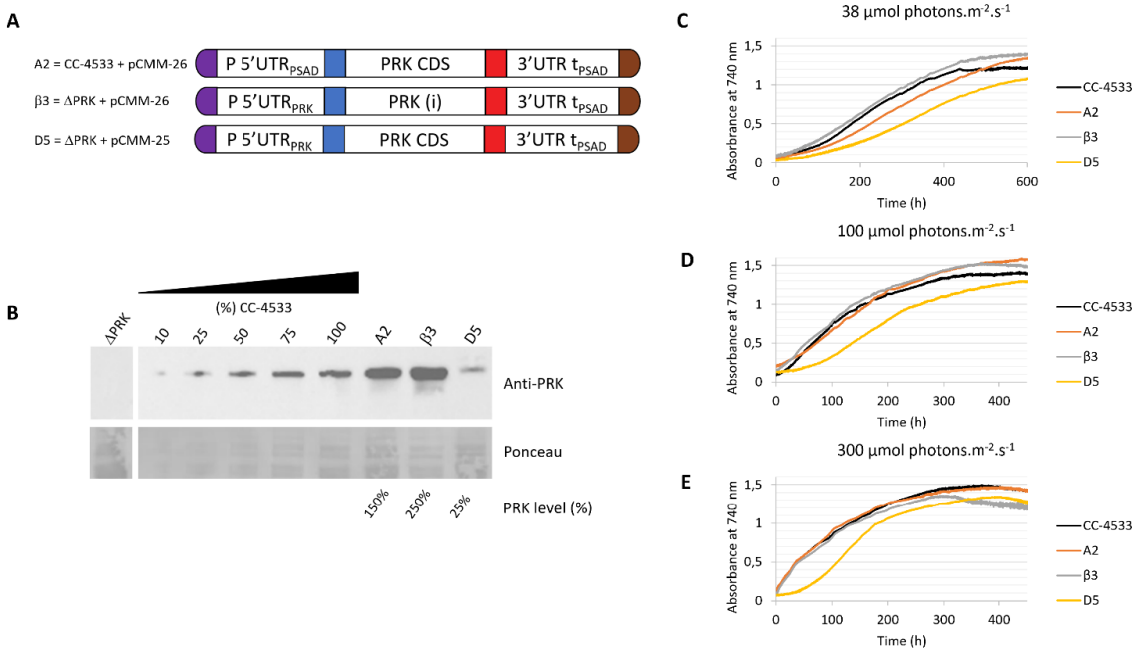

Figure 4. Overexpression of PRK. (A) Design of the transgene driving PRK expression and the genetic background (ΔPRK or CC-4533) for the A2, β3 and D5 strains (B) Anti-PRK western blot on total soluble protein extracts of the ΔPRK, CC-4533, and transformed strains as indicated. 100% corresponds to 12 µg of total protein. A gradient of the total protein extract of the strain CC-4533 was used for the quantification of the PRK content in the different complemented strains, indicated as PRK level (%). (C), (D), (E) Growth curves of CC-4533 and transformed strains. Cultures were inoculated at 10^5 cells/mL and incubated in HSM at 25°C under three distinct light intensities as indicated.

4. Conclusions

In the present study, we have characterized a PRK knock-out mutant of Chlamydomonas and utilized this strain to investigate the limitations imposed by PRK expression level on the CBBC. We demonstrated that PRK is essential for photosynthesis in *C. reinhardtii* through a comprehensive analysis of the mutant and its functional complementation. The essentiality of PRK for photoautotrophic growth was previously suggested by a large-scale systematic characterization of gene function in Chlamydomonas (Fauser et al., 2022). Previously, the only analyses of PRK deficiency in Chlamydomonas were obtained in the F-60 mutant generated by chemical mutagenesis and without a full validation by functional complementation (Moll and Levine, 1970). This mutant was also shown to spontaneously revert ((Smith, 2000) and personal observation of the authors). Through our functional complementation approach, we demonstrated that the level of PRK protein needs to

be as high as 86% of the level of the reference strain to allegedly restore the standard growth phenotype. Moreover, we established that, in the conditions tested, overexpression of PRK does not improve Chlamydomonas growth. This suggests that the endogenous PRK content is not limiting the CBBC in *Chlamydomonas reinhardtii*. PRK is therefore in excess in Chlamydomonas but this excess is much more limited than observed in tobacco where PRK limitation was only observed below 15% of the WT level (Paul et al., 1995; Banks et al., 1999). This implies that a slight decrease of PRK level or PRK activity would be sufficient to limit the CBBC in Chlamydomonas. This may allow PRK to play a more prominent role in the control of the CBBC turnover in Chlamydomonas, for example under conditions leading to light-dependent regulation of PRK activity mediated by thioredoxins and CP12 (Gurrieri et al., 2021; Gurrieri et al., 2023). Nevertheless, the CBBC functioning is different in algae compared to land plants, particularly because a carbon-concentration mechanism (CCM) in the pyrenoid increases carbon fixation by Rubisco (Barrett et al., 2021) and likely imposes a stronger requirement for RuBP production by PRK to sustain growth, especially in non-limiting light conditions. Metabolite profiling revealed that RuBP is indeed significantly more concentrated in algae and cyanobacteria compared to land plants (Clapero et al., 2023). This higher concentration of RuBP may be required to ensure that substantial concentration gradients drive rapid diffusion into the CCM compartment that houses Rubisco (Treves et al., 2022). Finally, the PRK knock-out strain along with the genetic elements we have generated may constitute useful tools to explore PRK regulation *in vivo* using functional complementation with PRK variants harboring targeted mutations such as mutations to serine/alanine of regulatory cysteines.

5. Conflict of Interest

All authors declare that the research was conducted in the absence of any commercial or financial relationships that could be construed as a potential conflict of interest.

6. Author Contributions

NDB, GF, MM, MZ, SDL and PC designed the study and analyzed the data. NDB, GF, MM, MZ, CCC, SDL and PC discussed and wrote the manuscript. NDB, GF, MM, LJ and PC performed the experiments.

7. Funding

This research and the article processing charges were funded by Centre National de la Recherche Scientifique, Sorbonne Université, Université Paris-Saclay and Agence Nationale de la Recherche grant CALVINDESIGN (ANR-17-CE05-001).

8. Acknowledgments

We thank Ferdinand Meneau, Dr Théo Le Moigne, Dr. Christophe Marchand, Dr Antoine Danon, and Dr. Julien Henri for stimulating discussions and suggestions.

9. References

Adler, L., Diaz-Ramos, A., Mao, Y., Pukacz, K.R., Fei, C., and McCormick, A.J. (2022). New horizons for building pyrenoid-based CO2-concentrating mechanisms in plants to improve yields. *Plant Physiol* 190(3), 1609-1627. doi: 10.1093/plphys/kiac373.

Amthor, J.S., Bar-Even, A., Hanson, A.D., Millar, A.H., Stitt, M., Sweetlove, L.J., et al. (2019). Engineering Strategies to Boost Crop Productivity by Cutting Respiratory Carbon Loss. *Plant Cell* 31(2), 297-314. doi: 10.1105/tpc.18.00743.

Atkinson, N., Mao, Y., Chan, K.X., and McCormick, A.J. (2020). Condensation of Rubisco into a proto-pyrenoid in higher plant chloroplasts. *Nat Commun* 11(1), 6303. doi: 10.1038/s41467-020-20132-0.

Baier, T., Jacobebbinghaus, N., Einhaus, A., Lauersen, K.J., and Kruse, O. (2020). Introns mediate post-transcriptional enhancement of nuclear gene expression in the green microalga Chlamydomonas reinhardtii. *PLoS Genet* 16(7), e1008944. doi: 10.1371/journal.pgen.1008944.

Baier, T., Wichmann, J., Kruse, O., and Lauersen, K.J. (2018). Intron-containing algal transgenes mediate efficient recombinant gene expression in the green microalga Chlamydomonas reinhardtii. *Nucleic Acids Res* 46(13), 6909-6919. doi: 10.1093/nar/gky532.

Banks, F.M., Driscoll, S.P., Parry, M.A., Lawlor, D.W., Knight, J.S., Gray, J.C., et al. (1999). Decrease in phosphoribulokinase activity by antisense RNA in transgenic tobacco. Relationship between photosynthesis, growth, and allocation at different nitrogen levels. *Plant Physiol* 119(3), 1125-1136. doi: 10.1104/pp.119.3.1125.

Bar-Even, A. (2018). Daring metabolic designs for enhanced plant carbon fixation. *Plant Sci* 273, 71-83. doi: 10.1016/j.plantsci.2017.12.007.

Bar-Even, A., Noor, E., Lewis, N.E., and Milo, R. (2010). Design and analysis of synthetic carbon fixation pathways. *Proc Natl Acad Sci U S A* 107(19), 8889-8894. doi: 10.1073/pnas.0907176107.

Barrett, J., Girr, P., and Mackinder, L.C.M. (2021). Pyrenoids: CO(2)-fixing phase separated liquid organelles. *Biochim Biophys Acta Mol Cell Res* 1868(5), 118949. doi: 10.1016/j.bbamcr.2021.118949.

Clapero, V., Arrivault, S., and Stitt, M. (2023). Natural variation in metabolism of the Calvin-Benson cycle. *Semin Cell Dev Biol*. doi: 10.1016/j.semcdb.2023.02.015.

Crozet, P., Navarro, F.J., Willmund, F., Mehrshahi, P., Bakowski, K., Lauersen, K.J., et al. (2018). Birth of a Photosynthetic Chassis: A MoClo Toolkit Enabling Synthetic Biology in the Microalga Chlamydomonas reinhardtii. *ACS Synth Biol* 7(9), 2074-2086. doi: 10.1021/acssynbio.8b00251.

da Fonseca-Pereira, P., Siqueira, J.A., Monteiro-Batista, R.C., Vaz, M., Nunes-Nesi, A., and Araujo, W.L. (2022). Using synthetic biology to improve photosynthesis for sustainable food production. *J Biotechnol* 359, 1-14. doi: 10.1016/j.jbiotec.2022.09.010.

de Carpentier, F., Le Peillet, J., Boisset, N.D., Crozet, P., Lemaire, S.D., and Danon, A. (2020). Blasticidin S Deaminase: A New Efficient Selectable Marker for Chlamydomonas reinhardtii. *Front Plant Sci* 11, 242. doi: 10.3389/fpls.2020.00242.

Ding, F., Wang, M., Zhang, S., and Ai, X. (2016). Changes in SBPase activity influence photosynthetic capacity, growth, and tolerance to chilling stress in transgenic tomato plants. *Sci Rep* 6, 32741. doi: 10.1038/srep32741.

Driever, S.M., Simkin, A.J., Alotaibi, S., Fisk, S.J., Madgwick, P.J., Sparks, C.A., et al. (2017). Increased SBPase activity improves photosynthesis and grain yield in wheat grown in greenhouse conditions. *Philos Trans R Soc Lond B Biol Sci* 372(1730). doi: 10.1098/rstb.2016.0384.

Durao, P., Aigner, H., Nagy, P., Mueller-Cajar, O., Hartl, F.U., and Hayer-Hartl, M. (2015). Opposing effects of folding and assembly chaperones on evolvability of Rubisco. *Nat Chem Biol* 11(2), 148-155. doi: 10.1038/nchembio.1715.

Eckardt, N.A., Ainsworth, E.A., Bahuguna, R.N., Broadley, M.R., Busch, W., Carpita, N.C., et al. (2023). Climate change challenges, plant science solutions. *Plant Cell* 35(1), 24-66. doi: 10.1093/plcell/koac303.

Erb, T.J., and Zarzycki, J. (2016). Biochemical and synthetic biology approaches to improve photosynthetic CO2-fixation. *Curr Opin Chem Biol* 34, 72-79. doi: 10.1016/j.cbpa.2016.06.026.

Fang, L., Lin, H.X., Low, C.S., Wu, M.H., Chow, Y., and Lee, Y.K. (2012). Expression of the Chlamydomonas reinhardtii sedoheptulose-1,7-bisphosphatase in Dunaliella bardawil leads to enhanced photosynthesis and increased glycerol production. *Plant Biotechnol J* 10(9), 1129-1135. doi: 10.1111/pbi.12000.

Fauser, F., Vilarrasa-Blasi, J., Onishi, M., Ramundo, S., Patena, W., Millican, M., et al. (2022). Systematic characterization of gene function in the photosynthetic alga Chlamydomonas reinhardtii. *Nat Genet* 54(5), 705-714. doi: 10.1038/s41588-022-01052-9.

Ferenczi, A., Pyott, D.E., Xipnitou, A., and Molnar, A. (2017). Efficient targeted DNA editing and replacement in Chlamydomonas reinhardtii using Cpf1 ribonucleoproteins and single-stranded DNA. *Proc Natl Acad Sci U S A* 114(51), 13567-13572. doi: 10.1073/pnas.1710597114.

Fuhrmann, M., Oertel, W., and Hegemann, P. (1999). A synthetic gene coding for the green fluorescent protein (GFP) is a versatile reporter in Chlamydomonas reinhardtii. *Plant J* 19(3), 353-361. doi: 10.1046/j.1365-313x.1999.00526.x.

Garcia, A., Gaju, O., Bowerman, A.F., Buck, S.A., Evans, J.R., Furbank, R.T., et al. (2023). Enhancing crop yields through improvements in the efficiency of photosynthesis and respiration. *New Phytol* 237(1), 60-77. doi: 10.1111/nph.18545.

Gleizer, S., Ben-Nissan, R., Bar-On, Y.M., Antonovsky, N., Noor, E., Zohar, Y., et al. (2019). Conversion of Escherichia coli to Generate All Biomass Carbon from CO(2). *Cell* 179(6), 1255-1263 e1212. doi: 10.1016/j.cell.2019.11.009.

Godfray, H.C., Beddington, J.R., Crute, I.R., Haddad, L., Lawrence, D., Muir, J.F., et al. (2010). Food security: the challenge of feeding 9 billion people. *Science* 327(5967), 812-818. doi: 10.1126/science.1185383.

Gorman, D.S., and Levine, R.P. (1965). Cytochrome f and plastocyanin: their sequence in the photosynthetic electron transport chain of Chlamydomonas reinhardi. *Proc Natl Acad Sci U S A* 54(6), 1665-1669. doi: 10.1073/pnas.54.6.1665.

Greiner, A., Kelterborn, S., Evers, H., Kreimer, G., Sizova, I., and Hegemann, P. (2017). Targeting of Photoreceptor Genes in Chlamydomonas reinhardtii via Zinc-Finger Nucleases and CRISPR/Cas9. *Plant Cell* 29(10), 2498-2518. doi: 10.1105/tpc.17.00659.

Gurrieri, L., Del Giudice, A., Demitri, N., Falini, G., Pavel, N.V., Zaffagnini, M., et al. (2019). Arabidopsis and Chlamydomonas phosphoribulokinase crystal structures complete the redox structural proteome of the Calvin-Benson cycle. *Proc Natl Acad Sci U S A* 116(16), 8048-8053. doi: 10.1073/pnas.1820639116.

Gurrieri, L., Fermani, S., Zaffagnini, M., Sparla, F., and Trost, P. (2021). Calvin-Benson cycle regulation is getting complex. *Trends Plant Sci* 26(9), 898-912. doi: 10.1016/j.tplants.2021.03.008.

Gurrieri, L., Sparla, F., Zaffagnini, M., and Trost, P. (2023). Dark complexes of the Calvin-Benson cycle in a physiological perspective. *Semin Cell Dev Biol*. doi: 10.1016/j.semcdb.2023.03.002.

Hammel, A., Sommer, F., Zimmer, D., Stitt, M., Muhlhaus, T., and Schroda, M. (2020). Overexpression of Sedoheptulose-1,7-Bisphosphatase Enhances Photosynthesis in Chlamydomonas reinhardtii and Has No Effect on the Abundance of Other Calvin-Benson Cycle Enzymes. *Front Plant Sci* 11, 868. doi: 10.3389/fpls.2020.00868.

Hennacy, J.H., and Jonikas, M.C. (2020). Prospects for Engineering Biophysical CO(2) Concentrating Mechanisms into Land Plants to Enhance Yields. *Annu Rev Plant Biol* 71, 461-485. doi: 10.1146/annurev-arplant-081519-040100.

Iwaki, T., Haranoh, K., Inoue, N., Kojima, K., Satoh, R., Nishino, T., et al. (2006). Expression of foreign type I ribulose-1,5-bisphosphate carboxylase/ oxygenase (EC 4.1.1.39) stimulates photosynthesis in cyanobacterium Synechococcus PCC7942 cells. *Photosynth Res* 88(3), 287-297. doi: 10.1007/s11120-006-9048-x.

Jaeger, D., Baier, T., and Lauersen, K.J. (2019). Intronserter, an advanced online tool for design of intron containing transgenes. *Algal Research* 42, 101588. doi: https://doi.org/10.1016/j.algal.2019.101588.

Janasch, M., Asplund-Samuelsson, J., Steuer, R., and Hudson, E.P. (2019). Kinetic modeling of the Calvin cycle identifies flux control and stable metabolomes in Synechocystis carbon fixation. *J Exp Bot* 70(3), 973-983. doi: 10.1093/jxb/ery382.

Jin, K., Chen, G., Yang, Y., Zhang, Z., and Lu, T. (2023). Strategies for manipulating Rubisco and creating photorespiratory bypass to boost C(3) photosynthesis: Prospects on modern crop improvement. *Plant Cell Environ* 46(2), 363-378. doi: 10.1111/pce.14500.

Kim, J., Lee, S., Baek, K., and Jin, E. (2020). Site-Specific Gene Knock-Out and On-Site Heterologous Gene Overexpression in Chlamydomonas reinhardtii via a CRISPR-Cas9-Mediated Knock-in Method. *Front Plant Sci* 11, 306. doi: 10.3389/fpls.2020.00306.

Kubis, A., and Bar-Even, A. (2019). Synthetic biology approaches for improving photosynthesis. *J Exp Bot* 70(5), 1425-1433. doi: 10.1093/jxb/erz029.

Lauersen, K.J., Wichmann, J., Baier, T., Kampranis, S.C., Pateraki, I., Moller, B.L., et al. (2018). Phototrophic production of heterologous diterpenoids and a hydroxy-functionalized derivative from Chlamydomonas reinhardtii. *Metab Eng* 49, 116-127. doi: 10.1016/j.ymben.2018.07.005.

Le Moigne, T., Boisset, N.D., de Carpentier, F., Crozet, P., Danon, A., Henri, J., et al. (2023). "Chapter 8 - Photoproduction of reducing power and the Calvin-Benson cycle," in *The Chlamydomonas Sourcebook (Third Edition),* eds. A.R. Grossman & F.-A. Wollman. (London: Academic Press), 273-315.

Lefebvre, S., Lawson, T., Zakhleniuk, O.V., Lloyd, J.C., Raines, C.A., and Fryer, M. (2005). Increased sedoheptulose-1,7-bisphosphatase activity in transgenic tobacco plants stimulates photosynthesis and growth from an early stage in development. *Plant Physiol* 138(1), 451-460. doi: 10.1104/pp.104.055046.

Li, X., Patena, W., Fauser, F., Jinkerson, R.E., Saroussi, S., Meyer, M.T., et al. (2019). A genome-wide algal mutant library and functional screen identifies genes required for eukaryotic photosynthesis. *Nat Genet* 51(4), 627-635. doi: 10.1038/s41588-019-0370-6.

Liang, F., and Lindblad, P. (2016). Effects of overexpressing photosynthetic carbon flux control enzymes in the cyanobacterium Synechocystis PCC 6803. *Metab Eng* 38, 56-64. doi: 10.1016/j.ymben.2016.06.005.

Liang, F., and Lindblad, P. (2017). Synechocystis PCC 6803 overexpressing RuBisCO grow faster with increased photosynthesis. *Metab Eng Commun* 4, 29-36. doi: 10.1016/j.meteno.2017.02.002.

Long, B.M., Hee, W.Y., Sharwood, R.E., Rae, B.D., Kaines, S., Lim, Y.L., et al. (2018). Carboxysome encapsulation of the CO(2)-fixing enzyme Rubisco in tobacco chloroplasts. *Nat Commun* 9(1), 3570. doi: 10.1038/s41467-018-06044-0.

Long, B.M., Rae, B.D., Rolland, V., Forster, B., and Price, G.D. (2016). Cyanobacterial CO2-concentrating mechanism components: function and prospects for plant metabolic engineering. *Curr Opin Plant Biol* 31, 1-8. doi: 10.1016/j.pbi.2016.03.002.

Long, S.P., Marshall-Colon, A., and Zhu, X.G. (2015). Meeting the global food demand of the future by engineering crop photosynthesis and yield potential. *Cell* 161(1), 56-66. doi: 10.1016/j.cell.2015.03.019.

Long, S.P., Zhu, X.G., Naidu, S.L., and Ort, D.R. (2006). Can improvement in photosynthesis increase crop yields? *Plant Cell Environ* 29(3), 315-330.

Lumbreras, V., and Purton, S. (1998). Recent advances in chlamydomonas transgenics. *Protist* 149(1), 23-27. doi: 10.1016/S1434-4610(98)70006-9.

Mackinder, L.C.M. (2018). The Chlamydomonas CO(2) -concentrating mechanism and its potential for engineering photosynthesis in plants. *New Phytol* 217(1), 54-61. doi: 10.1111/nph.14749.

Marcus, Y., Altman-Gueta, H., Wolff, Y., and Gurevitz, M. (2011). Rubisco mutagenesis provides new insight into limitations on photosynthesis and growth in Synechocystis PCC6803. *J Exp Bot* 62(12), 4173-4182. doi: 10.1093/jxb/err116.

Marri, L., Trost, P., Trivelli, X., Gonnelli, L., Pupillo, P., and Sparla, F. (2008). Spontaneous assembly of photosynthetic supramolecular complexes as mediated by the intrinsically unstructured protein CP12. *J Biol Chem* 283(4), 1831-1838. doi: 10.1074/jbc.M705650200.

Marri, L., Zaffagnini, M., Collin, V., Issakidis-Bourguet, E., Lemaire, S.D., Pupillo, P., et al. (2009). Prompt and easy activation by specific thioredoxins of calvin cycle enzymes of Arabidopsis thaliana associated in the GAPDH/CP12/PRK supramolecular complex. *Mol Plant* 2(2), 259-269. doi: 10.1093/mp/ssn061.

McFarlane, C.R., Shah, N.R., Kabasakal, B.V., Echeverria, B., Cotton, C.A.R., Bubeck, D., et al. (2019). Structural basis of light-induced redox regulation in the Calvin-Benson cycle in cyanobacteria. *Proc Natl Acad Sci U S A* 116(42), 20984-20990. doi: 10.1073/pnas.1906722116.

Meloni, M., Gurrieri, L., Fermani, S., Velie, L., Sparla, F., Crozet, P., et al. (2023). Ribulose-1,5-bisphosphate regeneration in the Calvin-Benson-Bassham cycle: Focus on the last three enzymatic steps that allow the formation of Rubisco substrate. *Front Plant Sci* 14, 1130430. doi: 10.3389/fpls.2023.1130430.

Michelet, L., Zaffagnini, M., Morisse, S., Sparla, F., Perez-Perez, M.E., Francia, F., et al. (2013). Redox regulation of the Calvin-Benson cycle: something old, something new. *Front Plant Sci* 4, 470. doi: 10.3389/fpls.2013.00470.

Moll, B., and Levine, R.P. (1970). Characterization of a Photosynthetic Mutant Strain of Chlamydomonas reinhardi Deficient in Phosphoribulokinase Activity. *Plant Physiol* 46(4), 576-580. doi: 10.1104/pp.46.4.576.

Ort, D.R., Merchant, S.S., Alric, J., Barkan, A., Blankenship, R.E., Bock, R., et al. (2015). Redesigning photosynthesis to sustainably meet global food and bioenergy demand. *Proc Natl Acad Sci U S A* 112(28), 8529-8536. doi: 10.1073/pnas.1424031112.

Patron, N.J., Orzaez, D., Marillonnet, S., Warzecha, H., Matthewman, C., Youles, M., et al. (2015). Standards for plant synthetic biology: a common syntax for exchange of DNA parts. *New Phytol* 208(1), 13-19. doi: 10.1111/nph.13532.

Paul, M.J., Knight, J.S., Habash, D., Parry, M.A.J., Lawlor, D.W., Barnes, S.A., et al. (1995). Reduction in phosphoribulokinase activity by antisense RNA in transgenic tobacco: effect on CO2 assimilation and growth in low irradiance. *The Plant Journal* 7(4), 535-542. doi: https://doi.org/10.1046/j.1365-313X.1995.7040535.x.

Raines, C.A. (2003). The Calvin cycle revisited. *Photosynth Res* 75(1), 1-10. doi: 10.1023/A:1022421515027.

Raines, C.A. (2011). Increasing photosynthetic carbon assimilation in C3 plants to improve crop yield: current and future strategies. *Plant Physiol* 155(1), 36-42. doi: 10.1104/pp.110.168559.

Raines, C.A. (2022). Improving plant productivity by re-tuning the regeneration of RuBP in the Calvin-Benson-Bassham cycle. *New Phytol* 236(2), 350-356. doi: 10.1111/nph.18394.

Roell, M.S., Schada von Borzykowski, L., Westhoff, P., Plett, A., Paczia, N., Claus, P., et al. (2021). A synthetic C4 shuttle via the β-hydroxyaspartate cycle in C3 plants. *Proc Natl Acad Sci U S A* 118(21). doi: 10.1073/pnas.2022307118.

Rosenthal, D.M., Locke, A.M., Khozaei, M., Raines, C.A., Long, S.P., and Ort, D.R. (2011). Over-expressing the C(3) photosynthesis cycle enzyme Sedoheptulose-1-7 Bisphosphatase improves photosynthetic carbon gain and yield under fully open air CO(2) fumigation (FACE). *BMC Plant Biol* 11, 123. doi: 10.1186/1471-2229-11-123.

Salesse-Smith, C.E., Sharwood, R.E., Busch, F.A., Kromdijk, J., Bardal, V., and Stern, D.B. (2018). Overexpression of Rubisco subunits with RAF1 increases Rubisco content in maize. *Nat Plants* 4(10), 802-810. doi: 10.1038/s41477-018-0252-4.

Salome, P.A., and Merchant, S.S. (2019). A Series of Fortunate Events: Introducing Chlamydomonas as a Reference Organism. *Plant Cell* 31(8), 1682-1707. doi: 10.1105/tpc.18.00952.

Satanowski, A., Dronsella, B., Noor, E., Vogeli, B., He, H., Wichmann, P., et al. (2020). Awakening a latent carbon fixation cycle in Escherichia coli. *Nat Commun* 11(1), 5812. doi: 10.1038/s41467-020-19564-5.

Schnell, R.A., and Lefebvre, P.A. (1993). Isolation of the Chlamydomonas regulatory gene NIT2 by transposon tagging. *Genetics* 134(3), 737-747. doi: 10.1093/genetics/134.3.737.

Schroda, M. (2019). Good News for Nuclear Transgene Expression in Chlamydomonas. *Cells* 8(12). doi: 10.3390/cells8121534.

Schwander, T., Schada von Borzyskowski, L., Burgener, S., Cortina, N.S., and Erb, T.J. (2016). A synthetic pathway for the fixation of carbon dioxide in vitro. *Science* 354(6314), 900-904. doi: 10.1126/science.aah5237.

Shin, S.E., Lim, J.M., Koh, H.G., Kim, E.K., Kang, N.K., Jeon, S., et al. (2016). CRISPR/Cas9-induced knockout and knock-in mutations in Chlamydomonas reinhardtii. *Sci Rep* 6, 27810. doi: 10.1038/srep27810.

Simkin, A.J., Lopez-Calcagno, P.E., and Raines, C.A. (2019). Feeding the world: improving photosynthetic efficiency for sustainable crop production. *J Exp Bot* 70(4), 1119-1140. doi: 10.1093/jxb/ery445.

Smith, B.D. (2000). *Isolation and analysis of Chlamydomonas reinhardtii phosphoribulokinase mutants and revertants.* Undergraduate Honors Thesis, University of Nebraska

South, P.F., Cavanagh, A.P., Liu, H.W., and Ort, D.R. (2019). Synthetic glycolate metabolism pathways stimulate crop growth and productivity in the field. *Science* 363(6422), eaat9077. doi: 10.1126/science.aat9077.

Stitt, M., Lunn, J., and Usadel, B. (2010). Arabidopsis and primary photosynthetic metabolism - more than the icing on the cake. *Plant J* 61(6), 1067-1091. doi: 10.1111/j.1365-313X.2010.04142.x.

Stitt, M., and Schulze, D. (1994). Does Rubisco control the rate of photosynthesis and plant growth? An exercise in molecular ecophysiology. *Plant, Cell and Environment* 17(5), 465-487. doi: 10.1111/j.1365-3040.1994.tb00144.x.

Sueoka, N. (1960). Mitotic Replication of Deoxyribonucleic Acid in Chlamydomonas Reinhardi. *Proc Natl Acad Sci U S A* 46(1), 83-91. doi: 10.1073/pnas.46.1.83.

Tamoi, M., Nagaoka, M., Miyagawa, Y., and Shigeoka, S. (2006). Contribution of fructose-1,6-bisphosphatase and sedoheptulose-1,7-bisphosphatase to the photosynthetic rate and carbon flow in the Calvin cycle in transgenic plants. *Plant Cell Physiol* 47(3), 380-390. doi: 10.1093/pcp/pcj004.

Thieulin-Pardo, G., Remy, T., Lignon, S., Lebrun, R., and Gontero, B. (2015). Phosphoribulokinase from Chlamydomonas reinhardtii: a Benson-Calvin cycle enzyme enslaved to its cysteine residues. *Mol Biosyst* 11(4), 1134-1145. doi: 10.1039/c5mb00035a.

Tilman, D., Balzer, C., Hill, J., and Befort, B.L. (2011). Global food demand and the sustainable intensification of agriculture. *Proc Natl Acad Sci U S A* 108(50), 20260-20264. doi: 10.1073/pnas.1116437108.

Treves, H., Lucius, S., Feil, R., Stitt, M., Hagemann, M., and Arrivault, S. (2022). Operation of Carbon-Concentrating Mechanisms in Cyanobacteria and Algae requires altered poising of the Calvin-Benson cycle. *bioRxiv*, 2022.2008.2023.504937. doi: 10.1101/2022.08.23.504937.

Trudeau, D.L., Edlich-Muth, C., Zarzycki, J., Scheffen, M., Goldsmith, M., Khersonsky, O., et al. (2018). Design and in vitro realization of carbon-conserving photorespiration. *Proc Natl Acad Sci U S A* 115(49), E11455-E11464. doi: 10.1073/pnas.1812605115.

Vavitsas, K., Crozet, P., Vinde, M.H., Davies, F., Lemaire, S.D., and Vickers, C.E. (2019). The Synthetic Biology Toolkit for Photosynthetic Microorganisms. *Plant Physiol* 181(1), 14-27. doi: 10.1104/pp.19.00345.

Vecchi, V., Barera, S., Bassi, R., and Dall'Osto, L. (2020). Potential and Challenges of Improving Photosynthesis in Algae. *Plants (Basel)* 9(1). doi: 10.3390/plants9010067.

Wang, L.M., Shen, B.R., Li, B.D., Zhang, C.L., Lin, M., Tong, P.P., et al. (2020). A Synthetic Photorespiratory Shortcut Enhances Photosynthesis to Boost Biomass and Grain Yield in Rice. *Mol Plant* 13(12), 1802-1815. doi: 10.1016/j.molp.2020.10.007.

Weber, E., Engler, C., Gruetzner, R., Werner, S., and Marillonnet, S. (2011). A modular cloning system for standardized assembly of multigene constructs. *PLoS One* 6(2), e16765. doi: 10.1371/journal.pone.0016765.

Wilson, R.H., Hayer-Hartl, M., and Bracher, A. (2019). Crystal structure of phosphoribulokinase from Synechococcus sp. strain PCC 6301. *Acta Crystallogr F Struct Biol Commun* 75(Pt 4), 278-289. doi: 10.1107/S2053230X19002693.

Wobbe, L., and Remacle, C. (2015). Improving the sunlight-to-biomass conversion efficiency in microalgal biofactories. *J Biotechnol* 201, 28-42. doi: 10.1016/j.jbiotec.2014.08.021.

Yoon, D.-K., Ishiyama, K., Suganami, M., Tazoe, Y., Watanabe, M., Imaruoka, S., et al. (2020). Transgenic rice overproducing Rubisco exhibits increased yields with improved nitrogen-use

efficiency in an experimental paddy field. *Nature Food* 1(2), 134-139. doi: 10.1038/s43016-020-0033-x.

Yu, A., Xie, Y., Pan, X., Zhang, H., Cao, P., Su, X., et al. (2020). Photosynthetic Phosphoribulokinase Structures: Enzymatic Mechanisms and the Redox Regulation of the Calvin-Benson-Bassham Cycle. *Plant Cell* 32(5), 1556-1573. doi: 10.1105/tpc.19.00642.

Zhu, X.G., de Sturler, E., and Long, S.P. (2007). Optimizing the distribution of resources between enzymes of carbon metabolism can dramatically increase photosynthetic rate: a numerical simulation using an evolutionary algorithm. *Plant Physiol* 145(2), 513-526. doi: 10.1104/pp.107.103713.

Zhu, X.G., Long, S.P., and Ort, D.R. (2010). Improving photosynthetic efficiency for greater yield. *Annu Rev Plant Biol* 61, 235-261. doi: 10.1146/annurev-arplant-042809-112206.

2.1.3 Conclusion

Au cours de cette étude, nous avons pu montrer que la PRK ne limite pas le flux du CBBC *in vivo* chez *C. reinhardtii*. Elle n'est cependant pas limitante au même niveau que celui décrit précédemment dans la littérature (Badger and Price, 1994; Paul et al., 1995; Banks et al., 1999). Cela pourrait permettre à la PRK de jouer un rôle plus important dans le contrôle du CBBC chez Chlamydomonas, par exemple dans des conditions conduisant à une régulation de l'activité de la PRK par les TRX ou par la formation du complexe GAPDH-CP12-PRK. Mon objectif initial était d'utiliser ce mutant pour étudier la régulation redox de la PRK *in vivo* chez Chlamydomonas en complémentant le mutant par des versions dépourvues d'une ou plusieurs cystéines régulatrices. Ces travaux ont été initiés mais n'ont pu être achevés faute de temps. Les résultats préliminaires obtenus avec diverses souches complémentées par des variants de PRK seront présentés dans la partie discussion et perspectives.

2.2 Nouvel outil de biologie synthétique chez Chlamydomonas

2.2.1 Introduction

Dans le cadre de mon travail de thèse, j'ai également participé au développement d'outils génétiques chez *Chlamydomonas reinhardtii*. Lorsque nous construisons des circuits génétiques, nous sommes amenés à utiliser plusieurs marqueurs de sélection. Puisque le nombre de marqueurs de sélection demeure assez restreint (4 gènes de résistance à un antibiotique et 2 marqueurs d'auxotrophie utilisés chez Chlamydomonas), il est toujours utile pour la communauté de disposer de nouvelles briques fonctionnelles contenant des gènes de résistance à de nouveaux antibiotiques.

Sous l'impulsion de Félix de Carpentier, ancien doctorant de notre équipe sous la direction d'Antoine Danon, nous avons conçu, construit et testé un nouveau marqueur de résistance à la blasticidine chez *C. reinhardtii*.

La blasticidine est un antibiotique produit par *Streptomyces griseochromogenes* qui agit comme un inhibiteur de la synthèse des protéines. La bactérie *Bacillus cereus* possède le gène BSR qui code pour la blasticidine S désaminase qui permet de détoxifier cet antibiotique, conférant la résistance à la cellule. La blasticidine S désaminase de *Bacillus cereus* a déjà été utilisée comme marqueur de sélection chez la levure (Fukuda and Kizaki,1999), les mammifères (Izumi *et al.*, 1991), les plantes (Kamakura *et al.*, 1990), et les microalgues, en particulier *Phaeodactylum tricornutum* (Buck *et al.*, 2018), *Nannochloropsis gaditana* (Ajjawi *et al.*, 2017) et *Volvox carteri* (Ortega-Escalante *et al.*, 2018). Nous avons donc décidé de tester ce marqueur chez Chlamydomonas et de l'adapter au standard MoClo afin de le rendre compatible avec les 119 briques développées pour le kit MoClo (Crozet et al., 2018).

Mon rôle dans ces travaux a consisté à caractériser phénotypiquement les souches transformées, en particulier pour analyser l'impact de la résistance à la blasticidine dans un photobioréacteur Algem.

2.2.2 Article 3

L'article intitulé « Blasticidin S deaminase: a new efficient selectable marker for *Chlamydomonas reinhardtii* » par Félix de Carpentier, Jeanne Le Peillet, Nicolas D. Boisset, Pierre Crozet, Stéphane D. Lemaire et Antoine Danon a été publié dans Frontiers in Plant Sciences en 2020.

frontiers in Plant Science

ORIGINAL RESEARCH
published: 05 March 2020
doi: 10.3389/fpls.2020.00242

Blasticidin S Deaminase: A New Efficient Selectable Marker for *Chlamydomonas reinhardtii*

*Félix de Carpentier[1,2†], Jeanne Le Peillet[1†], Nicolas D. Boisset[1,2], Pierre Crozet[1], Stéphane D. Lemaire[1] and Antoine Danon[1]**

[1] Institut de Biologie Physico-Chimique, UMR 8226, CNRS, Sorbonne Université, Paris, France, [2] Université Paris-Saclay, Saint-Aubin, France

OPEN ACCESS

Edited by:
Dimitris Petroutsos,
UMR 5168 Laboratoire de Physiologie Cellulaire Vegetale (LPCV), France

Reviewed by:
Xenie Johnson,
Commissariat à l'Energie Atomique et aux Energies Alternatives (CEA), France
Véronique Larosa,
University of Liège, Belgium
Ryutaro Tokutsu,
National Institute for Basic Biology, Japan

***Correspondence:**
Antoine Danon
antoine.danon@ibpc.fr

[†]These authors have contributed equally to this work

Specialty section:
This article was submitted to Plant Biotechnology, a section of the journal Frontiers in Plant Science

Received: 13 November 2019
Accepted: 17 February 2020
Published: 05 March 2020

Citation:
de Carpentier F, Le Peillet J, Boisset ND, Crozet P, Lemaire SD and Danon A (2020) Blasticidin S Deaminase: A New Efficient Selectable Marker for Chlamydomonas reinhardtii. Front. Plant Sci. 11:242. doi: 10.3389/fpls.2020.00242

Chlamydomonas reinhardtii is a model unicellular organism for basic or biotechnological research, such as the production of high-value molecules or biofuels thanks to its photosynthetic ability. To enable rapid construction and optimization of multiple designs and strains, our team and collaborators have developed a versatile Chlamydomonas Modular Cloning toolkit comprising 119 biobricks. Having the ability to use a wide range of selectable markers is an important benefit for forward and reverse genetics in Chlamydomonas. We report here the development of a new selectable marker based on the resistance to the antibiotic blasticidin S, using the *Bacillus cereus* blasticidin S deaminase (*BSR*) gene. The optimal concentration of blasticidin S for effective selection was determined in both liquid and solid media and tested for multiple laboratory strains. In addition, we have shown that our new selectable marker does not interfere with other common antibiotic resistances: zeocin, hygromycin, kanamycin, paromomycin, and spectinomycin. The blasticidin resistance biobrick has been added to the Chlamydomonas Modular Cloning toolkit and is now available to the entire scientific community.

Keywords: blasticidin, *Chlamydomonas reinhardtii*, antibiotic resistance, selectable marker, synthetic biology, modular cloning, algal biotechnology

INTRODUCTION

Chlamydomonas reinhardtii is a model microalga widely used for basic and biotechnological research such as photosynthesis, cilia/flagella, production of biofuels, or other molecules of interest (Georgianna and Mayfield, 2012; Barahimipour et al., 2016; Salomé and Merchant, 2019). In the last decades Chlamydomonas has been shown to be amenable to powerful genetic approaches including CRISPR-Cas9 gene editing (Jiang et al., 2014; Greiner et al., 2017; Kao and Ng, 2017). The creation of the Chlamydomonas Library Project (CLiP), which contains more than 62,000 mutants covering roughly 83% of Chlamydomonas genes (Li et al., 2019), has also greatly contributed to the development of Chlamydomonas reverse genetics. A wide range of molecular tools for engineering of the nuclear genome are also available in Chlamydomonas, most of which have been grouped in a Modular Cloning toolkit (Chlamy MoClo toolkit). This collection contains 119 biobricks (promoters, terminators, reporter genes, selectable markers, targeting peptides, antibiotic resistance genes, riboswitch, miRNA backbone, etc.), which can be easily assembled through Golden Gate cloning (Crozet et al., 2018). Most applications related to the manipulation

of nuclear gene expression require transformation of Chlamydomonas cells followed by selection of transformants on plates using a selectable marker, which is in most cases an antibiotic resistance gene enabling selection on a medium containing the appropriate antibiotic. In the case of multiple consecutive transformations several selectable markers are required. Therefore, it is essential for advanced genetic engineering to have as many selectable markers as possible. At the moment, six antibiotic resistances are commonly used in Chlamydomonas as selectable markers: zeocin (Stevens et al., 1996), hygromycin (Berthold et al., 2002), kanamycin (Barahimipour et al., 2016), paromomycin (Sizova et al., 2001), sulfadiazine (Tabatabaei et al., 2019), and spectinomycin (Meslet-Cladière and Vallon, 2011).

Blasticidin S (hereafter referred to as "blasticidin") is an antibiotic that inhibits cytosolic protein synthesis by blocking ribosomal translation termination (Svidritskiy et al., 2013). Blasticidin S deaminase (BSR) detoxifies blasticidin by catalyzing its deamination (Seto et al., 1966; Endo et al., 1987). The *BSR* gene has been successfully used as a selectable marker in mammals (Izumi et al., 1991), plants (Kamakura et al., 1990), yeasts (Kimura et al., 1994; Fukuda and Kizaki, 1999), and algae, including the diatom *Phaeodactylum tricornutum* (Buck et al., 2018) and the Chlamydomonas-related volvocine alga *Volvox carteri* (Ortega-Escalante et al., 2018).

We report here that blasticidin can be used as an antibiotic in Chlamydomonas, for all six laboratory strains tested. We show that BSR is functional in Chlamydomonas and can be used as a selectable marker, without conferring resistance to the other commonly used antibiotics. We also show that BSR can be used in combination with all other antibiotic resistance genes available in Chlamydomonas.

MATERIALS AND METHODS

Strains, Media, and Growth Conditions

If not otherwise specified, the reference strain used in the present study is CC-4533 (CMJ030), the CLiP library recipient strain used to generate the insertional mutants (Li et al., 2019). We also used other common laboratory strains CC-4051 (4A+) (Kim et al., 2005), CC-400 (cw15) (Roy Davies, 1972), CC-4425 (D66) (Schnell and Lefebvre, 1993), UVM4 (Neupert et al., 2009), and CC-124 (137c) (Pröschold et al., 2005). Chlamydomonas cells were grown on agar plates or liquid medium, using Tris-acetate-phosphate (TAP) medium (Gorman and Levine, 1965) at 25°C, under continuous light (40–60 μmol photon·m^{-2}·s^{-1}) and shaking (130 rpm). Growth analysis were performed in the Algem® labscale double photobioreactor systems (Algenuity, Stewartby, United Kingdom) under continuous light (200 μmol photons·m^{-2}·s^{-1}) and 120 rpm agitation in TAP or high salt medium (HSM) (Sueoka, 1960), with bubbling air. The absorbance at 740 nm was recorded every 10 min using the built-in sensor. The maximal growth rate was determined as the maximal slope of the growth curve (Δabs/Δtime). Linearity of the growth curve was estimated through linear regression every 200 min over a period of 13 h for TAP or 300 min over a period of 40 h for HSM condition. The slopes of these linear regressions were selected only for regressions displaying an $R^2 < 99.5\%$. Finally, the maximal slope was chosen as the maximal growth rate (**Supplementary Figure S2B**). Antibiotics used were blasticidin S (Sigma-Aldrich: SBR00022), zeocin (Invitrogen: R25005), hygromycin B (Sigma-Aldrich: H9773), kanamycin (Sigma-Aldrich: K1377), paromomycin (Sigma-Aldrich: P8692), or spectinomycin (Sigma-Aldrich: S4014). Chlamydomonas multi-well plates and Petri dishes were scanned using a Perfection V800 scanner (Epson).

Cell Death Quantification

Dead cells were detected using Evans blue (Sigma-Aldrich: E2129) at a final concentration of 0.2% w/v. Dead cells appear in blue whereas living cells that are impermeable to Evans blue remain green (Gaff and Okong'o-Ogola, 1971). Cells were observed with a microscope (Olympus BX43, Tokyo, Japan). For each sample multiple microscopic fields were analyzed and Evans blue-positive cells scored. For each value the percentage of dead cells was calculated on a minimum of 100 individuals.

Plasmid Construction

Protein and nucleic acid designs were performed *in silico* on Serial Cloner 2.6.1 software. *Bacillus cereus* BSR protein sequence (NCBI accession number: WP_076871832.1) was reverse translated using Chlamydomonas nuclear genome codon usage table[1]. The resulting *BSR* coding sequence was domesticated by removing *Bbs*I restriction sites, designed for the position B3–B5 of the common Plant MoClo syntax (Patron et al., 2015), synthetized (Twist Bioscience), and cloned by Golden Gate reaction with *Bsa*I-HFv2 (New England Biolabs) in pICH41308 (Weber et al., 2011) yielding plasmid pCM0-120, numbered according to the Chlamydomonas MoClo toolkit nomenclature (Crozet et al., 2018). Two other parts from the toolkit were used to build the *BSR* module (pCM1-029), the promoter $P_{A/R}$ coupled to the 5′UTR of RBCS2 (pCM0-020) and the 3′UTR of RBCS2 coupled to terminator T_{RBCS2} (pCM0-115) (Schroda et al., 2002; Crozet et al., 2018). The other antibiotic resistance genes were built using these same regulatory sequences and the coding sequence (CDS) from pCM0-077 (zeocin), pCM0-073 (hygromycin), pCM0-074 (paromomycin), pCM0-075 (kanamycin) and pCM0-076 (spectinomycin) generating the plasmids pCM1-030 (zeocin), pCM1-031 (hygromycin), pCM1-032 (kanamycin), pCM1-027 (paromomycin), and pCM1-033 (spectinomycin), respectively. All plasmid sequences are available in **Supplementary Files S1–S7**.

Chlamydomonas Transformation

Transformations were performed as previously described (Crozet et al., 2018). Briefly, Chlamydomonas cells were grown in TAP to early exponential phase (1–2 × 10^6 cells/mL), concentrated 100 times in TAP + 60 mM sucrose. After incubation of 250 μL of cells with DNA (55 fmol of purified resistance module excised with *Bbs*I-HF; New England Biolabs) at 4°C for 20 min, they were electroporated (2000 V/cm, 25 μF, no shunt resistance)

[1]www.kazusa.or.jp/codon/cgi-bin/showcodon.cgi?species=3055

and incubated for 16–20 h in 10 mL of TAP + 60 mM sucrose prior to be plated on TAP-agar complemented with appropriate antibiotic(s). Transformants were selected on TAP-agar medium containing blasticidin S (50 mg/L, unless otherwise specified), zeocin (15 mg/L), hygromycin B (20 mg/L), kanamycin (50 mg/L), paromomycin (20 mg/L), and/or spectinomycin (100 mg/L). Plates and transformants were analyzed after 5–7 days of growth in continuous light (50 μmol photon m^{-2} s^{-1}) at 25°C.

Insert Detection

Cells were pelleted (5 min, 2500 × *g*, room temperature) and lysed in 400 μL of extraction buffer (200 mM Tris-HCl pH 7.5; 200 mM NaCl; 25 mM EDTA; 0.5% SDS) for 10 min at 37°C under agitation (1400 rpm). After centrifugation (3 min, 17,000 × *g*, room temperature), the supernatant was harvested and the genomic DNA was precipitated with one volume of isopropanol for 10 min at room temperature, washed with 70% ethanol, dried and resuspended in water. PCR was performed using the Quick-Load® *Taq* 2× Master Mix (New England Biolabs) according to the manufacturer recommendations with the primers BSR.5 (5′-GCTGTACGAGGACAACAAGC-3′), TRBCS2.3 (5′-ACGGAGGATCGTTACAACC-3′), CBLP.5 (5′-GACGTCATCCACTGCCTGTG-3′), and CBLP.3 (5′-CGACGCATCCTCAACACACC-3′).

RESULTS

Chlamydomonas Is Sensitive to Blasticidin

To test the sensitivity of Chlamydomonas to blasticidin, the cells were grown in the presence of increasing blasticidin concentrations (25, 50, or 75 mg/L) in both solid and liquid cultures. Blasticidin was very effective to kill Chlamydomonas cells and the minimum efficient concentration was 50 mg/L in both conditions (**Figure 1A**). Many reference strains are used within the community and they present an important genetic diversity and substantial phenotypic differences (Gallaher et al., 2015). Compared to the reference strain of this study (CC-4533), some strain specific phenotypes, such as the absence of the cell wall, could alter blasticidin resistance. To assess whether this genetic diversity among common reference strains affects their sensitivity to blasticidin, CC-4051 (4A+), CC-400 (cw15), CC-4425 (D66+), UVM4, and CC-124 (137c) were cultivated on a solid medium supplemented or not with blasticidin (50 mg/L). In all cases, none of the strains survived in the presence of blasticidin, regardless of the initial number of cells tested (**Figure 1B**).

Blasticidin S Deaminase Can Be Used as a Selectable Marker in Chlamydomonas

To test whether the *BSR* module could be used as a selectable marker in Chlamydomonas, we engineered *B. cereus BSR* coding sequence to fit the optimal codon bias of Chlamydomonas nuclear genome. This has been already shown to improve transgene expression efficiency, including selection markers (Barahimipour et al., 2015, 2016). The engineered *BSR* coding sequence was then domesticated by removing *Bbs*I and *Bsa*I recognition motif and adding appropriate fusion sites of the Plant MoClo syntax (Patron et al., 2015). It was finally assembled with the parts $P_{A/R}$ (the hybrid promoter of *HSP70A* coupled to the 5′UTR of *RBCS2*) and T_{RBCS2} (coupling the 3′UTR and terminator of *RBCS2*) to form a functional module. $P_{A/R}$ is a chimeric constitutive promoter made up of *HSP70A* and *RBCS2* promoters that was proven to be very efficient in Chlamydomonas by significantly reducing gene silencing (Schroda et al., 2002). We also chose this promoter/terminator combination because it allows successful expression of the same *BSR* gene in Volvox (Ortega-Escalante et al., 2018). The resulting construct pCM1-029 (pCM stands for plasmid Chlamydomonas MoClo) is represented in **Figure 2A** using the MoClo nomenclature (Crozet et al., 2018). pCM0-120 and pCM1-029 plasmid sequences are available in **Supplementary Files S1, S2**, respectively. Cells transformed with pCM1-029 or an empty vector were incubated on plates containing blasticidin. Transformants appeared only when the cells were transformed with pCM1-029 (Blasticidin resistant cells are hereafter referred to as "Blast^R"), as shown in **Figure 2B**, indicating that *BSR* can be used as a selectable marker in Chlamydomonas. The insertion of the *BSR* module was confirmed by PCR in four independent Blast^R strains (**Supplementary Figure S1**).

To precisely evaluate the effect of blasticidin on the mortality of wild-type and Blast^R cells, we used Evans blue as a death marker (Gaff and Okong'o-Ogola, 1971). To avoid the heterogeneity that comes from the position of the transgene insertion locus, dozens of Blast^R colonies were collected from a Petri dish and then mixed in liquid culture (Blast^R culture). Wild-type and Blast^R cultures were grown in a 24-well plate with or without blasticidin, and the percentage of dead cells was evaluated several days after treatment. In the wild-type strain treated with blasticidin, the percentage of dead cells increased after 3 days and all the cells died after 5 days, while no significant levels of death was detected for Blast^R and untreated cells (**Figure 2C**). To assess a potential detrimental effect of BSR on Chlamydomonas, wild-type and Blast^R growth were quantified in a photobioreactor, in both mixotrophic (TAP) and autotrophic (HSM) conditions. No differences in the growth rate were observed suggesting that BSR does not affect growth or photosynthesis (**Supplementary Figure S2**).

Blasticidin Can Be Used in Combination With Other Antibiotics

To test the possible interactions of blasticidin with the other most commonly used selectable markers in Chlamydomonas, we first generated strains resistant to these antibiotics by transformation of wild-type cells with plasmids containing modules conferring resistance to zeocin (pCM1-030), hygromycin (pCM1-031), kanamycin (pCM1-032), paromomycin (pCM1-027), and spectinomycin (pCM1-033) under the control of the same regulatory sequences used for *BSR* in pCM1-029. Transformants were selected on plates containing the appropriate antibiotic

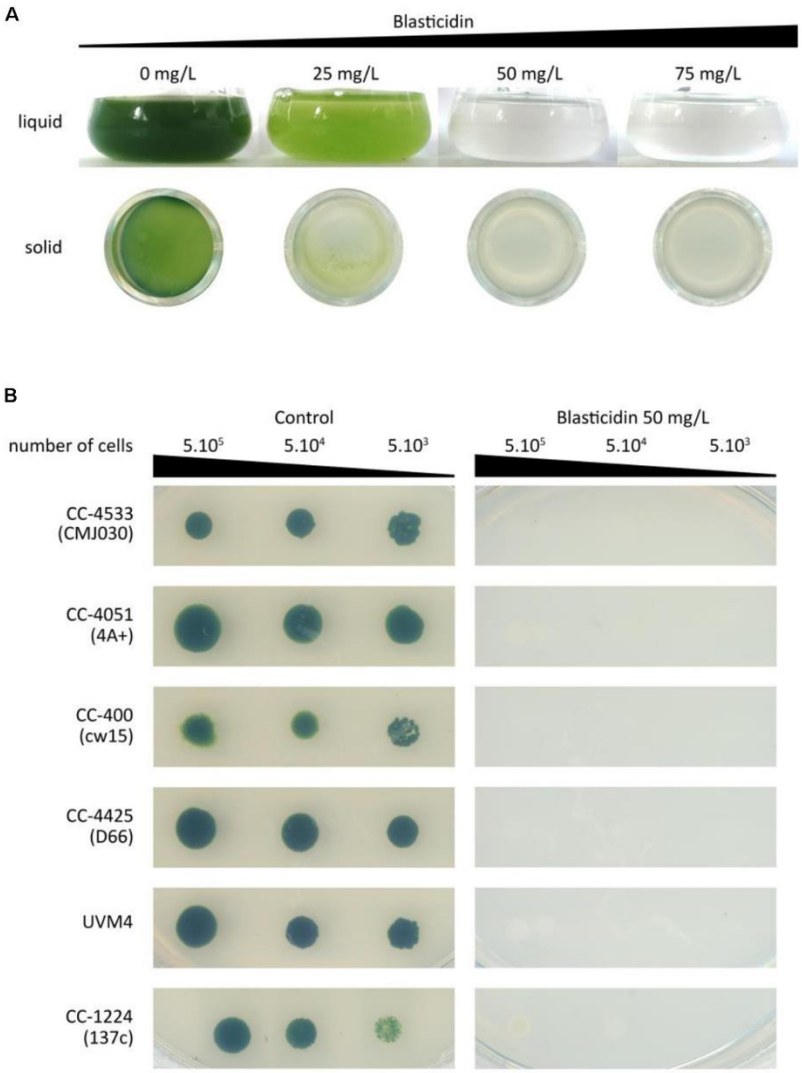

FIGURE 1 | Sensitivity of Chlamydomonas to blasticidin. **(A)** Chlamydomonas CC-4533 (CMJ030) was grown with increasing concentrations of blasticidin: 25, 50, or 75 mg/L, in both liquid and 24-well agar plates. For both liquid and solid media, cultures were photographed after 3 days of growth. **(B)** Spot tests were performed for six standard laboratory strains with or without blasticidin (50 mg/L). The results shown are representative of three biological replicates.

and pooled to take into account position effect, as for Blast^R culture. These cultures were called Zeo^R, Hygro^R, Kana^R, Paro^R, and Spec^R. The wild-type strain and the six antibiotic resistant cultures were cultivated in 96-well plates until exponential phase (5×10^6 cells/mL) prior to treatment with the different antibiotics. Five days after the addition of antibiotics, only the cells carrying the corresponding resistance gene survived the treatment, and importantly, only the Blast^R culture had survived upon blasticidin treatment (**Figure 3A**). It is to be noticed that Kana^R strains are also resistant to paromomycin (**Figure 3A**), as previously reported (Barahimipour et al., 2016).

If the resistance modules tested display no cross reactivity to one another, they can be combined to allow double selection. To use the *BSR* module and blasticidin in combination with another selectable marker, there must then be no interference between the different antibiotics and resistance modules. To verify possible interference, a single Blast^R strain was transformed with either pCM1-030 (zeocin resistance), pCM1-031 (hygromycin resistance), pCM1-032 (kanamycin resistance), pCM1-027 (paromomycin resistance), or pCM1-033 (spectinomycin resistance) (**Figure 3B**). Transformants were selected on plates containing both blasticidin and the appropriate antibiotic. For each combination tested, transformants resistant

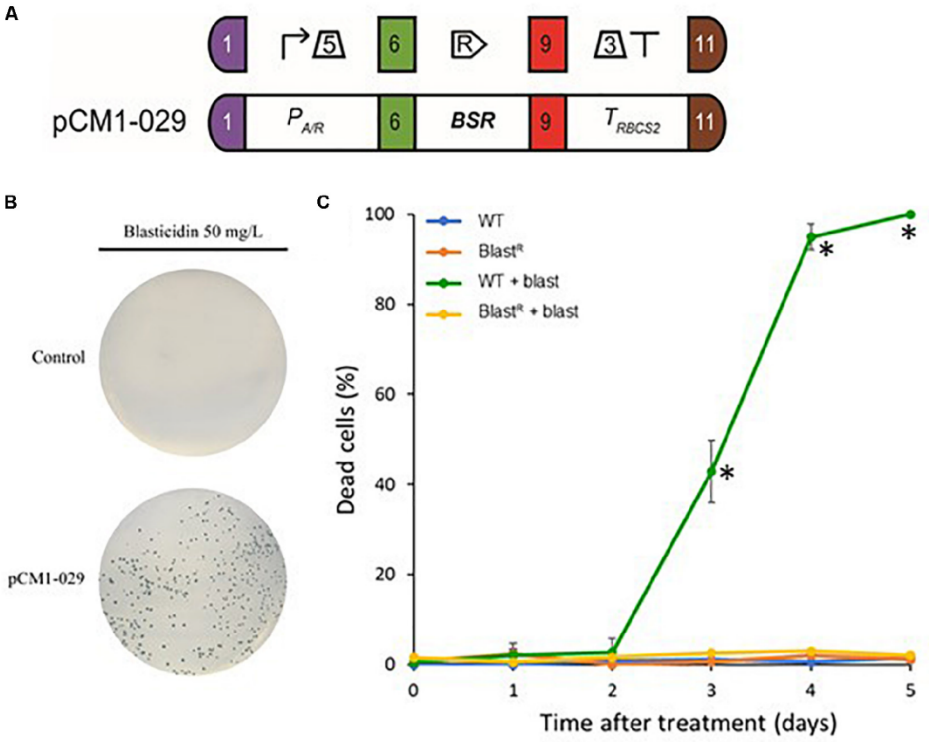

FIGURE 2 | Blasticidin S deaminase expression in Chlamydomonas. **(A)** The blasticidin resistance module pCM1-029 is built from a constitutive promoter ($P_{A/R}$ + 5′UTR of RBCS2), the BSR coding sequence and a terminator (3′UTR of RBCS2 + T_{RBCS2}) and was assembled using Golden Gate cloning. The numbers 1, 6, 9, and 11 stand for the standard fusion sites used for cloning (Crozet et al., 2018). SBOL2.0 visual syntax is shown above the module (Roehner et al., 2016). **(B)** CC-4533 cells were transformed with pCM1-029 or an empty vector (pICH47742) (Weber et al., 2011) and plated on TAP-agar supplemented with blasticidin (50 mg/L). Results are representative of three biological replicates. **(C)** The percentage of dead cells was evaluated using Evans blue in wild-type and Blast^R cultures with or without blasticidin, several days after treatment. Values represent the means and standard deviations of three independent experiments, symbol (*) shows the samples found to be significantly different doing an ANOVA analysis for each time points ($p < 0.001$).

to both antibiotics could be obtained (**Figure 3B**), indicating that no interference exists between the selectable markers tested.

DISCUSSION

Here we report the development of a new selectable marker for *C. reinhardtii*. Our data show that using blasticidin at a concentration of 50 mg/L ensures proper selection for all common laboratory strains of Chlamydomonas (**Figure 2C**). This concentration is slightly higher than the efficient concentration reported for *V. carteri* (Ortega-Escalante et al., 2018) or diatoms (Buck et al., 2018), but remains comparable with other antibiotics used in Chlamydomonas (Crozet et al., 2018).

We successfully engineered *BSR* coding sequence to adapt it to Chlamydomonas and no addition of intron was necessary for efficient expression, contrary to what was reported for *V. carteri* (Ortega-Escalante et al., 2018). Now that we have developed the blasticidin resistance module, seven antibiotic-based selectable markers are available for Chlamydomonas. This new tool can become important for advanced synthetic biology strategies requiring successive transformations of the same strain in combination with new engineering tools including the CLiP library (Li et al., 2019), the CRISPR/Cas technology (Jiang et al., 2014; Greiner et al., 2017; Kao and Ng, 2017) and the MoClo toolkit (Crozet et al., 2018). It is also important to increase the number of selectable markers available because the use of certain antibiotics should be taken with care. For instance zeocin is not always recommended since it can potentially cause DNA damages (Chankova et al., 2007; Čížková et al., 2019) and subsequent unwanted mutations. The kanamycin selectable marker *NPTII* is also conferring resistance to paromomycin (Barahimipour et al., 2015; **Figure 3A**) which makes it impossible to use in CLiP strains that are paromomycin resistant (Li et al., 2019). We show here that it is possible to use *BSR* and blasticidin in combination with all the other commonly used selectable markers in Chlamydomonas. *BSR* gene has been integrated as a new biobrick into the Chlamydomonas MoClo toolkit, and is now available to the entire community through the Chlamydomonas Resource Center[2].

[2]www.chlamycollection.org/

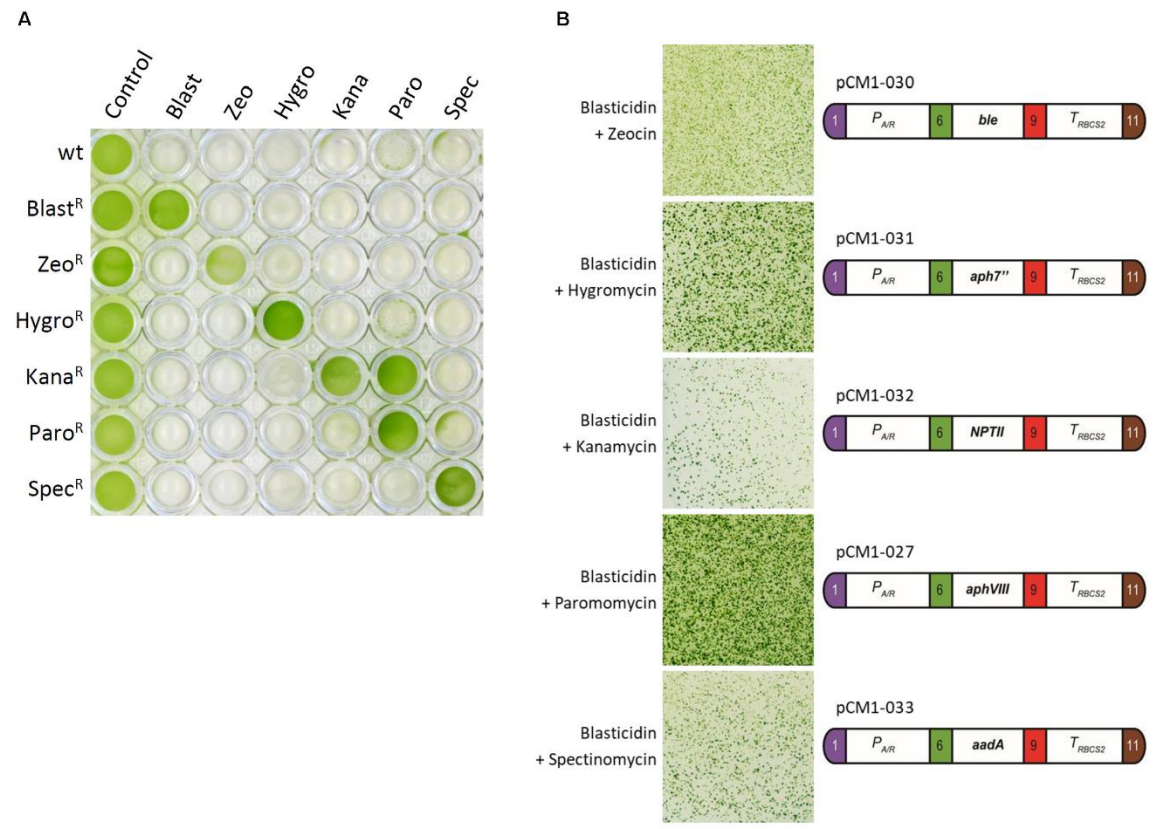

FIGURE 3 | Cross reactivity test. **(A)** Liquid cultures in exponential phase of wild-type strain and Zeo^R, Hygro^R, Kana^R, Paro^R, and Spec^R cultures were placed in a 96-well plate and treated with blasticidin (Blast, 50 mg/L), zeocin (Zeo, 15 mg/L), hygromycin B (Hygro, 20 mg/L), kanamycin (Kana, 50 mg/L), paromomycin (Paro, 20 mg/L), and spectinomycin (Spec, 100 mg/L) for 5 days. **(B)** A blasticidin resistant strain carrying pCM1-029 was independently transformed with the resistance modules to zeocin (pCM1-030), hygromycin (pCM1-031), kanamycin (pCM1-032), paromomycin (pCM1-027), and spectinomycin (pCM1-033). The numbers 1, 6, 9, and 11 stand for the standard fusion sites used for cloning (Crozet et al., 2018). Transformants were selected on plate containing both blasticidin and the appropriate antibiotic. The results showed are representative of three biological replicates. The full experiment with the different controls is available in **Supplementary Figure S3**.

DATA AVAILABILITY STATEMENT

All datasets generated for this study are included in the article/**Supplementary Material**.

AUTHOR CONTRIBUTIONS

FC, JL, PC, SL, and AD designed the study and analyzed the data. FC, JL, NB, PC, SL, and AD wrote the manuscript. FC, JL, NB, and AD performed the experiments.

FUNDING

This work was supported in part by the CNRS, Sorbonne Université, and Université Paris-Saclay, by Agence Nationale de la Recherche Grant 17-CE05-0001 CalvinDesign and by LABEX DYNAMO ANR-LABX-011.

ACKNOWLEDGMENTS

We thank Sandrine Bujaldon for providing the *Chlamydomonas reinhardtii* strains CC-4051, CC-400, and CC-124; Kevin Sarkissian for his help in the cloning; and Cyrielle Durand, Théo Le Moigne, Dr. Christophe Marchand, and Dr. Julien Henri for stimulating discussions and suggestions.

SUPPLEMENTARY MATERIAL

The Supplementary Material for this article can be found online at: https://www.frontiersin.org/articles/10.3389/fpls.2020.00242/full#supplementary-material

FIGURE S1 | Detection of the *BSR* module. pCM1-029 plasmid and the genomic DNA of the wild type (CC-4533) and four independent transformants Blast^R were used to amplify by PCR a fragment of the *BSR* resistance module. A product at the expected size (546 bp) was amplified only for pCM1-029 (positive control) and

the Blast^R transformants. Amplification of CBLP (Cre06.g278222) was used as a positive control for the experiment.

FIGURE S2 | Growth of wild-type (CC-4533) and Blast^R strains in a controlled photobioreactor. **(A)** Measurement of growth as detected by absorbance at 740 nm every 10 min, in TAP (mixotrophy) and HSM medium (autotrophy), light was set to 200 μmol photons·m^{-2}·s^{-1} with temperature and shaking set at 25°C and 120 rpm, respectively. **(B)** Quantification of the average growth rate of wild-type and Blast^R cells, corresponding to the growth curves shown in Graph **(A)**. Error bars represent the standard error to the mean of two biological replicates.

FIGURE S3 | Transformation of a blasticidin resistant strain with zeocin, hygromycin, kanamycin, paromomycin and spectinomycin resistance plasmids. A blasticidin resistant strain (Blast^R) carrying pCM1-029 was independently transformed with the resistance modules to zeocin (pCM1-030), hygromycin (pCM1-031), kanamycin (pCM1-032), paromomycin (pCM1-027), and spectinomycin (pCM1-033) or an empty vector (pICH50881). The numbers 1, 6, 9, and 11 stand for the standard fusion sites used for cloning (Crozet et al., 2018). Blast^R transformed cells were selected on plate containing both blasticidin and the appropriate antibiotic. CC-4533 was also transformed with the same five resistance modules or the empty vector and selected on the corresponding antibiotic with or without addition of blasticidin. The results showed are representative of three biological replicates.

FILE S1 | Annotated sequence of pCM0-120, the level 0 plasmid containing *BSR* coding sequence engineered for Chlamydomonas nuclear genome and designed for the position B3–B5 of the Chlamydomonas MoClo toolkit (Crozet et al., 2018).

FILE S2 | Annotated sequence of pCM1-029, the level 1 plasmid made up of the promoter AR ($P_{A/R}$ + 5′UTR of RBCS2), *BSR* coding sequence and the terminator of RBCS2 (3′UTR of RBCS2 + T_{RBCS2}) conferring blasticidin resistance in Chlamydomonas (Crozet et al., 2018).

FILE S3 | Annotated sequence of pCM1-027, the level 1 plasmid made up of the promoter AR ($P_{A/R}$ + 5′UTR of RBCS2), *aphVIII* coding sequence and the terminator of RBCS2 (3′UTR of RBCS2 + T_{RBCS2}) conferring paromomycin resistance in Chlamydomonas (Sizova et al., 2001; Crozet et al., 2018).

FILE S4 | Annotated sequence of pCM1-030, the level 1 plasmid made up of the promoter AR ($P_{A/R}$ + 5′UTR of RBCS2), *Ble* coding sequence and the terminator RBCS2 (3′UTR of RBCS2 + T_{RBCS2}) conferring zeocin resistance in Chlamydomonas (Stevens et al., 1996; Crozet et al., 2018).

FILE S5 | Annotated sequence of pCM1-031, the level 1 plasmid made up of the promoter AR ($P_{A/R}$ + 5′UTR of RBCS2), *aph7″* coding sequence and the terminator RBCS2 (3′UTR of RBCS2 + T_{RBCS2}) conferring hygromycin resistance in Chlamydomonas (Berthold et al., 2002; Crozet et al., 2018).

FILE S6 | Annotated sequence of pCM1-032, the level 1 plasmid made up of the promoter AR ($P_{A/R}$ + 5′UTR of RBCS2), *NPTII* coding sequence and the terminator RBCS2 (3′UTR of RBCS2 + T_{RBCS2}) conferring kanamycin resistance in Chlamydomonas (Barahimipour et al., 2016; Crozet et al., 2018).

FILE S7 | Annotated sequence of pCM1-029, the level 1 plasmid made up of the promoter AR ($P_{A/R}$ + 5′UTR of RBCS2), *aadA* coding sequence and the terminator RBCS2 (3′UTR of RBCS2 + T_{RBCS2}) conferring spectinomycin resistance in Chlamydomonas (Meslet-Cladière and Vallon, 2011; Crozet et al., 2018).

REFERENCES

Barahimipour, R., Neupert, J., and Bock, R. (2016). Efficient expression of nuclear transgenes in the green alga *Chlamydomonas*: synthesis of an HIV antigen and development of a new selectable marker. *Plant Mol. Biol.* 90, 403–418. doi: 10.1007/s11103-015-0425-8

Barahimipour, R., Strenkert, D., Neupert, J., Schroda, M., Merchant, S. S., and Bock, R. (2015). Dissecting the contributions of GC content and codon usage to gene expression in the model alga *Chlamydomonas reinhardtii*. *Plant J.* 84, 704–717. doi: 10.1111/tpj.13033

Berthold, P., Schmitt, R., and Mages, W. (2002). An engineered *Streptomyces hygroscopicus aph 7* Gene Mediates dominant resistance against hygromycin B in *Chlamydomonas reinhardtii*. *Protist* 153, 401–412. doi: 10.1078/14344610260450136

Buck, J. M., Río Bártulos, C., Gruber, A., and Kroth, P. G. (2018). Blasticidin-S deaminase, a new selection marker for genetic transformation of the diatom *Phaeodactylum tricornutum*. *PeerJ* 6:e5884. doi: 10.7717/peerj.5884

Chankova, S. G., Dimova, E., Dimitrova, M., and Bryant, P. E. (2007). Induction of DNA double-strand breaks by zeocin in *Chlamydomonas reinhardtii* and the role of increased DNA double-strand breaks rejoining in the formation of an adaptive response. *Radiat. Environ. Biophys.* 46, 409–416. doi: 10.1007/s00411-007-0123-2

Čížková, M., Slavková, M., Vítová, M., Zachleder, V., and Bišová, K. (2019). Response of the green alga *Chlamydomonas reinhardtii* to the DNA damaging agent zeocin. *Cells* 8:E735. doi: 10.3390/cells8070735

Crozet, P., Navarro, F. J., Willmund, F., Mehrshahi, P., Bakowski, K., Lauersen, K. J., et al. (2018). Birth of a photosynthetic chassis: a MoClo toolkit enabling synthetic biology in the microalga *Chlamydomonas reinhardtii*. *ACS Synth. Biol.* 7, 2074–2086. doi: 10.1021/acssynbio.8b00251

Endo, T., Furuta, K., Kaneko, A., Katsuki, T., Kobayashi, K., Azuma, A., et al. (1987). Inactivation of blasticidin S by *Bacillus cereus*. I. inactivation mechanism. *J. Antibiot.* 40, 1791–1793. doi: 10.7164/antibiotics.40.1791

Fukuda, H., and Kizaki, Y. (1999). A new transformation system of *Saccharomyces cerevisiae* with blasticidin S deaminase gene. *Biotechnol. Lett.* 21, 969–971. doi: 10.1023/A:1005613206138

Gaff, D. F., and Okong'o-Ogola, O. (1971). The Use of non-permeating pigments for testing the survival of cells. *J. Exp. Bot.* 22, 756–758. doi: 10.1093/jxb/22.3.756

Gallaher, S. D., Fitz-Gibbon, S. T., Glaesener, A. G., Pellegrini, M., and Merchant, S. S. (2015). Chlamydomonas genome resource for laboratory strains reveals a mosaic of sequence variation, identifies true strain histories, and enables strain-specific studies. *Plant Cell* 27, 2335–2352. doi: 10.1105/tpc.15.00508

Georgianna, D. R., and Mayfield, S. P. (2012). Exploiting diversity and synthetic biology for the production of algal biofuels. *Nature* 488, 329–335. doi: 10.1038/nature11479

Gorman, D. S., and Levine, R. P. (1965). Cytochrome f and plastocyanin: their sequence in the photosynthetic electron transport chain of *Chlamydomonas reinhardi*. *Proc. Natl. Acad. Sci. U.S.A.* 54, 1665–1669. doi: 10.1073/pnas.54.6.1665

Greiner, A., Kelterborn, S., Evers, H., Kreimer, G., Sizova, I., and Hegemann, P. (2017). Targeting of photoreceptor genes in *Chlamydomonas reinhardtii* via zinc-finger nucleases and CRISPR/Cas9. *Plant Cell* 29, 2498–2518. doi: 10.1105/tpc.17.00659

Izumi, M., Miyazawa, H., Kamakura, T., Yamaguchi, I., Endo, T., and Hanaoka, F. (1991). Blasticidin S-resistance gene (*bsr*): a novel selectable marker for mammalian cells. *Exp. Cell Res.* 197, 229–233. doi: 10.1016/0014-4827(91)90427-V

Jiang, W., Brueggeman, A. J., Horken, K. M., Plucinak, T. M., and Weeks, D. P. (2014). Successful transient expression of Cas9 and Single Guide RNA Genes in *Chlamydomonas reinhardtii*. *Eukaryot Cell* 13, 1465–1469. doi: 10.1128/EC.00213-14

Kamakura, T., Yoneyama, K., and Yamaguchi, I. (1990). Expression of the blasticidin S deaminase gene (*bsr*) in tobacco: fungicide tolerance and a new selective marker for transgenic plants. *Mol. Gen. Genet.* 223, 332–334. doi: 10.1007/bf00265072

Kao, P.-H., and Ng, I.-S. (2017). CRISPRi mediated phosphoenolpyruvate carboxylase regulation to enhance the production of lipid in *Chlamydomonas reinhardtii*. *Bioresour. Technol.* 245, 1527–1537. doi: 10.1016/j.biortech.2017.04.111

Kim, K.-S., Feild, E., King, N., Yaoi, T., Kustu, S., and Inwood, W. (2005). Spontaneous mutations in the ammonium transport gene AMT4 of *Chlamydomonas reinhardtii*. *Genetics* 170, 631–644. doi: 10.1534/genetics.105.041574

Kimura, M., Kamakura, T., Zhou Tao, Q., Kaneko, I., and Yamaguchi, I. (1994). Cloning of the blasticidin S deaminase gene (*BSD*) from *Aspergillus terreus* and its use as a selectable marker for *Schizosaccharomyces pombe*

and *Pyricularia oryzae*. *Mol. Gen. Genet.* 242, 121–129. doi: 10.1007/BF00391004

Li, X., Patena, W., Fauser, F., Jinkerson, R. E., Saroussi, S., Meyer, M. T., et al. (2019). A genome-wide algal mutant library and functional screen identifies genes required for eukaryotic photosynthesis. *Nat. Genet.* 51, 627–635. doi: 10.1038/s41588-019-0370-376

Meslet-Cladière, L., and Vallon, O. (2011). Novel shuttle markers for nuclear transformation of the green alga *Chlamydomonas reinhardtii*. *Eukaryotic Cell* 10, 1670–1678. doi: 10.1128/EC.05043-11

Neupert, J., Karcher, D., and Bock, R. (2009). Generation of *Chlamydomonas strains* that efficiently express nuclear transgenes. *Plant J.* 57, 1140–1150. doi: 10.1111/j.1365-313X.2008.03746.x

Ortega-Escalante, J. A., Kwok, O., and Miller, S. M. (2018). New Selectable Markers for *Volvox carteri* Transformation. *Protist* 170, 52–63. doi: 10.1016/j.protis.2018.11.002

Patron, N. J., Orzaez, D., Marillonnet, S., Warzecha, H., Matthewman, C., Youles, M., et al. (2015). Standards for plant synthetic biology: a common syntax for exchange of DNA parts. *New Phytol.* 208, 13–19. doi: 10.1111/nph.13532

Pröschold, T., Harris, E. H., and Coleman, A. W. (2005). Portrait of a species: *Chlamydomonas reinhardtii*. *Genetics* 170, 1601–1610. doi: 10.1534/genetics.105.044503

Roehner, N., Beal, J., Clancy, K., Bartley, B., Misirli, G., Grünberg, R., et al. (2016). Sharing structure and function in biological design with SBOL 2.0. *ACS Synth. Biol.* 5, 498–506. doi: 10.1021/acssynbio.5b00215

Roy Davies, D. (1972). Cell wall organisation in *Chlamydomonas reinhardi*. *Mol. Gen. Genet.* 115, 334–348. doi: 10.1007/BF00333172

Salomé, P. A., and Merchant, S. S. (2019). A series of fortunate events: introducing Chlamydomonas as a reference organism. *Plant Cell* 31, 1682–1707. doi: 10.1105/tpc.18.00952

Schnell, R. A., and Lefebvre, P. A. (1993). Isolation of the *Chlamydomonas* regulatory gene NIT2 by transposon tagging. *Genetics* 134, 737–747.

Schroda, M., Beck, C. F., and Vallon, O. (2002). Sequence elements within an HSP70 promoter counteract transcriptional transgene silencing in *Chlamydomonas*. *Plant J.* 31, 445–455. doi: 10.1046/j.1365-313X.2002.01371.x

Seto, H., Ôtake, N., and Yonehara, H. (1966). Biological transformation of Blasticidin S by *Aspergillus fumigatus* sp. *Agric. Biol. Chem.* 30, 877–886. doi: 10.1080/00021369.1966.10858693

Sizova, I., Fuhrmann, M., and Hegemann, P. (2001). A *Streptomyces rimosus aphVIII* gene coding for a new type phosphotransferase provides stable antibiotic resistance to *Chlamydomonas reinhardtii*. *Gene* 277, 221–229. doi: 10.1016/s0378-1119(01)00616-3

Stevens, D. R., Purton, S., and Rochaix, J.-D. (1996). The bacterial phleomycin resistance gene *ble* as a dominant selectable marker in *Chlamydomonas*. *Mol. Gen. Genet.* 251, 23–30. doi: 10.1007/BF02174340

Sueoka, N. (1960). Mitotic replication of deoxyribonucleic acid in *Chlamydomonas Reinhardi*. *Proc. Natl. Acad. Sci. U.S.A.* 46, 83–91. doi: 10.1073/pnas.46.1.83

Svidritskiy, E., Ling, C., Ermolenko, D. N., and Korostelev, A. A. (2013). Blasticidin S inhibits translation by trapping deformed tRNA on the ribosome. *Proc. Natl. Acad. Sci. U.S.A.* 110, 12283–12288. doi: 10.1073/pnas.1304922110

Tabatabaei, I., Dal Bosco, C., Bednarska, M., Ruf, S., Meurer, J., and Bock, R. (2019). A highly efficient sulfadiazine selection system for the generation of transgenic plants and algae. *Plant Biotechnol. J.* 17, 638–649. doi: 10.1111/pbi.13004

Weber, E., Engler, C., Gruetzner, R., Werner, S., and Marillonnet, S. (2011). A modular cloning system for standardized assembly of multigene constructs. *PLoS One* 6:e16765. doi: 10.1371/journal.pone.0016765

Conflict of Interest: The authors declare that the research was conducted in the absence of any commercial or financial relationships that could be construed as a potential conflict of interest.

Copyright © 2020 de Carpentier, Le Peillet, Boisset, Crozet, Lemaire and Danon. This is an open-access article distributed under the terms of the Creative Commons Attribution License (CC BY). The use, distribution or reproduction in other forums is permitted, provided the original author(s) and the copyright owner(s) are credited and that the original publication in this journal is cited, in accordance with accepted academic practice. No use, distribution or reproduction is permitted which does not comply with these terms.

2.2.3 Conclusion

Avec cette nouvelle brique, nous avons enrichi la palette d'outils génétiques disponibles chez Chlamydomonas. En l'ajoutant au kit de clonage modulaire, nous espérons pouvoir favoriser la construction dans ce châssis en offrant une plus grande flexibilité pour la conception des stratégies de bio-ingénierie.

3 DISCUSSION ET PERSPECTIVES

Mon travail de thèse s'inscrit dans le cadre de la thématique de notre équipe de recherche qui a pour objectif principal de comprendre et d'améliorer l'efficacité de la photosynthèse chez Chlamydomonas en employant des approches de biologie synthétique pour manipuler le CBBC *in vivo*.

Initialement, mes objectifs consistaient à :

1. Caractériser le mutant PRK ;
2. Déterminer quel niveau d'accumulation de PRK limite le CBBC et si une surproduction de l'enzyme peut améliorer la fixation du carbone ;
3. Utiliser le mutant PRK pour étudier la régulation redox de la PRK *in vivo* en complémentant le mutant par des versions dépourvues d'une ou plusieurs cystéines régulatrices.

Les deux premiers objectifs ont pu être poursuivis et ont permis de générer des outils qui seront importants pour la poursuite du travail. Le troisième a été initié mais n'a pu être achevé faute de temps. Toutefois, des résultats préliminaires obtenus récemment avec diverses souches complémentées par des variants de PRK seront présentés ci-après.

J'ai également au cours de ma thèse contribué au développement de nouveaux outils de biologie synthétique tel que la brique MoClo conférant la résistance à la blasticidine. De nombreuses briques génétiques ont également été obtenues dans le cadre de l'ingénierie du mutant PRK.

Les résultats obtenus ainsi que les perspectives ouvertes par mon travail de thèse seront discutés en détail dans ce chapitre.

3.1 Améliorer la fixation du carbone par l'ingénierie du CBBC

Améliorer la production de biomasse végétale a de multiples intérêts pour la production de nourriture, la production de molécules à haute valeur ajoutée, de biocarburants ou encore de molécules plateformes (Liang et al., 2018). Depuis la révolution verte, l'efficacité photosynthétique est devenue l'élément principal limitant la production de biomasse, et particulièrement la fixation du carbone par le cycle de Calvin-Benson-Bassham (Raines, 2022). L'étude du CBBC chez les plantes supérieures est ardue puisqu'aucun mutant n'est viable, ce qui n'est pas le cas chez *Chlamydomonas reinhardtii* (Salome and Merchant, 2019). Couplé au fait que son appareil photosynthétique est très similaire à celui des plantes terrestres, cela en fait donc un bon modèle pour étudier la photosynthèse.

Afin d'étudier par des approches de biologie synthétique le CBBC chez *Chlamydomonas reinhardtii*, il convient d'employer des méthodologies standardisées. Afin de commencer à les mettre en place, nous avons donc choisi la phosphoribulokinase (PRK) comme modèle d'étude car elle possède une activité unique au CBBC, que c'est un système assez maitrisé au laboratoire et qu'un mutant d'insertion à l'unique locus la codant était disponible.

3.1.1 Modulation de l'abondance de la PRK *in vivo*

Dans l'objectif de caractériser la PRK comme modèle du CBBC, nous avons étudié le mutant ΔPRK, ainsi qu'un certain nombre de lignées transgéniques exprimant un gène chimérique PRK ectopique (partie 2.1). Nous avons pu démontrer que la PRK est essentielle à la croissance photoautotrophique. Nous avons ensuite profité de la variation naturelle induite par la mutagénèse insertionnelle (effet de position) pour caractériser des lignées ayant différents niveaux d'expression. Idéalement, il serait intéressant de continuer cette étude à l'aide d'une seule lignée dans laquelle nous pourrions faire varier *in vivo* la quantité exprimée. Ce fut un projet que j'avais pour but de réaliser en utilisant le promoteur METE ou un riboswitch du gène THI4 (Crozet et al., 2018) pour contrôler finement l'expression de la PRK par les vitamines B1 (thiamine) et B12 (cobalamine), respectivement. Ces

deux éléments régulateurs négatifs sont inhibés par la vitamine respective, ce qui permet d'inhiber proportionnellement l'expression du gène cible en augmentant la concentration de vitamine. Cependant ce système n'a pas fonctionné pour plusieurs raisons.

Dans un premier temps, Chlamydomonas vit naturellement en symbiose avec les bactéries environnantes lui fournissant des vitamines (Croft et al., 2005). Nous pouvons utiliser la présence de ces vitamines pour finement faire varier la proportion des enzymes *in vivo*. Cependant, malgré mes essais, cette méthode n'a jamais fonctionné. Il n'est pas rare que nous retrouvions une contamination bactérienne très difficile à éliminer (provenant probablement du stock de la banque de mutants) mais qui ne semble pas affecter la croissance de l'algue. Chlamydomonas n'a plus ou pas ces voies de synthèse de vitamines, ce qui favorise l'interaction mutualiste avec des bactéries. En raison de ce mutualisme entre Chlamydomonas et une souche bactérienne, il s'avère que les bactéries sont capables de produire de la vitamine B1 et B12, et de les sécréter dans le milieu. Un système répressif qui fonctionne en réponse à ces vitamines ne pouvait donc pas fournir de résultats dans ces conditions.

Le deuxième problème est que pour utiliser un tel système répressif, le construit doit permettre d'obtenir une complémentation fonctionnelle totale du transgène. C'est-à-dire permettre que l'on puisse inhiber l'expression dans une souche ayant un niveau de protéine au moins égal à celui de la souche de référence (100%), voire plus. A partir d'une telle souche il est envisageable de moduler finement l'expression pour trouver la proportion exacte de PRK induisant un phénotype de croissance.

Ces deux problématiques ont été résolues, mais cela a pris plus de temps que prévu. En effet, après de nombreux mois d'efforts, j'ai réussi à décontaminer complétement la souche ΔPRK. J'ai ensuite pu la caractériser et la complémenter. Après avoir étudié ces souches, nous avons appris que les éléments géniques initialement choisis ne permettaient pas d'atteindre l'objectif du 100% de protéine par rapport à la référence. Après avoir cherché de nouveaux designs, (*cf*. 2.1), nous arrivons désormais à obtenir des surexpresseurs de la PRK. Il serait donc envisageable de réessayer cette stratégie en couplant

notre nouveau design basé sur une PRK avec introns à pMETE ou au Riboswitch THI4. Des designs similaires pourraient bien sûr être testés pour les autres enzymes du CBBC.

3.1.2 Notion d'enzyme limitante

Lors de l'étude du mutant ΔPRK et des lignées complémentées, nous avons observé qu'un niveau de 40%, relatif au niveau sauvage, de la protéine ne suffisait pas à restaurer la croissance au même niveau que le contrôle (*cf*. 2.1). Au contraire, chez le tabac, aucun effet sur la croissance n'est observé si les niveaux de PRK demeurent supérieurs à 15% de la lignée de référence (Paul et al., 1995; Banks et al., 1999). Nos résultats indiquent que chez Chlamydomonas, une souche avec une abondance en PRK correspondant à 85% de la souche de référence ne montre pas de phénotype de croissance (*cf*. 2.1). Ces résultats suggèrent que chez Chlamydomonas l'abondance de la PRK est limitante entre 40% et 85% de l'abondance de la souche de référence.

Un des outils utilisés pour caractériser l'impact d'une enzyme sur sa voie métabolique est le coefficient de contrôle du flux métabolique (Fell, 1997). Ce calcul (*cf*. 1.5.3) a initialement été développé par des biochimistes pour avoir un outil de mesure de l'importance de la quantité d'une enzyme sur une voie métabolique linéaire. Ce calcul a ensuite été utilisé, notamment par Christine Raines, sur le CBBC (Raines, 2003). Bien qu'utile pour comprendre si une des enzymes peut limiter le flux, nous pouvons penser que cette mesure n'est pas adaptée aux expériences *in vivo*.

En effet, il est important de rappeler que le calcul du coefficient de contrôle d'une enzyme sur une voie doit être considéré comme un outil d'étude, développé en faisant volontairement abstraction de certaines caractéristiques du système, comme les régulations. De plus, il faut admettre que les paramètres cinétiques obtenus *in vitro* seront identiques aux paramètres *in vivo,* ce qui n'est pas toujours le cas, notamment à cause des régulations, des concentrations des substrats... Ce calcul admet également que toutes les régulations transcriptionnelles et post traductionnelles sont connues (Fell, 1997) et que nous pouvons réaliser les mesures en contrôlant toutes les régulations. Or, ce n'est pas le cas pour le CBBC.

Une autre limitation de ce calcul est la différence de ploïdie des espèces étudiés. En effet, si l'organisme est haploïde ou diploïde, il faut aussi considérer les paramètres de dominance possible d'une copie vis-à-vis de son allèle. Nous ne pouvons pas non plus comparer directement des données obtenues sur différents organismes car les paramètres cinétiques des enzymes diffèrent, de même que leurs paramètres de croissance macroscopiques comme leurs besoins en azote (Fell, 1997).

Le fait de définir la PRK comme une enzyme essentielle mais non limitante pour le CBBC n'est finalement peut-être pas pertinent au regard du seul paramètre de son abondance. La limitation du flux métabolique est en premier lieu définie par l'activité enzymatique, qui dépend de la quantité d'enzyme, mais aussi de ses régulations post-traductionnelles. Et si la limitation de la PRK n'était pas uniquement liée à son abondance mais principalement à ses régulations post traductionnelles qui pourraient influer son action sur le flux métabolique ?

3.2 Étudier la régulation de la phosphoribulokinase *in vivo*

3.2.1 Régulations par les ponts disulfures régulateurs

La régulation de la PRK par l'oxydoréduction de ses ponts disulfures par les TRX a été bien caractérisée *in vitro*.

Le pont disulfure N-terminal C16-C55 régule l'activité enzymatique de la PRK alors que le pont C-terminal C243-C249 semble jouer un rôle dans la flexibilité de l'assemblage du complexe GAPDH/PRK/CP12 (Gurrieri et al., 2019). Grâce à la disponibilité du mutant ΔPRK et des outils pour le complémenter efficacement, il est possible d'envisager de tester l'importance fonctionnelle de la régulation redox de la PRK pour la première fois *in vivo*. Pour cela, nous avons construit 4 nouvelles unités transcriptionnelles pour exprimer des variants de la PRK ne pouvant former que le pont C-terminal (C243S-C249S, ΔC), que le pont N-terminal (C16S, ΔN), ou aucun des deux ponts (C16S-C243S-C249S, ΔN+C). Un contrôle sans altération des ponts disulfures a également été construit. Les substitutions des cystéines ont été

introduites par mutagénèse dirigée dans la brique MoClo correspondant à la séquence codante de la PRK avec intron. Cette brique a été incluse dans une unité transcriptionnelle sous le contrôle d'un promoteur/5'UTR PSAD et d'un 3'UTR/terminateur PSAD (Figure 25).

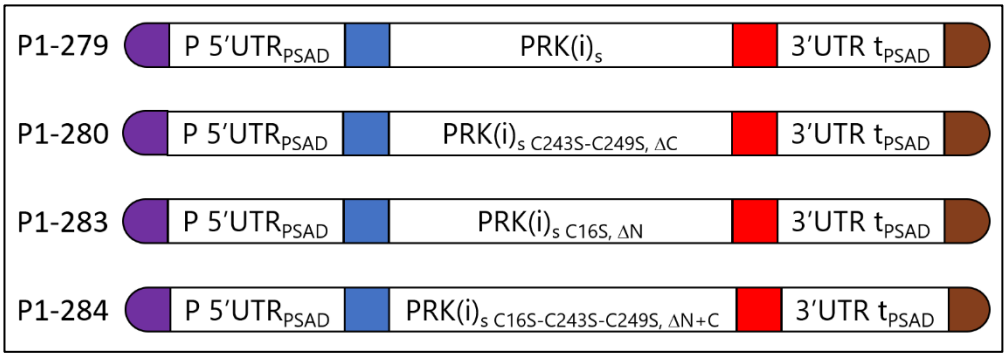

Figure 25. Représentation schématique des unités de transcription codant les PRK WT, ΔC, ΔN et ΔN+C
Les différents vecteurs construits pour étudier des formes mutées de PRK insensibles aux régulations par les thiorédoxines ont été générées. Le plasmide p1-279 est le contrôle sans mutation. Les mutants du pont N-terminal (C16S, ΔN), C-terminal (C243S-C249S) ou bien les deux sont annotés p1-280, p1-283 ou p1-284, respectivement.

Le mutant ΔPRK a été transformé avec les construits de la figure 2 puis les clones ont été sélectionnés sur milieu minimum. Les transformants ont été sélectionnés sur milieu minimum puis plusieurs clones ont été analysés par western-blot anti-PRK afin de sélectionner des souches complémentées ayant des niveaux comparables de PRK. Ces analyses ont été effectuées par Manuel Jesús Ponce Mallén, post-doctorant (co-direction S. Lemaire, Paris, José-Luis Crespo/Esther Pérez-Pérez, Séville).

Tous les transformants, quelle que soit la construction utilisée (Figure 25), présentent une accumulation de la PRK supérieure ou égale à la souche de référence (Figure 26). Pour chaque construction (Figure 25), une souche unique a été sélectionnée pour réaliser des tests préliminaires de phénotypage (en rouge dans la Figure 26). Ces souches présentent toutes des niveaux plus forts que celui de la souche de référence. Nous avons sélectionné des souches présentant

les niveaux de PRK les plus proches possibles, autour de 260% du contrôle sauvage.

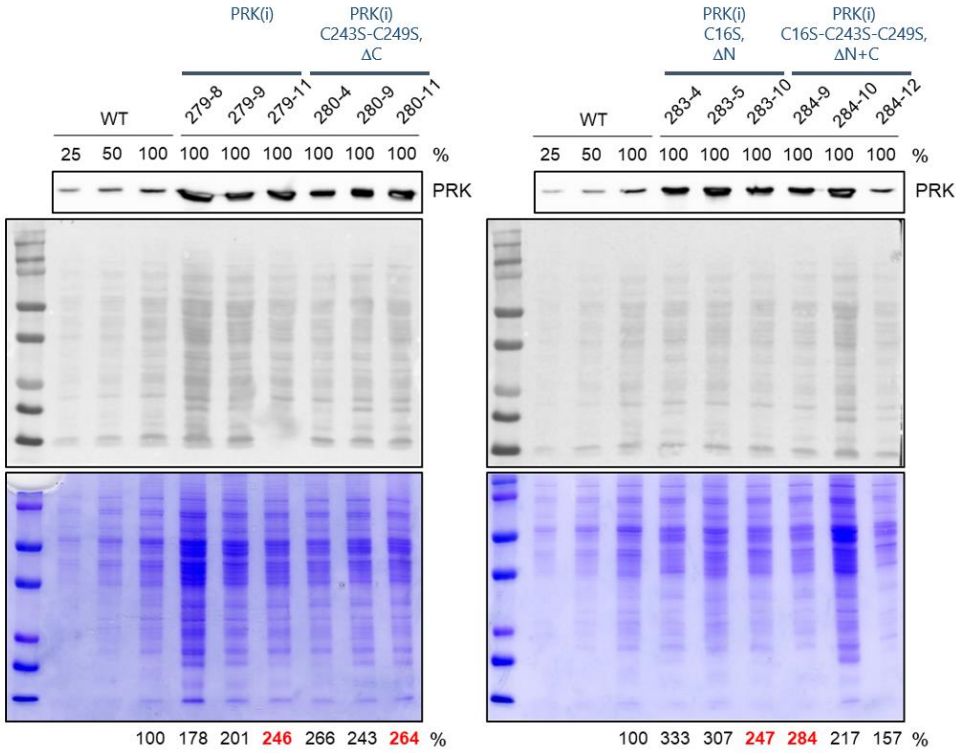

Figure 26. Immuno-blot anti-PRK sur des extraits totaux de protéines solubles chez la souche de référence CC-4533, notée WT, avec 3 quantités différentes chargées (100% correspond à 12 µg) et les transformants sélectionnés. La souche 279 est le contrôle sans mutation. Les mutants du pont C-terminal (C243S-C249S, ΔC), du pont N-terminal (C16S, ΔN), ou bien des deux (C16S-C243S-C249S, ΔN+C) sont annotés 280, 283 et 284, respectivement. Dans la partie inférieure, le témoin de charge est représenté par une coloration au bleu de Coomassie. (Travaux effectués par Manuel Jesús Ponce Mallén). L'abondance de la PRK dans chaque souche a été estimée par quantification du signal et normalisation par rapport à la référence (WT) et sont indiqués en dessous du gel. Les souches dont la quantité relative est inscrite en rouge sont celles sélectionnées pour des expériences préliminaires de phénotypage.

Les premiers résultats concernant l'impact de ces mutations sur la croissance des cellules à différentes intensités lumineuses sont présentés dans la Figure 27. La vitesse de croissance a été déterminée

à partir de cultures en photobioréacteurs. Différentes intensités lumineuses ont été testées pour observer l'impact de la quantité de pouvoir réducteur, qui augmente en fonction de l'intensité lumineuse, sur le pool de PRK sauvage et mutées. Les courbes de croissance des souches montrent des différences dépendantes de l'intensité lumineuse et des mutations introduites. En effet, en lumière faible (15 µmoles photons m^{-2} s^{-1}) ou en lumière moyenne (50 µmoles photons m^{-2} s^{-1}), les souches ΔN (283) et ΔN+C (284) présentent une croissance plus rapide que la souche exprimant la version sauvage (279) (Figure 27A). Leur taux de croissance a été déterminé et il est clairement supérieur à celui du contrôle (279). Ces différences ne sont pas observées en lumière forte, à une intensité lumineuse de 500 µmoles photons m^{-2} s^{-1}. Au contraire, la souche ΔC (280) présente une croissance similaire à celle de la souche contrôle (279) à toutes les intensités lumineuses. Après normalisation par rapport au contrôle (279), les mutants ΔN (283) et ΔN+C (284) présentent clairement des taux de croissance plus élevés en lumière faible et moyenne mais pas en lumière forte. De plus, le phénomène semble plus marqué en lumière faible qu'en lumière moyenne.

Ainsi, les deux variants mutés pour le pont disulfure N-terminal (ΔN et ΔN+C) présentent une croissance plus rapide que celle du contrôle (Figure 27). Ces résultats, bien que préliminaires, sont particulièrement intéressants. Il a été montré *in vitro* que le pont N-terminal de la PRK est réduit par des TRX dont le niveau de réduction est dépendant de l'intensité lumineuse, ce qui permet de coupler l'activité de la chaîne de transfert d'électrons à l'activation de la PRK. Les différences observées entre les conditions d'illumination peuvent donc s'interpréter en considérant l'état redox des TRX. On peut supposer qu'à une intensité inférieure à 500 µmol photons m^2 s^{-1}, la chaine de transfert des électrons génère, *a priori*, une quantité de pouvoir réducteur suffisante pour que le pool de TRX puisse être totalement réduit, et puisse donc activer totalement la PRK. A l'inverse, plus l'intensité lumineuse sera faible, plus le pool de TRX sera oxydé entrainant une diminution de l'activation de la PRK. Eliminer le pont disulfure N-terminal permet ainsi de s'affranchir de la régulation TRX *in vivo* qui semble donc limiter la croissance aux faibles intensités lumineuses. Ces résultats semblent montrer que la régulation par le

pont disulfure C16-C55 active bien la protéine *in vivo*, d'une façon lumière dépendante, validant les études réalisées *in vitro* depuis de nombreuses années (Gurrieri et al., 2019). Toutes les régulations redox des enzymes du CBBC identifiées *in vitro* pourraient être testées de la même manière (SBPase, FBPase, PGK, Rubisco Activase…).

A.

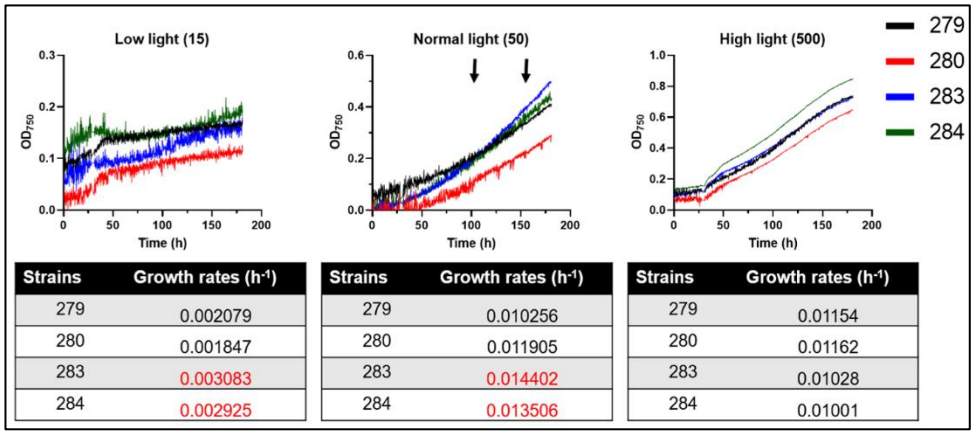

Strains	Growth rates (h⁻¹)
279	0.002079
280	0.001847
283	0.003083
284	0.002925

Strains	Growth rates (h⁻¹)
279	0.010256
280	0.011905
283	0.014402
284	0.013506

Strains	Growth rates (h⁻¹)
279	0.01154
280	0.01162
283	0.01028
284	0.01001

B.

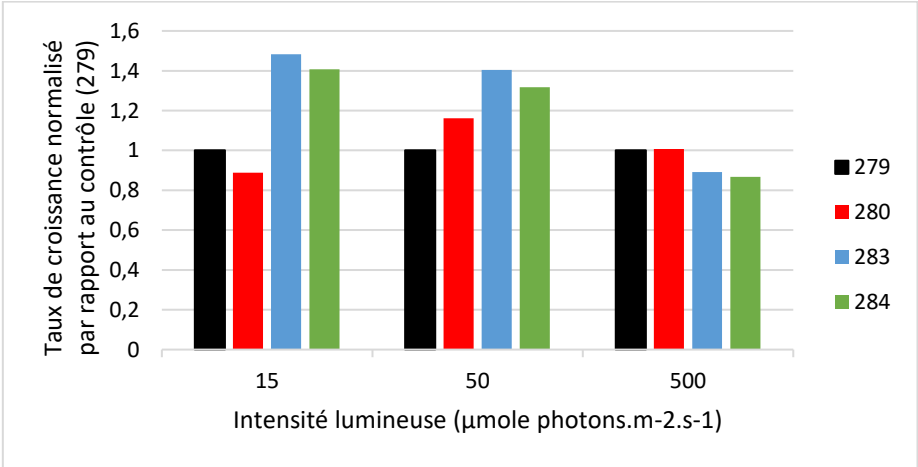

Figure 27. Première analyse de la croissance des variants PRK ΔN, ΔC et ΔN+C à différentes intensités de lumière. (Travaux effectués par Manuel Jesús Mallén Ponce). La souche 279 est le contrôle sans mutation. Les mutants du pont C-terminal (C243S-C249S, ΔC), du pont N-terminal (C16S, ΔN), ou bien des deux (C16S-C243S-C249S, ΔN+C) sont annotés 280, 283 et 284, respectivement. A. Données brutes des courbes de croissance avec les taux de croissance indiqués. B. Taux de croissance présentée en A normalisés par rapport au contrôle (279).

Ces premiers résultats suggèrent également que la régulation par les TRX pourraient être un levier d'amélioration du CBBC *in vivo*. En effet, alors que la surexpression de la PRK seule ne permet pas d'augmenter le taux de croissance, une surexpression combinée à une abolition de l'activation par les TRX semble une stratégie prometteuse à explorer à l'avenir. La modulation dépendante de la lumière des enzymes du CBBC par les TRX permet un ajustement fin de l'activité du CBBC probablement nécessaire pour une croissance et une survie optimale dans la nature sous des cycles lumière/obscurité photopériodiques naturels et dans un large éventail de conditions environnementales. Les microalgues ne sont cependant pas optimisées pour la croissance dans des conditions contrôlées de croissance en lumière continue. Dans ces conditions, l'existence de l'activation dépendante de la lumière par les TRX pourrait limiter l'efficacité du CBBC, comme le suggèrent nos résultats préliminaires. Ainsi, la conception d'enzymes du CBBC modifiées quant à leur régulation dépendante des TRX pourrait avoir un impact important sur la production de biomasse et l'efficacité de la fixation du carbone pour les cultures de Chlamydomonas cultivées dans des conditions contrôlées.

Enfin ces résultats n'ont pas montré de phénotype de croissance associé à la mutation du pont C-terminal seul (Figure 27). Ce pont contrôlerait indirectement l'activité PRK en modulant la formation du complexe GAPDH/CP12/PRK (Thieulin-Pardo et al., 2015). La fonction proposée du complexe tripartite serait de bloquer les enzymes en amont et en aval de la Rubisco pendant la nuit (Le Moigne et al., 2023). Il s'agirait donc d'un mécanisme plus lent et ne dépendant pas de l'intensité lumineuse, comme observé pour la souche 280 (Figure 27). Si la formation du complexe joue essentiellement un rôle inhibiteur à l'obscurité, il est cohérent de ne pas observer de phénotype pour le mutant ΔC dans nos conditions de culture en lumière continue.

Je tiens toutefois à rappeler que ces résultats sont très préliminaires car ces analyses du taux de croissance des mutants n'ont été effectuées qu'une seule fois. Il faudra bien évidemment confirmer ces résultats prometteurs en répétant l'expérience dans des conditions similaires. Il faudra également tester la croissance dans des conditions d'alternance lumière/obscurité afin d'explorer un rôle éventuel du pont C-terminal, mais également sur une gamme plus fine d'intensité lumineuses,

notamment entre 50 et 500 µmol photons m^2 s^{-1}. Des analyses complémentaires seront également nécessaires pour mieux caractériser ces souches dans les différentes conditions de croissance. Il sera intéressant de mesurer l'activité PRK ainsi que l'abondance des métabolites du CBBC par une approche métabolomique. Il pourra aussi être intéressant de mesurer l'état redox de la PRK par des expériences de redox-western et celui de la chaine de transfert des électrons par des mesures de cinétique de fluorescence.

3.2.2 Régulations par phosphorylation

Si la régulation par les TRX est bien connue (*cf*. 1.5.2 et 1.5.5), d'autres modifications post-traductionnelles ont été observées sur les enzymes du CBBC, y compris la PRK, mais dont la fonction est encore inconnue. C'est le cas de la phosphorylation, qui est une des modifications post-traductionnelles (PTM) les plus répandues chez tous les organismes (Hunter, 2007). D'après plusieurs études de phosphoprotéomique (Wang et al., 2014; Ma et al., 2018; McConnell et al., 2018), nous savons que 10 des 11 enzymes du CBBC chez *C. reinhardtii* sont phosphorylées, sans en connaître les fonctions. Un des points particulièrement intéressant que ces études révèlent est que beaucoup de protéines chloroplastiques sont phosphorylées mais relativement peu de protéines kinases et phosphatases ont été caractérisées dans ce compartiment cellulaire (White-Gloria et al., 2018).

Il est tout à fait possible que ces PTMs puissent être un des facteurs contrôlant l'activité que nous pourrions modifier pour augmenter l'efficacité photosynthétique de Chlamydomonas. Il a été identifié chez la PRK 4 sites de phosphorylation (T4, T57, S204 et S281). En remplaçant ces serines et thréonines par une alanine ou une aspartate, générant ainsi des variants phospho-mutant ou phosphomimétique, respectivement, il serait possible d'étudier l'impact de ces phosphorylations. En utilisant les outils développés et le savoir acquis, tels que le MoClo, la méthodologie de phénotypage et le design des circuits génétiques, nous pourrions rapidement construire des souches complémentant le mutant ΔPRK pour en identifier les fonctions. Bien sûr, la phosphorylation est un exemple, mais d'autres PTMs et d'autres enzymes du CBBC peuvent être analysées de la même manière.

3.3 Pourquoi la PRK est une cible pertinente pour l'amélioration de la fixation du carbone chez *Chlamydomonas reinhardtii*

La PRK est essentielle à la photosynthèse, nous l'avons démontré chez *C. reinhardtii* (*cf*. 2.1). Elle est très abondante (0,25% des protéines totales (Hammel et al., 2020) et son activité est spécifique du CBBC (Le Moigne et al., 2023). En modifiant non pas uniquement son abondance, mais aussi sa régulation par les TRX, il semblerait que nous puissions augmenter la production de biomasse. La notion de limitation du flux ne prend en compte que principalement l'abondance d'une enzyme. Il serait judicieux de développer un modèle comprenant aussi les régulations. En effet, il est tout à fait possible que les régulateurs, dans notre cas la quantité, la spécificité et le niveau de réduction des TRX, soient le facteur limitant le flux du CBBC et donc la production de biomasse.

Nous avons observé qu'une quantité de PRK inférieure ou égale à environ 40% du niveau endogène chez Chlamydomonas impacte la croissance. En augmentant la quantité native de PRK, la vitesse de croissance de la souche n'est pas impactée dans les conditions testées. Cela semble donc indiquer que la PRK est présente en quantité suffisante, voire en excès, par rapport aux autres enzymes du CBBC (*cf*. 2.1.2). Il est cependant aussi possible d'expliquer ce résultat par l'hypothèse que seule une partie du pool total d'enzyme serait activé par les TRXs, et donc pourrait fonctionner dans le CBBC. Ainsi, même en doublant la quantité de PRK, la proportion active ne serait pas modifiée puisque dépendante de la quantité de TRX réduite. Les résultats préliminaires obtenus par Manuel Jesús Mallén Ponce (*cf*. 3.2.1) semblent confirmer cette hypothèse. La piste de la PRK comme cible d'amélioration du flux du CBBC n'est donc pas exclue.

Par ailleurs, la PRK n'est pas trouvée uniquement chez les organismes photosynthétiques. En effet, la PRK est présente chez les bactéries et les Archaea (Kono et al., 2017). Or quelle peut être la fonction de la PRK dans un organisme non-photosynthétique ? Un début de réponse pourrait venir d'une étude d'Andrea M. Ochsner, qui montre que la PRK apparait essentielle à la méthylotrophie chez *Methylobacterium*

extorquens (Ochsner et al., 2017). Le mutant de la PRK dans cet organisme méthylotrophe ne croît pas sur un milieu avec du méthanol. La conservation du gène chez certains organismes semble indiquer l'existence d'une autre fonction non caractérisée jusqu'à aujourd'hui pour la PRK. Les connaissances acquises chez les organismes photosynthétiques pourraient donc être utilisés pour comprendre et même améliorer ces enzymes.

3.4 Perspectives : approche de paléobiochimie du CBBC

Mes travaux sur la PRK, et en particulier la méthodologie mise en place, ont permis d'ouvrir la voie à différentes études. Nous étudions la PRK actuelle issue de milliards d'années d'évolution. La phylogénétique a depuis de nombreuses années permit d'étudier les trajets évolutifs naturels. Des algorithmes d'inférence des séquences des protéines ancestrales, identifiées par la construction de phylogénies robustes, ont été développés (Toone, 2006; Yang, 2007; Garcia and Kaçar, 2019). Les séquences ainsi obtenues permettent de comparer les propriétés des séquences ancestrales avec leurs descendantes (Benner, 2017).

L'émergence de la biologie synthétique a permis des approches de paléobiochimie visant à synthétiser puis exprimer ces séquences ancestrales dans des organismes actuels pour étudier leurs caractéristiques structurales, biochimiques ou fonctionnelles (Ingles-Prieto et al., 2013; Shih et al., 2016; Schulz et al., 2022).

Puisque le CBBC est un facteur principal limitant l'efficacité de la photosynthèse, nous pouvons nous demander pourquoi une voie métabolique si importante n'a pas été plus optimisée ? Si l'une des hypothèses est que le CBBC est toujours soumis à l'évolution, il apparait pourtant avec le cas de la Rubisco que cela fait maintenant longtemps qu'elle n'est plus améliorée par bricolage moléculaire. En effet, l'évolution a sélectionné la photorespiration, les mécanismes de concentration du carbone ou encore la photosynthèse en C4 plutôt qu'une amélioration de la Rubisco. Cela pourrait s'expliquer par le fait que la Rubisco actuelle est devenue difficile à améliorer dans le contexte naturel. Si la Rubisco peut être améliorée par rational design, son évolvabilité est complexe (Durao et al., 2015), ce qui pourrait être lié à une contrainte de son chemin évolutif, comme le suggèrent des

analyses phylogénétiques (Bouvier et al., 2021). En d'autres termes, cette enzyme n'est pas une bonne base pour l'évoluer vers des solutions présentant une meilleure *fitness* (définie ici comme la capacité d'une protéine à réaliser une fonction). Une autre raison serait tout simplement qu'il n'existe pas de meilleure solution dans ce chemin évolutif et que la Rubisco actuelle est à une *fitness* maximale.

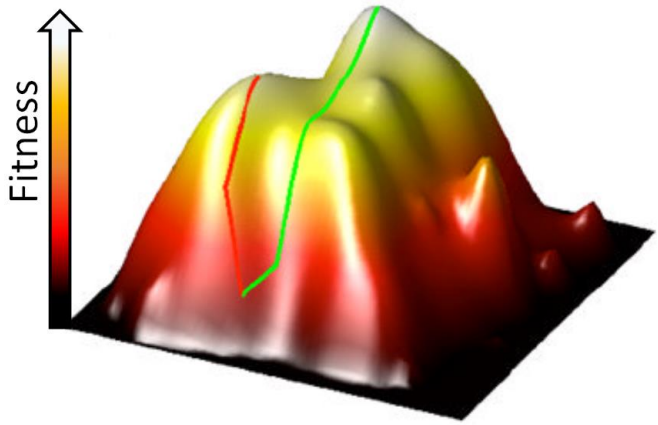

Figure 28. Exemple de fitness landscape des protéines.

Adapté de Romero et Arnold. Différents chemins évolutifs de la fitness d'une protéine (dans quelle mesure une protéine donnée remplit une fonction donnée) en fonction de sa séquence. Les deux lignes représentent des trajectoires différentes de l'évolution (dirigée). La trajectoire rouge a atteint un optimum local inférieur à celui théoriquement possible (vert) (Romero and Arnold, 2009).

Dans les deux cas, il est possible que d'autres chemins évolutifs existent et soient plus performants que celui choisi par hasard au cours de l'évolution naturelle (Romero and Arnold, 2009) (Figure 28). Nous pourrions donc tenter, en appliquant une approche de paléobiochimie de ressusciter des protéines ancestrales pour les faire réévoluer dans de nouvelles conditions environnementales. Une pression de sélection différente de celle exercée au cours de l'histoire évolutive naturelle pourrait permettre de créer de nouvelles trajectoires évolutives, en particulier pour les enzymes du CBBC.

Grâce à mon travail sur la PRK, tous les outils étaient disponibles pour pouvoir commencer ce projet ambitieux sur la PRK. Certaines

séquences ancestrales de PRK ont pu être inférées par Ingrid Lafontaine (Institut de Biologie Physico-Chimique) puis synthétisées. Leur fonctionnalité, leur fitness, sont en cours d'évaluation *in vitro* et *in vivo* par Maria Meloni et Marta Bertolini après un travail préliminaire réalisé par Giusi Favoino et Tanguy Chotel.

Ces séquences seront ensuite soumises à des expériences d'évolution dirigée dans l'objectif de savoir si des chemins évolutifs différents existent, et pourraient mener à des versions de l'enzyme avec une meilleur efficacité.

Giusi Favoino a obtenu des résultats préliminaires intéressants (Figure 29). Le mutant ΔPRK a pu être complémenté avec la séquence du dernier ancêtre commun aux algues verte de la PRK. Les données issues de mon travail (résultats partie 1) ont permis d'obtenir à la fois la méthodologie de sélection et les éléments génétiques nécessaires à une bonne expression du transgène.

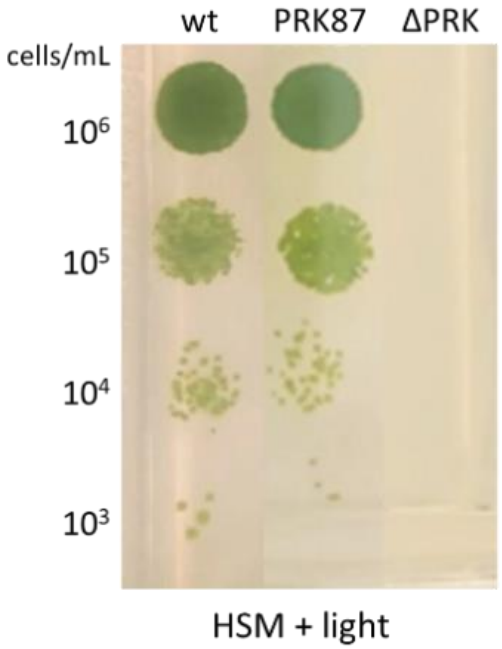

Figure 29. Spot test réalisé par Giusi Favoino sur la complémentation du mutant PRK par une séquence ancestrale de celle-ci dans des conditions de croissance en milieu minimum + lumière (50 µmol photons m^{-2} s^{-1}).

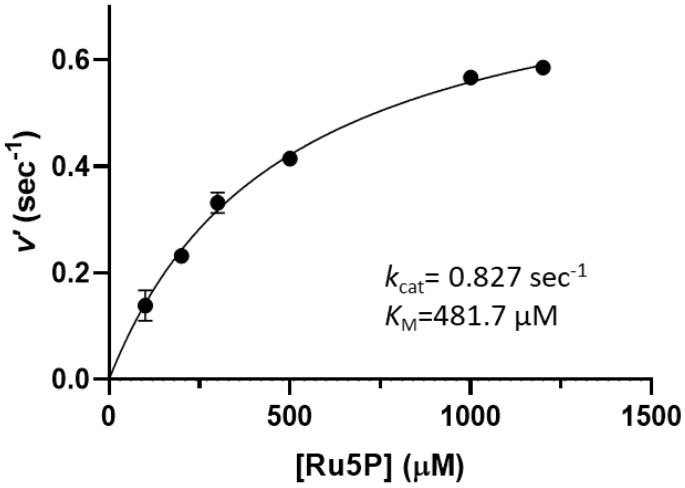

Figure 30. Paramètres fonctionnels d'une PRK ancestrale. Résultats obtenus par Maria Meloni.

Le dernier ancêtre commun des Archeae a été produit et purifié dans E. coli. *Son affinité pour le Ru5P ($K_{M\ Ru5P}$) et sa constante catalytique ($k_{cat\ Ru5P}$) ont été déterminées.*

Par ailleurs Maria Meloni a obtenu des résultats intéressants sur une PRK ancestrale, le dernier ancêtre commun des Archaea. Cette protéine a été produite chez *E. coli*, purifiée et utilisée pour déterminer ses paramètres cinétiques (Figure 30). Si l'on compare ces données à celles déjà connues de la PRK de *C. reinhardtii* ($k_{cat\ Ru5P}$= 262 sec^{-1}, $K_{M\ Ru5P}$= 87,5 µM), elles sont très éloignées. En effet, le k_{cat} de la paleo-PRK est 300 fois plus faible que celui de l'enzyme de Chlamydomonas et son K_M est cinq fois plus haut. Cette enzyme semble donc considérablement moins efficace que celle existant aujourd'hui. Cela renforce l'hypothèse que la PRK a bien évolué sur ses paramètres catalytiques. Si les résultats tendent à montrer cela sur toutes les protéines testées, alors nous avons déjà identifié un chemin évolutif.

Ces résultats encourageants permettront surement de mettre en place la bonne méthodologie pour ce projet de paléobiochimie.

3.5 Outils de biologie synthétique pour Chlamydomonas

La transformation d'un transgène, sa sélection et son expression sont

des problématiques de base de la biologie moléculaire et les outils génétiques nécessaires ont une importance centrale en biologie de synthèse.

3.5.1 Expression du gène PRK

Pour mener à bien la complémentation fonctionnelle du mutant ΔPRK chez Chlamydomonas, nous avons réalisé plusieurs cycles de design/build/test/learn. Cela nous a permis de comprendre, au moins partiellement, le rôle des éléments régulateurs du gène PRK pour une forte expression du transgène. En effet, nous avons en premier lieu utilisé un design qui nous semblait être la meilleure option pour obtenir une forte expression de la PRK. Basé sur nos connaissances, nous avions utilisé le promoteur, le 5'UTR et le 3'UTR/Terminateur du gène PSAD pour contrôler l'expression de la séquence codante de la PRK sans introns. En effet, nous avions précédemment montré que cette combinaison de briques issues du gène PSAD était la plus performante pour permettre la production de la nanoluciferase à partir d'une séquence codante également dépourvue d'introns (Crozet et al., 2018). Nos résultats ont montré que cette construction n'était pas optimale puisque le maximum d'expression obtenu, dans les conditions testées, ne dépassait pas 40% du niveau protéique de la souche de référence. Nous avons alors utilisé un nouveau design intégrant les éléments régulateurs du gène PRK. En effet, nous savons que la PRK représente environ 0,25% de la quantité totale de protéines d'une cellule (Hammel et al., 2020). Cela suggère que les éléments régulateurs du gène PRK, permettent ce très fort niveau d'expression. Nos analyses ont montré que combiné avec une séquence codante sans introns, le promoteur de la PRK ne suffisait pas pour obtenir une expression au moins équivalente à celle de la souche de référence. En revanche, nous avons observé une forte augmentation du niveau d'expression de notre transgène en utilisant la séquence génomique de la région codante du gène PRK, c'est-à-dire la séquence naturelle avec tous ses introns. Cette forte expression est observée aussi bien avec le promoteur/5'UTR du gène PRK qu'avec le promoteur/5'UTR du gène PSAD, ce qui suggère que c'est bien la présence des introns qui permet un fort niveau d'expression. Il est désormais bien établi que la présence d'introns dans la construction synthétique est souvent nécessaire pour assurer une expression élevée d'un transgène chez

Chlamydomonas (Lumbreras et Purton, 1998; Fuhrmann et al., 1999; Lauersen et al., 2018; Schroda, 2019; Baier et al., 2020). Il serait intéressant de déterminer si un ou plusieurs introns spécifiques du gène de la PRK sont responsables de ce phénomène, comme c'est le cas pour le premier intron du gène rbsc2, codant pour la petite sous-unité de la Rubisco (Baier *et al*. 2018, Baier *et al*. 2020). Pour cela il serait intéressant d'utiliser des construits synthétiques exprimant différents gènes rapporteurs (nanoluciférase et protéines fluorescentes présents dans le kit MoClo) dans lesquels un ou plusieurs introns de la PRK ont été introduits à l'aide de l'outil *Intronserter* développé pour Chlamydomonas (Jaeger et al., 2019). Il est intéressant de noter que ce sont des introns des gènes codant des enzymes du CBBC qui semblent avoir une fonction d'enhancer. Il existe peut-être des éléments régulateurs communs à ceux-ci. Des analyses bioinformatiques pourraient nous aider à répondre à cette question. Si tel était le cas, ces introns pourraient être utilisés de façon encore plus rationnelle pour le design de circuits génétiques.

En termes d'outils, le promoteur et les introns de la PRK que j'ai clonés et intégrés aux briques du kit MoClo pourront permettre de nouveaux designs pour des expressions fortes de transgènes chez *C. reinhardtii*.

3.5.2 La PRK comme marqueur de sélection ?

La multiplication des circuits génétiques dont les fonctions pourront s'additionner, à l'instar des modules électroniques composant les dispositifs informatiques, nécessitera de disposer de différents marqueurs de sélection pour s'assurer de la présence de chaque module. Le développement de nouveaux marqueurs de sélection, tel que le gène de résistance à la blasticidine, demeure donc un aspect important des développements en ingénierie biologique. La méthodologie décrite dans notre publication (*cf*. 2.2), en particulier la matrice de vérification que les gènes de résistance à un antibiotique ne confèrent la résistance qu'à une molécule, pourra être appliquée pour d'autres couples gène/molécule active.

Il existe encore des gènes de résistance disponibles chez les bactéries et les champignons qui pourront être adaptés à *C. reinhardtii*. Nous pouvons également imaginer l'utilisation de complémentations

fonctionnelles comme moyen aisé de sélection, comme l'utilisation de marqueurs d'auxotrophie comme LEU, HIS ou TRP couramment utilisés chez la levure ou chez les bactéries.

En effet, l'étude du mutant PRK nous a fourni des informations très utiles. La PRK étant essentielle à la photosynthèse, la complémentation du mutant PRK, même avec une expression modeste, permet de restaurer la croissance photoautotrophique perdue chez le mutant. Cette différence phénotypique pourra permettre d'utiliser le mutant PRK comme fond génétique afin de sélectionner aisément des transformants contenant le circuit génétique souhaité. Ce marqueur d'auxotrophie pourrait être utilisé pour réduire l'utilisation d'antibiotiques qui peuvent entraîner des conséquences néfastes sur la souche utilisée ou même pour l'environnement.

3.5.3 Impacts sociétaux de la biologie de synthèse

La biologie de synthèse offre des opportunités sans précédent pour transformer la société et relever des défis mondiaux. Toutefois, il est crucial d'aborder ces avancées avec prudence et de veiller à ce que les retombées positives soient équilibrées avec les préoccupations éthiques, environnementales et sociétales.

Depuis l'émergence de la biologie de synthèse, de nombreuses applications industrielles ont vu le jour, donnant naissance à un marché considérable, désigné sous le terme de bioéconomie ou économie du « *made by biology* ». Le marché mondial des biotechnologies et de la bioéconomie représente plus de 2 000 milliards d'euros dans l'Union Européenne (Flores Bueso et Tangney, 2017). La biologie de synthèse y joue un rôle important et devrait connaître un taux de croissance annuel moyen de 28%[1]. Cette expansion rapide ouvre la voie à une transformation de nos modes de production et de consommation, avec pour objectif de réduire l'impact de notre société sur la planète.

La biologie de synthèse et les biotechnologies en général suscitent de

[1] https://www.bccresearch.com/market-research/biotechnology/synthetic-biology-global-markets.htm

grands espoirs quant à leur potentiel pour résoudre divers problèmes mondiaux tels que la production durable d'énergie, la lutte contre les maladies et la sécurité alimentaire. Cependant, ces avancées technologiques soulèvent également des questions éthiques, sociales et environnementales. Les peurs et les préoccupations concernant l'utilisation de ces outils et technologies sont de plus en plus discutées afin de garantir que leurs bénéfices soient maximisés tout en identifiant et en atténuant les risques qui leurs sont associés (Wang and Zhang, 2019).

Il est essentiel d'impliquer les parties prenantes, telles que les décideurs politiques, les chercheurs, les industriels et le grand public, dans un dialogue ouvert et transparent sur les implications de la biologie de synthèse. Cela permettra de promouvoir une régulation adéquate et un développement responsable de cette discipline scientifique. De plus, l'éducation et la sensibilisation du public joueront un rôle crucial dans l'acceptation et l'adoption des innovations issues de la biologie de synthèse.

3.5.4 Considérations éthiques et environnementales en biologie de synthèse

Etant donné le potentiel de développement des applications de la biologie de synthèse, il est important d'examiner attentivement les implications éthiques, sociales et juridiques de ces technologies émergentes.

Sans énoncer tous les risques potentiels à différents niveaux, je trouve important en premier lieu de s'interroger sur la finalité de nos travaux dans la société et sur les risques liés à l'utilisation de nos technologies afin de définir quelles actions nous pouvons entreprendre à l'échelle du laboratoire.

D'un point de vue environnemental, une question préoccupante est de savoir si une souche que nous avons créée avec une fixation améliorée du carbone pourrait, si elle était introduite dans la nature, entrer en compétition avec des organismes existants. Bien qu'une souche de laboratoire pourrait présenter une croissance plus rapide, il est difficile de déterminer si, en cas de contamination environnementale, cette

souche pourrait supplanter des espèces sauvages. Les souches que nous utilisons dans les laboratoires évoluent dans des conditions idéales et contrôlés, sans compétiteurs, ni prédateurs et disposant de tous les nutriments nécessaires et cela depuis des décennies. Il est peu probable qu'elles puissent rivaliser avec des espèces naturelles résistantes aux stress environnementaux. Néanmoins, cela reste une possibilité. De plus, la possibilité d'une contamination de l'environnement par transfert horizontal de gène doit être envisagée.

La question n'est pas spécifique à mon sujet et différentes stratégies ont déjà été envisagées. Au-delà de la manipulation des souches modifiées dans un espace confiné et de leur destruction après utilisation, il est possible de prévenir les risques de contamination accidentelles en intégrant aux souches modifiées un ou plusieurs mécanismes de bio-confinement (Marliere, 2009). Par exemple, un système dit « *kill switch* » a été imaginé chez Chlamydomonas par l'équipe IGEM de Sorbonne Université 2020 (https://2020.igem.org/Team:Sorbonne_U_Paris/Description), qui repose sur un mécanisme de mort cellulaire programmée induit par le rayonnement UV et basé sur le relargage par clivage d'une nucléase ancrée sur la membrane plasmique contrôlé par la dimérisation de COP1 et UVR8. Ce *kill switch* permettrait de cultiver les algues dans des systèmes de culture équipés de filtres UV et d'assurer qu'en cas de contamination accidentelle de l'environnement, les algues, qui seront exposées à l'ensemble du spectre lumineux, seront tuées prématurément. Un autre système, le « *suicide system* » développé chez *E. coli*, permet de contrôler artificiellement la production d'une toxine pour s'assurer que la souche ne puisse pas survivre si elle se retrouve en dehors des conditions de culture établies. Ce système est basé sur l'établissement d'une auxotrophie pour une molécule synthétique, l'acide aminé 3-iodo-L-tyrosine, nécessaire pour la production d'une protéine inhibant la toxine colicine E3 (F. Wang & Zhang, 2019). D'autres types d'auxotrophies sont également envisageables. Toutefois, compte tenu des possibilités de contournements d'une unique stratégie de bio-confinement, il est crucial de mettre en place un ensemble de mesures comprenant plusieurs verrous pour réduire le risque de contamination accidentelle.

Il est important de rester humble et de reconnaître que nous ne

pouvons maitriser tous les risques en raison de la complexité du vivant. Nous étudions le vivant en regardant uniquement là où nous le pouvons. La biologie de synthèse est un domaine qui nous permet de repousser nos limites, de voir plus loin, d'apprendre et de conceptualiser une partie de la complexité du vivant. Etudier, construire, comprendre la nature, la photosynthèse, le cycle de Calvin Benson Bassham, nous permettra, espérons-le, d'améliorer notre système de production et plus largement d'apporter de grands bénéfices à notre civilisation. Il est donc essentiel de continuer à explorer et à innover dans ce domaine tout en restant conscients des responsabilités éthiques et environnementales qui en découlent.

Outre les considérations environnementales, il est crucial d'aborder les implications sociales et éthiques de la biologie de synthèse. Par exemple, les questions liées à l'accès et à la répartition des bénéfices des technologies émergentes doivent être examinées. Il est important d'assurer une distribution équitable des avantages et de veiller à ce que les pays en développement ne soient pas laissés pour compte. De plus, les questions de propriété intellectuelle et de brevetabilité des découvertes et innovations dans ce domaine sont également pertinentes et doivent être étudiées avec soin pour garantir un partage équitable des connaissances et favoriser la collaboration scientifique. Enfin, il est important d'engager un dialogue ouvert et transparent avec le public et les parties prenantes concernant les développements et les risques associés à la biologie de synthèse. Une communication claire et une éducation appropriée peuvent aider à dissiper les craintes et les malentendus, et à promouvoir une acceptation plus large de ces technologies potentiellement transformatrices.

En conclusion, la biologie de synthèse offre un potentiel considérable pour améliorer la durabilité de notre société et résoudre de nombreux défis mondiaux. Cependant, il est essentiel de rester attentif aux implications éthiques, environnementales et sociales de ces technologies et de mettre en place des mécanismes appropriés pour en minimiser les risques. En adoptant une approche responsable et éclairée, nous pouvons tirer le meilleur parti de la biologie de synthèse tout en protégeant notre environnement et notre société.

4 MATÉRIELS ET MÉTHODES

4.1 Matériels

4.1.1 Chlamydomonas reinhardtii

4.1.1.1 Souches

La souche de référence, parfois appelée sauvage ou *wild type* (WT), de Chlamydomonas utilisée a été la CC-4533 (CMJ030) qui est le fond génétique de la banque CLiP (Li *et al*, 2019). De cette banque de mutants, la souche LMJ.RY0402.119555 a été utilisée, dont l'insertion aléatoire de la cassette CIB1 portant le gène de résistance à la paromycine se trouve dans l'exon 7 du gène de la PRK (Cre12.g554800).

La souche D66 (Schnell and Lefebvre, 1993) a été utilisée pour le clonage du cDNA de la PRK.

4.1.1.2 Liste des souches utilisées

Nom de la souche	Fond génétique	Insertion
ΔPRK	LMJ.RY0402.119555	CIB1(résistance à la paromomycine)
CC-4533	cMJ030	
C12	ΔPRK	pM-11
C2	ΔPRK	pM-11
C4	ΔPRK	pM-11
C5	ΔPRK	pM-11
C6	ΔPRK	pM-11
C11	ΔPRK	pM-11

A	CC-4533	pM-162
B	CC-4533	pM-163
α	ΔPRK	pM-162
β	ΔPRK	pM-163
D	ΔPRK	pM1-11
No name	CC-4533	P1-128
No name	CC-1224	p1-128
No name	CC-4051	p1-128
No name	CC-4425	p1-128
No name	UVM4	p1-128
No name	CC-400	p1-128

4.1.1.3 Milieux de culture

Les souches de Chlamydomonas ont été cultivées en condition hétérotrophe ou mixotrophe dans du milieu Tris Acétate Phosphate (TAP, Gormant and Levine, 1965) à l'obscurité ou à la lumière, respectivement. Pour les cultiver en conditions phototrophe, un milieu minimum, le High Salt Medium (HSM, Sueoka, 1959), a été utilisé. Pour des cultures solides, 15 g/L d'agar for plant cell (Sigma-Aldrich) ont été ajoutés.

Les compositions exactes du TAP et HSM sont en annexe 1.

Lorsque nécessaire, un antibiotique a été ajouté aux milieux : paromomycine (20 µg/mL), hygromycine (20 µg/mL), spectinomycine (100 µg/mL), zeocyne (15 µg/mL) ou blasticidine (50 µg/mL) (Sigma-Aldrich).

4.1.2 Escherichia coli

4.1.2.1 Souche utilisée

La souche utilisée, NEB10β, pour tous les clonages provenait du fournisseur *New England Biolabs* (ref : C3019H).

Génotype de la souche NEB10β : Δ(ara-leu) 7697 araD139 fhuA ΔlacX74 galK16 galE15 e14- ϕ80dlacZΔM15 recA relA1 endA1 nupG rpsL (StrR) rph spoT1 Δ(mrr-hsdRMS-mcrBC)

4.1.2.2 Milieu de culture

Les bactéries ont été cultivées en milieu LB liquide ou solide (Sigma-Aldrich), supplémenté de l'antibiotique adapté : ampicilline (100 µg/mL), kanamycine (50 µg/mL) ou spectinomycine (50 µg/mL). Pour les sélections en milieu solide, du X-gal (80 µg /mL, Sigma-Aldrich) a également été ajouté.

4.1.3 Plasmides construits

4.1.3.1 p1-128

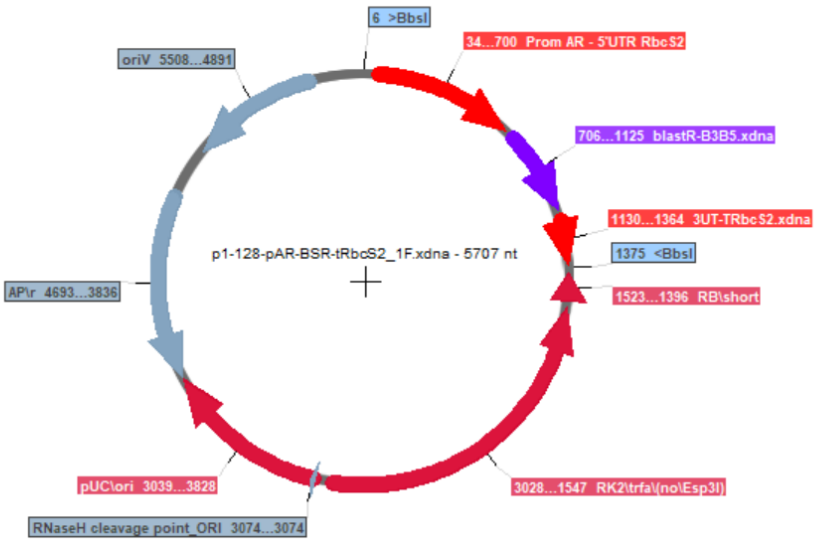

4.1.3.2 pM-11

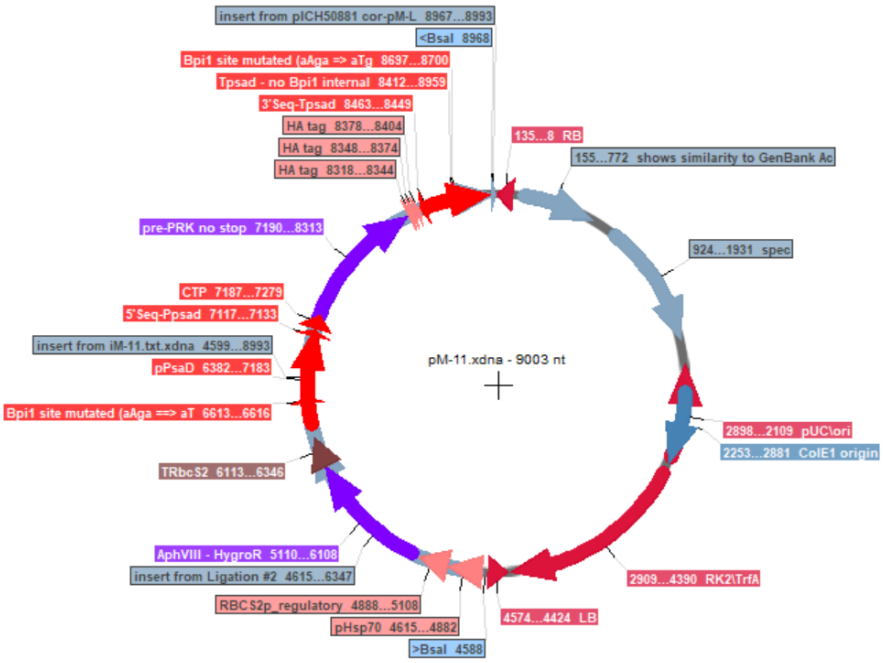

4.1.3.3 pM-162

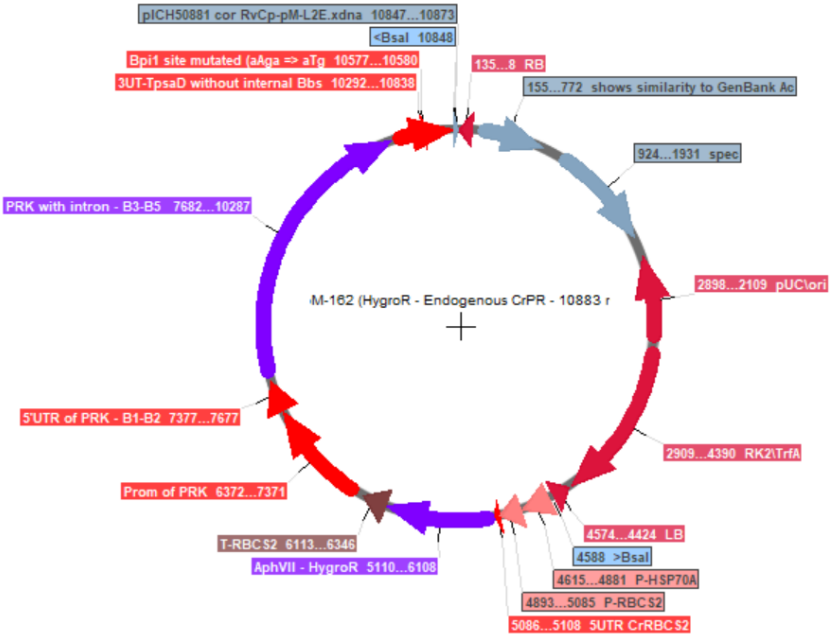

4.1.3.4 pM-163

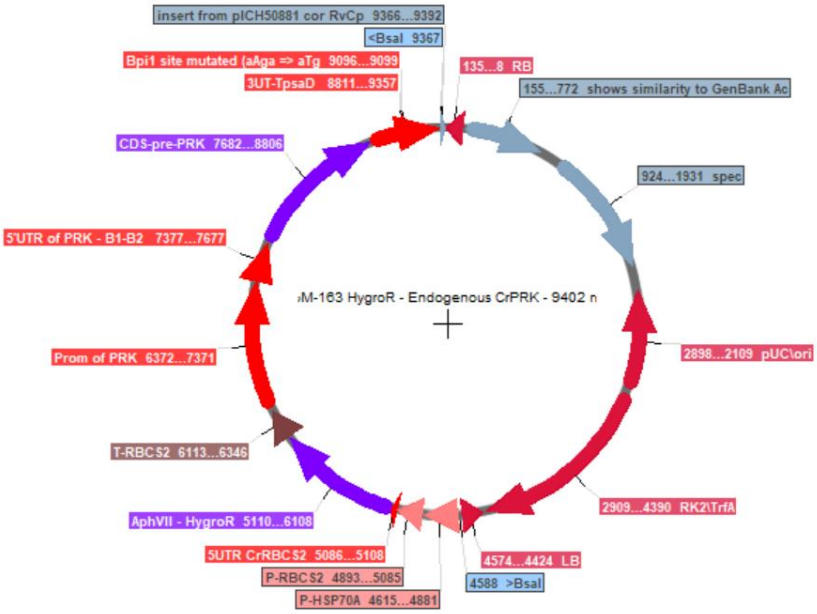

4.2 Méthodes

4.2.1 Méthodes de biologie moléculaire

Le travail *in silico* a été effectué sur Serial cloner 2.6.1 et Phytozome (https://phytozome-next.jgi.doe.gov/) (Blaby *et al.*, 2014).

4.2.1.1 Enzymes de clonage utilisées

Toutes les enzymes utilisées ont été fournies par *New Englands Biolabs* (Ipswitch, NY, USA) en version HF (High Fidelity) quand disponibles, soit *Bsa*I-HFv2, *Bbs*I-HF et T4 DNA ligase.

4.2.1.2 Clonage modulaire

Les plasmides pM-11, pM-162, pM-163 (*cf.* 4.1.3) ont été clonés par golden gate avec les plasmides du kit MoClo Chlamydomonas avec la méthode publiée dans (Crozet *et al.*, 2018) avec les plasmides receveurs de (Weber *et al.*, 2011). Les constructions ont été effectuées *in silico* sur le logiciel Serial Cloner 2.6.1 avant chaque réalisation. La

séquence de la protéine phosphoribulokinase PRK (Cre12.g55480; uniprot accession 19824) a été designée pour la position B4 du Chlamy MoClo (Crozet *et al.*, 2018) et obtenue par PCR sur ADNc pour la version sans intron, et sur ADN génomique pour la version avec introns.

Tous les plasmides récepteurs sont dérivés du kit MoClo original (Weber *et al.*, 2011). La séquence d'ADNc de la phosphoribulokinase PRK (Cre12.g554800 ; Uniprot accession P19824) a été obtenue par RT-PCR sur des extraits d'ARNm provenant d'une souche D66 (Schnell et Lefebvre, 1993) en utilisant les amorces TTGAAGACTTAATGGCTTTCACTATGCGCGC et TTGAAGACAACGACCACGGGCACAACGTCC. La séquence codante PRK résultante a été conçue pour la position B3-B4 du kit Chlamydomonas MoClo (Crozet *et al.*, 2018), et clonée dans le plasmide pAGM1287 (Weber *et al.*, 2011).

Deux autres constructions de niveau 0 ont été obtenues par PCR sur l'ADN génomique de la souche CC-4533 (*cf.* 1.2.2.4) en utilisant les amorces suivantes : TTGAAGACTTCTCAGGAGCCCTGGGCTTTAGCCCC et AAGAAGACAACTCGAGTACATGATGCATGTAACCAGCAATGAT pour le promoteur de PRK, TTGAAGACTTCTCATACTGCGTCTTGGGTCGGTGCGCT et CAGAAGACAACTCGCATTGGTAACAGCTCGACGC pour le 5'UTR de PRK, et TTGAAGACTTCTCAAATGGCTTTCACTATGCGCGC et TTGAAGACTTCTCAAATGGCTTTCACTATGCGCGCGC pour le CDS de PRK avec introns.
Chaque brique génique a été clonée dans le plasmide pAGM9121 (Patron *et al.*, 2015).

Les plasmides de niveau 1 ont été construits dans pICH47742 avec le promoteur et le 5'UTR du gène PSAD (Cre05.g238332) ou PRK, et le 3'UTR/Terminateur du gène PSAD contrôlant l'expression du CDS de PRK avec ou sans ses introns endogènes. Les plasmides de niveau M ont été construits dans pAGM8031 en combinant p1-013 (gène de résistance à l'hygromycine) (de Carpentier *et al.*, 2020) avec l'unité transcriptionnelle PRK, ce qui a donné pM-11 / pCMM-24 (PPSAD-PRKCDS), pM-162 / pCMM-25 (PPRK-PRKCDS) et pM-163 / pCMM-26

(PPRK-PRK(i)).

Le plasmide de niveau 1 conférant la résistance à la blasticidine pCM1-034 a été construit par assemblage du promoteur et 5'UTR PSAD (pCM0-016), du gène rapporteur mVenus (pCM0-086) et du terminateur et 3'UTR PSAD (pCM0-144) dans le plasmide accepteur pICH47732. L'unité de transcription de résistance à la blasticidine pCM1-029 a été assemblée à partir du promoteur PA/R couplé au 5'UTR de RBCS2 (pCM0-020), du gène BSR (pCM0-120) et du 3'UTR de RBCS2 couplé au terminateur RBCS2 (pCM0-115) dans le plasmide pICH47742. Les unités de transcription pCM1-034 (mVenus) et pCM1-029 (résistance à la blasticidine) ont été combinées dans le plasmide récepteur pAGM8031 pour obtenir le plasmide de niveau M pCMM-23.

Chaque réaction de MoClo a été réalisée avec 20 fmol de chaque brique, module ou plasmide receveur, dans un volume de 20 µL contenant 10 unités d'enzyme de restriction (*Bbs*I ou *Bsa*I) et 400 unités de T4 ligase. Les réactions ont été incubées dans un thermocycleur avec 3 cycles de 37°C 10 min puis 16°C 10 min, suivis d'une incubation finale à 37°C pendant 10 min.

4.2.1.3 Transformation d'*E. coli*

Les cellules d'*E. coli* NEB10β (ref NEB : C3019H) chemio-compétentes ont été transformées à l'aide d'un choc thermique. Un aliquote de cellules stockées à -80°C a été décongelé sur glace puis mélangé à l'ADN (4 µL d'une réaction Golden Gate de 20 µL) et incubé pendant 20 min à 4°C. Après un choc thermique à 42°C pendant 55 secondes, les cellules sont incubées à 4°C pendant 2 min avant d'être concentrée par centrifugation à 4000 *g* pendant 5 min à température ambiante. Le culot est resuspendu dans environ 100 µL avant d'être étalé sur boite LB Agar complémentée de l'antibiotique adéquat et de X-gal, le cas échéant. Les colonies blanches sont les souches devant porter le plasmide d'intérêt.

4.2.1.4 Mini-préparation d'ADN plasmidique d'*E. coli*

Des clones résistants à l'antibiotique, et blancs si un screen blanc/bleu a été réalisé en présence de X-gal, sont mis en culture dans du LB

complémenté de l'antibiotique approprié. Après 8 à 16h de culture à 37°C, les cellules sont collectées par centrifugation à 4000 *g* pendant 5 min à température ambiante. Le culot est ensuite soumis à une extraction plasmidique par lyse alcaline avec le kit de Macherey-Nagel (ref 740588.50) Les ADN plasmidiques purifiés sont ensuite dosés au spectrophotomètre de type *Nanodrop* par mesure d'absorbance à 260 nm. Enfin, un contrôle qualité est effectué sur ces plasmides par restriction différentielle. Dans le cas des plasmides de niveau 0, un deuxième contrôle qualité par séquençage (méthode de Sanger, sous-traité à Eurofins Genomics) a été réalisé.

4.2.2 Méthodes relatives à Chlamydomonas

4.2.2.1 Entretien et conservation

L'entretien et la conservation ont été effectuées sur boite solide TAP agar ou dans des cryotubes contenant 1 mL de TAP agar complémenté de cefotaxine sodium salt (Sigma-Aldrich) à une concentration de 50 g/L et repiquées à raison d'une fois par semaine pour un usage régulier ou de 1 fois toutes les deux semaines pour une conservation de souches. Un ensemble de souches mutant, WT et complémentés ont été congelées en utilisant le kit de cryopréservation pour algue de Gene art (invitrogen).

4.2.2.2 Transformation de Chlamydomonas

Pour les transformations de Chlamydomonas, l'insert a été séparé du plasmide le portant par l'enzyme de restriction adéquate, *Bsa*I ou *Bbs*I pour les pM ou p1, respectivement, et purifié à partir d'un gel d'agarose après électrophorèse et nettoyage par le kit Macherey-Nagel (PCR clean-up kit REF 740609.50). L'éluat final est dosé par spectrophotométrie au Nanodrop à 260 nm.

Les transformations de Chlamydomonas ont été réalisées selon le protocole de Stéphane Lemaire précédemment publié (De Carpentier *et al.*, 2020) pour l'obtention des souches A, B, Cx, D. L'antibiotique utilisé était l'hygromycine et le plasmide pM-11 (4.1.3.1).
Les cellules de *Chlamydomonas reinhardtii* ont été cultivées en TAP jusqu'à une concentration de 1 à 2 x 10^6 cellules/mL et concentrées

100 fois dans du TAP-sucrose 60 mM. Pour chaque transformation, 250 µL de suspension cellulaire ont été incubés au moins 20 min à 4°C en présence de 250 à 500 ng d'insert purifié. Les cellules ont été électroporées à 2000 $V.cm^{-1}$, 25 µF et sans résistance puis incubées dans 10 mL de TAP sucrose 60 mM pendant 16 à 20 h en faible lumière avant d'être étalées sur boites de TAP-agar supplémentées de l'antibiotique adéquat. Les transformants ont été génotypés après 5 à 7 jours de croissance à 100 µmol photons m^{-2} s^{-1}.

Une autre technique de transformation a été adaptée de la méthode publiée par Onishi et Pringle en 2016 (Onishi et Pringle, 2016). Les transformants α et β ont été générés à partir des plasmides pM162 (*cf*. 4.1.3.2) et pM-163 (*cf*. 4.1.3.2). Les colonies transformées ont été sélectionnées à partir de leur capacité de restaurer l'autotrophie du mutant ΔPRK en cas d'intégration du transgène.

Des cultures de *Chlamydomonas reinhardtii* en croissance exponentielle ont été concentrées à 2 x 10^8 cellules/mL dans 240 µL tampon CHES (10 mM CHES pH9,25 (Sigma-Aldrich : C2885), 40 mM sucrose et 10 mM sorbitol) contenant 1 µg de l'insert désiré. Le mélange a ensuite été incubé à 15°C sous agitation (700 rpm) pendant au moins 20 min et électroporé (1500 $V.cm^{-1}$, 25 µF et pas de résistance). Les cellules ont été incubées 16 à 20 h dans 13 mL de TAP-sucrose, puis étalées sur boîtes de HSM-agar et cultivées pendant 5 à 7 jours en lumière continue (100 µmol photons m^{-2} s^{-1}).

4.2.2.3 Extraction d'ADN génomique de *C. reinhardtii* et génotypage

L'ADN génomique a été extrait à partir d'une culture en TAP liquide en lumière continue (100 µmol photons m^{-2} s^{-1}) des colonies positives à la sélection. Les cellules cultivées jusqu'à 4-5 x 10^6 cellules.mL^{-1} ont été récoltées par centrifugation à 2500 *g* pendant 5 min à température ambiante (RT), puis lysées dans 400 µL de tampon d'extraction (Tris-HCl 0,2 M pH 7,5 ; NaCl 200 mM ; EDTA 25 mM ; SDS 0,5 %) pendant 10 min à 37 °C sous agitation (1400 rpm). Après centrifugation à 17000 *g* pendant 3 minutes à RT, l'ADN génomique contenu dans le surnageant a été précipité avec un volume d'isopropanol pendant 10 minutes à RT et recueilli par centrifugation à 17000 *g* pendant 10 minutes à RT. Le culot d'ADN a ensuite été lavé avec de l'éthanol à

70% (17000 *g* pendant 3 minutes à RT) puis séché à l'air avant d'être remis en suspension dans de l'eau MilliQ.

La détection de la présence de l'insertion de la cassette CIB1 ou l'insertion du plasmide pM-11 dans la souche mutante LMJ.RY0402.119555 a été réalisée à l'aide d'une PCR en utilisant le Quick-load 2x master mix (New England Biolab, M0271L) selon les recommandations du fabricant. Les amorces Plex5 (AAGGACGCTGACATG) et Plm1 (CCTGATGGATGGTTC) ont été utilisées pour la cassette CIB1 et Plex5 (AAGGACGCTGACATG) Plpsad3U (TTGAAGACAATCATCTCAATGGGTGTG) pour l'insert du plasmide pM-11. Le contrôle CC-4533 a été effectué avec les amorces Plex5 et Plen3U (AGGTGCCAAAGCAAC).

4.2.2.4 Extraction d'ARNm totaux de *C. reinhardtii* et reverse transcription

Vingt millions de cellules d'une culture en phase exponentielle de croissance (1-5 x 10^6 cellules.mL^{-1}) sont centrifugées (3000 *g* pendant 2 min à 4°C). Le culot de cellules est immédiatement remis en suspension dans 1 ml de tampon TRIzol Reagent (Gibco BRL), puis les polysaccharides et les membranes sont éliminés par centrifugation (12000 *g* pendant 10 min à 4°C). 200 µL de chloroforme sont ajoutés au surnageant puis, après agitation, le mélange est incubé pendant 2 minutes à température ambiante (RT). Après centrifugation (12000 *g* pendant 15 min à 4°C), trois phases apparaissent (en bas, les protéines, en haut, les ARN, et à l'interface des deux, les ADN). La phase du haut contenant les ARNs est prélevée précautionneusement sans toucher à la phase des ADN. 500 µL d'isopropanol sont ajoutés et, après agitation, sont incubés pendant 10 minutes à RT avant d'être centrifugés (12000 *g* pendant 15 min à 4°C) afin de précipiter l'ARN. Le culot est ensuite lavé avec 1 mL d'éthanol 70% (le mélange est vortexé puis centrifugé à 8000 *g* pendant 10 min à 4°C). Le culot est séché à l'air à RT jusqu'à ce qu'il devienne translucide (20 à 30 minutes environ). Les ARN totaux sont ensuite remis en suspension dans 20 µL d'eau MilliQ stérile.

Les ARN totaux ainsi préparés sont conservés à -20°C.

4.2.2.5 Spot test de C. reinhardtii

Les cellules de Chlamydomonas sont cultivées jusqu'à atteindre la phase exponentielle de croissance (1-5 x 10^6 cellules.mL^{-1}) puis diluées dans du TAP ou du HSM à une concentration de 1 millions de cellules.mL^{-1} dans une plaque 96 puits stérile. Trois dilutions en séries sont effectuées afin d'obtenir des cellules à une concentration de 1.10^6 à 1.10^4 cellules/mL. A partir de cette plaque, 10 µL de chaque souche et chaque dilution sont déposés sur boite TAP-agar ou HSM-agar. Les boites une fois sèches sont incubées en chambre de culture à une température de 25°C et à des intensités lumineuses variables. Un scan des boites est effectué à un temps variable en fonction du milieu à l'aide d'un scanner Perfection V800 photo (Epson).

4.2.2.6 Culture des cellules en photo-bioreacteur

Les analyses de croissance sont effectuées dans le système Algem® labscale double photobioreactor (Algenuity, Stewartby, United Kingdom) sous lumière continue 100 µmol photons m^{-2} s^{-1} à une agitation de 120 rpm dans du TAP ou du HSM. La culture est ensemencée à 0,1 x 10^6 cellules.mL^{-1}. L'absorbance à 740 nm est mesurée dans le photo-bioréacteur toutes les 10 min. La vitesse maximale de croissance est déterminée par la mesure de la pente maximale de la courbe de croissance (Δabs/Δtemps).

4.2.3 Méthodes de biochimie

4.2.3.1 Extraction des protéines totales

Les cellules de Chlamydomonas sont cultivées jusqu'à atteindre la phase exponentielle de croissance (1-5 x 10^6 cellules.mL^{-1}) en TAP ou HSM et concentrées 100 fois dans du tampon d'extraction (30 mM Tris-HCl pH7,9, 1 mM EDTA et une tablette pour 50 mL d'antiprotéase Sigmafast™ protease inhibitor cocktail tablets, EDTA free). Environ 150 µL de billes de verre (G8772 Sigma-Aldrich) sont ajoutés pour chaque échantillon. Les cellules sont lysées par 2 cycles de [10 secondes de vortex, 1 min à 4°C] puis centrifugées deux fois à 21000 *g* pendant 10 min à 4°C. Le surnageant clarifié contenant les protéines solubles totales est ensuite dosé par la méthode BCA (Sigma-Aldrich).

Après réalisation d'une gamme étalon avec de la BSA (Bovine Serum Albumine, (Sigma-Aldrich), 3 prises par échantillon sont utilisées pour réaliser une réaction avec le BCA (acide bicinchoninique) et l'absorbance est mesurée à 562 nm.

4.2.3.2 Western-blot

Les protéines solubles totales sont dénaturées dans le milieu de dénaturation (30 mM Tris-HCl pH6,5, 10% SDS, bleu de bromophénol, 10% glycérol) après chauffage à 95°C pendant 10 min. Elles sont ensuite soumises à une électrophorèse en gel de polyacrylamide-SDS (SDS-PAGE). Typiquement, un gel de résolution de 8% d'acrylamide était utilisé. Après environ 1h30 de migration en voltage continu (100 V) dans du tampon Tris-Glycine-SDS, les protéines du gel sont transférées sur une membrane de nitrocellulose (Sigma Aldrich) à l'aide d'un Trans-blot (Sigma Aldrich) dans un tampon Tris-Glycine-SDS (comme précédemment) complémenté de 20% d'éthanol. Après 30 min de transfert semi-sec à 15 V, les protéines de la membrane sont colorées à l'aide du rouge Ponceau (0,1% ponceau et 5% acide acétique 141194, Sigma Aldrich), pendant 1 min à RT sous agitation (30 rpm) avant que la membrane soit lavée à l'eau deux fois. Une acquisition d'image est réalisée à ce moment à l'aide d'un Chemidoc (Bio-Rad). La membrane est ensuite bloquée à l'aide d'une solution de lait écrémé (Régilait) 5% solubilisé dans du TBS 1x (Tris-Buffered Saline) pendant 1 h à RT sous agitation. L'anticorps primaire, dilué dans une solution de lait écrémé (Régilait) 1% solubilisé dans du TBS est ensuite incubé pendant une nuit à 4°C sous agitation.

La détection de la PRK a été faite à l'aide d'un anticorps polyclonal primaire généré chez le lapin (Covalab) contre la protéine recombinante. Cet anticorps a été utilisé à une dilution de 1/5000.

Après 4 lavages de 5 min à RT avec environ 30 mL de TBS-T (TBS 1x + 1% de Tween 20) sous agitation, un anticorps secondaire anti-lapin couplé à une péroxydase est utilisé à 1/10000 dans une solution de lait écrémé (Régilait) 1% solubilisé dans du TBS. Après 4 nouveaux lavages de 5 min à RT avec environ 30 mL de TBS-T sous agitation, la révélation est réalisée grâce au kit commercial ECL peroxydase assay (GE Healthcare, Chicago IL USA) et avec un Chemidoc (Bio-Rad, Hercules

CA USA).

4.2.3.3 Mesure d'activité de la PRK

La mesure d'activité de la PRK est une mesure de suivi sa consommation d'ATP via un couplage équimolaire avec le pyruvate kinase et la lactate déshydrogénase. La consommation du NADH utilité par la lactate déshydrogénase est suivi via spectrophotométrie à une longueur d'onde de 340 nm.

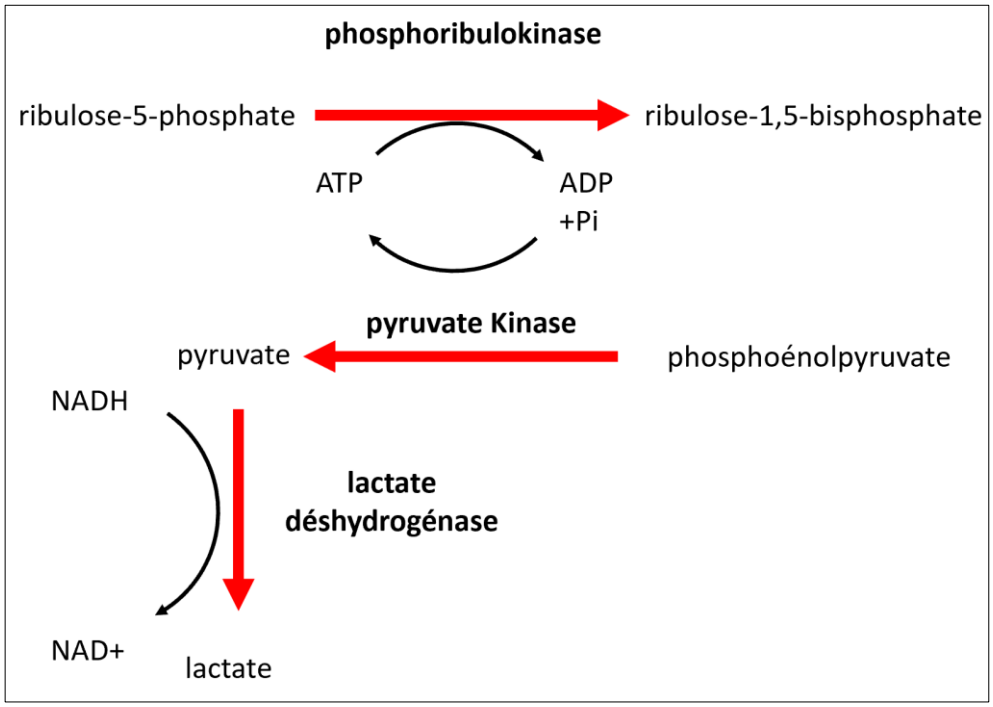

Figure 31. Réaction de couplage de la mesure d'activité de la phosphoribulokinase.

Cette mesure est réalisée sur des échantillons de protéines totales qui ont été dessalées sur une colonne Sephadex G-25 (GE Healthcare). Les échantillons ont ensuite été dosés par la méthode BCA. L'objectif étant de mesurer l'activité totale de la PRK, l'échantillon est incubé 30 min avec 30 mM de DTT à 30°C.

La réaction enzymatique en système couplé est réalisée dans un milieu réactionnel composé de 50 mM Tris-HCl pH 7,5; 1 mM EDTA, 40 mM KCl, 10 mM $MgCl_2$, de pyruvate kinase/lactate déshydrogénase 600-

1000 unités/mL et 900-1400 unités/mL respectivement (Sigma Aldrich : P0294), 2,5 mM phosphoénolpyruvate, 2 mM ATP (stock resuspendu dans du 0,1 M Tris-HCl pH7,9), 0,2 mM NADH. La réaction se mesure dans un volume total de 500 µL comprenant l'échantillon réduit (entre 300 µg et 500 µg). La mesure commence par l'ajout de 25 mM de ribulose-5-phosphate (Sigma Aldrich : 83899) après que la ligne de base devient droite et stable afin de mesurer l'activité parasite des déshydrogénases de l'échantillon consommant du NADH.

5 RÉFÉRENCES

Aboelmy, M. H., and Peterhansel, C. (2014). Enzymatic characterization of Chlamydomonas reinhardtii glycolate dehydrogenase and its nearest proteobacterial homologue. *Plant Physiology and Biochemistry* 79, 25–30. doi: 10.1016/j.plaphy.2014.03.009.

Adams, B. L. (2016). The Next Generation of Synthetic Biology Chassis: Moving Synthetic Biology from the Laboratory to the Field. *ACS Synth Biol* 5, 1328–1330. doi: 10.1021/acssynbio.6b00256.

Adler, L., Díaz-Ramos, A., Mao, Y., Pukacz, K. R., Fei, C., and McCormick, A. J. (2022). New horizons for building pyrenoid-based CO2-concentrating mechanisms in plants to improve yields. *Plant Physiol* 190, 1609–1627. doi: 10.1093/plphys/kiac373.

Aigner, H., Wilson, R. H., Bracher, A., Calisse, L., Bhat, J. Y., Hartl, F. U., *et al.* (2017). Plant RuBisCo assembly in E. coli with five chloroplast chaperones including BSD2. *Science (1979)* 358, 1272–1278. doi: 10.1126/science.aap9221.

Allahverdiyeva, Y., Mustila, H., Ermakova, M., Bersanini, L., Richaud, P., Ajlani, G., *et al.* (2013). Flavodiiron proteins Flv1 and Flv3 enable cyanobacterial growth and photosynthesis under fluctuating light. *Proc Natl Acad Sci U S A* 110, 4111–4116. doi: 10.1073/pnas.1221194110.

Allen, J. F. (2003). Cyclic, pseudocyclic and noncyclic photophosphorylation: new links in the chain. *Trends Plant Sci* 8, 15–19.

Alric, J. (2010). Cyclic electron flow around photosystem I in unicellular green algae. *Photosynth Res* 106, 47–56. doi: 10.1007/s11120-010-9566-4.

Amendola, S., Kneip, J. S., Meyer, F., Perozeni, F., Cazzaniga, S., Lauersen, K. J., *et al.* (2023). Metabolic Engineering for Efficient Ketocarotenoid Accumulation in the Green Microalga Chlamydomonas reinhardtii. *ACS Synth Biol* 12, 820–831. doi: 10.1021/acssynbio.2c00616.

Amthor, J. S., Bar-Even, A., Hanson, A. D., Millar, A. H., Stitt, M., Sweetlove,

L. J., *et al*. (2019). Engineering Strategies to Boost Crop Productivity by Cutting Respiratory Carbon Loss. *Plant Cell* 31, 297–314. doi: 10.1105/tpc.18.00743.

Arsova, B., Hoja, U., Wimmelbacher, M., Greiner, E., Ustun, S., Melzer, M., *et al*. (2010). Plastidial thioredoxin z interacts with two fructokinase-like proteins in a thiol-dependent manner: evidence for an essential role in chloroplast development in Arabidopsis and Nicotiana benthamiana. *Plant Cell* 22, 1498–1515. doi: 10.1105/tpc.109.071001 tpc.109.071001 [pii].

Asim, M., Zhang, Y., Sun, Y., Guo, M., Khan, R., Wang, X. L., *et al*. (2022). Leaf senescence attributes: the novel and emerging role of sugars as signaling molecules and the overlap of sugars and hormones signaling nodes. *Crit Rev Biotechnol*, 1–19. doi: 10.1080/07388551.2022.2094215.

Atkinson, N., Mao, Y., Chan, K. X., and McCormick, A. J. (2020). Condensation of Rubisco into a proto-pyrenoid in higher plant chloroplasts. *Nat Commun* 11, 6303. doi: 10.1038/s41467-020-20132-0.

Badger, M. R., and Price, G. D. (1994). The Role of Carbonic Anhydrase in Photosynthesis. *Annu Rev Plant Physiol Plant Mol Biol* 45, 369–392. doi: 10.1146/annurev.pp.45.060194.002101.

Baier, T., Jacobebbinghaus, N., Einhaus, A., Lauersen, K. J., and Kruse, O. (2020). Introns mediate post-Transcriptional enhancement of nuclear gene expression in the green microalga Chlamydomonas reinhardtii. *PLoS Genet* 16. doi: 10.1371/journal.pgen.1008944.

Baier, T., Wichmann, J., Kruse, O., and Lauersen, K. J. (2018). Intron-containing algal transgenes mediate efficient recombinant gene expression in the green microalga Chlamydomonas reinhardtii. *Nucleic Acids Res* 46, 6909–6919. doi: 10.1093/nar/gky532.

Banks, F. M., Driscoll, S. P., Parry, M. A. J., Lawlor, D. W., Knight, J. S., Gray, J. C., *et al*. (1999). Decrease in phosphoribulokinase activity by antisense RNA in transgenic tobacco. Relationship between photosynthesis, growth, and allocation at different nitrogen levels. *Plant Physiol* 119, 1125–1136.

Barahimipour, R., Neupert, J., and Bock, R. (2016). Efficient expression of nuclear transgenes in the green alga Chlamydomonas: synthesis of an HIV antigen and development of a new selectable marker. *Plant Mol Biol* 90, 403–418. doi: 10.1007/s11103-015-0425-8.

Barahimipour, R., Strenkert, D., Neupert, J., Schroda, M., Merchant, S. S., and Bock, R. (2015). Dissecting the contributions of GC content and codon usage to gene expression in the model alga Chlamydomonas reinhardtii. *Plant Journal* 84, 704–717. doi: 10.1111/tpj.13033.

Bar-Even, A. (2018). Daring metabolic designs for enhanced plant carbon fixation. *Plant Sci* 273, 71–83. doi: 10.1016/j.plantsci.2017.12.007.

Bar-Even, A., Noor, E., Lewis, N. E., and Milo, R. (2010). Design and analysis of synthetic carbon fixation pathways. *Proc Natl Acad Sci U S A* 107, 8889–8894. doi: 10.1073/pnas.0907176107.

Barnosky, A. D., Matzke, N., Tomiya, S., Wogan, G. O. U., Swartz, B., Quental, T. B., *et al*. (2011). Has the Earth's sixth mass extinction already arrived? *Nature* 471, 51–57. doi: 10.1038/nature09678.

Barrett, J., Girr, P., and Mackinder, L. C. M. (2021). Pyrenoids: CO2-fixing phase separated liquid organelles. *Biochim Biophys Acta Mol Cell Res* 1868. doi: 10.1016/j.bbamcr.2021.118949.

Bassham, J. A., Benson, A. A., Kay, L. D., Harris, A. Z., Wilson, A. T., and Calvin, M. (1954). The Path of Carbon in Photosynthesis. XXI. The Cyclic Regeneration of Carbon Dioxide Acceptor. *J Am Chem Soc* 76, 1760–1770. doi: 10.1021/ja01636a012.

Bedhomme, M., Adamo, M., Marchand, C. H., Couturier, J., Rouhier, N., Lemaire, S. D., *et al*. (2012). Glutathionylation of cytosolic glyceraldehyde-3-phosphate dehydrogenase from the model plant Arabidopsis thaliana is reversed by both glutaredoxins and thioredoxins in vitro. *Biochem J* 445, 337–347. doi: 10.1042/BJ20120505.

Benner, S. (2017). Uniting natural history with the molecular sciences. the ultimate multidisciplinarity. *Acc Chem Res* 50, 498–502. doi: 10.1021/acs.accounts.6b00496.

Benson, A. A., Bassham, J. A., Calvin, M., Hall, A. G., Hirsch, H. E., Kawaguchi, S., *et al*. (1952). The path of carbon in photosynthesis. XV. Ribulose and sedoheptulose. *J Biol Chem* 196, 703–716. Available at: http://www.ncbi.nlm.nih.gov/pubmed/12981011.

Bergner, S. V, Scholz, M., Trompelt, K., Barth, J., Gäbelein, P., Steinbeck, J., *et al*. (2015). STATE TRANSITION7-Dependent Phosphorylation Is Modulated by Changing Environmental Conditions, and Its Absence Triggers Remodeling of Photosynthetic Protein Complexes. *Plant Physiol* 168, 615–634. doi: 10.1104/pp.15.00072.

Berthold, P., Schmitt, R., and Mages, W. (2002). Introduction An Engineered Streptomyces hygroscopicus aph 7′′ Gene Mediates Dominant Resistance against Hygromycin B in Chlamydomonas reinhardtii. Available at: http://www.urbanfischer.de/journals/protist.

Blaby, I. K., Blaby-Haas, C. E., Perez-Perez, M. E., Schmollinger, S., Fitz-Gibbon, S., Lemaire, S. D., *et al*. (2015). Genome-wide analysis on Chlamydomonas reinhardtii reveals the impact of hydrogen peroxide on protein stress responses and overlap with other stress transcriptomes. *Plant J* 84, 974–988. doi: 10.1111/tpj.13053.

Blaby, I. K., Glaesener, A. G., Mettler, T., Fitz-Gibbon, S. T., Gallaher, S. D., Liu, B., *et al*. (2013). Systems-level analysis of nitrogen starvation–induced modifications of carbon metabolism in a Chlamydomonas reinhardtii starchless mutant. *Plant Cell* 25, 4305–4323.

Boehm, M., Alahuhta, M., Mulder, D. W., Peden, E. A., Long, H., Brunecky, R., *et al*. (2016). Crystal structure and biochemical characterization of Chlamydomonas FDX2 reveal two residues that, when mutated, partially confer FDX2 the redox potential and catalytic properties of FDX1. *Photosynth Res* 128, 45–57. doi: 10.1007/s11120-015-0198-6.

Boeke, J. D., Church, G., Hessel, A., Kelley, N. J., Arkin, A., Cai, Y., *et al*. (2016). GENOME ENGINEERING. The Genome Project-Write. *Science* 353, 126–127. doi: 10.1126/science.aaf6850.

Bouvier, J. W., Emms, D. M., Rhodes, T., Bolton, J. S., Brasnett, A., Eddershaw, A., *et al*. (2021). Rubisco Adaptation Is More Limited by Phylogenetic Constraint Than by Catalytic Trade-off. 38, 2880–2896. doi:

10.1093/molbev/msab079.

Buchanan, B. B. (2016). The Path to Thioredoxin and Redox Regulation in Chloroplasts. *Annu Rev Plant Biol* 67, 1–24. doi: 10.1146/annurev-arplant-043015-111949.

Buck, J. M., Bártulos, C. R., Gruber, A., and Kroth, P. G. (2018). Blasticidin-S deaminase, a new selection marker for genetic transformation of the diatom Phaeodactylum tricornutum. *PeerJ* 2018. doi: 10.7717/peerj.5884.

Burki, F., Shalchian-Tabrizi, K., Minge, M., Skjæveland, Å., Nikolaev, S. I., Jakobsen, K. S., *et al*. (2007). Phylogenomics reshuffles the eukaryotic supergroups. *PLoS One* 2, 1–6. doi: 10.1371/journal.pone.0000790.

Cameron, D. E., Bashor, C. J., and Collins, J. J. (2014). A brief history of synthetic biology. *Nat Rev Microbiol*. doi: 10.1038/nrmicro3239.

Casini, A., Storch, M., Baldwin, G. S., and Ellis, T. (2015). Bricks and blueprints: Methods and standards for DNA assembly. *Nat Rev Mol Cell Biol*. doi: 10.1038/nrm4014.

Cello, J., Paul, A. V., and Wimmer, E. (2002). Chemical synthesis of poliovirus cDNA: Generation of infectious virus in the absence of natural template. *Science (1979)* 297, 1016–1018. doi: 10.1126/science.1072266.

Chankova, S. G., Dimova, E., Dimitrova, M., and Bryant, P. E. (2007). Induction of DNA double-strand breaks by zeocin in Chlamydomonas reinhardtii and the role of increased DNA double-strand breaks rejoining in the formation of an adaptive response. *Radiat Environ Biophys* 46, 409–416. doi: 10.1007/s00411-007-0123-2.

Chapman, M. S., Suh, S. W., Curmi, P. M., Cascio, D., Smith, W. W., and Eisenberg, D. S. (1988). Tertiary structure of plant RuBisCO: domains and their contacts. *Science (1979)* 241, 71–74. doi: 10.1126/science.3133767.

Charoenwattanasatien, R., Zinzius, K., Scholz, M., Wicke, S., Tanaka, H., Brandenburg, J. S., *et al*. (2020). Calcium sensing via EF-hand 4 enables

thioredoxin activity in the sensor-responder protein calredoxin in the green alga Chlamydomonas reinhardtii. *J Biol Chem* 295, 170–180. doi: 10.1074/jbc.RA119.008735.

Chaux, F., Burlacot, A., Mekhalfi, M., Auroy, P., Blangy, S., Richaud, P., *et al*. (2017). Flavodiiron Proteins Promote Fast and Transient O(2) Photoreduction in Chlamydomonas. *Plant Physiol* 174, 1825–1836. doi: 10.1104/pp.17.00421.

Chiadmi, M., Navaza, A., Miginiac-Maslow, M., Jacquot, J. P., and Cherfils, J. (1999). Redox signalling in the chloroplast: structure of oxidized pea fructose-1,6-bisphosphate phosphatase. *EMBO J* 18, 6809–6815. Available at: http://www.ncbi.nlm.nih.gov/entrez/query.fcgi?cmd=Retrieve&db=PubMed&dopt=Citation&list_uids=10581254.

Chibani, K., Wingsle, G., Jacquot, J. P., Gelhaye, E., and Rouhier, N. (2009). Comparative genomic study of the thioredoxin family in photosynthetic organisms with emphasis on Populus trichocarpa. *Mol Plant* 2, 308–322. doi: ssn076 [pii] 10.1093/mp/ssn076.

Čížková, M., Slavková, M., Vítová, M., Zachleder, V., and Bišová, K. (2019). Response of the green alga Chlamydomonas reinhardtii to the DNA damaging agent zeocin. *Cells* 8. doi: 10.3390/cells8070735.

Clapero, V., Arrivault, S., and Stitt, M. (2023). Natural variation in metabolism of the Calvin-Benson cycle. *Semin Cell Dev Biol*. doi: 10.1016/j.semcdb.2023.02.015.

Courteille, A., Vesa, S., Sanz-Barrio, R., Cazale, A. C., Becuwe-Linka, N., Farran, I., *et al*. (2013). Thioredoxin m4 controls photosynthetic alternative electron pathways in Arabidopsis. *Plant Physiol* 161, 508–520. doi: 10.1104/pp.112.207019 pp.112.207019 [pii].

Cowie, R. H., Bouchet, P., and Fontaine, B. (2022). The Sixth Mass Extinction: fact, fiction or speculation? *Biological Reviews* 97, 640–663. doi: 10.1111/brv.12816.

Craig, R. J., Gallaher, S. D., Shu, S., Salomé, P. A., Jenkins, J. W., Blaby-Haas, C. E., *et al*. (2023). The Chlamydomonas Genome Project, version 6:

Reference assemblies for mating-type plus and minus strains reveal extensive structural mutation in the laboratory. *Plant Cell* 35, 644–672. doi: 10.1093/plcell/koac347.

Croft, M. T., Lawrence, A. D., Raux-Deery, E., Warren, M. J., and Smith, A. G. (2005). Algae acquire vitamin B12 through a symbiotic relationship with bacteria. *Nature* 438, 90–93. doi: 10.1038/nature04056.

Crozet, P., Navarro, F. J., Willmund, F., Mehrshahi, P., Bakowski, K., Lauersen, K. J., *et al*. (2018). Birth of a Photosynthetic Chassis: A MoClo Toolkit Enabling Synthetic Biology in the Microalga Chlamydomonas reinhardtii. *ACS Synth Biol* 7, 2074–2086. doi: 10.1021/acssynbio.8b00251.

da Fonseca-Pereira, P., Siqueira, J. A., Monteiro-Batista, R. C., Vaz, M., Nunes-Nesi, A., and Araujo, W. L. (2022). Using synthetic biology to improve photosynthesis for sustainable food production. *J Biotechnol* 359, 1–14. doi: 10.1016/j.jbiotec.2022.09.010.

Dai, S., Friemann, R., Glauser, D. A., Bourquin, F., Manieri, W., Schürmann, P., *et al*. (2007). Structural snapshots along the reaction pathway of ferredoxin-thioredoxin reductase. *Nature* 448, 92–96. Available at: http://www.ncbi.nlm.nih.gov/entrez/query.fcgi?cmd=Retrieve&db=PubMed&dopt=Citation&list_uids=17611542.

Dang, K. V, Plet, J., Tolleter, D., Jokel, M., Cuine, S., Carrier, P., *et al*. (2014). Combined increases in mitochondrial cooperation and oxygen photoreduction compensate for deficiency in cyclic electron flow in Chlamydomonas reinhardtii. *Plant Cell* 26, 3036–3050. doi: 10.1105/tpc.114.126375.

De Carpentier, F., Le Peillet, J., Boisset, N. D., Crozet, P., Lemaire, S. D., and Danon, A. (2020). Blasticidin S Deaminase: A New Efficient Selectable Marker for Chlamydomonas reinhardtii. *Front Plant Sci* 11, 242. doi: 10.3389/fpls.2020.00242.

Dean Price, G., Badger, M. R., and von Caemmerer, S. (2011). The prospect of using cyanobacterial bicarbonate transporters to improve leaf photosynthesis in C3 crop plants. *Plant Physiol* 155, 20–26. doi: 10.1104/pp.110.164681.

Desplats, C., Mus, F., Cuiné, S., Billon, E., Cournac, L., and Peltier, G. (2009). Characterization of Nda2, a plastoquinone-reducing type II NAD (P) H dehydrogenase in Chlamydomonas chloroplasts. *Journal of Biological Chemistry* 284, 4148–4157.

Diaz, M. G., Hernandez-Verdeja, T., Kremnev, D., Crawford, T., Dubreuil, C., and Strand, A. (2018). Redox regulation of PEP activity during seedling establishment in Arabidopsis thaliana. *Nat Commun* 9, 50. doi: 10.1038/s41467-017-02468-2.

Dietz, K. J. (2011). Peroxiredoxins in plants and cyanobacteria. *Antioxid Redox Signal* 15, 1129–1159. doi: 10.1089/ars.2010.3657.

Ding, F., Wang, M., Zhang, S., and Ai, X. (2016). Changes in SBPase activity influence photosynthetic capacity, growth, and tolerance to chilling stress in transgenic tomato plants. *Sci Rep* 6, 32741. doi: 10.1038/srep32741.

Dong, Y., Sun, F., Ping, Z., Ouyang, Q., and Qian, L. (2020). DNA storage: Research landscape and future prospects. *Natl Sci Rev* 7, 1092–1107. doi: 10.1093/nsr/nwaa007.

Driever, S. M., Simkin, A. J., Alotaibi, S., Fisk, S. J., Madgwick, P. J., Sparks, C. A., *et al*. (2017). Increased sbpase activity improves photosynthesis and grain yield in wheat grown in greenhouse conditions. *Philosophical Transactions of the Royal Society B: Biological Sciences* 372. doi: 10.1098/rstb.2016.0384.

Durao, P., Aigner, H., Nagy, P., Mueller-Cajar, O., Hartl, F. U., and Hayer-Hartl, M. (2015). Opposing effects of folding and assembly chaperones on evolvability of Rubisco. *Nat Chem Biol* 11, 148–155. doi: 10.1038/nchembio.1715.

Eckardt, N. A., Ainsworth, E. A., Bahuguna, R. N., Broadley, M. R., Busch, W., Carpita, N. C., *et al*. (2023). Climate change challenges, plant science solutions. *Plant Cell* 35, 24–66. doi: 10.1093/plcell/koac303.

Eckardt, N. A., Snyder, G. W., Portis, A. R., and Ogren, W. L. (1997). Growth and photosynthesis under high and low irradiance of Arabidopsis thaliana antisense mutants with reduced ribulose-1,5-bisphosphate

carboxylase/oxygenase activase content. *Plant Physiol* 113, 575–586. doi: 10.1104/pp.113.2.575.

Endy, D. (2005). Foundations for engineering biology. *Nature*. doi: 10.1038/nature04342.

Endy, D. (2011). Building a new biology. *Comptes Rendus Chimie* 14, 424–428. doi: 10.1016/j.crci.2010.11.013.

Engel, B. D., Schaffer, M., Kuhn Cuellar, L., Villa, E., Plitzko, J. M., and Baumeister, W. (2015). Native architecture of the Chlamydomonas chloroplast revealed by in situ cryo-electron tomography. *Elife* 4. doi: 10.7554/eLife.04889.

Engler, C., Kandzia, R., and Marillonnet, S. (2008). A one pot, one step, precision cloning method with high throughput capability. *PLoS One* 3. doi: 10.1371/journal.pone.0003647.

English, M. A., Gayet, R. V., and Collins, J. J. (2021). Designing Biological Circuits: Synthetic Biology within the Operon Model and beyond. *Annu Rev Biochem* 90, 221–244. doi: 10.1146/annurev-biochem-013118-111914.

Erb, T. J., and Zarzycki, J. (2016). Biochemical and synthetic biology approaches to improve photosynthetic CO2-fixation. *Curr Opin Chem Biol* 34, 72–79. doi: 10.1016/J.CBPA.2016.06.026.

Ermakova, M., Lopez-Calcagno, P. E., Furbank, R. T., Raines, C. A., and von Caemmerer, S. (2023). Increased sedoheptulose-1,7-bisphosphatase content in Setaria viridis does not affect C4 photosynthesis. *Plant Physiol* 191, 885–893. doi: 10.1093/plphys/kiac484.

Fang, L., Lin, H. X., Low, C. S., Wu, M. H., Chow, Y., and Lee, Y. K. (2012). Expression of the Chlamydomonas reinhardtii sedoheptulose-1,7-bisphosphatase in Dunaliella bardawil leads to enhanced photosynthesis and increased glycerol production. *Plant Biotechnol J* 10, 1129–1135. doi: 10.1111/pbi.12000.

Farr, T. J., Huppe, H. C., and Turpin, D. H. (1994). Coordination of Chloroplastic Metabolism in N-Limited Chlamydomonas reinhardtii by

Redox Modulation (I. The Activation of Phosphoribulosekinase and Glucose-6-Phosphate Dehydrogenase Is Relative to the Photosynthetic Supply of Electrons). *Plant Physiol* 105, 1037–1042. doi: 10.1104/pp.105.4.1037.

Fauser, F., Vilarrasa-Blasi, J., Onishi, M., Ramundo, S., Patena, W., Millican, M., *et al*. (2022). Systematic characterization of gene function in the photosynthetic alga Chlamydomonas reinhardtii. *Nat Genet* 54, 705–714. doi: 10.1038/s41588-022-01052-9.

Federici, F., Rudge, T. J., Pollak, B., Haseloff, J., and Gutiérrez, R. A. (2013). Synthetic Biology: Opportunities for Chilean Bioindustry and education. *Biol Res* 46, 383–393. doi: 10.4067/S0716-97602013000400010.

Fei, C., Wilson, A. T., Mangan, N. M., Wingreen, N. S., and Jonikas, M. C. (2022). Modelling the pyrenoid-based CO2-concentrating mechanism provides insights into its operating principles and a roadmap for its engineering into crops. *Nat Plants* 8, 583–595. doi: 10.1038/s41477-022-01153-7.

Fell, D. A., and Fell, D. (1997). Understanding the Control of Metabolism Cell cycle simulation View project Metabolic control analysis View project Understanding the Control of Metabolism. Available at: https://www.researchgate.net/publication/317369476.

Feng, L., Li, H., Jiao, J., Li, D., Zhou, L., Wan, J., *et al*. (2009). Reduction in SBPase Activity by Antisense RNA in Transgenic Rice Plants: Effect on Photosynthesis, Growth, and Biomass Allocation at Different Nitrogen Levels. *Journal of Plant Biology* 52, 382–394. doi: 10.1007/s12374-009-9049-3.

Ferenczi, A., Pyott, D. E., Xipnitou, A., and Molnar, A. (2017). Efficient targeted DNA editing and replacement in Chlamydomonas reinhardtii using Cpf1 ribonucleoproteins and single-stranded DNA. *Proc Natl Acad Sci U S A* 114, 13567–13572. doi: 10.1073/pnas.1710597114.

Fermani, S., Ripamonti, A., Sabatino, P., Zanotti, G., Scagliarini, S., Sparla, F., *et al*. (2001). Crystal structure of the non-regulatory A(4)isoform of spinach chloroplast glyceraldehyde-3-phosphate dehydrogenase

complexed with NADP. *J Mol Biol* 314, 527–542. Available at: http://www.ncbi.nlm.nih.gov/entrez/query.fcgi?cmd=Retrieve&db=PubMed&dopt=Citation&list_uids=11846565.

Fermani, S., Sparla, F., Falini, G., Martelli, P. L., Casadio, R., Pupillo, P., *et al*. (2007). Molecular mechanism of thioredoxin regulation in photosynthetic A2B2-glyceraldehyde-3-phosphate dehydrogenase. *Proc Natl Acad Sci U S A* 104, 11109–11114. Available at: http://www.ncbi.nlm.nih.gov/entrez/query.fcgi?cmd=Retrieve&db=PubMed&dopt=Citation&list_uids=17573533.

Fermani, S., Sparla, F., Marri, L., Thumiger, A., Pupillo, P., Falini, G., *et al*. (2010). Structure of photosynthetic glyceraldehyde-3-phosphate dehydrogenase (isoform A4) from Arabidopsis thaliana in complex with NAD. *Acta Crystallogr Sect F Struct Biol Cryst Commun* 66, 621–626. doi: 10.1107/S1744309110013527.

Fermani, S., Trivelli, X., Sparla, F., Thumiger, A., Calvaresi, M., Marri, L., *et al*. (2012). Conformational selection and folding-upon-binding of intrinsically disordered protein CP12 regulate photosynthetic enzymes assembly. *J Biol Chem* 287, 21372–21383. doi: 10.1074/jbc.M112.350355 M112.350355 [pii].

Flores Bueso, Y., and Tangney, M. (2017). Synthetic Biology in the Driving Seat of the Bioeconomy. *Trends Biotechnol* 35, 373–378. doi: 10.1016/J.TIBTECH.2017.02.002.

Ford, M. M., Smythers, A. L., McConnell, E. W., Lowery, S. C., Kolling, D. R. J., and Hicks, L. M. (2019). Inhibition of TOR in Chlamydomonas reinhardtii Leads to Rapid Cysteine Oxidation Reflecting Sustained Physiological Changes. *Cells* 8. doi: 10.3390/cells8101171.

Forti, G. (2008). The role of respiration in the activation of photosynthesis upon illumination of dark adapted Chlamydomonas reinhardtii. *Biochim Biophys Acta* 1777, 1449–1454. doi: 10.1016/j.bbabio.2008.08.011.

Fuhrmann, M., Oertel, W., and Hegemann, P. (1999). A synthetic gene coding for the green fluorescent protein (GFP) is a versatile reporter in Chlamydomonas reinhardtii. *Plant J* 19, 353–361. doi: 10.1046/j.1365-

313x.1999.00526.x.

Fukuda, H., and Kizaki, Y. (1999). A new transformation system of Saccharomyces cerevisiae with blasticidin S deaminase gene.

Furbank, R. T., Chitty, J. A., Von Caemmerer, S., and Jenkins, C. L. D. (1996). Antisense RNA Inhibition of RbcS Gene Expression Reduces Rubisco Level and Photosynthesis in the C4 Plant Flaveria bidentis. *Plant Physiol* 111, 725–734. doi: 10.1104/pp.111.3.725.

Gaff, D. F. (1971). The Use of Non-permeating Pigments for Testing the Survival of Cells.

Gaigbe-Togbe, V., Bassarsky, L., Gu, D., Spoorenberg, T., and Zeifman, L. (2022). *World Population Prospects 2022*. Available at: https://www.un.org/development/desa/pd/sites/www.un.org.development.desa.pd/files/wpp2022_summary_of_results.pdf.

Gallaher, S. D., Fitz-Gibbon, S. T., Glaesener, A. G., Pellegrini, M., and Merchanta, S. S. (2015). Chlamydomonas genome resource for laboratory strains reveals a mosaic of sequence variation, identifies true strain histories, and enables strain-specific studies. *Plant Cell* 27, 2335–2352. doi: 10.1105/tpc.15.00508.

Gallaher, S. D., Fitz-Gibbon, S. T., Strenkert, D., Purvine, S. O., Pellegrini, M., and Merchant, S. S. (2018). High-throughput sequencing of the chloroplast and mitochondrion of Chlamydomonas reinhardtii to generate improved de novo assemblies, analyze expression patterns and transcript speciation, and evaluate diversity among laboratory strains and wild isolates. *Plant Journal* 93, 545–565. doi: 10.1111/tpj.13788.

Garcia, A., Gaju, O., Bowerman, A. F., Buck, S. A., Evans, J. R., Furbank, R. T., *et al.* (2023). Enhancing crop yields through improvements in the efficiency of photosynthesis and respiration. *New Phytol* 237, 60–77. doi: 10.1111/nph.18545.

Garcia, A. K., and Kaçar, B. (2019). How to resurrect ancestral proteins as proxies for ancient biogeochemistry. *Free Radic Biol Med* 140, 260–269. doi: 10.1016/j.freeradbiomed.2019.03.033.

Garcia-Murria, M. J., Karkehabadi, S., Marin-Navarro, J., Satagopan, S., Andersson, I., Spreitzer, R. J., *et al*. (2008). Structural and functional consequences of the replacement of proximal residues Cys(172) and Cys(192) in the large subunit of ribulose-1,5-bisphosphate carboxylase/oxygenase from Chlamydomonas reinhardtii. *Biochem J* 411, 241–247. doi: 10.1042/BJ20071422.

Garcia-Murria, M. J., Sudhani, H. P. K., Marin-Navarro, J., Sanchez Del Pino, M. M., and Moreno, J. (2018). Dissecting the individual contribution of conserved cysteines to the redox regulation of RubisCO. *Photosynth Res* 137, 251–262. doi: 10.1007/s11120-018-0497-9.

Garcia-Sanchez, M. I., Gotor, C., Jacquot, J. P., Stein, M., Suzuki, A., and Vega, J. M. (1997). Critical residues of Chlamydomonas reinhardtii ferredoxin for interaction with nitrite reductase and glutamate synthase revealed by site-directed mutagenesis. *Eur J Biochem* 250, 364–368. doi: 10.1111/j.1432-1033.1997.0364a.x.

Gardner, T. S., Cantor, C. R., and Collins, J. J. (2000). Construction of a genetic toggle switch in Escherichia coli. *Nature* 403, 339–342. doi: 10.1038/35002131.

George M. Church, Yuan Gao, and Kosuri, S. (2012). Next-Generation Digital Information. *Science express* 399, 533–534. doi: 10.1038/21092.

Gerotto, C., Alboresi, A., Meneghesso, A., Jokel, M., Suorsa, M., Aro, E. M., *et al*. (2016). Flavodiiron proteins act as safety valve for electrons in Physcomitrella patens. *Proc Natl Acad Sci U S A* 113, 12322–12327. doi: 10.1073/pnas.1606685113.

Gibson, D. G., Glass, J. I., Lartigue, C., Noskov, V. N., Chuang, R. Y., Algire, M. A., *et al*. (2010). Creation of a bacterial cell controlled by a chemically synthesized genome. *Science (1979)* 329, 52–56. doi: 10.1126/science.1190719.

Gleizer, S., Ben-Nissan, R., Bar-On, Y. M., Antonovsky, N., Noor, E., Zohar, Y., *et al*. (2019). Conversion of Escherichia coli to Generate All Biomass Carbon from CO(2). *Cell* 179, 1255-1263 e12. doi: 10.1016/j.cell.2019.11.009.

Godfray, H. C., Beddington, J. R., Crute, I. R., Haddad, L., Lawrence, D., Muir, J. F., *et al*. (2010). Food security: the challenge of feeding 9 billion people. *Science (1979)* 327, 812–818. doi: 10.1126/science.1185383.

Goodenough, U., Blaby, I., Casero, D., Gallaher, S. D., Goodson, C., Johnson, S., *et al*. (2014). The path to triacylglyceride obesity in the sta6 strain of Chlamydomonas reinhardtii. *Eukaryot Cell* 13, 591–613.

Gorman, D. S., and Levine, R. P. (1965). Cytochrome f and plastocyanin: their sequence in the photosynthetic electron transport chain of Chlamydomonas reinhardi. *Proc Natl Acad Sci U S A* 54, 1665–1669. doi: 10.1073/pnas.54.6.1665.

Gormant, D. S., and Levine, R. P. (1965). Cytochrome F and plastocyanin: Their sequence in the photosynthetic electron transport chain of Chlamydomonas reinhardtii.

Graciet, E., Gans, P., Wedel, N., Lebreton, S., Camadro, J. M., and Gontero, B. (2003). The small protein CP12: a protein linker for supramolecular complex assembly. *Biochemistry* 42, 8163–8170. Available at: http://www.ncbi.nlm.nih.gov/entrez/query.fcgi?cmd=Retrieve&db=PubMed&dopt=Citation&list_uids=12846565.

Greiner, A., Kelterborn, S., Evers, H., Kreimer, G., Sizova, I., and Hegemann, P. (2017). Targeting of photoreceptor genes in Chlamydomonas reinhardtii via zinc-finger nucleases and CRISPR/Cas9. *Plant Cell* 29, 2498–2518. doi: 10.1105/tpc.17.00659.

Gross, G., and Eshhar, Z. (2016). Therapeutic Potential of T Cell Chimeric Antigen Receptors (CARs) in Cancer Treatment: Counteracting Off-Tumor Toxicities for Safe CAR T Cell Therapy. *Annu Rev Pharmacol Toxicol* 56, 59–83. doi: 10.1146/annurev-pharmtox-010814-124844.

Gurrieri, L., Del Giudice, A., Demitri, N., Falini, G., Pavel, N. V, Zaffagnini, M., *et al*. (2019). Arabidopsis and Chlamydomonas phosphoribulokinase crystal structures complete the redox structural proteome of the Calvin-Benson cycle. *Proc Natl Acad Sci U S A* 116, 8048–8053. doi: 10.1073/pnas.1820639116.

Gurrieri, L., Fermani, S., Zaffagnini, M., Sparla, F., and Trost, P. (2021). Calvin-

Benson cycle regulation is getting complex. *Trends Plant Sci* 26, 898–912. doi: 10.1016/j.tplants.2021.03.008.

Gurrieri, L., Sparla, F., Zaffagnini, M., and Trost, P. (2023). Dark complexes of the Calvin-Benson cycle in a physiological perspective. *Semin Cell Dev Biol*. doi: 10.1016/j.semcdb.2023.03.002.

Gütle, D. D., Roret, T., Muller, S. J., Couturier, J., Lemaire, S. D., Hecker, A., *et al*. (2016). Chloroplast FBPase and SBPase are thioredoxin-linked enzymes with similar architecture but different evolutionary histories. *Proc Natl Acad Sci U S A* 113, 6779–6784. doi: 10.1073/pnas.1606241113.

Haake, V., Geiger, M., Walch-Liu, P., Engels, C., Zrenner, R., and Stitt, M. (1999). Changes in aldolase activity in wild-type potato plants are important for acclimation to growth irradiance and carbon dioxide concentration, because plastid aldolase exerts control over the ambient rate of photosynthesis across a range of growth condition. *Plant Journal* 17, 479–489. doi: 10.1046/j.1365-313X.1999.00391.x.

Haake, V., Zrenner, R., Sonnewald, U., and Stitt, M. (1998). A moderate decrease of plastid aldolase activity inhibits photosynthesis, alters the levels of sugars and starch, and inhibits growth of potato plants. *Plant Journal* 14, 147–157. doi: 10.1046/j.1365-313X.1998.00089.x.

Hammel, A., Sommer, F., Zimmer, D., Stitt, M., Mühlhaus, T., and Schroda, M. (2020). Overexpression of Sedoheptulose-1,7-Bisphosphatase Enhances Photosynthesis in Chlamydomonas reinhardtii and Has No Effect on the Abundance of Other Calvin-Benson Cycle Enzymes. *Front Plant Sci* 11. doi: 10.3389/fpls.2020.00868.

Harpel, M. R., and Hartman, F. C. (1994). Chemical Rescue by Exogenous Amines of a Site-Directed Mutant of Ribulose 1,5-Bisphosphate Carboxylase/Oxygenase That Lacks a Key Lysyl Residue. *Biochemistry* 33, 5553–5561. doi: 10.1021/bi00184a026.

Harris, E. H. (2001). Chlamydomonas as a model organism. *Annu Rev Plant Physiol Plant Mol Biol* 52, 363–406. doi: 10.1146/annurev.arplant.52.1.363.

Harrison, E. P., Olcer, H., Lloyd, J. C., Long, S. P., and Raines, C. A. (2001). Small decreases in SBPase cause a linear decline in the apparent RuBP regeneration rate, but do not affect Rubisco carboxylation capacity. *J Exp Bot* 52, 1779–1784. doi: 10.1093/jexbot/52.362.1779.

Harrison, E. P., Willingham, N. M., Lloyd, J. C., and Raines, C. A. (1997). Reduced sedoheptulose-1,7-bisphosphatase levels in transgenic tobacco lead to decreased photosynthetic capacity and altered carbohydrate accumulation. *Planta* 204, 27–36. doi: 10.1007/s004250050226.

He, S., Chou, H. T., Matthies, D., Wunder, T., Meyer, M. T., Atkinson, N., *et al*. (2020). The structural basis of Rubisco phase separation in the pyrenoid. *Nat Plants* 6, 1480–1490. doi: 10.1038/s41477-020-00811-y.

Henkes, S., Sonnewald, U., Badur, R., Flachmann, R., and Stitt, M. (2001). A small decrease of plastid transketolase activity in antisense tobacco transformants has dramatic effects on photosynthesis and phenylpropanoid metabolism. *Plant Cell* 13, 535–551. doi: 10.1105/tpc.13.3.535.

Hennacy, J. H., and Jonikas, M. C. (2020). Prospects for Engineering Biophysical CO(2) Concentrating Mechanisms into Land Plants to Enhance Yields. *Annu Rev Plant Biol* 71, 461–485. doi: 10.1146/annurev-arplant-081519-040100.

Hertle, A. P., Blunder, T., Wunder, T., Pesaresi, P., Pribil, M., Armbruster, U., *et al*. (2013). PGRL1 is the elusive ferredoxin-plastoquinone reductase in photosynthetic cyclic electron flow. *Mol Cell* 49, 511–523. doi: 10.1016/j.molcel.2012.11.030 S1097-2765(12)00989-6 [pii].

Heyduk, T., Michalczyk, R., and Kochman, M. (1991). Long-range effects and conformational flexibility of aldolase. *J Biol Chem* 266, 15650–15655.

Hirasawa, M., Tripathy, J. N., Sommer, F., Somasundaram, R., Chung, J. S., Nestander, M., *et al*. (2010). Enzymatic properties of the ferredoxin-dependent nitrite reductase from Chlamydomonas reinhardtii. Evidence for hydroxylamine as a late intermediate in ammonia production. *Photosynth Res* 103, 67–77. doi: 10.1007/s11120-009-9512-5.

Hirt, H., Al-Babili, S., Almeida-Trapp, M., Antoine, M., Aranda, M., Bartels, D., *et al*. (2023). PlantACT! – how to tackle the climate crisis. *Trends Plant Sci*. doi: 10.1016/j.tplants.2023.01.005.

Hochmal, A. K., Zinzius, K., Charoenwattanasatien, R., Gabelein, P., Mutoh, R., Tanaka, H., *et al*. (2016). Calredoxin represents a novel type of calcium-dependent sensor-responder connected to redox regulation in the chloroplast. *Nat Commun* 7, 11847. doi: 10.1038/ncomms11847.

Hodges, M., Dellero, Y., Keech, O., Betti, M., Raghavendra, A. S., Sage, R., *et al*. (2016). Perspectives for a better understanding of the metabolic integration of photorespiration within a complex plant primary metabolism network. doi: 10.1093/jxb/erw145.

Huang, C., Yu, Q. B., Lv, R. H., Yin, Q. Q., Chen, G. Y., Xu, L., *et al*. (2013). The reduced plastid-encoded polymerase-dependent plastid gene expression leads to the delayed greening of the Arabidopsis fln2 mutant. *PLoS One* 8, e73092. doi: 10.1371/journal.pone.0073092.

Hudson, G. S., Evans, J. R., Von Caemmerer, S., Arvidsson, Y. B. C., and Andrews, T. J. (1992). Reduction of ribulose-1,5-bisphosphate carboxylase/oxygenase content by antisense RNA reduces photosynthesis in transgenic tobacco plants. *Plant Physiol* 98, 294–302. doi: 10.1104/pp.98.1.294.

Hunter, T. (2007). The Age of Crosstalk: Phosphorylation, Ubiquitination, and Beyond. *Mol Cell* 28, 730–738. doi: 10.1016/j.molcel.2007.11.019.

Hutchison, C. A., Chuang, R. Y., Noskov, V. N., Assad-Garcia, N., Deerinck, T. J., Ellisman, M. H., *et al*. (2016). Design and synthesis of a minimal bacterial genome. *Science (1979)* 351. doi: 10.1126/science.aad6253.

Iezzi, B., Brady, R., Sardag, S., Eu, B., and Skerlos, S. (2019). Growing bricks: Assessing biocement for lower embodied carbon structures. in *Procedia CIRP* (Elsevier B.V.), 470–475. doi: 10.1016/j.procir.2019.01.061.

Ingles-Prieto, A., Ibarra-Molero, B., Delgado-Delgado, A., Perez-Jimenez, R., Fernandez, J. M., Gaucher, E. A., *et al*. (2013). Conservation of protein structure over four billion years. *Structure* 21, 1690–1697. doi:

10.1016/j.str.2013.06.020.

IPCC (2022). Summary for Policymakers: Climate Change 2022_ Impacts, Adaptation and Vulnerability_Working Group II contribution to the Sixth Assessment Report of the Intergovernamental Panel on Climate Change. doi: 10.1017/9781009325844.Front.

Iwaki, T., Haranoh, K., Inoue, N., Kojima, K., Satoh, R., Nishino, T., *et al*. (2006). Expression of foreign type I ribulose-1,5-bisphosphate carboxylase/ oxygenase (EC 4.1.1.39) stimulates photosynthesis in cyanobacterium Synechococcus PCC7942 cells. *Photosynth Res* 88, 287–297. doi: 10.1007/s11120-006-9048-x.

Izumi, M., Miyazawa, H., Kamakura, T., Yamaguchi, I., Endo, T., and Hanaoka, F. (1992). Blasticidin S-resistance gene (bsr) : a novel selectable marker for mammalian cells.

Jacob, F., Perrin, D., Sánchez, C., and Monod, J. (2005). The operon: A group of genes with expression coordinated by an operator. *C R Biol* 328, 514–520. doi: 10.1016/j.crvi.2005.04.005.

Jacquot, J. P., Stein, M., Suzuki, A., Liottet, S., Sandoz, G., and Miginiac-Maslow, M. (1997). Residue Glu-91 of Chlamydomonas reinhardtii ferredoxin is essential for electron transfer to ferredoxin-thioredoxin reductase. *FEBS Lett* 400, 293–296. Available at: http://www.ncbi.nlm.nih.gov/entrez/query.fcgi?cmd=Retrieve&db=PubMed&dopt=Citation&list_uids=9009217.

Jaeger, D., Baier, T., and Lauersen, K. J. (2019). Intronserter, an advanced online tool for design of intron containing transgenes. *Algal Res* 42, 101588. doi: https://doi.org/10.1016/j.algal.2019.101588.

Janasch, M., Asplund-Samuelsson, J., Steuer, R., and Hudson, E. P. (2019). Kinetic modeling of the Calvin cycle identifies flux control and stable metabolomes in Synechocystis carbon fixation. *J Exp Bot* 70, 1017–1031. doi: 10.1093/jxb/ery382.

Jans, F., Mignolet, E., Houyoux, P.-A., Cardol, P., Ghysels, B., Cuiné, S., *et al*. (2008). A type II NAD (P) H dehydrogenase mediates light-independent plastoquinone reduction in the chloroplast of

Chlamydomonas. *Proceedings of the National Academy of Sciences* 105, 20546–20551.

Jin, K., Chen, G., Yang, Y., Zhang, Z., and Lu, T. (2023). Strategies for manipulating Rubisco and creating photorespiratory bypass to boost C3 photosynthesis: Prospects on modern crop improvement. *Plant Cell Environ* 46, 363–378. doi: 10.1111/pce.14500.

Johnson, X., Steinbeck, J., Dent, R. M., Takahashi, H., Richaud, P., Ozawa, S., *et al*. (2014). Proton gradient regulation 5-mediated cyclic electron flow under ATP- or redox-limited conditions: a study of ΔATpase pgr5 and ΔrbcL pgr5 mutants in the green alga Chlamydomonas reinhardtii. *Plant Physiol* 165, 438–452. doi: 10.1104/pp.113.233593.

Kamakura, T., Yoneyama, K., and Yamaguchi, Isamu (1990). Expression of the blasticidin S deaminase gene (bsr) in tobacco: Fungicide tolerance and a new selective marker for transgenic plants. Springer-Verlag.

Kao, P. H., and Ng, I. S. (2017). CRISPRi mediated phosphoenolpyruvate carboxylase regulation to enhance the production of lipid in Chlamydomonas reinhardtii. *Bioresour Technol* 245, 1527–1537. doi: 10.1016/j.biortech.2017.04.111.

Karas, B. J., Diner, R. E., Lefebvre, S. C., McQuaid, J., Phillips, A. P. R., Noddings, C. M., *et al*. (2015). Designer diatom episomes delivered by bacterial conjugation. *Nat Commun* 6. doi: 10.1038/ncomms7925.

Kaye, Y., Huang, W., Clowez, S., Saroussi, S., Idoine, A., Sanz-Luque, E., *et al*. (2019). The mitochondrial alternative oxidase from Chlamydomonas reinhardtii enables survival in high light. *Journal of Biological Chemistry* 294, 1380–1395.

Kebeish, R., Niessen, M., Thiruveedhi, K., Bari, R., Hirsch, H. J., Rosenkranz, R., *et al*. (2007). Chloroplastic photorespiratory bypass increases photosynthesis and biomass production in Arabidopsis thaliana. *Nat Biotechnol* 25, 593–599. doi: 10.1038/nbt1299.

Képès, F. (2011). Biologie synthétique et intégrative. *Comptes Rendus Chimie* 14, 420–423. doi: http://dx.doi.org/10.1016/j.crci.2010.11.012.

Kerfeld, C. A., and Melnicki, M. R. (2016). Assembly, function and evolution of cyanobacterial carboxysomes. *Curr Opin Plant Biol* 31, 66–75. doi: 10.1016/j.pbi.2016.03.009.

Kessler, E. (1973). Effect of anaerobiosis on photosynthetic reactions and nitrogen metabolism of algae with and without hydrogenase. *Arch Mikrobiol* 93, 91–100.

Kim, J., Lee, S., Baek, K., and Jin, E. (2020). Site-Specific Gene Knock-Out and On-Site Heterologous Gene Overexpression in Chlamydomonas reinhardtii via a CRISPR-Cas9-Mediated Knock-in Method. *Front Plant Sci* 11, 306. doi: 10.3389/fpls.2020.00306.

Kim, K. S., Feild, E., King, N., Yaoi, T., Kustu, S., and Inwood, W. (2005). Spontaneous mutations in the ammonium transport gene AMT4 of Chlamydomonas reinhardtii. *Genetics* 170, 631–644. doi: 10.1534/genetics.105.041574.

Kimura, M., Kamakura, T., Zhon Tao, Q., Kaneko, I., and Yamaguchi, I. (1994). Cloning of the blastieidin S deaminase gene (BSD) from Aspergillus terreus and its use as a selectable marker for Schizosaccharomyces pombe and Pyricularia oryzae.

Klein, U. (1986). Compartmentation of glycolysis and of the oxidative pentose-phosphate pathway in Chlamydomonas reinhardii. *Planta* 167, 81–86.

Kong, F., Burlacot, A., Liang, Y., Légeret, B., Alseekh, S., Brotman, Y., *et al*. (2018). Interorganelle communication: Peroxisomal MALATE DEHYDROGENASE2 connects lipid catabolism to photosynthesis through redox coupling in Chlamydomonas. *Plant Cell* 30, 1824–1847.

Kong, F., Yamaoka, Y., Ohama, T., Lee, Y., and Li-Beisson, Y. (2019). Molecular genetic tools and emerging synthetic biology strategies to increase cellular oil content in chlamydomonas reinhardtii. *Plant Cell Physiol* 60, 1184–1196. doi: 10.1093/pcp/pcz022.

Kono, T., Mehrotra, S., Endo, C., Kizu, N., Matusda, M., Kimura, H., *et al*. (2017). A RuBisCO-mediated carbon metabolic pathway in methanogenic archaea. *Nat Commun* 8. doi: 10.1038/ncomms14007.

Koßmann, J., Sonnewald, U., and Willmitzer, L. (1994). Reduction of the chloroplastic fructose-1,6-bisphosphatase in transgenic potato plants impairs photosynthesis and plant growth. *The Plant Journal* 6, 637–650. doi: 10.1046/j.1365-313X.1994.6050637.x.

Kouprina, N., Petrov, N., Molina, O., Liskovykh, M., Pesenti, E., Ohzeki, J. I., *et al*. (2018). Human Artificial Chromosome with Regulated Centromere: A Tool for Genome and Cancer Studies. *ACS Synth Biol* 7, 1974–1989. doi: 10.1021/acssynbio.8b00230.

Krishnan, A., Kumaraswamy, G. K., Vinyard, D. J., Gu, H., Ananyev, G., Posewitz, M. C., *et al*. (2015). Metabolic and photosynthetic consequences of blocking starch biosynthesis in the green alga C hlamydomonas reinhardtii sta6 mutant. *The Plant Journal* 81, 947–960.

Kubis, A., and Bar-Even, A. (2019). Synthetic biology approaches for improving photosynthesis. *J Exp Bot* 70, 1425–1433. doi: 10.1093/jxb/erz029.

Kuken, A., Sommer, F., Yaneva-Roder, L., Mackinder, L. C., Hohne, M., Geimer, S., *et al*. (2018). Effects of microcompartmentation on flux distribution and metabolic pools in Chlamydomonas reinhardtii chloroplasts. *Elife* 7. doi: 10.7554/eLife.37960.

Lauersen, K. J., Wichmann, J., Baier, T., Kampranis, S. C., Pateraki, I., Moller, B. L., *et al*. (2018). Phototrophic production of heterologous diterpenoids and a hydroxy-functionalized derivative from Chlamydomonas reinhardtii. *Metab Eng* 49, 116–127. doi: 10.1016/j.ymben.2018.07.005.

Lawson, T., Bryant, B., Lefebvre, S., Lloyd, J. C., and Raines, C. A. (2006). Decreased SBPase activity alters growth and development in transgenic tobacco plants. *Plant Cell Environ* 29, 48–58. doi: 10.1111/j.1365-3040.2005.01399.x.

Le Moigne, T., Boisset, N. D., de Carpentier, F., Crozet, P., Danon, A., Henri, J., *et al*. (2023). "Chapter 8 - Photoproduction of reducing power and the Calvin-Benson cycle," in *The Chlamydomonas Sourcebook (Third Edition)*, eds. A. R. Grossman and F.-A. Wollman (London: Academic Press), 273–315. doi: https://doi.org/10.1016/B978-0-12-821430-

5.00016-X.

Le Moigne, T., Gurrieri, L., Crozet, P., Marchand, C. H., Zaffagnini, M., Sparla, F., *et al*. (2021). Crystal structure of chloroplastic thioredoxin z defines a type-specific target recognition. *Plant Journal* 107, 434–447. doi: 10.1111/tpj.15300.

Lee, J. Y., Marotzke, J., Bala, G., Cao, L., Corti, S., Dunne, J. P., *et al*. (2021). *IPCC. Climate change 2021: The physical science basis*.

Lefebvre, S., Lawson, T., Zakhleniuk, O. V, Lloyd, J. C., Raines, C. A., and Fryer, M. (2005). Increased sedoheptulose-1,7-bisphosphatase activity in transgenic tobacco plants stimulates photosynthesis and growth from an early stage in development. *Plant Physiol* 138, 451–460. doi: 10.1104/pp.104.055046.

Lemaire, S. D., Guillon, B., Le Marechal, P., Keryer, E., Miginiac-Maslow, M., and Decottignies, P. (2004). New thioredoxin targets in the unicellular photosynthetic eukaryote Chlamydomonas reinhardtii. *Proc Natl Acad Sci U S A* 101, 7475–7480. doi: 10.1073/pnas.0402221101.

Lemaire, S. D., Michelet, L., Zaffagnini, M., Massot, V., and Issakidis-Bourguet, E. (2007). Thioredoxins in chloroplasts. *Curr Genet* 51, 343–365. doi: 10.1007/s00294-007-0128-z.

Lemaire, S. D., Quesada, A., Merchan, F., Corral, J. M., Igeno, M. I., Keryer, E., *et al*. (2005). NADP-malate dehydrogenase from unicellular green alga Chlamydomonas reinhardtii. A first step toward redox regulation? *Plant Physiol* 137, 514–521. doi: 10.1104/pp.104.052670.

Lemaire, S. D., Stein, M., Issakidis-Bourguet, E., Keryer, E., Benoit, V. V, Pineau, B., *et al*. (1999). The complex regulation of ferredoxin/thioredoxin-related genes by light and the circadian clock. *Planta* 209, 221–229. doi: 10.1007/s004250050626.

Lemaire, S. D., Tedesco, D., Crozet, P., Michelet, L., Fermani, S., Zaffagnini, M., *et al*. (2018). Crystal Structure of Chloroplastic Thioredoxin f2 from Chlamydomonas reinhardtii Reveals Distinct Surface Properties. *Antioxidants (Basel)* 7. doi: 10.3390/antiox7120171.

Lemaire, S., Keryer, E., Stein, M., Schepens, I., Issakidis-Bourguet, E., Gérard-Hirne, C., *et al*. (1999). Heavy-metal regulation of thioredoxin gene expression in chlamydomonas reinhardtii. *Plant Physiol* 120, 773–778. doi: 10.1104/pp.120.3.773.

Levine, R. P. (1960). A screening technique for photosynthetic mutants in unicellular algae. *Nature* 188, 339–340.

Li, X., Patena, W., Fauser, F., Jinkerson, R. E., Saroussi, S., Meyer, M. T., *et al*. (2019). A genome-wide algal mutant library and functional screen identifies genes required for eukaryotic photosynthesis. *Nat Genet* 51, 627–635. doi: 10.1038/s41588-019-0370-6.

Li, X., Zhang, R., Patena, W., Gang, S. S., Blum, S. R., Ivanova, N., *et al*. (2015). An indexed, mapped mutant library enables reverse genetics studies of biological processes in chlamydomonas reinhardtii. *Plant Cell* 28, 367–387. doi: 10.1105/tpc.15.00465.

Liang, F., Lindberg, P., and Lindblad, P. (2018). Engineering photoautotrophic carbon fixation for enhanced growth and productivity. *Sustain Energy Fuels* 2, 2583–2600. doi: 10.1039/c8se00281a.

Liang, F., and Lindblad, P. (2016). Effects of overexpressing photosynthetic carbon flux control enzymes in the cyanobacterium Synechocystis PCC 6803. *Metab Eng* 38, 56–64. doi: 10.1016/j.ymben.2016.06.005.

Liang, F., and Lindblad, P. (2017). Synechocystis PCC 6803 overexpressing RuBisCO grow faster with increased photosynthesis. *Metab Eng Commun* 4, 29–36. doi: 10.1016/j.meteno.2017.02.002.

Liu, K., Yuan, C., Li, H., Chen, K., Lu, L., Shen, C., *et al*. (2018). A qualitative proteome-wide lysine crotonylation profiling of papaya (Carica papaya L.). *Sci Rep* 8, 8230. doi: 10.1038/s41598-018-26676-y.

Long, B. M., Hee, W. Y., Sharwood, R. E., Rae, B. D., Kaines, S., Lim, Y. L., *et al*. (2018). Carboxysome encapsulation of the CO2-fixing enzyme Rubisco in tobacco chloroplasts. *Nat Commun* 9. doi: 10.1038/s41467-018-06044-0.

Long, B. M., Rae, B. D., Rolland, V., Forster, B., and Price, G. D. (2016). Cyanobacterial CO2-concentrating mechanism components: function and prospects for plant metabolic engineering. *Curr Opin Plant Biol* 31, 1–8. doi: 10.1016/j.pbi.2016.03.002.

Long, S. P., Marshall-Colon, A., and Zhu, X. G. (2015). Meeting the global food demand of the future by engineering crop photosynthesis and yield potential. *Cell* 161, 56–66. doi: 10.1016/J.CELL.2015.03.019.

Long, S. P., Zhu, X. G., Naidu, S. L., and Ort, D. R. (2006). Can improvement in photosynthesis increase crop yields? *Plant Cell Environ* 29, 315–330. Available at: http://www.ncbi.nlm.nih.gov/pubmed/17080588.

Löwe, H., and Kremling, A. (2021). In-Depth Computational Analysis of Natural and Artificial Carbon Fixation Pathways. *BioDesign Research* 2021. doi: 10.34133/2021/9898316.

Lumbreras, V., and Purton, S. (1998). Recent advances in chlamydomonas transgenics. *Protist* 149, 23–7. doi: 10.1016/S1434-4610(98)70006-9.

Ma, W., Weckwerth, W., and Roustan, V. (2018). Quantitative Phosphoproteomic and System-Level Analysis of TOR Inhibition Unravel Distinct Organellar Acclimation in Chlamydomonas reinhardtii. doi: 10.3389/fpls.2018.01590.

Mackinder, L. C. M. (2018). The Chlamydomonas CO(2) -concentrating mechanism and its potential for engineering photosynthesis in plants. *New Phytol* 217, 54–61. doi: 10.1111/nph.14749.

Mackinder, L. C. M., Chen, C., Leib, R. D., Patena, W., Blum, S. R., Rodman, M., *et al*. (2017). A Spatial Interactome Reveals the Protein Organization of the Algal CO2-Concentrating Mechanism. *Cell* 171, 133-147 e14. doi: 10.1016/j.cell.2017.08.044.

Mackinder, L. C., Meyer, M. T., Mettler-Altmann, T., Chen, V. K., Mitchell, M. C., Caspari, O., *et al*. (2016). A repeat protein links Rubisco to form the eukaryotic carbon-concentrating organelle. *Proc Natl Acad Sci U S A* 113, 5958–5963. doi: 10.1073/pnas.1522866113.

Maier, A., Fahnenstich, H., von Caemmerer, S., Engqvist, M. K. M., Weber, A.

P. M., Flügge, U. I., *et al*. (2012). Transgenic introduction of a glycolate oxidative cycle into A. Thaliana chloroplasts leads to growth improvement. *Front Plant Sci* 3, 1–12. doi: 10.3389/fpls.2012.00038.

Makino, A., and Sage, R. F. (2007). Temperature response of photosynthesis in transgenic rice transformed with "sense" or "antisense" rbcS. *Plant Cell Physiol* 48, 1472–1483. doi: 10.1093/pcp/pcm118.

Makino, A., Shimada, T., Takumi, S., Kaneko, K., Matsuoka, M., Shimamoto, K., *et al*. (1997). Does decrease in ribulose-1,5-bisphosphate carboxylase by antisense rbcS lead to a higher N-use efficiency of photosynthesis under conditions of saturating CO2 and light in rice plants? *Plant Physiol* 114, 483–491. doi: 10.1104/pp.114.2.483.

Malaterre, C., Jeancolas, C., and Nghe, P. (2022). The Origin of Life: What Is the Question? *Astrobiology* 22, 851–862. doi: 10.1089/ast.2021.0162.

Marco, P., Elman, T., and Yacoby, I. (2019). Binding of ferredoxin NADP(+) oxidoreductase (FNR) to plant photosystem I. *Biochim Biophys Acta Bioenerg* 1860, 689–698. doi: 10.1016/j.bbabio.2019.07.007.

Marcus, Y., Altman-Gueta, H., Wolff, Y., and Gurevitz, M. (2011). Rubisco mutagenesis provides new insight into limitations on photosynthesis and growth in Synechocystis PCC6803. *J Exp Bot* 62, 4173–4182. doi: 10.1093/jxb/err116.

Mark Peplow (2016). Synthetic biology's first malaria drug meets market. *Nature* 32, 8–17. doi: 10.12968/prma.2022.32.8.8.

Marliere, P. (2009). The farther, the safer: A manifesto for securely navigating synthetic species away from the old living world. Syst Synth Biol 3, 77–84. doi: 10.1007/s11693-009-9040-9.

Marri, L., Pesaresi, A., Valerio, C., Lamba, D., Pupillo, P., Trost, P., *et al*. (2010). In vitro characterization of Arabidopsis CP12 isoforms reveals common biochemical and molecular properties. *J Plant Physiol* 167, 939–950. doi: 10.1016/j.jplph.2010.02.008 S0176-1617(10)00100-8 [pii].

Marri, L., Trost, P., Pupillo, P., and Sparla, F. (2005). Reconstitution and Properties of the Recombinant Phosphoribulokinase Supramolecular

Complex. *Plant Physiol* 139, 1433–1443. doi: 10.1104/pp.105.068445.1.

Marri, L., Trost, P., Trivelli, X., Gonnelli, L., Pupillo, P., and Sparla, F. (2008). Spontaneous assembly of photosynthetic supramolecular complexes as mediated by the intrinsically unstructured protein CP12. *J Biol Chem* 283, 1831–1838. doi: 10.1074/jbc.M705650200.

Marri, L., Zaffagnini, M., Collin, V., Issakidis-Bourguet, E., Lemaire, S. D., Pupillo, P., *et al*. (2009). Prompt and easy activation by specific thioredoxins of calvin cycle enzymes of Arabidopsis thaliana associated in the GAPDH/CP12/PRK supramolecular complex. *Mol Plant* 2, 259–269. doi: 10.1093/mp/ssn061.

Martin V, Pitera D, Withers S, Newman J, and Keasling J (2003). Engineering a mevalonate pathway in Escherichia coli for production of terpenoids. *Nat Biotechnol* 21, 796–802.

Mathy, G., Cardol, P., Dinant, M., Blomme, A., Gérin, S., Cloes, M., *et al*. (2010). Proteomic and functional characterization of a Chlamydomonas reinhardtii mutant lacking the mitochondrial alternative oxidase 1. *J Proteome Res* 9, 2825–2838.

Matt, P., Krapp, A., Haake, V., Mock, H. P., and Stitt, M. (2002). Decreased Rubisco activity leads to dramatic changes of nitrate metabolism, amino acid metabolism and the levels of phenylpropanoids and nicotine in tobacco antisense RBCS transformants. *Plant Journal* 30, 663–677. doi: 10.1046/j.1365-313X.2002.01323.x.

Matthew Johnson, P. P., and Johnson, M. P. (2016). An overview of photosynthesis. *Essays Biochem* 60, 255–273. doi: 10.1042/EBC20160016.

McConnell, E. W., Werth, E. G., and Hicks, L. M. (2018). The phosphorylated redox proteome of Chlamydomonas reinhardtii: Revealing novel means for regulation of protein structure and function. *Redox Biol* 17, 35–46. doi: 10.1016/j.redox.2018.04.003.

McFarlane, C. R., Shah, N. R., Kabasakal, B. V, Echeverria, B., Cotton, C. A. R., Bubeck, D., *et al*. (2019). Structural basis of light-induced redox regulation in the Calvin-Benson cycle in cyanobacteria. *Proc Natl Acad*

Sci U S A 116, 20984–20990. doi: 10.1073/pnas.1906722116.

McGrath, J. M., and Long, S. P. (2014). Can the cyanobacterial carbon-concentrating mechanism increase photosynthesis in crop species? A theoretical analysis. *Plant Physiol* 164, 2247–2261. doi: 10.1104/pp.113.232611.

Mehrshahi, P., Nguyen, G., Gorchs Rovira, A., Sayer, A., Llavero-Pasquina, M., Lim Huei Sin, M., *et al*. (2020). Development of Novel Riboswitches for Synthetic Biology in the Green Alga Chlamydomonas. *ACS Synth Biol* 9, 1406–1417. doi: 10.1021/acssynbio.0c00082.

Meloni, M., Gurrieri, L., Fermani, S., Velie, L., Sparla, F., Crozet, P., *et al*. (2023). Ribulose-1,5-bisphosphate regeneration in the Calvin-Benson-Bassham cycle: Focus on the last three enzymatic steps that allow the formation of Rubisco substrate. *Front Plant Sci* 14, 1130430. doi: 10.3389/fpls.2023.1130430.

Meng, F., and Ellis, T. (2020). The second decade of synthetic biology: 2010–2020. *Nat Commun* 11, 1–4. doi: 10.1038/s41467-020-19092-2.

Merchant, S. S. (2019). A Series of Fortunate Events : Introducing Chlamydomonas as. 31, 1682–1707. doi: 10.1105/tpc.18.00952.

Meslet-Cladière, L., and Vallon, O. (2011). Novel shuttle markers for nuclear transformation of the green alga Chlamydomonas reinhardtii. *Eukaryot Cell* 10, 1670–1678. doi: 10.1128/EC.05043-11.

Mettler, T., Muhlhaus, T., Hemme, D., Schottler, M. A., Rupprecht, J., Idoine, A., *et al*. (2014). Systems Analysis of the Response of Photosynthesis, Metabolism, and Growth to an Increase in Irradiance in the Photosynthetic Model Organism Chlamydomonas reinhardtii. *Plant Cell* 26, 2310–2350. doi: 10.1105/tpc.114.124537.

Michael B. Elowitz, and Stanislas Leibler (2000). A synthetic oscillatory networkof transcriptional regulators. *Nature* 403, 335–338.

Michelet, L., Roach, T., Fischer, B. B., Bedhomme, M., Lemaire, S. D., and Krieger-Liszkay, A. (2013). Down-regulation of catalase activity allows transient accumulation of a hydrogen peroxide signal in C

hlamydomonas reinhardtii. *Plant Cell Environ* 36, 1204–1213.

Michelet, L., Zaffagnini, M., Morisse, S., Sparla, F., Pérez-Pérez, M. E., Francia, F., *et al*. (2013). Redox regulation of the Calvin-Benson cycle: Something old, something new. *Front Plant Sci* 4, 1–21. doi: 10.3389/fpls.2013.00470.

Michelet, L., Zaffagnini, M., Vanacker, H., Le Marechal, P., Marchand, C., Schroda, M., *et al*. (2008). In vivo targets of S-thiolation in Chlamydomonas reinhardtii. *J Biol Chem* 283, 21571–21578. doi: 10.1074/jbc.M802331200.

Milanez, S., Mural, R. J., and Hartman, F. C. (1991). Roles of cysteinyl residues of phosphoribulokinase as examined by site-directed mutagenesis. *Journal of Biological Chemistry* 266, 10694–10699. doi: 10.1016/s0021-9258(18)99279-3.

Miller, T. E., Beneyton, T., Schwander, T., Diehl, C., Girault, M., McLean, R., *et al*. (2020). Light-powered CO2 fixation in a chloroplast mimic with natural and synthetic parts. *Science (1979)* 368, 649–654. doi: 10.1126/science.aaz6802.

Miyagawa, Y., Tamoi, M., and Shigeoka, S. (2001). Overexpression of a cyanobacterial fructose-1,6-/sedoheptulose-1,7-bisphosphatase in tobacco enhances photosynthesis and growth. *Nat Biotechnol* 19, 965–969. doi: 10.1038/nbt1001-965.

Moll, B., and Levine, R. P. (1970). Characterization of a Photosynthetic Mutant Strain of Chlamydomonas reinhardi Deficient in Phosphoribulokinase Activity. *Plant Physiol* 46, 576–580. doi: 10.1104/pp.46.4.576.

Moparthi, S. B., Thieulin-Pardo, G., De Torres, J., Ghenuche, P., Gontero, B., and Wenger, J. (2015). FRET analysis of CP12 structural interplay by GAPDH and PRK. *Biochem Biophys Res Commun* 458, 488–493. doi: 10.1016/J.BBRC.2015.01.135.

Morisse, S., Michelet, L., Bedhomme, M., Marchand, C. H., Calvaresi, M., Trost, P., *et al*. (2014). Thioredoxin-dependent redox regulation of chloroplastic phosphoglycerate kinase from Chlamydomonas

reinhardtii. *J Biol Chem* 289, 30012–30024. doi: 10.1074/jbc.M114.597997.

Mosebach, L., Heilmann, C., Mutoh, R., Gabelein, P., Steinbeck, J., Happe, T., *et al*. (2017). Association of Ferredoxin:NADP(+) oxidoreductase with the photosynthetic apparatus modulates electron transfer in Chlamydomonas reinhardtii. *Photosynth Res* 134, 291–306. doi: 10.1007/s11120-017-0408-5.

Moses, T., and Goossens, A. (2017). Plants for human health: Greening biotechnology and synthetic biology. *J Exp Bot* 68, 4009–4011. doi: 10.1093/jxb/erx268.

Moses, T., Mehrshahi, P., Smith, A. G., and Goossens, A. (2017). Synthetic biology approaches for the production of plant metabolites in unicellular organisms. *J Exp Bot* 68, 4057–4074. doi: 10.1093/jxb/erx119.

Nee, G., Zaffagnini, M., Trost, P., and Issakidis-Bourguet, E. (2009). Redox regulation of chloroplastic glucose-6-phosphate dehydrogenase: a new role for f-type thioredoxin. *FEBS Lett* 583, 2827–2832. doi: S0014-5793(09)00571-7 [pii] 10.1016/j.febslet.2009.07.035.

Neupert, J., Karcher, D., and Bock, R. (2009). Generation of Chlamydomonas strains that efficiently express nuclear transgenes. *Plant Journal* 57, 1140–1150. doi: 10.1111/j.1365-313X.2008.03746.x.

Nielsen, A. A. K., Der, B. S., Shin, J., Vaidyanathan, P., Paralanov, V., Strychalski, E. A., *et al*. (2016). Genetic circuit design automation. *Science (1979)* 352. doi: 10.1126/science.aac7341.

Ochsner, A. M., Christen, M., Hemmerle, L., Peyraud, R., Christen, B., and Vorholt, J. A. (2017). Transposon Sequencing Uncovers an Essential Regulatory Function of Phosphoribulokinase for Methylotrophy. *Current Biology* 27, 2579-2588.e6. doi: 10.1016/j.cub.2017.07.025.

Oguntona, O. A., and Aigbavboa, C. O. (2023). Nature inspiration, imitation, and emulation: Biomimicry thinking path to sustainability in the construction industry. *Front Built Environ* 9, 1–12. doi: 10.3389/fbuil.2023.1085979.

Ohad, I., Siekevitz, P., and Palade, G. E. (1967). Biogenesis of chloroplast membranes. I. Plastid dedifferentiation in a dark-grown algal mutant (Chlamydomonas reinhardi). *J Cell Biol* 35, 521–552. doi: 10.1083/jcb.35.3.521.

Ölçer, H., Lloyd, J. C., and Raines, C. A. (2001). Photosynthetic capacity is differentially affected by reductions in sedoheptulose-1,7-bisphosphatase activity during leaf development in transgenic tobacco plants. *Plant Physiol* 125, 982–989. doi: 10.1104/pp.125.2.982.

Ort, D. R., Merchant, S. S., Alric, J., Barkan, A., Blankenship, R. E., Bock, R., *et al*. (2015). Redesigning photosynthesis to sustainably meet global food and bioenergy demand. *Proc Natl Acad Sci U S A* 112, 8529–8536. doi: 10.1073/pnas.1424031112.

Ortega-Escalante, J. A., Kwok, O., and Miller, S. M. (2019). New Selectable Markers for Volvox carteri Transformation. *Protist* 170, 52–63. doi: 10.1016/j.protis.2018.11.002.

Page, M. D., Allen, M. D., Kropat, J., Urzica, E. I., Karpowicz, S. J., Hsieh, S. I., *et al*. (2012). Fe sparing and Fe recycling contribute to increased superoxide dismutase capacity in iron-starved Chlamydomonas reinhardtii. *Plant Cell* 24, 2649–2665.

Pasquini, M., Fermani, S., Tedesco, D., Sciabolini, C., Crozet, P., Naldi, M., *et al*. (2017). Structural basis for the magnesium-dependent activation of transketolase from Chlamydomonas reinhardtii. *Biochim Biophys Acta Gen Subj* 1861, 2132–2145. doi: 10.1016/j.bbagen.2017.05.021.

Patron, N. J. (2014). DNA assembly for plant biology: techniques and tools This review comes from a themed issue on Physiology and metabolism. *Curr Opin Plant Biol* 19, 14–19. doi: 10.1016/j.pbi.2014.02.004.

Patron, N. J., Orzaez, D., Marillonnet, S., Warzecha, H., Matthewman, C., Youles, M., *et al*. (2015). Standards for plant synthetic biology: A common syntax for exchange of DNA parts. *New Phytologist* 208, 13–19. doi: 10.1111/nph.13532.

Paul, M. J., Driscoll, S. P., Andralojc, P. J., Knight, J. S., Gray, J. C., and Lawlor, D. W. (2000). Decrease of phosphoribulokinase activity by antisense

RNA in transgenic tobacco: Definition of the light environment under which phosphoribulokinase is not in large excess. *Planta* 211, 112–119. doi: 10.1007/s004250000269.

Paul, M. J., Knight, J. S., Habash, D., Parry, M. A. J., Lawlor, D. W., Barnes, S. A., *et al*. (1995). Reduction in phosphoribulokinase activity by antisense RNA in transgenic tobacco: effect on CO2 assimilation and growth in low irradiance. *The Plant Journal* 7, 535–542. doi: 10.1046/j.1365-313X.1995.7040535.x.

Peden, E. A., Boehm, M., Mulder, D. W., Davis, R., Old, W. M., King, P. W., *et al*. (2013). Identification of global ferredoxin interaction networks in Chlamydomonas reinhardtii. *J Biol Chem* 288, 35192–35209. doi: 10.1074/jbc.M113.483727.

Pérez-Pérez, M. E., Mauries, A., Maes, A., Tourasse, N. J., Hamon, M., Lemaire, S. D., *et al*. (2017). The Deep Thioredoxome in Chlamydomonas reinhardtii: New Insights into Redox Regulation. *Mol Plant* 10, 1107–1125. doi: 10.1016/j.molp.2017.07.009.

Petersen, J., Teich, R., Becker, B., Cerff, R., and Brinkmann, H. (2006). The GapA/B gene duplication marks the origin of Streptophyta (charophytes and land plants). *Mol Biol Evol* 23, 1109–1118. doi: msj123 [pii] 10.1093/molbev/msj123.

Poddar, H., Breitling, R., and Takano, E. (2020). Towards engineering and production of artificial spider silk using tools of synthetic biology. *Engineering Biology* 4, 1–6. doi: 10.1049/enb.2019.0017.

Portis Jr., A. R., and Heldt, H. W. (1976). Light-dependent changes of the Mg2+ concentration in the stroma in relation to the Mg2+ dependency of CO2 fixation in intact chloroplasts. *Biochim Biophys Acta* 449, 434–436. doi: 10.1016/0005-2728(76)90154-7.

Pröschold, T., Harris, E. H., and Coleman, A. W. (2005). Portrait of a species: Chlamydonomas reinhardtii. *Genetics* 170, 1601–1610. doi: 10.1534/genetics.105.044503.

Quick, W. P., Schurr, U., Fichtner, K., Schulze, E. -D, Rodermel, S. R., Bogorad, L., *et al*. (1991). The impact of decreased Rubisco on photosynthesis,

growth, allocation and storage in tobacco plants which have been transformed with antisense rbcS. *The Plant Journal* 1, 51–58. doi: 10.1111/j.1365-313X.1991.00051.x.

Raines, C. A. (2003). The Calvin cycle revisited. *Photosynth Res* 75, 1–10. doi: 10.1023/A:1022421515027.

Raines, C. A. (2006). Transgenic approaches to manipulate the environmental responses of the C3 carbon fixation cycle. *Plant Cell Environ* 29, 331–339. doi: 10.1111/j.1365-3040.2005.01488.x.

Raines, C. A. (2011). Increasing photosynthetic carbon assimilation in C3 plants to improve crop yield: current and future strategies. *Plant Physiol* 155, 36–42. doi: 10.1104/pp.110.168559.

Raines, C. A. (2022). Improving plant productivity by re-tuning the regeneration of RuBP in the Calvin–Benson–Bassham cycle. *New Phytologist* 236, 350–356. doi: 10.1111/nph.18394.

Raines, C. A., Harrison, E. P., Ölçer, H., and Lloyd, J. C. (2000). Investigating the role of the thiol-regulated enzyme sedoheptulose-1,7-bisphosphatase in the control of photosynthesis. *Physiol Plant* 110, 303–308. doi: 10.1034/j.1399-3054.2000.1100303.x.

Richardson, S. M., Mitchell, L. A., Stracquadanio, G., Yang, K., Dymond, J. S., DiCarlo, J. E., *et al*. (2017). Design of a synthetic yeast genome. *Science (1979)* 355, 1040–1044. doi: 10.1126/SCIENCE.AAF4557/SUPPL_FILE/AAF4557S1.MP4.

Ro, D. K., Paradise, E. M., Quellet, M., Fisher, K. J., Newman, K. L., Ndungu, J. M., *et al*. (2006). Production of the antimalarial drug precursor artemisinic acid in engineered yeast. *Nature* 440, 940–943. doi: 10.1038/nature04640.

Roehner, N., Beal, J., Clancy, K., Bartley, B., Misirli, G., Grünberg, R., *et al*. (2016). Sharing Structure and Function in Biological Design with SBOL 2.0. *ACS Synth Biol* 5, 498–506. doi: 10.1021/acssynbio.5b00215.

Roell, M. S., Schada von Borzykowski, L., Westhoff, P., Plett, A., Paczia, N., Claus, P., *et al*. (2021). A synthetic C4 shuttle via the β-hydroxyaspartate

cycle in C3 plants. *Proc Natl Acad Sci U S A* 118. doi: 10.1073/pnas.2022307118.

Rolland, N., Atteia, A., Decottignies, P., Garin, J., Hippler, M., Kreimer, G., *et al*. (2009). Chlamydomonas proteomics. *Curr Opin Microbiol* 12, 285–291. doi: 10.1016/j.mib.2009.04.001.

Romero, P. A., and Arnold, F. H. (2009). Exploring protein fitness landscapes by directed evolution. *Nat Rev Mol Cell Biol* 10, 866–876. doi: 10.1038/nrm2805.

Rooke, J. (2013). Synthetic biology as a source of global health innovation See, for example, "'Current Uses of Synthetic Biology'". *Syst Synth Biol* 488, 67–72. doi: 10.1007/s11693-013-9117-3.

Rosales-Mendoza, S., María, L., Paz-Maldonado, T., Ruth, •, and Soria-Guerra, E. (2012). Chlamydomonas reinhardtii as a viable platform for the production of recombinant proteins: current status and perspectives. doi: 10.1007/s00299-011-1186-8.

Rosenthal, D. M., Locke, A. M., Khozaei, M., Raines, C. A., Long, S. P., and Ort, D. R. (2011). Over-expressing the C(3) photosynthesis cycle enzyme Sedoheptulose-1-7 Bisphosphatase improves photosynthetic carbon gain and yield under fully open air CO(2) fumigation (FACE). *BMC Plant Biol* 11, 123. doi: 10.1186/1471-2229-11-123.

Roy Davies, D. (1972). Cell Wall Organisation in Chlamydomonas reinhardi The Role of Extra-Nuclear Systems.

Ryan Georgianna, D., and Mayfield, S. P. (2012). Exploiting diversity and synthetic biology for the production of algal biofuels. *Nature* 488, 329–335. doi: 10.1038/nature11479.

Salesse-Smith, C. E., Sharwood, R. E., Busch, F. A., Kromdijk, J., Bardal, V., and Stern, D. B. (2018). Overexpression of Rubisco subunits with RAF1 increases Rubisco content in maize. *Nat Plants* 4, 802–810. doi: 10.1038/s41477-018-0252-4.

Salomé, P. A., and Merchant, S. S. (2019). A series of fortunate events: Introducing chlamydomonas as a reference organism. *Plant Cell* 31,

1682–1707. doi: 10.1105/tpc.18.00952.

Salvucci, M. E., and Ogren, W. L. (1985). A Chlamydomonas reinhardii mutant with catalytically and structurally altered ribulose-5-phosphate kinase. *Planta* 165, 340–347. doi: 10.1007/BF00392230.

Saroussi, S. I., Wittkopp, T. M., and Grossman, A. R. (2016). The Type II NADPH Dehydrogenase Facilitates Cyclic Electron Flow, Energy-Dependent Quenching, and Chlororespiratory Metabolism during Acclimation of Chlamydomonas reinhardtii to Nitrogen Deprivation. *Plant Physiol* 170, 1975–1988. doi: 10.1104/pp.15.02014.

Satanowski, A., Dronsella, B., Noor, E., Vögeli, B., He, H., Wichmann, P., *et al*. (2020). Awakening a latent carbon fixation cycle in Escherichia coli. *Nat Commun* 11, 1–14. doi: 10.1038/s41467-020-19564-5.

Scaife, M. A., Nguyen, G. T. D. T., Rico, J., Lambert, D., Helliwell, K. E., and Smith, A. G. (2015). Establishing Chlamydomonas reinhardtii as an industrial biotechnology host. *Plant Journal*. doi: 10.1111/tpj.12781.

Schnell, R. A., and Lefebvre, P. A. (1993). Isolation of the Chlamydomonas regulatory gene NIT2 by transposon tagging. *Genetics* 134, 737–747. doi: 10.1093/genetics/134.3.737.

Schroda, M. (2019). Good News for Nuclear Transgene Expression in Chlamydomonas. *Cells* 8. doi: 10.3390/cells8121534.

Schroda, M., Beck, C. F., and Vallon, O. (2002). Sequence elements within an HSP70 promoter counteract transcriptional transgene silencing in Chlamydomonas.

Schroda, M., and Remacle, C. (2022). Molecular Advancements Establishing Chlamydomonas as a Host for Biotechnological Exploitation. *Front Plant Sci* 13. doi: 10.3389/fpls.2022.911483.

Schulz, L., Guo, Z., Zarzycki, J., Steinchen, W., Schuller, J. M., Heimerl, T., *et al*. (2022). Evolution of increased complexity and specificity at the dawn of form I Rubiscos. *Science (1979)* 378, 155–160. doi: 10.1126/science.abq1416.

Schwander, T., Schada von Borzyskowski, L., Burgener, S., Cortina, N. S., and

Erb, T. J. (2016). A synthetic pathway for the fixation of carbon dioxide in vitro. *Science (1979)* 354, 900–904. doi: 10.1126/science.aah5237.

Seto, H., Ōtake, N., and Yonehara, H. (1966). Biological transformation of blasticidin s by aspergillus fumigatus sp. *Agric Biol Chem* 30, 877–886. doi: 10.1080/00021369.1966.10858693.

Shao, N., Beck, C. F., Lemaire, S. D., and Krieger-Liszkay, A. (2008). Photosynthetic electron flow affects H2O2 signaling by inactivation of catalase in Chlamydomonas reinhardtii. *Planta* 228, 1055–1066. doi: 10.1007/s00425-008-0807-0.

Shih, P. M., Occhialini, A., Cameron, J. C., Andralojc, P. J., Parry, M. A. J., and Kerfeld, C. A. (2016). Biochemical characterization of predicted Precambrian RuBisCO. *Nat Commun* 7, 1–11. doi: 10.1038/ncomms10382.

Shimakawa, G., Ishizaki, K., Tsukamoto, S., Tanaka, M., Sejima, T., and Miyake, C. (2017). The Liverwort, Marchantia, Drives Alternative Electron Flow Using a Flavodiiron Protein to Protect PSI. *Plant Physiol* 173, 1636–1647. doi: 10.1104/pp.16.01038.

Shin, S. E., Lim, J. M., Koh, H. G., Kim, E. K., Kang, N. K., Jeon, S., *et al*. (2016). CRISPR/Cas9-induced knockout and knock-in mutations in Chlamydomonas reinhardtii. *Sci Rep* 6, 27810. doi: 10.1038/srep27810.

Siebke, K., Von Caemmerer, S., Badger, M., and Furbank, R. T. (1997). Expressing an RbcS antisense gene in transgenic Flaveria bidentis leads to an increased quantum requirement for Co2 fixed in photosystems I and II. *Plant Physiol* 115, 1163–1174. doi: 10.1104/pp.115.3.1163.

Simkin, A. J., López-Calcagno, P. E., and Raines, C. A. (2019). Feeding the world: Improving photosynthetic efficiency for sustainable crop production. *J Exp Bot* 70, 1119–1140. doi: 10.1093/jxb/ery445.

Singh, A. V., Rahman, A., Sudhir Kumar, N. V. G., Aditi, A. S., Galluzzi, M., Bovio, S., *et al*. (2012). Bio-inspired approaches to design smart fabrics. *Mater Des* 36, 829–839. doi: 10.1016/j.matdes.2011.01.061.

Sizova, I., Fuhrmann, M., and Hegemann, P. (2001). A Streptomyces rimosus

aphVIII gene coding for a new type phosphotransferase provides stable antibiotic resistance to Chlamydomonas reinhardtii. Available at: www.elsevier.com/locate/gene.

Smith, B. D. (2000). Bryan's Thesis 1-24-14.

South, P. F., Cavanagh, A. P., Liu, H. W., and Ort, D. R. (2019). Synthetic glycolate metabolism pathways stimulate crop growth and productivity in the field. *Science (1979)* 363. doi: 10.1126/SCIENCE.AAT9077.

Sparla, F., Fermani, S., Falini, G., Zaffagnini, M., Ripamonti, A., Sabatino, P., *et al*. (2004). Coenzyme Site-directed Mutants of Photosynthetic A4-GAPDH Show Selectively Reduced NADPH-dependent Catalysis, Similar to Regulatory AB-GAPDH Inhibited by Oxidized Thioredoxin. *J Mol Biol* 340, 1025–1037. doi: https://doi.org/10.1016/j.jmb.2004.06.005.

Sparla, F., Zaffagnini, M., Wedel, N., Scheibe, R., Pupillo, P., and Trost, P. (2005). Regulation of photosynthetic GAPDH dissected by mutants. *Plant Physiol* 138, 2210–2219. Available at: http://www.ncbi.nlm.nih.gov/entrez/query.fcgi?cmd=Retrieve&db=PubMed&dopt=Citation&list_uids=16055685.

Stevens, D. R., Roehaix, J.-D., and Purton, S. (1996). The bacterial phleomycin resistance gene ble as a dominant selectable marker in Chlamydomonas.

Stitt, M., Lunn, J., and Usadel, B. (2010). Arabidopsis and primary photosynthetic metabolism - More than the icing on the cake. *Plant Journal* 61, 1067–1091. doi: 10.1111/j.1365-313X.2010.04142.x.

Stitt, M., and Schulze, D. (1994). Does Rubisco control the rate of photosynthesis and plant growth? An exercise in molecular ecophysiology. *Plant Cell Environ* 17, 465–487. doi: 10.1111/J.1365-3040.1994.TB00144.X.

Strenkert, D., Schmollinger, S., Gallaher, S. D., Salome, P. A., Purvine, S. O., Nicora, C. D., *et al*. (2019). Multiomics resolution of molecular events during a day in the life of Chlamydomonas. *Proc Natl Acad Sci U S A*

116, 2374–2383. doi: 10.1073/pnas.1815238116.

Subramanian, V., Wecker, M. S. A., Gerritsen, A., Boehm, M., Xiong, W., Wachter, B., *et al*. (2019). Ferredoxin5 Deletion Affects Metabolism of Algae during the Different Phases of Sulfur Deprivation. *Plant Physiol* 181, 426–441. doi: 10.1104/pp.19.00457.

Sueoka, N. (1960). Mitotic Replication of Deoxyribonucleic Acid in Chlamydomonas Reinhardi. *Proc Natl Acad Sci U S A* 46, 83–91. doi: 10.1073/pnas.46.1.83.

Sun, H., Liu, X., Li, F., Li, W., Zhang, J., Xiao, Z., *et al*. (2017). First comprehensive proteome analysis of lysine crotonylation in seedling leaves of Nicotiana tabacum. *Sci Rep* 7, 3013. doi: 10.1038/s41598-017-03369-6.

Sun, J., Qiu, C., Qian, W., Wang, Y., Sun, L., Li, Y., *et al*. (2019). Ammonium triggered the response mechanism of lysine crotonylome in tea plants. *BMC Genomics* 20, 340. doi: 10.1186/s12864-019-5716-z.

Sun, Y., Valente-Paterno, M., Bakhtiari, S., Law, C., Zhan, Y., and Zerges, W. (2019). Photosystem Biogenesis Is Localized to the Translation Zone in the Chloroplast of Chlamydomonas. *Plant Cell* 31, 3057–3072. doi: 10.1105/tpc.19.00263.

Svidritskiy, E., Ling, C., Ermolenko, D. N., and Korostelev, A. A. (2013). Blasticidin S inhibits translation by trapping deformed tRNA on the ribosome. *Proc Natl Acad Sci U S A* 110, 12283–12288. doi: 10.1073/pnas.1304922110.

Syeda, R., Xu, J., Dubin, A. E., Coste, B., Mathur, J., Huynh, T., *et al*. (2015). Chemical activation of the mechanotransduction channel Piezo1. *Elife* 4. doi: 10.7554/eLife.07369.

Tabatabaei, I., Dal Bosco, C., Bednarska, M., Ruf, S., Meurer, J., and Bock, R. (2019). A highly efficient sulfadiazine selection system for the generation of transgenic plants and algae. *Plant Biotechnol J* 17, 638–649. doi: 10.1111/pbi.13004.

Tagliani, A., Rossi, J., Marchand, C. H., De Mia, M., Tedesco, D., Gurrieri, L.,

et al. (2021). Structural and functional insights into nitrosoglutathione reductase from Chlamydomonas reinhardtii. *Redox Biol* 38, 101806. doi: 10.1016/j.redox.2020.101806.

Tamoi, M., Nagaoka, M., Miyagawa, Y., and Shigeoka, S. (2006). Contribution of fructose-1,6-bisphosphatase and sedoheptulose-1,7-bisphosphatase to the photosynthetic rate and carbon flow in the Calvin cycle in transgenic plants. *Plant Cell Physiol* 47, 380–390. doi: 10.1093/pcp/pcj004.

Tarrago, L., Laugier, E., Zaffagnini, M., Marchand, C., Le Marechal, P., Rouhier, N., *et al*. (2009). Regeneration mechanisms of Arabidopsis thaliana methionine sulfoxide reductases B by glutaredoxins and thioredoxins. *J Biol Chem* 284, 18963–18971. Available at: http://www.ncbi.nlm.nih.gov/entrez/query.fcgi?cmd=Retrieve&db=PubMed&dopt=Citation&list_uids=19457862.

Rapport de l'Académie des technologies (2020).

Terashima, M., Specht, M., and Hippler, M. (2011). The chloroplast proteome: a survey from the Chlamydomonas reinhardtii perspective with a focus on distinctive features. *Curr Genet* 57, 151–168. doi: 10.1007/s00294-011-0339-1.

Terauchi, A. M., Lu, S. F., Zaffagnini, M., Tappa, S., Hirasawa, M., Tripathy, J. N., *et al*. (2009). Pattern of expression and substrate specificity of chloroplast ferredoxins from Chlamydomonas reinhardtii. *J Biol Chem* 284, 25867–25878. doi: 10.1074/jbc.M109.023622.

Thieulin-Pardo, G., Remy, T., Lignon, S., Lebrun, R., and Gontero, B. (2015). Phosphoribulokinase from Chlamydomonas reinhardtii: a Benson-Calvin cycle enzyme enslaved to its cysteine residues. *Mol Biosyst* 11, 1134–1145. doi: 10.1039/c5mb00035a.

Tilman, D., Balzer, C., Hill, J., and Befort, B. L. (2011). Global food demand and the sustainable intensification of agriculture. *Proc Natl Acad Sci U S A* 108, 20260–20264. doi: 10.1073/pnas.1116437108.

Tirard, S. (2015). La biologie synthétique : de Stéphane Leduc Á Craig Vanter… et retour ? *Cahiers François Viète*, 137–150. doi:

10.4000/cahierscfv.2968.

Toone, E. J. (2006). Mechanisms of Protein Evolution and their Application to Protein Engineering. *Advances in enzymology and related subjects*. doi: 10.1002/9780471224464.

Toyoshige Endo (1987). Inactivation of Blasticidin S by Bacillus cereus.

Treves, H., Lucius, S., Feil, R., Stitt, M., Hagemann, M., and Arrivault, S. (2022). Operation of Carbon-Concentrating Mechanisms in Cyanobacteria and Algae requires altered poising of the Calvin-Benson cycle. *bioRxiv*, 2022.08.23.504937. doi: 10.1101/2022.08.23.504937.

Trost, P., Fermani, S., Marri, L., Zaffagnini, M., Falini, G., Scagliarini, S., *et al*. (2006). Thioredoxin-dependent regulation of photosynthetic glyceraldehyde-3-phosphate dehydrogenase: autonomous vs. CP12-dependent mechanisms. *Photosynth Res* 89, 263–275. Available at: http://www.ncbi.nlm.nih.gov/entrez/query.fcgi?cmd=Retrieve&db=PubMed&dopt=Citation&list_uids=17031544.

Trudeau, D. L., Edlich-Muth, C., Zarzycki, J., Scheffen, M., Goldsmith, M., Khersonsky, O., *et al*. (2018). Design and in vitro realization of carbon-conserving photorespiration. *Proc Natl Acad Sci U S A* 115, E11455–E11464. doi: 10.1073/pnas.1812605115.

van der Linde, K., Gutsche, N., Leffers, H. M., Lindermayr, C., Müller, B., Holtgrefe, S., *et al*. (2011). Regulation of plant cytosolic aldolase functions by redox-modifications. *Plant Physiol Biochem* 49, 946–957. doi: 10.1016/j.plaphy.2011.06.009.

Vavitsas, K., Crozet, P., Vinde, M. H., Davies, F., Lemaire, S. D., and Vickers, C. E. (2019). The Synthetic Biology Toolkit for Photosynthetic Microorganisms. *Plant Physiol* 181, 14–27. doi: 10.1104/pp.19.00345.

Vavitsas, K., Kugler, A., Satta, A., Hatzinikolaou, D. G., Lindblad, P., Fewer, D. P., *et al*. (2021). Doing synthetic biology with photosynthetic microorganisms. *Physiol Plant* 173, 624–638. doi: 10.1111/ppl.13455.

Vecchi, V., Barera, S., Bassi, R., and Dall'Osto, L. (2020). Potential and Challenges of Improving Photosynthesis in Algae. *Plants (Basel)* 9. doi:

10.3390/plants9010067.

Villeret, V., Huang, S., Zhang, Y., Xue, Y., and Lipscomb, W. N. (1995). Crystal structure of spinach chloroplast fructose-1,6-bisphosphatase at 2.8 A resolution. *Biochemistry* 34, 4299–4306. Available at: http://www.ncbi.nlm.nih.gov/entrez/query.fcgi?cmd=Retrieve&db=PubMed&dopt=Citation&list_uids=7703243.

Von Caemmerer, S., Millgate, A., Farquhar, G. D., and Furbank, R. T. (1997). Reduction of ribulose-1,5-bisphosphate carboxylase/oxygenase by antisense RNA in the C4 plant Flaveria bidentis leads to reduced assimilation rates and increased carbon isotope discrimination. *Plant Physiol* 113, 469–477. doi: 10.1104/pp.113.2.469.

Wagner, V., Gessner, G., Heiland, I., Kaminski, M., Hawat, S., Scheffler, K., *et al*. (2006). Analysis of the phosphoproteome of Chlamydomonas reinhardtii provides new insights into various cellular pathways. *Eukaryot Cell* 5, 457–468. Available at: http://www.ncbi.nlm.nih.gov/entrez/query.fcgi?cmd=Retrieve&db=PubMed&dopt=Citation&list_uids=16524901.

Walker, D. (1992). *Energy, plants and man*. Univ Science Books.

Wang, F., and Zhang, W. (2019). Synthetic biology: Recent progress, biosafety and biosecurity concerns, and possible solutions. *J Biosaf Biosecur* 1, 22–30. doi: 10.1016/J.JOBB.2018.12.003.

Wang, H., Gau, B., Slade, W. O., Juergens, M., Li, P., and Hicks, L. M. (2014). The global phosphoproteome of chlamydomonas reinhardtii reveals complex organellar phosphorylation in the flagella and thylakoid membrane. *Molecular and Cellular Proteomics* 13, 2337–2353. doi: 10.1074/mcp.M114.038281.

Wang, H., Yan, X., Aigner, H., Bracher, A., Nguyen, N. D., Hee, W. Y., *et al*. (2019). Rubisco condensate formation by CcmM in beta-carboxysome biogenesis. *Nature* 566, 131–135. doi: 10.1038/s41586-019-0880-5.

Wang, L., Jiang, S., Chen, C., He, W., Wu, X., Wang, F., *et al*. (2018). Synthetic Genomics: From DNA Synthesis to Genome Design. *Angewandte Chemie - International Edition* 57, 1748–1756. doi:

10.1002/anie.201708741.

Wang, L. M., Shen, B. R., Li, B. D., Zhang, C. L., Lin, M., Tong, P. P., *et al*. (2020). A Synthetic Photorespiratory Shortcut Enhances Photosynthesis to Boost Biomass and Grain Yield in Rice. *Mol Plant* 13, 1802–1815. doi: 10.1016/j.molp.2020.10.007.

Way, J. C., Collins, J. J., Keasling, J. D., and Silver, P. A. (2014). Integrating biological redesign: Where synthetic biology came from and where it needs to go. *Cell* 157, 151–161. doi: 10.1016/j.cell.2014.02.039.

Weber, A., Menzlaff, E., Arbinger, B., Gutensohn, M., Eckerskorn, C., and Fluegge, U.-I. (1995). The 2-oxoglutarate/malate translocator of chloroplast envelope membranes: molecular cloning of a transporter containing a 12-helix motif and expression of the functional protein in yeast cells. *Biochemistry* 34, 2621–2627.

Weber, E., Engler, C., Gruetzner, R., Werner, S., and Marillonnet, S. (2011). A modular cloning system for standardized assembly of multigene constructs. *PLoS One* 6. doi: 10.1371/journal.pone.0016765.

Werner, S., Engler, C., Weber, E., Gruetzner, R., and Marillonnet, S. (2012). Fast track assembly of multigene constructs using golden gate cloning and the MoClo system. *Bioeng Bugs* 3, 38–43. doi: 10.4161/bbug.3.1.18223.

Werth, E. G., McConnell, E. W., Couso Lianez, I., Perrine, Z., Crespo, J. L., Umen, J. G., *et al*. (2019). Investigating the effect of target of rapamycin kinase inhibition on the Chlamydomonas reinhardtii phosphoproteome: from known homologs to new targets. *New Phytol* 221, 247–260. doi: 10.1111/nph.15339.

Werth, E. G., McConnell, E. W., Gilbert, T. S., Couso Lianez, I., Perez, C. A., Manley, C. K., *et al*. (2017). Probing the global kinome and phosphoproteome in Chlamydomonas reinhardtii via sequential enrichment and quantitative proteomics. *Plant J* 89, 416–426. doi: 10.1111/tpj.13384.

White-Gloria, C., Johnson, J. J., Marritt, K., Kataya, A., Vahab, A., and Moorhead, G. B. (2018). Protein kinases and phosphatases of the

plastid and their potential role in starch metabolism. *Front Plant Sci* 9, 1–8. doi: 10.3389/fpls.2018.01032.

Wilson, R. H., Hayer-Hartl, M., and Bracher, A. (2019). Crystal structure of phosphoribulokinase from Synechococcus sp. strain PCC 6301. *Acta Crystallogr F Struct Biol Commun* 75, 278–289. doi: 10.1107/S2053230X19002693.

Wobbe, L., and Remacle, C. (2015). Improving the sunlight-to-biomass conversion efficiency in microalgal biofactories. *J Biotechnol* 201, 28–42. doi: 10.1016/j.jbiotec.2014.08.021.

Wollman, F.-A., Girard-Bascou Société Française de Génétique Président Nicolas P résident, J. A., Jacob, lonneur F., Berger Pinon C Stoll Secrétaire général M Solignac Trésorier P-M Sinet, R. H., and emheim Bolotin-Fukuhara M Fellous J Génermont B Michel R Motta A Nicolas S Sommer P Thuriaux D de Vienne Secrétaire M-L Prunier, A. M. (1994). Une algue pour l'étude de la génétique des organites : Chlamydomonas reinhardtii.

Xu, M., Luo, J., Li, Y., Shen, L., Zhang, X., Yu, J., *et al*. (2021). First comprehensive proteomics analysis of lysine crotonylation in leaves of peanut (Arachis hypogaea L.). *Proteomics* 21, e2000156. doi: 10.1002/pmic.202000156.

Yahya, R. Z., Wellman, G. B., Overmans, S., and Kyle, J. (2023). Engineered production of isoprene from the model green microalga Chlamydomonas reinhardtii. 1–27.

Yan, N., Fan, C., Chen, Y., and Hu, Z. (2016). The potential for microalgae as bioreactors to produce pharmaceuticals. *Int J Mol Sci* 17. doi: 10.3390/ijms17060962.

Yang, W., Wittkopp, T. M., Li, X., Warakanont, J., Dubini, A., Catalanotti, C., *et al*. (2015). Critical role of Chlamydomonas reinhardtii ferredoxin-5 in maintaining membrane structure and dark metabolism. *Proc Natl Acad Sci U S A* 112, 14978–14983. doi: 10.1073/pnas.1515240112.

Yang, Z. (2007). PAML 4: Phylogenetic analysis by maximum likelihood. *Mol Biol Evol* 24, 1586–1591. doi: 10.1093/molbev/msm088.

Yeh, H.-L., Lin, T.-H., Chen, C.-C., Cheng, T.-X., Chang, H.-Y., and Lee, T.-M. (2019). Monodehydroascorbate reductase plays a role in the tolerance of Chlamydomonas reinhardtii to photooxidative stress. *Plant Cell Physiol* 60, 2167–2179.

Yoon, D.-K., Ishiyama, K., Suganami, M., Tazoe, Y., Watanabe, M., Imaruoka, S., *et al*. (2020). Transgenic rice overproducing Rubisco exhibits increased yields with improved nitrogen-use efficiency in an experimental paddy field. *Nat Food* 1, 134–139. doi: 10.1038/s43016-020-0033-x.

Yu, A., Xie, Y., Pan, X., Zhang, H., Cao, P., Su, X., *et al*. (2020). Photosynthetic Phosphoribulokinase Structures: Enzymatic Mechanisms and the Redox Regulation of the Calvin-Benson-Bassham Cycle. *Plant Cell* 32, 1556–1573. doi: 10.1105/tpc.19.00642.

Zaffagnini, M., Bedhomme, M., Groni, H., Marchand, C. H., Puppo, C., Gontero, B., *et al*. (2012). Glutathionylation in the photosynthetic model organism Chlamydomonas reinhardtii: a proteomic survey. *Mol Cell Proteomics* 11, M111 014142. doi: 10.1074/mcp.M111.014142.

Zaffagnini, M., De Mia, M., Morisse, S., Di Giacinto, N., Marchand, C. H., Maes, A., *et al*. (2016). Protein S-nitrosylation in photosynthetic organisms: A comprehensive overview with future perspectives. *Biochim Biophys Acta* 1864, 952–966. doi: 10.1016/j.bbapap.2016.02.006.

Zaffagnini, M., Fermani, S., Costa, A., Lemaire, S. D., and Trost, P. (2013). Plant cytoplasmic GAPDH: redox post-translational modifications and moonlighting properties. *Front Plant Sci* 4, 450. doi: 10.3389/fpls.2013.00450.

Zaffagnini, M., Fermani, S., Marchand, C. H., Costa, A., Sparla, F., Rouhier, N., *et al*. (2019). Redox Homeostasis in Photosynthetic Organisms: Novel and Established Thiol-Based Molecular Mechanisms. *Antioxid Redox Signal* 31, 155–210. doi: 10.1089/ars.2018.7617.

Zaffagnini, M., Michelet, L., Sciabolini, C., Di Giacinto, N., Morisse, S., Marchand, C. H., *et al*. (2014). High-resolution crystal structure and redox properties of chloroplastic triosephosphate isomerase from

Chlamydomonas reinhardtii. *Mol Plant* 7, 101–120. doi: 10.1093/mp/sst139.

Zhan, Y., Dhaliwal, J. S., Adjibade, P., Uniacke, J., Mazroui, R., and Zerges, W. (2015). Localized control of oxidized RNA. *J Cell Sci* 128, 4210–4219. doi: 10.1242/jcs.175232.

Zhan, Y., Marchand, C. H., Maes, A., Mauries, A., Sun, Y., Dhaliwal, J. S., *et al*. (2018). Pyrenoid functions revealed by proteomics in Chlamydomonas reinhardtii. *PLoS One* 13, e0185039. doi: 10.1371/journal.pone.0185039.

Zhu, X. G., De Sturler, E., and Long, S. P. (2007). Optimizing the distribution of resources between enzymes of carbon metabolism can dramatically increase photosynthetic rate: A numerical simulation using an evolutionary algorithm. *Plant Physiol* 145, 513–526. doi: 10.1104/pp.107.103713.

Zhu, X. G., Long, S. P., and Ort, D. R. (2010). Improving photosynthetic efficiency for greater yield. *Annu Rev Plant Biol* 61, 235–261. doi: 10.1146/annurev-arplant-042809-112206.

6 ANNEXES

Annexe 1

Milieux de culture pour *Chlamydomonas reinhardtii*

Pour 1 litre	**TAP (Tris Acétate Phosphate) 1x**	**HSM (High Salt Minimal) 1x**
H_2O MilliQ	975 ml	925 ml
Tris base	2,42 g	-
[1]4x Beijerinck salts	25 ml	25 ml
[2](K)PO_4 1 M, pH 7	1 ml	-
[3]2x PO_4	-	50 ml
[4]Trace (Hutner + fer)	1 ml	1 ml
Acide acétique	ajuster à pH 7 avec l'acide acétique : ~1 ml	-
HCl concentré	pour finir d'ajuster le pH	-

Remarque : ne pas ajouter plus d'1 ml d'acide acétique (source d'acétate) pour préparer la solution TAP, sinon il y aura plus d'acétate fourni aux Chlamydomonas. Pour finir d'ajuster le pH, ajouter de l'HCl si nécessaire. Pour produire des gamètes (TAP-N), le pH doit être ajusté un peu au-dessus de 7 (7,1 ou 7,2), car le pH diminue toujours un peu à l'autoclave, et si le pH est trop bas, les Chlamydomonas ne donneront pas de gamètes.

Les milieux solides sont obtenus en ajoutant de l'agar 1,5% (p/v) sauf pour les croisements qui nécessitent une densité supérieure et pour lesquels de l'agar 3% (p/v) est ajouté.

Autoclaver immédiatement 30 minutes à 115°C pour éviter toute contamination.

1. 4x Beijerinck salts :

- 16 g NH_4Cl ou supprimer le composé pour un milieu TAP sans azote (-N)
- 2 g $CaCl_2.2H_2O$
- 4 g $MgSO_4.7H_2O$ ou 3,3 g $MgCl_2.6H_2O$ pour un milieu TAP sans soufre (-S)

ajuster à 1 l avec de l'eau MilliQ.

2. (K)PO_4 1 M, pH 7 :

- 250 ml K_2HPO_4 1 M

~ 170 ml KH_2PO_4 1 M

3. 2x PO_4 :

- 14,34 g de K_2HPO_4 (80 mM)
- 7,26 g de KH_2PO_4 (50 mM)

ajuster à pH 6,9 avec du KOH et à 1 l avec de l'eau MilliQ.

4. Trace :

- Méthode 1 :

1) Dissoudre dans 550 ml d'eau MilliQ dans l'ordre indiqué :

- 11,40 g H_3BO_3
- 22,00 g $ZnSO_4.7H_2O$
- 5,06 g $MnCl_2.4H_2O$
- 4,99 g $FeSO_4.7H_2O$
- 1,61 g $CoCl_2.6H_2O$
- 1,57 g $CuSO_4.5H_2O$
- 1,10 g $(NH_4)_6Mo_7O_{24}.4H_2O$

puis chauffer à 100°C.

=> ajouter les différents composés dans l'ordre, en ajoutant le suivant après dissolution totale du précédent.

2) Dissoudre 50 g de Na_2EDTA dans 250 ml d'eau MilliQ en chauffant, puis ajouter à la solution précédente à 100°C.

3) Chauffer le mélange à 100°C, puis le refroidir à 80-90°C et ajuster le pH à 6,5-6,8 avec du KOH 20% (moins de 100 ml).

Le pH-mètre doit d'abord être calibré à 75°C ; la température du mélange doit rester supérieure à 70°C.

4) Ajuster à 1 l avec de l'eau MilliQ, et laisser se former un précipité couleur rouille pendant 2 semaines à température ambiante, dans un erlenmeyer de 2 l bouché avec un coton. La solution va passer de vert à violet.

5) Filtrer plusieurs fois à travers trois couches de Whatman No. 1 sous aspiration (entonnoir Büchner). Conserver la solution violacée à 4°C dans un flacon opaque.

- Méthode 2 :

1) Dissoudre les sels ci-dessous dans 400 ml d'eau MilliQ dans l'ordre indiqué :

   - 4,99 g $FeSO_4.7H_2O$
   - 50 g Na_2EDTA

Pour dissoudre le Na_2EDTA, il est nécessaire d'augmenter le pH en ajoutant des pastilles de KOH jusqu'à ce que la solution prenne une coloration jaune/orangée.

2) Dissoudre les sels ci-dessous dans 400 ml d'eau MilliQ dans l'ordre indiqué :

- 22,00 g $ZnSO_4.7H_2O$
- 11,40 g H_3BO_3
- 5,06 g $MnCl_2.4H_2O$

- 1,61 g $CoCl_2.6H_2O$
- 1,57 g $CuSO_4.5H_2O$
- 1,10 g $(NH_4)_6Mo_7O_{24}.4H_2O$

Cette solution a une couleur rosée.

3) Mélanger les deux solutions ci-dessus et ajuster le pH à 6,5 avec des pastilles de KOH puis des solutions de KOH de concentration décroissante.

4) Ajuster le volume à 1 l avec de l'eau MilliQ, et laisser se former un précipité couleur rouille pendant 2 semaines à température ambiante, dans un erlenmeyer de 2 l bouché avec un coton. La solution va passer de vert à violet.

5) Filtrer plusieurs fois à travers trois couches de Whatman No. 1 sous aspiration (entonnoir Büchner). Conserver la solution violacée à 4°C dans un flacon opaque.

Annexe 2

Données supplémentaires de l'article 3 - Blasticidin S Deaminase: A New Efficient Selectable Marker for Chlamydomonas reinhardtii

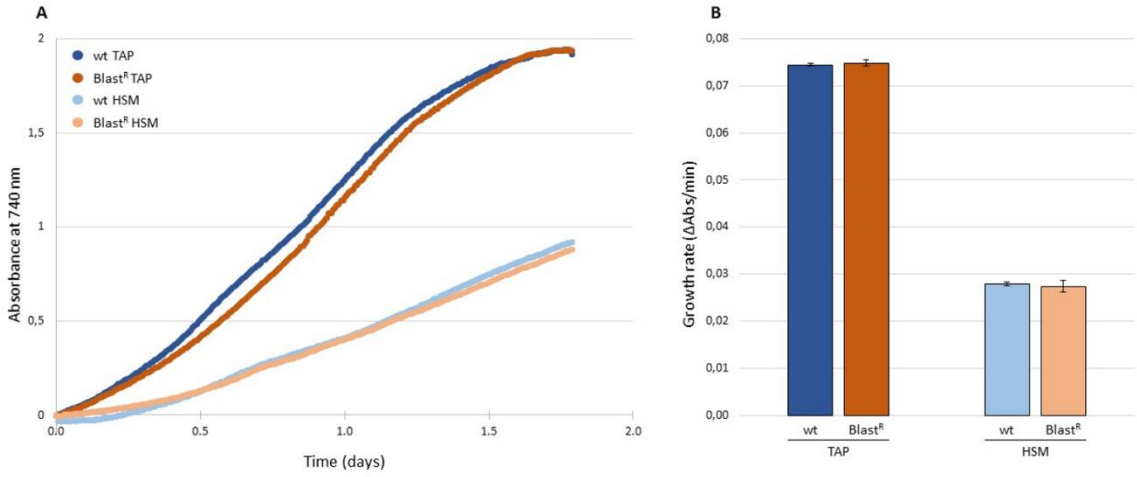

Figure 32. Croissance des souches sauvages (CC-4533) et des souches BlastR dans un photobioréacteur contrôlé. (A) Mesure de la croissance détectée par l'absorbance à 740 nm toutes les 10 minutes, en milieu TAP (mixotrophie) et en milieu HSM (autotrophie), la lumière étant réglée à 200 µmol photons m^{-2} s^{-1} avec une température et un agitateur réglé à 25°C et 120 rpm, respectivement. (B) Quantification du taux de croissance moyen des cellules CC-4533 et des cellules BlastR, correspondant aux courbes de croissance présentées dans le graphique (A). Les barres d'erreur représentent l'erreur standard par rapport à la moyenne de deux réplicats biologiques (De Carpentier et al., 2020).